Universidade Federal de Minas Gerais
Instituto de Geociências
Departamento de Geografia

Samuel Rodrigues Ribeiro

MORFOGÊNESE E EVOLUÇÃO PALEOGEOGRÁFICA DA FOZ DO RIO TOCANTINS, ESTADO DO PARÁ, DURANTE O HOLOCENO

Belo Horizonte
2022

Samuel Rodrigues Ribeiro

MORFOGÊNESE E EVOLUÇÃO PALEOGEOGRÁFICA DA FOZ DO RIO TOCANTINS, ESTADO DO PARÁ, DURANTE O HOLOCENO

Tese apresentada ao Programa de Pós-Graduação em Geografia da Universidade Federal de Minas Gerais, como requisito parcial à obtenção do título de Doutor em Geografia.

Área de concentração: Análise Ambiental

Linha de Pesquisa: Geografia Física

Orientador: Prof. Dr. Roberto Célio Valadão

Coorientadora: Profa. Dra. Makênia Oliveira Soares Gomes

Belo Horizonte
2022

R484m
2022

Ribeiro, Samuel Rodrigues.

Morfogênese e evolução paleogeográfica da foz do Rio Tocantins, estado do Pará, durante o Holoceno [manuscrito] / Samuel Rodrigues Ribeiro. – 2022.

191 f., enc.: il. (principalmente color.)

Orientador: Roberto Célio Valadão.

Coorientadora: Makênia Oliveira Soares Gomes.

Tese (doutorado) – Universidade Federal de Minas Gerais, Departamento de Geografia, 2022.

Área de concentração: Análise Ambiental.

Linha de pesquisa: Geografia Física.

Inclui bibliografia.

1. Geomorfologia – Teses. 2. Hidrodinâmica – Teses. 3. Palinologia – Teses. 4. Tocantins, Rio – Teses. 5. Amazônia – Teses. I. Valadão, Roberto Célio. II. Gomes, Makênia Oliveira Soares. III. Universidade Federal de Minas Gerais. Departamento de Geografia. IV. Título.

CDU: 551.4

Ficha catalográfica elaborada por Graciane Aparecida de Paula – CRB-6/3404
Biblioteca “Vitória Pedersoli”, Instituto de Geociências da UFMG

UNIVERSIDADE FEDERAL DE MINAS GERAIS
INSTITUTO DE GEOCIÊNCIAS
COLEGIADO DO CURSO DE PÓS-GRADUAÇÃO EM GEOGRAFIA

FOLHA DE APROVAÇÃO

"MORFOGÊNESE E EVOLUÇÃO PALEOGEOGRÁFICA DA FOZ DO RIO TOCANTINS, ESTADO DO PARÁ, DURANTE O HOLOCENO"

SAMUEL RODRIGUES RIBEIRO

Tese de Doutorado defendida e aprovada, no dia 12 de julho de 2022, pela Banca Examinadora designada pelo Colegiado do Programa de Pós-Graduação em Geografia da Universidade Federal de Minas Gerais constituída pelos seguintes professores:

Adilson Viana Soares Júnior
UNIFESP

Edgardo Manuel Latrubesse
CIAMB/UFG

Mariah Izar Francisquini Correia
CENA/USP

Fábio Soares de Oliveira
IGC/UFMG

Roberto Célio Valadão – Orientador
IGC/UFMG

Belo Horizonte, 12 de julho de 2022.

Documento assinado eletronicamente por **Adilson Viana Soares Junior**, **Usuário Externo**, em 12/07/2022, às 18:57, conforme horário oficial de Brasília, com fundamento no art. 5º do Decreto nº 10.543, de 13 de novembro de 2020.

Documento assinado eletronicamente por **Fabio Soares de Oliveira**, **Professor do Magistério Superior**, em 12/07/2022, às 18:58, conforme horário oficial de Brasília, com fundamento no art. 5º do Decreto nº 10.543, de 13 de novembro de 2020.

Documento assinado eletronicamente por **Mariah Izar Francisquini Correia**, **Usuária Externa**, em 12/07/2022, às 19:00, conforme horário oficial de Brasília, com fundamento no art. 5º do Decreto nº 10.543, de 13 de novembro de 2020.

Documento assinado eletronicamente por **Roberto Celio Valadao**, **Professor do Magistério Superior**, em 12/07/2022, às 19:16, conforme horário oficial de Brasília, com fundamento no art. 5º do Decreto nº 10.543, de 13 de novembro de 2020.

Documento assinado eletronicamente por **Edgardo Manuel Latrubesse**, **Usuário Externo**, em 19/07/2022, às 16:47, conforme horário oficial de Brasília, com fundamento no art. 5º do Decreto nº 10.543, de 13 de novembro de 2020.

A autenticidade deste documento pode ser conferida no site https://sei.ufmg.br/sei/controlador_externo.php?acao=documento_conferir&id_orgao_acesso_externo=0, informando o código verificador **1539243** e o código CRC **8DB998FA**.

A Raimundo e Carmelina,
meus pais,
pelo amor desdobrado,
os ensinamentos e os valores humanos que me teceram,
dedico.

AGRADECIMENTOS

A Deus, o Espírito que sempre está comigo, cercando de bondade e graça. Agradeço-O por ter sustentado e protegido meus passos, e cuidado de minha vida até aqui;

Ao Instituto de Geociências da Universidade Federal de Minas Gerais, por intermédio do Programa de Pós-Graduação em Geografia, pela oportunidade de formação profissional;

Ao Prof. Dr. Roberto Valadão pela amizade, a honra da confiança, a liberdade de pensar, a acessibilidade, o saber transmitido e o magistério que inspira;

À Profa. Dra. Makênia Gomes (UEMG), pela forma especial que me recebeu, dispensou confiança, incentivou a execução da pesquisa e oportunizou o ingresso no Laboratório de Paleontologia e Macroevolução (LPM-CPMTC/UFMG);

Aos demais membros do Laboratório de Paleontologia e Macroevolução, em particular, ao diretor, Prof. Dr. Jonathas Bittencourt, agradeço por ter colocado o LMP ao interesse da pesquisa, por sua solicitude e a confiança depositada; à Dra. Karin Meyer (*in memorian*) por ter planejado, erguido e garantido a infraestrutura e insumos para a execução também desta pesquisa, e à Gabriela Pires, pela amizade e cooperação;

À Coordenação de Aperfeiçoamento de Pessoal de Nível Superior (CAPES), pela concessão da bolsa de Doutorado;

À titular da Secretaria de Pós-Graduação de Geografia, pelo suporte às demandas acadêmicas;

A Raimundo Ribeiro, João Paulo, Joárison Mendes e Jessé Mendes, que prestaram irrestrito suporte operacional durante a execução das campanhas campo, tanto em terra, quanto nos desconhecidos rios do Estuário de Marapatá. O sucesso obtido nos trabalhos de campo toma parte na braveza e a generosidade de vocês;

Aos queridos Jesiel Silva, pelo apoio veicular e, a Marcos Higor, pela habilidade com a qual nos levou a desbravar sítios de interesse da pesquisa no interior do continente;

Aos proprietários de sítios amostradas e/ou monitorados ao longo das ilhas, por permitirem o acesso e coletas, e aos mateiros, pela provisão de informação em campo;

À Renata Jordan, pela fraterna amizade, generosidade e recepção na UFMG; por seu espírito positivo que sempre proporcionou momentos de alegria e otimismo acadêmico;

À Raquel Alves, pelo amoroso zelo, cuidado e doação. Agradeço ainda por segurar minha mão ao longo desta fase;

Aos meus tios Nélio e Nazaré, pela carinhosa acolhida e apoio prestados durante fase tão decisiva de minha vida profissional;

Às minhas avós Maria e Roberta, pelo amor singelo, afável e cheio de alegria;

Por fim, reservo profunda gratidão à minha família, em especial, aos meus pais, meus irmãos e sobrinhos, pelo incessante amor, conforto e o encorajamento que me desperta a superar os desafios da jornada, e por sempre acreditarem em mim.

O homem teve seu tempo sob o Sol
Sonhou entender um único grão de areia
Deu vida à poesia, mas um dia ele mesmo deixará de existir,
Cumprimente a última luz da biblioteca.

Holopainen, J.

RESUMO

Ilhas são extensões de terra emersas, com distribuição geográfica difusa em quase todos os grandes rios tropicais. Na zona costeira da Amazônia, as ilhas estão concentradas entre os rios Amazonas, Pará e Tocantins, onde sua ocorrência generalizada contrasta com a subatenção recebida nos estudos geomorfológicos. Consequentemente, a gênese insular é pouco compreendida, em particular no sistema estabelecido na foz do Rio Tocantins. O escopo desta tese é investigar os mecanismos relacionados à evolução paleogeográfica holocênica da foz do Rio Tocantins, Estado do Pará, com base em múltiplos indicadores (dados oceanográficos, morfo-topográfico e estrutural, registro de perfil de poços, testemunhos de sedimento, feições sedimentares, palinologia, isótopos estáveis e datação C-14). Os resultados sugerem que o rearranjo do Rio Tocantins é o estágio central da paleogeografia costeira regional. No final do Pleistoceno, esse rio divergiu da Bacia do Amazonas e abriu nova rota oriental em direção ao Oceano Atlântico. O deslocamento da camada laterítica sobrejacente à sucessão sedimentar é indicador de eventos de subsidência concomitantes ao rearranjo fluvial. Essa sucessão compreende ciclos de *fining-upward* atribuídos a depósito de preenchimento de canal de maré, provavelmente relacionados à configuração transgressiva. A imposição da foz do Rio Tocantins em direção ao mar modelou a paisagem holocênica. Primeiro, abriu-se o vale inciso de Maratauíra, dando início ao destacamento à franja de terra da margem continental na foz do Tocantins. A incursão marinha seguinte invadiu a região, com pico de $2 \pm 0{,}5$ m acima do atual, formando ambientes salobros dominados por manguezais entre 8410 e 1490 anos cal AP. Os manguezais sofreram declínio espacial entre 1490 e 700 anos cal AP, coincidindo com a formação de turfeiras. Em contraste, a vegetação de água doce floresceu e tornou-se dominante. Essa dinâmica paleoecológica testemunhada na paisagem é consistente com a queda do nível relativo do mar, responsável pela migração da condição salobra em direção à linha de costa. Nos últimos sete séculos, dada a fisionomia insular ascendente dos dias de hoje, as principais alterações na paisagem envolveram a subida e estabilização do nível relativo do mar na posição atual, o afogamento da rede de rios de marés com planícies dominadas pela floresta de água doce, e a separação completa da franja terrestre do domínio continental. Portanto, esse sistema insular é de curto prazo, com tendência genética e evolutiva de longo prazo. Concernente ao mecanismo estruturador da paleogeografia, a atividade tectônica e a mudança do nível do mar foram preponderantes até ~1500 anos cal AP, enquanto a hidrodinâmica teve maior envolvimento na evolução tardia. Atualmente, o papel dessa última forçante se expressa na morfodinâmica, mediante o regime de marés que subordina ~40% do trecho insular a eventos de inundação estuarina. Endereçada à região de grande potencial no âmbito da Geografia Física, as interevidências morfológicas, tectônicas, paleoecológicas, sedimentares e biogeoquímicas reunidas neste estudo fornecem dados que auxiliam na reconstrução do quadro paleogeográfico da interface terra-mar no nordeste costeiro do Estado do Pará através do Holoceno, incluindo novos sinais de nível do mar alto no litoral norte brasileiro. Em conjunto, os achados proporcionam avanços significativos para se compreender, de modo mais efetivo, a evolução da Amazônia diante de um quadro marcado pela carência de investigações geomorfológicas.

Palavras-chave: Amazônia. Complexo Insular. Hidrodinâmica. Palinologia. Neotectônica. Nível Relativo do Mar.

ABSTRACT

The islands have a wide geographical distribution over nearly every major tropical river. In the coastal zone of the Amazon, they occur mainly between the Amazon, Pará, and Tocantins Rivers. This extensive occurrence contrasts with the attention they have received from geomorphological studies. Consequently, insular genesis is poorly understood, particularly in the system established at the mouth of the Tocantins. This study aimed to investigate the mechanisms related to the paleogeographic evolution of the mouth of the Tocantins River, State of Pará, during the Holocene, using a multi-proxy approach (oceanographic, morpho-topographic, and structural data, well drilling records, sediment cores, sedimentary features, palynology, stable isotope analysis and 14C-dating). The results suggest that the coastal adjustment of the Tocantins River is the central stage of the regional paleogeography. This river diverged from the Amazon basin and opened a new eastern route towards the Atlantic Ocean at the end of the Pleistocene. The displacement of the laterite layer overlying the sedimentary succession reflects subsidence events concurrent with the fluvial rearrangements. This succession comprises fining-upward cycles attributed to a tidal channel fill deposit, which is likely related to the transgressive configuration. The imposition of the mouth of the Tocantins towards the sea drove changes in the Holocene landscape. First, the incised valley of Maratauíra was opened, initiating the detachment of the fringe of land from the continental margin at the mouth of the Tocantins. Subsequently, the marine incursion invaded the region, attaining a peak of 2 ± 0,5 m above the present level, forming brackish environments dominated by mangroves between 8408 and 1485 cal yr BP. Mangroves suffered a spatial decline between 1485 and 700 cal yr BP, coinciding with the formation of peat bogs. In contrast, the freshwater vegetation flourished and became dominant. The paleoecological dynamics witnessed by the landscape are consistent with a fall in the relative sea level, which forced migration from brackish conditions towards the shoreline. In the last seven centuries, given the rising island physiognomy of the present day, the main changes in the landscape have involved the rise and stabilization of the sea level in the current position, drowning of the tidal river network with plains dominated by the floodplain, and complete separation of the land fringe from the continental domain. Therefore, this insular morphology is short-term, with long-term genetic and evolutionary trends. Regarding the landscape structuration mechanism, tectonic activity and sea-level change were predominant up to ~1500 cal yr BP, whereas hydrodynamics was more involved in late evolution. Currently, the role of this forcing is expressed in the morphodynamics through the tidal regime, which subordinates ~40% of the insular stretch to estuarine flood events. In addition to the region of great potential in the scope of Physical Geography, the morphological, tectonic, paleoecological, sedimentary, and biogeochemical inter-evidence gathered in this study provides data that help in the reconstruction of the paleogeographic picture of the land-sea interface of the northeastern portion of the state of Pará during the Holocene, including new signs regarding the highstand sea level on the northern Brazilian coast.

Keywords: Amazon. Insular Complex. Hydrodynamic. Palynology. Relative Sea-level. Neotectonic.

RÉSUMÉ

Les îles ont une distribution géographique dispersée dans presque tous les grands fleuves tropicaux. Dans la zone côtière de l'Amazonie, les îles sont concentrées entre les fleuves Amazonas, Pará et Tocantins où leur occurrence généralisée contraste avec le peu d'attention reçue dans les études géomorphologiques. De ce fait, la genèse insulaire est mal comprise, notamment dans le système établi à l'embouchure du fleuve Tocantins. Le cadre de cette thèse est d'étudier les mécanismes liés à l'évolution paléogéographique holocène de l'embouchure du fleuve Tocantins, État du Pará, sur la base de multiples indicateurs (données océanographiques, morpho-topographiques et structurelles, des rapports du profil de puits, des dépôts sédimentaires, des caractéristiques sédimentaires, de la palynologie, des isotopes stables et datation au C-14). Les résultats proposent que l'ajustement côtier du fleuve Tocantins soit l'étape centrale de la paléogéographie côtière régionale. À la fin du Pléistocène, le fleuve Tocantins s'est séparé du bassin du fleuve Amazonas et a ouvert une nouvelle voie orientale vers l'Océan Atlantique. Le déplacement de la couche latéritique au-dessus de la séquence sédimentaire est révélateur d'évènements d'affaissement simultanés au réarrangement fluvial. Cette succession comprend des cycles de fining-upward attribués au dépôt de remplissage de canal de marée, probablement liés à la configuration transgressive. L'imposition de l'embouchure du fleuve Tocantins vers la mer a façonné le paysage holocène. Tout d'abord, la vallée incisée de Maratauíra a été ouverte initiant le détachement à la frange de terre de la marge continentale à l'embouchure du Tocantins. L'incursion marine suivante a envahi la région avec un pic de 2 ± 0,5m au-dessus de l'actuel, formant des environnements saumâtres dominés par des mangroves entre 8410 et 1490 ans cal AP. Les mangroves ont subi un déclin spatial entre 1490 et 700 ans cal AP correspondant à la formation de tourbières. En revanche, la végétation d'eau douce a fleuri et est devenue dominante. Cette dynamique paléoécologique observée dans le paysage est cohérente avec la chute du niveau relatif de la mer, responsable de la migration de l'état saumâtre vers la côte. Au cours des sept derniers siècles, compte tenu de la physionomie insulaire ascendante d'aujourd'hui, les principaux changements dans le paysage ont impliqué la montée et la stabilisation du niveau relatif de la mer à sa position actuelle, la noyade du réseau des fleuves marécageuses dont les plaines sont dominées par la forêt d'eau douce, et la séparation complète de la frange terrestre de la domination continentale. Par conséquent, ce système insulaire est à court terme avec une tendance génétique et évolutive à long terme. En ce qui concerne le mécanisme structurant de la paléogéographie, l'activité tectonique et le changement du niveau de la mer ont été prépondérants jusqu'à ~1,5 ans cal AP, tandis que l'hydrodynamique a été davantage impliquée dans l'évolution tardive. Actuellement, le rôle de ce dernier mécanisme s'exprime dans la morpho-dynamique par le régime de marées, qui cause l'inondation de ~40% de la portion insulaire. Adressée à la région à fort potentiel dans le domaine de la Géographie Physique, les évidences morphologiques, tectoniques, paléoécologiques, sédimentaires et biogéochimiques rassemblées dans cette étude apportent des données qui aident à la reconstruction de l'encadrement paléogéographique de l'interface terre-mer dans la côte nord-est de l'État du Pará par l'Holocène, y compris de nouveaux signes de niveau de la haute mer sur la côte nord brésilienne. En même temps, les résultats fournissent des avancées significatives pour mieux comprendre l'évolution de l'Amazonie face à un cadre marqué par le manque de recherches géomorphologiques.

Mots-clés: Amazonie. Complexe insulaire. Hydrodynamique. Palynologie. Néotectonique. Niveau relatif de la mer.

LISTA DE FIGURAS

APRESENTAÇÃO

CAPÍTULO 1. EFEITOS MARINHO E FLUVIAL NA DINÂMICA DOS AMBIENTES INUNDÁVEIS DO ESTUÁRIO SUPERIOR DO RIO PARÁ, NORTE DO BRASIL

CHAPTER 2. SPATIAL AND TEMPORAL PATTERNS OF COASTAL DRAINAGE REARRANGEMENT BY LARGE TROPICAL RIVERS IN A PASSIVE MARGIN SETTING

LISTA DE TABELAS

CHAPTER 2. SPATIAL AND TEMPORAL PATTERNS OF COASTAL DRAINAGE REARRANGEMENT BY LARGE TROPICAL RIVERS IN A PASSIVE MARGIN SETTING

CHAPTER 3. PALEOECOLOGICAL INDICATORS OF THE HIGHSTAND SEA LEVEL ON THE AMAZONIAN SUPRALITTORAL UNTIL THE LAST TWO MILLENNIA

CHAPTER 4. FROM BRACKISH TO FRESHWATER ENVIRONMENT: IMPACTS OF THE HOLOCENE RELATIVE SEA LEVEL CHANGE ON THE TOCANTINS MOUTH LANDSCAPE TRANSITION, NORTH BRAZILIAN COASTAL AREA

SUMÁRIO

CHAPTER 2: SPATIAL AND TEMPORAL PATTERNS OF COASTAL DRAINAGE REARRANGEMENT BY LARGE TROPICAL RIVERS IN A PASSIVE MARGIN SETTING

APRESENTAÇÃO

1. Enunciado do problema

O Rio Tocantins possui extensão mesocontinental. Estende-se do Planalto Central até o estuário do Rio Pará, na Costa Norte do Brasil, após transcorrer cerca de 1960 km (MMA, 2006). Na faixa latitudinal que atravessa, verifica-se significativa variabilidade de climas, biomas, sistemas de relevo e arcabouço geológico, cuja interação resulta em um complexo mosaico geomórfico. Alguns fatos desse mosaico geomórfico têm sua dinâmica marcada pela assinatura de mecanismos auto-organizados e atuais (a exemplo das marés e do trabalho fluvial), ao passo que alguns outros fatos se vinculam a mecanismos episódicos (neotectonismo, variação climática e mudança do nível do mar), cuja manifestação se deu em tempo, escala espacial e condição ambiental subatuais. Um possível exemplo de fato geomórfico que expressa dinâmica no tempo recente e tendência genética em tempo profundo está na foz do Rio Tocantins, onde um sistema de ilha supralitorânea (SIS) foi estabelecido (Fig. 1b).

Ilhas normalmente são definidas como extensões de terra, de tamanho subcontinental, cercadas por água ou cursos d'água, e que persistem por tempo suficiente para fixar a vegetação (OSTERKAMP, 1998). Essas porções emersas estão presentes em quase todos os grandes rios tropicais da Terra, como por exemplo, Anavilhanas, no Amazonas (LATRUBESSE & STEVAUX, 2015), Ilha Grande, no Paraná (SOUZA-FILHO, 1993), Mbandaka no Congo (RUNGE, 2008) e Majuli, em Brahmaputra (SARMA & PHUKAN 2004). Na Zona Costeira do Pará (ZCP), entre a foz dos rios Amazonas, Pará e Tocantins (Fig. 1a–c), as ilhas assumem destaque na paisagem e fazem parte de um sistema geologicamente recente, informalmente, incluídas na série das Formações aluviais (Barbosa et al., 1974).

O SIS é, provavelmente, o maior conjunto de terras emersas do nordeste do Estado do Pará e sua individualização resulta da conexão, em sentido horário, entre os rios Maiauatá, Tocantins, Pará e Maratauíra (Fig. 1a). Esses rios compõem dois pares de orientação ligeiramente simétrica entre si: Tocantins e Maratauíra compõem o primeiro par, com orientação SW-NE, ao passo que, Pará e Maiauatá correspondem ao segundo, orientados em WSW-ENE. A composição desses pares fluviais confere ao trecho insular o recorte planimétrico similar ao paralelogramo. Internamente, a configuração de drenagem é marcada por canais afogados e apadronizados (Fig.1b).

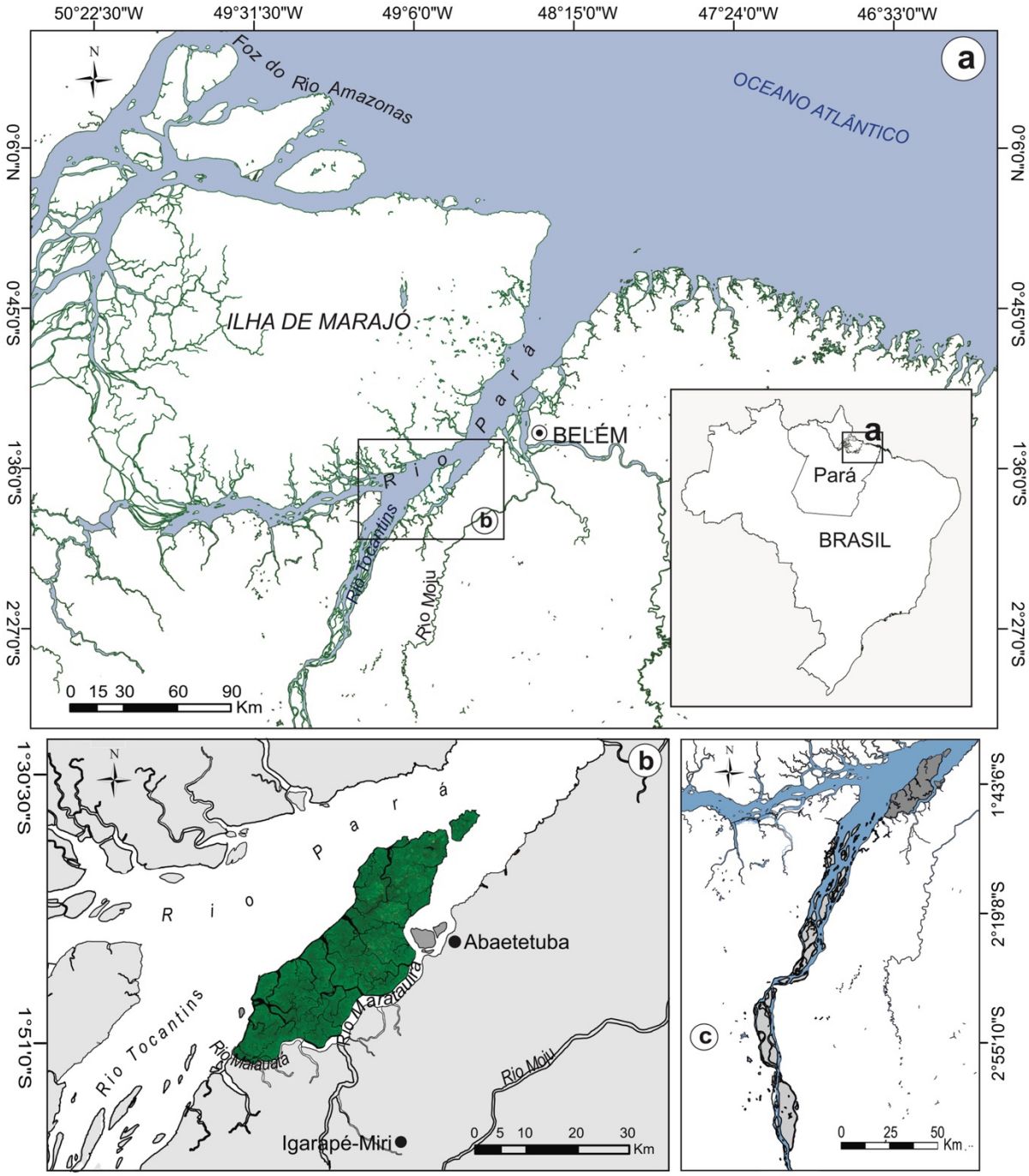

Figura 1. Zona Costeira do Pará (ZCP) constituída de grandes sistemas de ilhas distribuídas entre os rios Amazonas, Pará e Tocantins (a). Note o baixo curso do Tocantins, tamponado por ilhas (c). Na parte inferior esquerda da figura, destaca-se o sistema de ilha supralitorâneo (SIS), na foz dos rios Tocantins e Maratauíra (b).

O SIS pode ser referido como uma zona de interflúvio entre o Maratauíra e Baixo Tocantins. Por outro lado, sua imposição no estuário do Rio Pará confere ao SIS a fisionomia de barreira em relação ao segmento médio desse rio (Fig. 1b). Especula-se se essas ilhas poderiam ser produto de sedimentação fluvial, compreendida por barras arenosas subaquáticas que evoluíram para ilhas supralitorâneas. Questiona-se, ainda, se teriam elas relação com um antigo aparelho deltaico (cf. AB'SÁBER, 2004; 2006), construído nas intermediações dos rios Pará e Tocantins durante o

Último Máximo Glacial (UMG). Em perspectiva geométrica, a localização do SIS na margem leste do Tocantins sugere, por vezes, paleocontinuidade marginal. Teriam essas ilhas sido parte do domínio continental, posteriormente destacado e posto à deriva na foz do Rio Tocantins? Tais questões expõem o espectro de hipóteses que se incorporam à investigação sobre a origem e o significado do SIS no contexto de evolução paleogeográfica.

Ao mesmo tempo em que o SIS tem contrapartes no ambiente fluvial, sua localização estuarina faz desse trato insular parte da ZCP, subordinando-o diretamente à influência marinha, e atribuindo-lhe, consequentemente, o caráter transicional. Logo, o SIS comunica uma gradação de processos marinhos e fluviais que convergem nesse setor, controlando componentes sensíveis da paisagem atual, imprimindo suas assinaturas, enquanto geram produtos geomórficos particulares. Se no tempo presente o SIS mostra ter uma dinâmica diretamente atrelada a processos fluviomarinhos, é crucial questionar se a longo prazo esses mesmos processos também estiveram presentes, em coparticipação, na evolução da paisagem. Portanto, o caráter transicional e o longo prazo sugerem que investigar a origem do SIS consiste na apreciação conjunta de influências marinha e fluvial e de trânsito multiescalar, respectivamente.

O trânsito multiescalar é crucial na investigação morfogenética, pois possibilita englobar eventos episódicos de longo prazo (i.e. antes do Quaternário Superior), os quais respondem pela estruturação da paisagem regional. Esses eventos não constituem a centralidade da pesquisa, mas assumem relevância e se articulam a ela na medida em que são tidos por essenciais ao raciocínio geomorfológico que se busca construir para desvendar a origem insular.

1.1 Forçantes ambientais no trânsito multiescalar na Amazônia

A estruturação da paisagem cenozoica amazônica, *lato sensu*, atende a três forçantes episódicas principais, quais sejam: neotectônica, mudança climática e a variação do nível do mar. O papel dessas forçantes tem sido reconhecido na geologia, geomorfologia e na fitoecologia, de tal modo que sua magnitude e frequência resultaram na elaboração de diferentes produtos geomórficos de efetiva expressão geográfica. Aqui, a aplicação do termo ‘episódico’ não visa emprestar a essas forçantes o sentido de manifestação intercalada e/ou etapista, visto que podem ter sua atuação compartilhada no tempo e espaço. Ao contrário disso, o termo referencia a manifestação como inconstante, não organizada e com pulsos de ressurgência separada por intervalos de quiescência de milhares (variação climática e de mudança do nível do mar) a milhão de anos (manifestação tectônica).

Até a década de 1980 a hipótese climática e, consequentemente, as mudanças do nível do mar prevaleciam como fatores capazes de explicar mais fortemente a configuração da

geomorfologia da Amazônia (cf. BARBOSA et al., 1974). Mais tarde surgiram estudos enfatizando a influência da neotectônica na configuração da paisagem neogênica em termos de evolução do relevo (FRANZINELLI & IGREJA, 1990; COSTA & HASSUI, 1991; BORGES et al., 1995), do arranjo nos padrões do empilhamento sedimentar (FRANZINELLI e PIUCI 1988; FERNANDES et al., 1995; COSTA et al., 1996) e da composição e direcionamento da rede de drenagem (CUNHA, 1991; BEMERGUY & COSTA, 1991; BEMERGUY et al., 1995; BEMERGUY, 1997; COSTA et al., 2001). Pesquisas desenvolvidas na Ilha de Marajó (ROSSETTI & GÓES, 2007; ROSSETTI et al., 2008, SOUZA et al., 2014) e no nordeste paraense (BANDEIRA, 2007; PALHETA, 2008; SOARES JÚNIOR et al., 2011; CORRÊA, 2015) sustentaram a neotectônica do Quaternário Superior como responsável pela reativação de falhas pré-existentes e pela geração de novas falhas que afetaram a Formação Barreiras, os sedimentos Pós-Barreiras, a geometria de aquíferos subterrâneos, a posição da linha de costa e a organização de cursos flúvio-estuarinos. De acordo com COSTA *et al*. (1996; 2001), a neotectônica responde pelo traçado da drenagem do Tocantins, o qual teria sido estabelecido na transição do Pleistoceno Superior-Holoceno (COSTA et al., 1996; ROSSETTI & VALERIANO, 2007; SOARES JÚNIOR et al., 2011). Se a foz contemporânea do Tocantins deriva de ajuste fluvial, investigar esse evento talvez seja um dos fundamentos para se desvendar a trajetória de formação do SIS.

Concernente à mudança do clima, essa forçante foi reclamada para explicar a denudação e o reafeiçoamento do relevo (AB'SÁBER, 1966; BARBOSA et al., 1974), a diversidade na composição fitoecológica (BROWN JR. & AB'SÁBER, 1979) e a especiação biológica (HAFFER, 1969; AB'SÁBER, 1979) em domínio continental. Embora na região o modelado seja de superfícies rebaixadas, geralmente interrompidas por serras com topos semiconcordantes, comumente interpretado como produto de desagregação sob clima mais árido em condição de quiescência tectônica, os vestígios que mais satisfatoriamente proveem a compreensão da forçante climática foram fornecidos pela vegetação. Nesse contexto, cabe destaque às clássicas pesquisas de Hooghiemstra & van der Hammen (2000) e van der Hammen & Absy (1994), as quais, mediante emprego de métodos bioestratigráfico e palinológico, defenderam mudanças fitoecológicas representadas pela dinâmica entre floresta úmida e savana/campo. A substituição de comunidades herbáceas por gêneros arbóreos tem sido correlacionada a pulsos climáticos, com transição de período seco para úmido, respectivamente. Sob outro enfoque, as oscilações climáticas representam o gatilho às mudanças do nível do mar, com efetivo impacto na geomorfologia costeira.

As variações do nível marinho foram indicadas pelo conteúdo fossilífero da Formação Pirabas (PETRI, 1957; FERREIRA, 1977), bem como através de fácies e assinaturas de icnofósseis

relacionadas à configuração ambiental estuarina na Formação Barreiras (ARAI et al., 1988; ROSSETTI et al., 1990; GÓES et al., 1990). Não obstante a cronocorrelação desses depósitos miocênicos às oscilações globais (e.g., HAQ et al., 1987), que melhoraram a visão sobre paleocurvas marinhas no litoral, as curvas do nível do mar do Pleistoceno Superior ao Holoceno são as mais bem conhecidas e provavelmente cruciais por uma dupla característica: aos impactos que atribuem à configuração do litoral dos dias atuais; e aos indicadores que permanecem chave na paisagem, subsidiando, assim, as reconstituições paleoambientais.

Globalmente, a queda do nível do mar durante o UMG levou à progradação costeira, escavou vales profundos e formou depósitos deltaicos. Em contraste, a transgressão seguinte retrogradou paleolinhas de costa, com desenvolvimento de estuários mediante o afogamento das antigas feições escavadas (DALRYMPLE & CHOI, 2007; CLEMENT et al., 2017; KELLETAT, 2019; GHANDOUR et al., 2021; YEN et al., 2021). Na Amazônia, o emprego de *multi-proxy* (sedimentologia, estratigrafia, palinologia, isótopos estáveis e datação C-14) tem mostrado que a transgressão promoveu a expansão de ecossistemas litorâneos (BEHLING et al., 2001; COHEN et al., 2005; VEDEL et al., 2006; COHEN et al., 2012; GUIMARÃES et al., 2012), a evolução dos sistemas deposicionais (MASLIN et al., 2006; ROSSETTI et al., 2013; BEZERRA et al., 2015;) e a formação de vales afogados (BARBOSA et al., 1974; AB'SÁBER, 2000). Considerando esse impacto litorâneo, questiona-se: a referida elevação do nível do mar foi de magnitude suficiente para afetar o setor supralitorâneo, isto é, aquelas zonas posicionadas > 50 km da linha de costa, tal como as da foz do Tocantins?

Ao lado das três forçantes de impacto regional (morfogênese), é relevante considerar o ambiente moderno que envolve o SIS, qual seja, o estuário. Em estuários, os processos hidrodinâmicos contínuos e cíclicos representados por marés, corrente de marés e descarga fluvial reagem uns sobre os outros gerando uma variedade de depósitos e estruturas sedimentares, migração lateral de canais, transporte direto de sedimentos terra-mar (DALRYMPLE & CHOI, 2007) e, talvez, a própria formação de ilhas (cf. RIBEIRO & VALADÃO, 2020). Diante do exposto até aqui, o SIS, ao integrar a fisiografia estuarina, poderia conter traços evolutivos atrelados à influência de marés?

Considerando essa possibilidade, a hidrodinâmica seria compatível à nova forçante, porém sua natureza é oposta às forçantes anteriores, uma vez que opera em escala local (estuário) mediante processos cíclicos e auto-organizados transcorridos em curto intervalo de tempo (dia/hora). Assim, entender a magnitude e a frequência com a qual a hidrodinâmica afeta a porção insular consiste em percurso metodológico estratégico capaz de auxiliar na correta interpretação

de seus produtos, bem como poderá impedir que mudanças engendradas na paisagem pela morfodinâmica sejam erroneamente atribuídas às forças morfogenéticas.

Face ao breve antecedente histórico-geomorfológico, ao focar a evolução paleogeográfica das ilhas na foz do Rio Tocantins, Norte do Brasil, através do Holoceno, este estudo considera forçantes de ordem escalar local e regional. Ressalta-se, ademais, que o efeito da hidrodinâmica nesse setor é pouco compreendido, e não há evidências na literatura acerca de impactos da variação do clima, mudanças do nível do mar e da neotectônica sobre sua geomorfologia, paleoecologia, constituição dos sistemas deposicionais e vegetação, cabendo a este trabalho o objetivo de investigá-los mediante a integração de dados oceanográficos, morfo-topográfico e estrutural, fácies sedimentares, palinologia, isótopos estáveis ($\delta^{13}C$ & $\delta^{15}N$), datação C-14 e análise elementar da matéria orgânica sedimentar (C/N).

1.2 Premissas da Pesquisa

O raciocínio geomorfológico norteador da pesquisa baseia-se nas seguintes premissas:

I. O ajuste fluvial do Rio Tocantins representa o estágio central da paleogeografia do nordeste costeiro do Estado do Pará;

II. A evolução da paisagem comunica uma gradação de processos articulados às influências marinha e fluvial, de tal modo que investigar essa evolução depende de sua apreciação conjunta;

III. A morfogênese do SIS tem contrapartes em três forçantes regionais de natureza episódica e de longo prazo [1. Neotectônica; 2. Mudança climática; 3. Variação do nível do mar] e, sua morfodinâmica, relaciona-se à quarta forçante [4. Hidrodinâmica], cuja atuação é local, e seu caráter é cíclico, auto-organizado e de curto prazo;

IV. O papel dessa coleção de forçantes pode ser desvendado pelas assinaturas preservadas no ambiente;

V. Os processos mais relevantes que controlam a paisagem contemporânea podem ter atuado também no passado, o que resultaria em produtos semelhantes, mas cronologicamente distintos;

VI. O SIS é fato geomórfico com raízes morfogenéticas ancoradas no contexto espaço-temporal profundo.

1.3 Hipóteses

Considerando o estado da arte, são apresentadas as seguintes hipóteses:

a) O SIS presente na foz do Tocantins pode ter sido parte do continente;

b) O desmembramento do SIS pode ter ocorrido entre o Pleistoceno terminal e o Holoceno inicial;

c) Causas tectônicas podem ter controlado os ajustes na paisagem;

d) A queda do nível do mar do período glacial pode ter levado à incisão de vales, entre eles, o Maratauíra;

e) A subida do nível do mar pós-glacial gerou ambientes salobros no interior do continente, com predomínio do ecossistema de manguezal;

f) A hidrodinâmica estuarina teve participação na oferta e disponibilidade de sedimentos terrígenos e marinhos aos sistemas deposicionais.

1.4 Objetivo Geral

O escopo deste trabalho é o de contribuir para a elucidação de mecanismos associados à estruturação e evolução da paisagem da foz do Rio Tocantins, Estado do Pará, durante o Holoceno.

1.4.1 Objetivos Específicos

- Identificar as forçantes responsáveis pela gênese do sistema de ilhas;
- Determinar a cronologia dos eventos e associá-los às possíveis mudanças do clima e nível do mar manifestas durante o Holoceno;
- Identificar e caracterizar os paleoambientes;
- Caracterizar a influência das marés e do influxo fluvial nos ambientes inundáveis;
- Determinar a origem da matéria orgânica dos depósitos sedimentares.

1.5 Escopo e percurso metodológico da Tese

Face à colocação do problema, premissas da investigação, hipóteses e objetivos, o desenho metodológico consiste na integração de métodos e técnicas para aquisição e processamento de dados de campo, sensores remotos e analíticos de laboratório. Os resultados provenientes deste estudo são apresentados em quatro artigos que correspondem, respectivamente, aos capítulos 1, 2, 3 e 4. O capítulo 5 reúne os resultados desses artigos sob a égide de uma discussão em que se retoma, inclusive, as intenções da pesquisa (Fig. 2).

A estruturação deste volume atende diretamente ao encadeamento da investigação, a qual se baseia no levantamento de processos atuais (Artigo 1), na intenção de expandir as possibilidades para desvendar o passado paleogeográfico (Artigo 2), detectar forçantes externas (Artigo 3) e reconstituir a trajetória ambiental até os dias atuais (Artigo 4). Após o título, os objetivos, procedimentos e principais achados dos artigos são sintetizados a seguir.

Capítulo 1 – Efeitos marinho e fluvial na dinâmica dos ambientes inundáveis do Estuário Superior do Rio Pará, Norte do Brasil. Nesse manuscrito buscou-se compreender como a hidrodinâmica estuarina interage com os ambientes emersos e dinamiza a paisagem da foz do Rio

Tocantins. O percurso metodológico consistiu em três etapas: 1) campanhas de campo Jan-2019, Jun-2019 e Jan-2020; 2) aquisição de dados de marégrafos e de vazão fluvial; e 3) interpretação de produtos cartográficos e imagens de radar. Os resultados forneceram a visão geral do sistema estuarino, ao mesmo tempo em que permitiram caracterizar a topografia insular. Consequentemente, foi possível compreender melhor como a magnitude, a frequência das marés e o aporte fluvial têm subordinado essas ilhas à inundação, o que acaba por condicionar o quadro ecológico e a composição morfológica e sedimentar.

Capítulo 2 – Spatial and temporal patterns of coastal drainage rearrangement by large tropical rivers in a passive margin setting. Com enfoque paleogeográfico, esse manuscrito investiga e caracteriza as principais forçantes que respondem pela morfogênese e evolução da paisagem da foz do Rio Tocantins desde o Pleistoceno Superior. O percurso metodológico consistiu em: 1) interpretação de produtos de sensor remoto, dados vetoriais e morfoestruturais; 2) trabalhos de campo em Jan-2019, Jun-2019 e Jan-2020; e 3) analítico de cronologia. Os resultados indicam que a gênese do SIS tem contrapartes no rearranjo da drenagem do Rio Tocantins, após abrir seu curso para o leste. São reconhecidas influências tectônicas e de variações do nível do mar na evolução da paisagem até o Holoceno tardio.

Capítulo 3 – Paleoecological indicators of the highstand sea level on the Amazonian supralittoral until the last two millennia. Nesse manuscrito objetivou-se detectar sinais da incursão marinha na área de estudo. O percurso metodológico consistiu em: 1) trabalho de campo em Jan/2019; 2) processamento palinológico; e 3) análises isotópicas (^{13}C, ^{15}N e C/N) e de dados cronológicos. Os resultados permitem propor que o nível do mar atingiu nível mais alto que o atual, o que resultou no desenvolvimento de um paleo-manguezal antes do Holoceno Médio.

Capítulo 4 – From brackish to freshwater environment: impacts of the Holocene relative sea level change on the Tocantins mouth landscape transition, North Brazilian coastal area. Endereçado à reconstituição paleoambiental da foz do Tocantins e Maratauíra, esse manuscrito resultou do seguinte encaminhamento metodológico: 1) trabalho de campo Jan/2019 e Jan-2022; 2) processamento palinológico; e 3) análises isotópicas (^{13}C, ^{15}N e C/N) e de dados cronológicos. Os resultados expressam a súbita mudança na paisagem transcorrida durante o Holoceno tardio, relacionada às mudanças do nível relativo do mar. A trajetória ambiental do Holoceno médio aos dias atuais é recuperada a partir de inter-evidências ecológicas, geomorfológicas e sedimentares.

Capítulo 5 – Da compartimentação do objeto à construção de uma Tese. Nesse capítulo faz-se a retomada de premissas e objetivos que nortearam a investigação, relacionando-os aos

resultados obtidos. As ideias apresentadas versam sobre a natureza da pesquisa, mediante a busca por se correlacionar os resultados alcançados, o significado que porventura têm esses resultados para a produção do conhecimento no âmbito da Geografia Física e Geomorfologia e áreas afins, além de relacionar questões que ainda permanecem abertas e fatos que demandam estudos mais sistemáticos concernentes à paleogeografia da Amazônia.

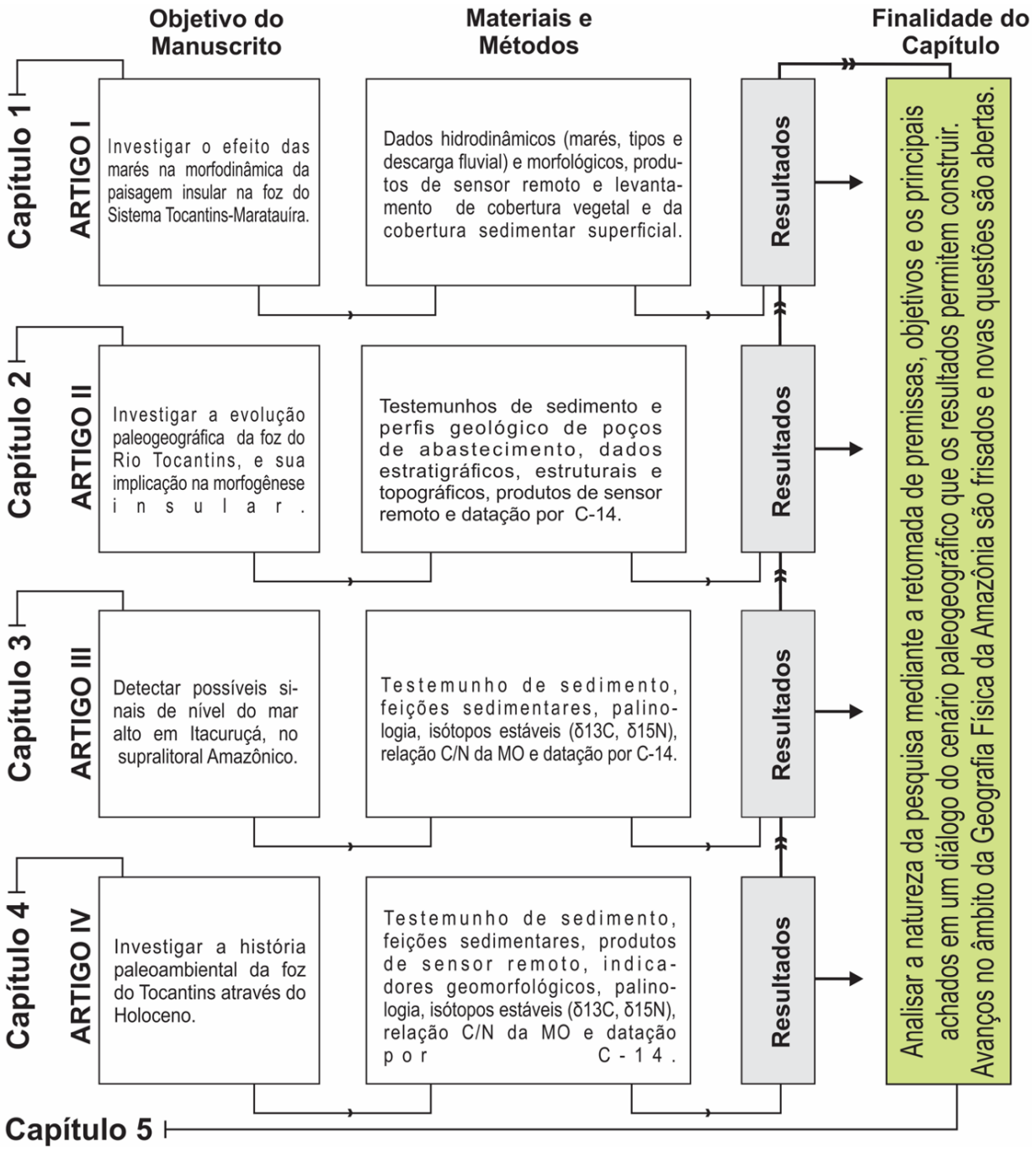

Figura 2. Estrutura e organização da pesquisa, segundo capítulos - artigos. O fluxograma não contempla a Apresentação e seus componentes.

Referências

AB'SÁBER, A. N. Superfícies aplainadas e terraços na Amazônia. Geomorfologia, São Paulo,n. 4, p. 1–10, 1966.

AB'SÁBER, A. N. Fundamentos da Geomorfologia Costeira do Brasil Atlântico Inter e Subtropical. Revista Brasileira de Geomorfologia, v. 1, n. 1, p. 27–43, 2000.

AB'SÁBER, A. N. A história complexa dos deltas. Scientific American Brasil, São Paulo, v.3,n. 29, p. 114, 2004.

AB'SÁBER, A. N. Brasil: paisagens de exceção: o Litoral e o Pantanal Mato-Grossense – patrimônios básicos. Cotia, SP: Ateliê Editorial, 2006. 182p

ARAI, M.; UESUGUI, N.; ROSSETTI, D. F.; GÓES, A. M. Considerações sobre a idade do grupo Barreiras no nordeste do estado do Pará. 35. In: Cong. Bras. Geol., Belém, p. 3–31, 1988.

BANDEIRA, I. C. N. Neotectônica e estruturação dos sistemas hidrogeológicos da região de Castanhal, PA. Dissertação (Mestrado em Geologia). Programa de Pós-Graduação em Geologiae Geoquímica, Universidade Federal do Pará, Belém, PA. 144 p. 2008.

BARBOSA, G. V.; RENNÓ, C. V.; FRANCO, E. M. S. Geomorfologia da Folha SA-22 Belém.In: DNPM (Ed.). Folha SA.22 Belém: geologia, geomorfologia, solos, vegetação, uso potencialda terra, Rio de Janeiro. 1974, p. 70–130.

BEMERGUY, R. Morfotectônica e Evolução Paleogeográfica da Região da Calha do Rio Amazonas. Tese (Doutorado em Geologia). Programa de Pós-Graduação em Geologia e Geoquímica, Universidade Federal do Pará, Belém, PA. 200 p. 1997.

BEMERGUY, R.L.; COSTA, J.B.S. Considerações sobre o sistema de drenagem da Amazôniae sua relação com o arcabouço tectono-estrutural. Boletim do Museu Paraense Emílio Goeldi. (Série Ciências da Terra), v. 3, 75–97, 1991.

BEMERGUY, R. L.; COSTA, J. B. S.; HASUI, Y.; BORGES M. S. Tectônica e paleogeografiada calha do Rio Amazonas. In: Simpósio Nacional de Estudos Tectônicos, 5. Rio Grande do Sul, p. 419–420, 1988.

BEZERRA, I. S. A. A.; NOGUEIRA, A. C. R.; GUIMARÃES, J. T. F.; TRUCKENBRODT, W. Late pleistocene sea-level changes recorded in tidal and fluvial deposits from Itaubal Formation, onshore portion of the Foz do Amazonas Basin, Brazil. Brazilian J. Geol. v. 45, p. 63–78, 2015.

BORGES, M. S.; COSTA, J. B. S.; BEMERGUY, R. L.; FERREIRA Jr., C. R. P.; HASUI, Y. A esculturação da paisagem do litoral norte do Brasil e sua relação com os movimentos neotectônicos do Quaternário. In: Simpósio Nacional de Estudos Tectônicos, 5. Rio Grande doSul, p. 423–424, 1988.

BROWN JR., K. S.; AB'SÁBER, A. N. Ice-age Forest Refuges and Evolutionm in the Neotropics: Correlation of Paleoclimatological, Geomorphological and Pedological Data with Modern Biological Endemism. Paleoclimas, São Paulo, n. 5, p. 1–30, 1979.

CLEMENT, A. M.; TACKETT, L. S. Facies stacking and distribution in the Gabbs Formation (Late Triassic, west-Central Nevada, U.S.A.): An environmental baseline to the end-Triassic carbonate crisis. Sedimentary Geology, v 425, p. 106021, 2017.

COHEN, M. C. L.; BEHLING, H.; LARA, R. J. Amazonian mangrove dynamics during the last millennium: The relative sea-level and the Little Ice Age. Rev. Palaeobot. Palynol., v. 136,p. 93–108, 2005.

COHEN, M. C. L.; PESSENDA, L. C. R.; BEHLING, H.; ROSSETTI, D. F.; FRANÇA, M. C.; GUIMARÃES, J.T.F.; FRIAES, Y.; SMITH, C.B. Holocene palaeoenvironmental history of the Amazonian mangrove belt. Quat. Sci. Rev., v. 55, p. 50–58, 2012.

CORRÊA, A. J. R. Aplicação de sísmica de alta resolução em ambiente estuarino amazônico, na investigação de estruturas neotectônicas. Dissertação (Mestrado em Geofísica) - Programa de Pós-Graduação em Geofísica, Universidade Federal do Pará, Belém. 82 p. 2015.

COSTA, J. B. S.; BEMERGUY, R. L.; HASUI, Y.; BORGES, M. da S.; FERREIRA JR., C. R. P.; BEZERRA, P. É. L.; COSTA, M. L.; FERNANDES, J. M. G. Neotectônica da Região Amazônica: Aspectos Tectônicos, Geomorfológicos e Deposicionais. Geonomos, v. 4, p. 23– 43, 1996.

COSTA, J. B. S.; BEMERGUY, R-L.; HASUI, Y.; BORGES, M. S. B. Tectonics and paleogeography along the Amazon river. J. South Am. Earth Sci., v. 14, p. 335–347, 2001.

COSTA, J. B. S.; HASUI, Y. O quadro geral da evolução tectônica da Amazônia. In: Simpósio Nacional de Estudos Tectônicos, 3, Rio Claro, p. 142–145, 2001.

CUNHA, F. M. B. Morfologia e neotectonismo do Rio Amazonas. In: Simpósio de Geologia da Amazônia, 3, Belém, p. 193-210, 1991.

DALRYMPLE, R. W. Tidal depositional systems. In: James, N. P., Dalrymple, R. W., (Eds). Facies Models 4. Geological Association of Canada, St. John′s, p. 201–232, 2010.

DALRYMPLE, R.W.; CHOI, K. Morphologic and facies trends through the fluvial-marine transition in tide-dominated depositional systems: A schematic framework for environmental and sequence-stratigraphic interpretation. Earth-Science Rev., v. 81, p. 135– 174, 2007.

FERREIRA, C. S. Fácies da Formação Pirabas (Mioceno Inferior): novos conceitos e ampliações. Anais da Academia Brasileira de Ciências, 49, p. 353, 1977.

FRANZINELLI, E.; PIUCI, J. Evidências de neotectonismo na Bacia Amazônica. In: Congresso Latino-Americano de Geologia, 7, Belém, p. 80–90, 1988.

FRANZINELLI, E.; IGREJA, H.L.S. Utilização do sensoriamento remoto na investigação da área do baixo Rio Negro e Grande Manaus. In: Simpósio Nacional De Estudos Tectônicos, 6. Rio Grande do Sul, p. 641–648, 1990.

GHANDOUR, I. M.; AL-ZUBIERI, A. G.; BASAHAM, A. S.; MANNAA, A. A.; AL-DUBAI, T. A.; JONES, B. G. Mid-Late Holocene Paleoenvironmental and Sea Level Reconstruction onthe Al Lith Red Sea Coast, Saudi Arabia. Frontiers in Marine Science, v. 8, p. 1–20, 2021.

GÓES, A. M.; ROSSETTI, D. F.; NOGUEIRA, A. C. R.; TOLEDO, P. M. Modelo Deposicional preliminar da Formação Pirabas no Nordeste do Estado do Pará. Bol. do Mus. Para. Emílio Goeldi, Ciências da Terra, v. 2, p. 3–15, 1990.

GUIMARÃES, J. T. F.; COHEN, M. C. L.; PESSENDA, L. C. R.; FRANÇA, M. C.; SMITH, C. B.; NOGUEIRA, A. C. R. Mid- and late-Holocene sedimentary process and palaeovegetation changes near the mouth of the Amazon River. Holocene, v. 22, p. 359–370, 2012.

HAFFER, J. Speciation in Amazoni Forest Bir Most species probably originated forest refuges during dry climatic periods. Science, v. 165, p. 131–137, 1969.

KELLETAT, D.H. Holocene Coastal Geomorphology. In: Finkl C.W., Makowski C. (eds) Encyclopedia of Coastal Science. Encyclopedia of Earth Sciences Series. Springer, p. 977–980, 2019.

LATRUBESSE, E. M.; STEVAUX, J. C. The Anavilhanas and Mariuá Archipelagos: Fluvial Wonders from the Negro River, Amazon Basin. World Geomorphological Landscapes, p. 157–169, 2015.

MASLIN, M.; KNUTZ, P. C.; RAMSAY, T. Millennial-scale sea-level control on avulsion events on the Amazon Fan. Quaternary Science Review, v. 25, p. 3338–3345, 2006.

MMA. Ministério do Meio Ambiente. 2006. Caderno da região geográfica do Tocantins-Araguaia. Brasília.

OSTERKAMP, W. R. Processes of fluvial island formation, with examples from plum creek, Colorado and Snake River, Idaho. Wetlands, v. 18, p. 530–545, 1998.

PALHETA, E. S. M. Estudo da compartimentação e arcabouço neotectônico da Ilha de Mosqueiro, Pará, empregado na prospecção hídrica subterrânea. Tese (Doutorado em Geologia). Programa de Pós-Graduação em Geologia e Geoquímica, Universidade Federal do Pará, Belém, PA. 241 p. 2008.

PETRI, S. Foraminíferos miocênicos da Formação Pirabas. Boletim da Faculdade de Filosofia, Ciências e Letras da Universidade de São Paulo (Geologia), v. 16, p. 1–79, 1957.

RIBEIRO, S. R.; VALADÃO, R. C. Processos fluviomarinhos associados à formação da Ilha Rasa, Sul da Baía de Marapatá,Nordeste do Pará, Brasil. Arquivos de Ciências do Mar, v. 53, p. 110–119, 2020.

ROSSETTI, D. F.; GÓES, A. M.; TRUCKENBRODT, W. A influência marinha nos Sedimentos Barreiras. Bol. Mus. Para. Emilio Goeldi, Ser. Cienc. Terra, v. 2, p. 17–29, 1990.

ROSSETTI, D. F.; GÓES, A. M.; VALERIANO, M. M.; MIRANDA.; M. C. C. Quaternary tectonics in a passive margin: Marajó Island, Northern Brazil. Journal of Quaternary Science, v. 23, p. 121–35, 2008.

ROSSETTI, D. F.; VALERIANO, M. M. Evolution of the lowest amazon basin modeled from the integration of geological and SRTM topographic data. Catena, v. 70, p. 253–265, 2007.

RUNGE, J. The Congo River, Central Africa. Large Rivers. Geomorphol. Manag., p. 293–309, 2007.

SARMA, J. N.; PHUKAN, M.K. Origin and some geomorphological changes of Majuli Island of the Brahmaputra River in Assam, India. Geomorphology, v. 60, p. 1–19, 2004.

SOARES JÚNIOR, A. V.; HASUI, Y.; COSTA, J. B. S.; MACHADO, F. B. Evolução do rifteamento e paleogeografia da margem Atlântica Equatorial do Brasil: Triássico ao Holoceno. Geociencias, v. 30, p. 669–692, 2011.

SOUZA, L. S. B.; ROSSETTI, D. F.; ELIAS, V. R.; PRADO, R. L. Neotectonics in Marajó Island, State of Pará (Brazil) revealed by vertical electric sounding integrated with remote sensing and geological data. An. Acad. Bras. Cienc., v. 85, p. 73–86, 2013.

SOUZA-FILHO, E. E. Aspectos da geologia e estatigrafia dos depósitos sedimentares do Rio Paraná entre Porto Primavera (MS) e Guaira (PR). PhD Thesis, University of São Paulo, São Paulo. Tese (Doutorado em Geociências). Programa de Pós-Graduação em em Geologia Sedimentar, Universidade de São Paulo, São Paulo, SP. 214 p. 1993.

van der HAMMEN, T.; ABSY, M. L. Amazonia during the last glacial. Palaeogeogr. Palaeoclimatol. Palaeoecol., v. 109, p. 247–261, 1994.

van der HAMMEN, T, T., HOOGHIEMSTRA, H. Neogene and Quaternary history of vegetation, climate, and plant diversity in Amazonia. Quat. Sci. Rev. v. 19, p. 725–742, 2000.

VEDEL, V.; BEHLING, H.; COHEN, M.; LARA, R. Holocene mangrove dynamics and sea-level changes in northern Brazil, inferences from the Taperebal core in northeastern Pará State. Veg. Hist. Archaeobot., v. 15, p. 115–123, 2006.

YEN, H. P. H.; NHAN, T. T. T.; NGHI, T.; TOAN, N. Q.; KHIEN, H. A.; LAM, D. D.; van LONG, H.; THANH, D. X.; HUNG, N. T.; TRANG, N. T. H.; DIEN, T. N.; TUYEN, N. T.; TRUONG, T. X.; DUNG, T. T.; THAO, N. T. P.; LAN, V. Q. Late Pleistocene-Holocene sedimentary evolution in the coastal zone of the Red River Delta. Heliyon, v. 7, p. e05872, 2021.

CAPÍTULO 1:

EFEITOS MARINHO E FLUVIAL NA DINÂMICA DOS AMBIENTES INUNDÁVEIS DO ESTUÁRIO SUPERIOR DO RIO PARÁ, NORTE DO BRASIL[1]

[1]Artigo publicado na Revista Brasileira de Geomorfologia, v. 22, n. 4, p. 886–898, 2021.

Resumo – Nas regiões litorâneas, os ambientes inundáveis ocorrem no baixo curso dos rios e de seus afluentes, onde o ciclo diário de inundação comandado por marés resulta em condições hidrodinâmicas de considerável complexidade. Na costa norte do Brasil, na adjacência do Sistema Tocantins-Maratauíra (STM), estuário do Rio Pará, os ambientes inundáveis reúnem características físicas que incluem uma geografia insular de retaguarda continental, intensa descarga fluvial e um regime de marés com amplitude de até 6 m. A fim de compreender como os ambientes inundáveis desse estuário são afetados por marés, este trabalho se apoia em abordagem *multi-proxy* (hidrodinâmica, topografia, vegetação, morfologia e cobertura sedimentar superficial) para a delimitação do estuário do rio Pará em zonas e para a investigação dos ambientes inundáveis do STM, relacionando-os à zona estuarina correspondente. Baseado nos resultados alcançados, três ambientes inundáveis e um não inundável foram reconhecidos. Esses ambientes integram o Estuário Superior do Rio Pará e têm seu ciclo de inundação regido por mesomarés. Por outro lado, devido à alta descarga fluvial, a paisagem ecológica é constituída essencialmente por ecossistemas de água doce. Os resultados revelam que os ambientes mais suscetíveis à inundação se situam no intervalo entre 0 e 3 m e representam 39% do complexo insular. Paradoxalmente, a maior ocorrência destes ambientes inundáveis é no setor sul (40,6%), direcionado ao continente, realçando a natureza dinâmica e mais instável desse setor em relação ao setor norte (21,1%), direcionado ao mar. As evidências mostram ainda que a maré representa uma das principais forçantes indutoras da hidrodinâmica local, tornando os cursos integrados à rede de drenagem do STM compatíveis com a designação de rios de maré. Os resultados proveem melhor compreensão acerca da morfodinâmica da paisagem moderna e, ao mesmo tempo, expõem sua vulnerabilidade, tendo em vista sua ocupação humana.

Palavras-chave: Complexo insular; Fitoecologia; Tocantins-Maratauíra; Zonas estuarinas.

1. Introdução

O estuário é um sistema transicional aberto, caracterizado pela intensa troca de matéria e energia entre oceano e continente. Ele se estende da foz de um vale, onde o mar adentra o continente, até o limite terrestre em que a energia de maré é capaz de reverter a corrente fluvial. Essa reversão causa perceptíveis oscilações no nível da água a montante. Comumente, os estuários são divididos em três zonas definidas pela razão média da entrada de energia das marés *versus* energia fluvial: (i) estuário dominado por marés; (ii) estuário de energia mista (maré-fluvial); e (iii) estuário de domínio fluvial, mas com influência de maré (JAY; SMITH,

1990; HOITINK; JAY, 2016). Essa últimazona, também denominada estuário superior, além de tradicionalmente ser a menos estudada em relação às adjacentes, tende a compartilhar características dos rios de maré. Em um rio de maré, embora o fluxo seja influenciado por marés e a corrente assuma caráter bidirecional (COHEN; MCCARTHY, 1963; VRIEND, 2003; CARR et al., 2004), suas águas não apresentam salinidade detectável KJERFVE; MAGILL, 1989; COOK; SOMMERFIELD; WONG, 2007), pois a maré penetra muito além da influência salina, fenômeno típico no Rio Amazonas (WELLS, 1995).

No golfo norte do Brasil, paralelo ao Amazonas, um vasto conjunto de estuários se desenvolve acoplado à rede de drenagem do Rio Pará (Fig. 1a). Esse rio constitui o mais amplo vale escavado do litoral brasileiro (58,5 km),uma vez que não apresenta formações insulares em sua foz, a despeito do Amazonas. Tal configuração geomorfológica imprime no rio Pará, ao que tudo indica, características ambientais distintas daquelas vigentes no Amazonas ao estabelecer zonas estuarinas no interior do continente. Na calha do Rio Pará, o Sistema Tocantins- Maratauíra (STM) superpõe sua desembocadura e aporta mais de 60% (i. e. 10.900 m^3/s [ANA, 2019]) do volume total que esse rio descarrega no Atlântico. Ao mesmo tempo em que o STM transfere seu fluxo ao Rio Pará, durante a enchente, os efeitos marinhos avançam e se propagam na retaguarda do continente. A interação entre a descargafluvial e o regime de marés semidiurnas, essa última com amplitude de até 6 m (EL-ROBRINI et al., 2018), resulta em intenso hidrodinamismo que engendra processos e efeitos sobre os ambientes estuarinos de montante ainda pouco compreendidos.

Baseado nas interações físicas que afetam e controlam o segmento principal do estuário do Rio Pará, Corrêa (2005) reportou o domínio de correntes de marés. Gregório e Mendes (2009), por sua vez, notaram característica de estuário de energia mista ao trecho investigado por Corrêa (2005), a jusante do STM. Diante do exposto, é provávelque o Tocantins-Maratauíra apresente característica entre estuário de energia mista e estuário de domínio fluvial (Fig. 1b). Definir sua posição e identificar os mecanismos que o regem contribuirá sobremaneira para a compreensão de sua hidrodinâmica e, consequentemente, de seus ambientes inundáveis.

No contexto do litoral amazônico, os ambientes inundáveis (várzea) ocupam o baixo curso dos rios e de seustributários, e têm seu ciclo de inundação diário comandado pelo regime das marés (LIMA; TOURINHO; COSTA, 2001). No caso do STM os ambientes inundáveis correspondem a extensa planície recortada pela drenagem local, atribuindo-lhe uma geografia insular (Fig. 1c). Apesar da morfologia da área constar de tabuleiros, esses se restringem ao interior do continente e apresentam caimento topográfico suave para o oeste (Maratauíra e

Tocantins), constituindo uma rampa sedimentar de topografia inferior (i. e. planície) em sua porção mesoterminal(Fig. 1d). A planície tem elevação ≤ 5 m (FURTADO; PONTE, 2013).

Tendo em vista essa configuração geomorfológica, estima-se que a hidrodinâmica estuarina exerça o controle da porção insular (até 5 m), devido à amplitude das marés (até 6 m). Apesar do balanço altimetria *versus* amplitude de maré reforçar essa hipótese, é possível que nem todo o ambiente insular sujeito à hidrodinâmica local seja frequentemente afetado por marés, tendo em vista sua acomodação em trecho montante localizado a cerca de 180km da atual linha de costa. Consequentemente, as ilhas que integram o STM devem apresentar particularidades ambientais que decorrem de resposta espaço-temporal distinta ao ciclo de inundação, em que algumas áreas se ajustam ao efetivo controle das marés, enquanto outras apresentam maior estabilidade. Nesse caso, os aspectos morfológicos e fitoecológicos e a constituição sedimentar dos ambientes inundáveis passam a ser regulados pelo gradiente da influência estuarina. É relevante ainda mencionar que compreender como essa área é atingida pelas inundações auxilia sobremaneira no estabelecimento de estratégias voltadas para o planejamento e gestão de suasocupações e atividades humanas, haja vista a vulnerabilidade dos ambientes estuarinos à subida do nível relativo do mar (e.g., MACPHERSON; HAIGH; PATTIARATCHI, 2011).

A fim de identificar a hidrodinâmica estuarina, mediante reconhecimento da frequência com que as marés afetam os ambientes inundáveis no Sistema Tocantins-Maratauíra, este estudo emprega dados hidrodinâmicos, topográficos, morfológicos, ecológicos e da cobertura sedimentar superficial na proposição de compartimentação do estuário do Rio Pará, Norte do Brasil. A proposta aqui desenvolvida enfatiza o caráter intrínseco de cada zona estuarina e estabelece os critérios de sua delimitação.

2. Área de Estudo

A área de estudo, localizada no segmento montante do Rio Pará, foz do Tocantins e Maratauíra, compreende trecho continental e agrupamentos de ilhas. Dentre esses agrupamentos o principal é Urubuéua, pertencente aos municípios de Abaetetuba (82,7%) e Igarapé-Miri (18,3%). Face ao seu caráter multi-insular com mais de 100 ilhas contabilizadas, neste trabalho optou-se por reunir todas elas sob a designação de Complexo Insular do Oeste Abaetetubense (CIOA), o qual ocupa área de 410 km² (Fig. 1b). O CIOA integra o estuário do Rio Pará, cujas marés alcançam amplitudes de até 6 m durante a sizígia.

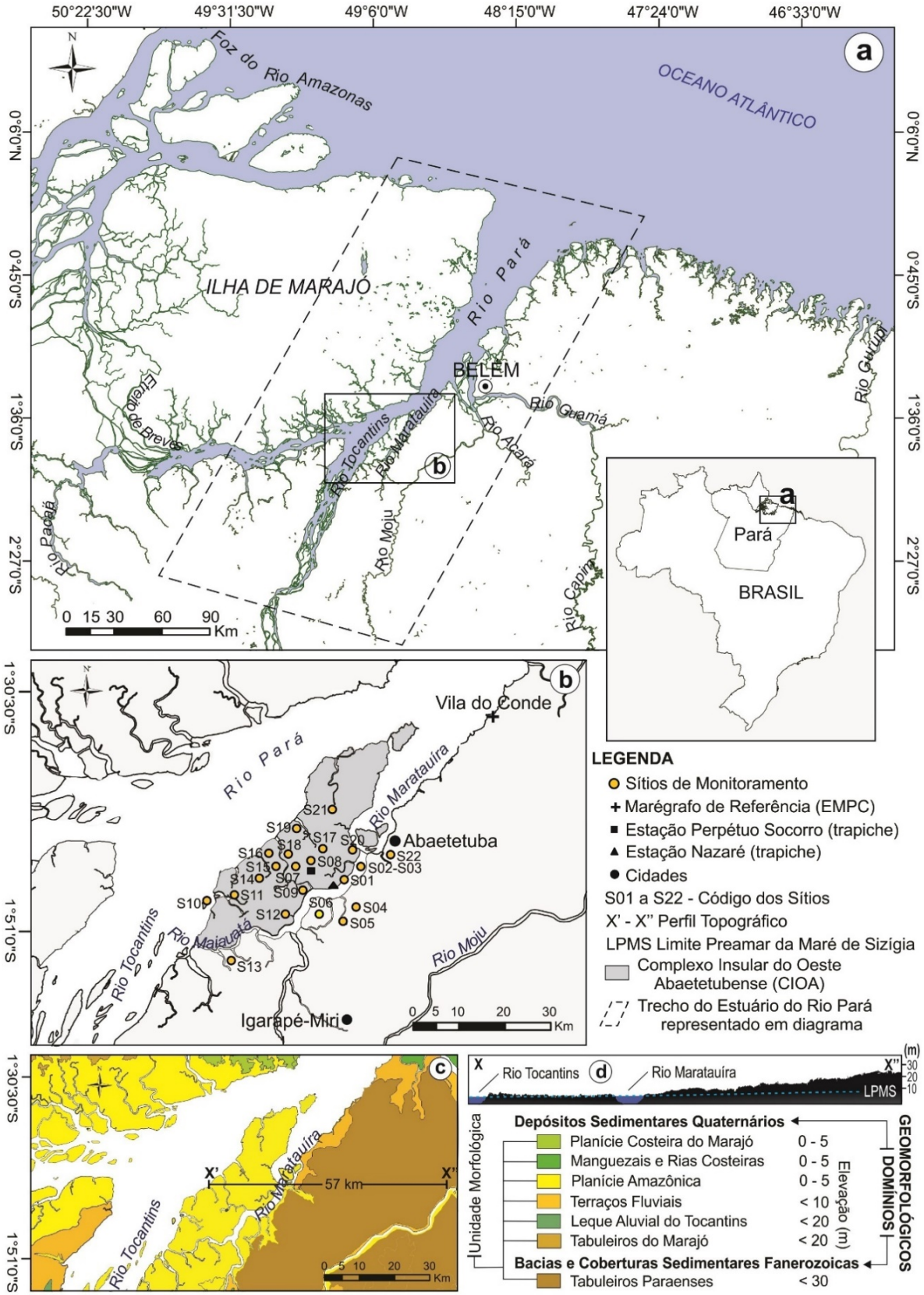

Figura 1. Litoral do Estado do Pará, Costa Norte do Brasil, com destaque para o Rio Pará e os principais corpos hídricos que compõem seu estuário (a). A área de estudo situada à foz do Sistema Tocantins-Maratauíra (b) foi realçada, incluindo sua caracterização morfológica (c) e topográfica (d).

O clima é tropical quente e úmido, tipo Am da classificação de Köppen, com valores médios anuais de temperatura em 27 °C, umidade relativa do ar em 85% e precipitação pluviométrica entre 2.300 e 2.800 mm (FAPESPA, 2016). Duas estações são reconhecidas na região, definidas por mudanças sazonais da Zona de Convergência Intertropical (ZCIT). Durante os meses de março e abril, a ZCIT migra da latitude 14º N para 2° S (SOUZA-FILHO et al., 2009), estaciona sobre a costa paraense, o que acarreta maior umidade e volume de chuva (estação chuvosa - dezembro a maio). A ZCIT faz o movimento inverso de agosto a setembro, o que reduz as chuvas e define a estação seca - junho a novembro (MORAES et al., 2005).

O relevo é modesto e plano em razão da estrutura geológica subjacente. A morfologia consta de tabuleiros paraenses (≤ 30 m), terraços (5 - 10 m) e planícies (≤ 5) (Fig. 1c). Os tabuleiros, de acordo com Dantas e Teixeira (2013), são embasados por rochas sedimentares pouco litificadas de idade neogênica. Essa superfície registra inclinação suave para oeste (Fig. 1d), estabelecendo contato com os terraços fluviais e esse último com as planícies. As planícies ocupam todo o CIOA e a franja do continente e são constituídas por sedimentos fluviais, marinhos e fluviomarinhos. Enquanto as planícies formam ambientes holocênicos, sujeitos à inundação, os terraços são cronocorrelatos ao Pleistoceno e estão acima do alcance da maré (FURTADO; PONTE, 2013) (Fig. 1c).

3. Materiais e Métodos

3.1 Trabalho de campo

3.1.1 Determinação altimétrica dos ambientes inundáveis e amplitudes de marés

Três campanhas de campo foram executadas (duas na estação chuvosa (jan/2018, jan. e mar/2020) e uma na estação seca (jun/2019)) para monitoramento de maré, coleta de dados altimétricos e de declividade, levantamento de cobertura vegetal e dos depósitos sedimentares superficiais. Devido à ausência de estações maregráficas locais, dois trapiches foram designados para definir o Nível de Redução (NR) geral, determinar as amplitudes de marés e a altimetria dos ambientes inundáveis. Para o monitoramento e mapeamento dos ambientes inundáveis, 22 sítios foram selecionados baseado em análise integrada de mapeamento (geologia, geomorfologia, vegetação e hidrografia) e da possibilidade de acesso em campo.

Do quantitativo de sítios selecionado para monitoramento (22), 18 se localizam no CIOA e 4 no domínio continental (Fig. 1b). A declividade nesses sítios foi determinada por clinômetro analógico de leitura direta, seguido da coleta de coordenadas geográficas através de aparelho GPS (*Global Positioning System*), sendo a altimetria obtida por meio do monitoramento de

marés. Para o monitoramento de marés, duas estações foram designadas: Trapiche Perpétuo Socorro e Trapiche Nazaré (Fig. 1b).

As estações Perpétuo Socorro e Nazaré cobrem os sítios do CIOA e do continente em um raio de 18 e 9 km, respectivamente. A escolha desses trapiches considerou a posição geográfica que ocupam e a existência de estacas fixadas em substrato não suscetíveis à exposição durante eventos de maré baixa. As estacas de mensuração desses trapiches foram calibradas tomando por referência o Marégrafo do Porto de Vila do Conde (MPC), localizado na Baía do Capim. O MPC dista 35,4 km de Nazaré e 36,1 km de P. Socorro (Fig. 2B). Dados da régua do MPC e posição do seu Nível de Redução (RN) são apresentados na Figura 2A.

A calibração das estações Perpétuo Socorro e Nazaré foi executada em 12-jan-2020, quando a projeção da baixa-mar no MPC foi de 0 cm em relação ao seu Nível de Redução (DHN, 2020). Então, assim que a maré atingiu a baixa-mar em Nazaré e em Perpétuo Socorro, o nível indicado pela água nas estacas foi demarcado e considerado o Nível de Baixa-mar Calibrada (NBC). Em face da distância desses locais em relação ao MPC, uma defasagem no horário da baixa-mar entre as estações foi registrada (Fig. 2A). Neste trabalho o NR de P. Socorro e Nazaré é igual a 0 cm (valor obtido no NBC de 12-jan-2020).

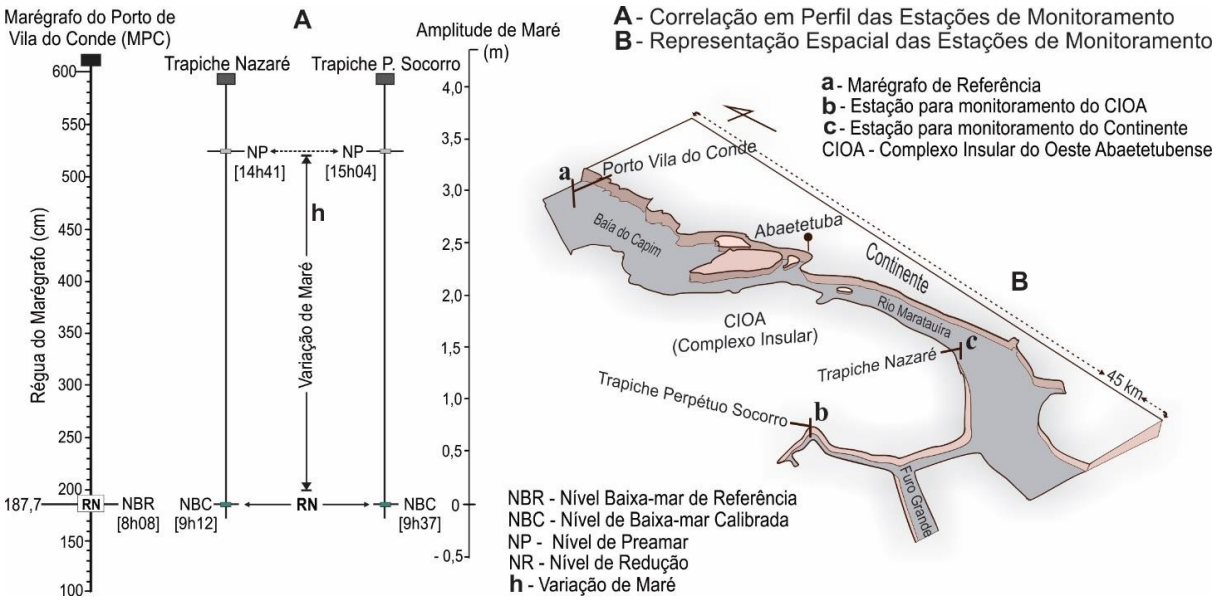

Figura 2. Esboço integrado das estações P. Socorro e Nazaré, as quais foram calibradas em relação ao Marégrafo do Porto de Vila do Conde (A), incluindo a situação geográfica das estações (B).

Definido o NR geral, bastões não graduados de madeira, alumínio ou policloreto de vinila (PVC) contendo o código do sítio correspondente foram afixados no substrato dos locais de monitoramento antes da enchente. Posteriormente, com a maré cheia, o Nível de Preamar (NP) indicado nos bastões foi demarcado, e de modo semelhante, esse NP foi registrado em Nazaré

e P. Socorro (Fig. 2A). Em seguida, o intervalo entre a superfície dossítios e o NP dos bastões foi mensurado em centímetros e os valores calculados com base na amplitude de maré (NR *versus* NP) fornecida por suas respectivas estações. Desse modo, a altimetria dos sítios foi aferida e nivelada em relação ao NR. O resultado obtido foi plotado em diagrama hidrotopográfico e introduzido em *software* de geoprocessamento para a condução do mapeamento dos ambientes inundáveis.

3.1.2 Levantamento da cobertura vegetal

Cinco levantamentos da cobertura vegetal foram realizados (4 no CIOA e 1 na franja continental). O método utilizado consistiu em transectos, sentido rio-ilhas e rio-continente. Os tipos botânicos interceptados e/ou adjacentes aos transectos reconhecidos por mateiro através do nome popular (vulgar) foram registrados, acrescidos de descrição fisionômica, forma de vida e ambiente físico-ecológico ocupado pelo espécime. Além de transectos, algumas trilhas foram exploradas e setores restritos acessados via navegação. Quanto ao nome popular das espécies levantadas em campo, em sua quase totalidade consta no registro oficial do Herbário do Museu Paraense Emílio Goeldi (MPEG) (<www.reflora.jbrj.gov.br/reflora>), o que facilitou a identificação, comparação e obtenção da nomenclatura científica. Além disso, foram acessadas obras de referência que tratam da floresta típica de ambientes inundáveis da costa paraense (e.g., LIMA; TOURINHO; COSTA, 2001) e de levantamentos da estrutura vegetal da várzea (e.g., ALMEIDA; AMARAL; SILVA, 2004) e estuário amazônico (e.g., QUEIROZ et al., 2007).

3.1.3 Sensoriamento Remoto e Geoprocessamento

Dois grupos de dados foram levantados e processados. O primeiro envolveu mapeamento prévio de geomorfologia, geologia, vegetação e hidrografia com uso de dados vetoriais do tipo *shapefile* (<www.ibge.gov.br/geociencias/downloads-geociencias>), e o segundo constou de mapeamento topográfico com imagens de radar do sensor ALOS PALSAR (<www.search.asf.alaska.edu>). O geodatabase foi tratado e processado através de ferramentas e recursos integrados à plataforma do *software* Arcgis 10.2®. O tratamento de imagens ALOS PALSAR envolveu correção e padronização de Datum e filtragem, seguido de extração de curvas de nível, construção do Modelo Digital de Elevação (MDE) e geração de perfil topográfico. O fator topográfico fornecido pelo MDE, elementar ao mapeamento dos ambientes, teve boa resposta para o continente. Para as ilhas e franja continental, com superfícies em nível de planície (≤ 5 m), o resultado incorporou distorções flagradas durante trabalhos de campo, de modo que os 22 sítios levantados foram plotados sobre a imagem para a

correção, classificação e delimitação manual dos ambientes inundáveis. Cotas topográficas < 8 m relacionadas ao CIOA e à franja continental adjacentes aos 22 sítios expressam maior confiabilidade, tendo em vista a aferição da altimetria desses sítios baseada no Nível de Redução (NR). Por outro lado, cotas > 10 m que ocorrem no continente, expressam valores cotados do MDE.

3.2 Caracterização de processos físicos estuarinos

Para a caracterização dos principais processos físicos de macroescala do Rio Pará (marés e descarga fluvial), foram levantados dados referentes a quatro estações maregráficas distribuídas ao longo desse rio: 1. Atracadouro de Breves, na "nascente"; 2. Porto de Vila do Conde, no curso médio; 3. Ilha de Mosqueiro, no curso baixo; e 4. Ilha dos Guarás, na desembocadura – Fig. 4, disponibilizados pela Diretoria Nacional de Hidrografia e Navegação (<www.dhn.mar.mil.br>). Somaram-se a elas as medições de campo efetivadas nas estações Perpétuo Socorro e Nazaré através de monitoramento durante marés de sizígia (12 a 15-jan e entre 9 e 23-mar de 2020) e de quadratura(5 a 8-jan-2020). A definição de tipos e amplitude de maré seguiu Davies (1964) e, para a classificação das águas em razão da concentração de salinidade, optou-se por Elliott e McLusky (2002), os quais adotam o Sistema de Venice. Os valores de salinidade reunidos foram compilados de estudos publicados e pesquisas aplicadas em diferentes setores do Rio Pará. Concernente à componente fluvial, essa foi baseada em séries históricas de vazão do Rio Tocantins, cuja aquisição, incluindo dados de precipitação, se deu através da Rede Hidrometeorológica (<www.snirh.gov.br/hidrotelemetria>), a plataforma de monitoramento digital da Agência Nacional de Água (ANA, 2019).

4. Resultados

4.1 Compartimentos do Estuário do Rio Pará

O estuário do Rio Pará pode ser definido, do ponto de vista processo-resposta, como dominado por marés (SCHUBEL; HAYES; PRITCHARD, 1974; DALRYMPLE; ZAITLIN; BOYD, 1992). A ausência de promontórios perpendiculares ao fluxo e de barra em pontal em sua desembocadura paralela à linha de costa são indicadores do controle por correntes de marés, as quais transportam e transferem sua carga sedimentar à corrente oceânica (DYER, 1979). Estuários que apresentam desembocaduras com essas características geomorfológicas comumente exibem seção transversal do leito mais estável, pois as fortes correntes de maré limitam o desenvolvimento de depósitos transversais no flanco submerso da foz (BRYCE; LARCOMBE; RIDD, 1998). Por outro lado, barras longitudinais orientadas na direção das

correntes de maré tendem a integrar o sistema sedimentar típico desses estuários (CORRÊA, 2005; FITZGERALD et al., 2000), a exemplo do Victoria River, no norte da Austrália (cf. HARRIS et al.,2002).

No estuário do Rio Pará, três compartimentos ou zonas foram definidas e descritas e a terminologia adotada seguiu Dionne (1963). Essas zonas são: I - Estuário Inferior ou de Marajó (EIP); II - Estuário Médio ou de Guajará (EMP); III - Estuário Superior ou de Marapatá (ESP) (Fig. 4). Cabe ressaltar que, embora essa proposta de compartimentação atenda a interesses geográficos desta pesquisa [classificar/delimitar estuários é uma tarefa complexa, haja vista a soma de processos que reagem uns sobre os outros no tempo e no espaço e conferem ao estuário constante mudança], ela guarda direta associação com o gradiente superficial de salinidade.

4.1.1 Estuário Inferior (Marajó)

O Estuário Inferior (EIP) corresponde à zona terminal do Rio Pará, conectado ao sistema oceânico do Atlântico. Ele possui aproximadamente 50 km de extensão, compreendido entre a foz, na linha de costa, e o limite transversal **y**, o qual intercepta áreas a montante das cidades de Salvaterra (1), a oeste, e de Vigia (11), a leste (Fig. 4-I). O estuário de Marajó é dominado por macromarés, que podem alcançar 5,7 m durante a sizígia na ilha dos Guarás (12) (Figs. 3a e 4).

De acordo com Prestes et al. (2014), a vazão do Rio Pará atinge pico de 300.000 m³/s durante a vazante e de 200.000 m³/s na enchente, induzindo intensos processos de circulação hidrodinâmica, com estratificação, turbulência, difusão e avanço de sal para o estuário. Esses efeitos exercem maior controle sobre o estuário proximal, por isso, o EIP apresenta a mais elevada concentração salina. Embora ocorram oscilações sazonais e diluição da concentração salina decorrente da alta vazão na estação chuvosa, os valores médios de salinidade aferidos em trechos adjacentes à margem reportados por Ramos (2007) e Bezerra et al. (2013) superam 2,5 g/kg.

Rosário et al. (2016) demonstraram o comportamento do gradiente salino do Rio Pará ao longo do ano, considerando três períodos: alta descarga, média (transição) e baixa descarga. Segundo os dados desses autores, o segmento definido como Estuário Inferior exibe gradiente de salinidade média no período de alta e baixa descarga em torno de 3 e 9 PSU, respectivamente. Face à tendência de manutenção do gradiente de salinidade anual > 2 PSU, o Estuário Superior pode ser classificado como de água salobra (oligohalino). Ademais, a penetração salina no Rio Pará diferencia o litoral leste do litoral oeste do estado, esse último comandado pelo Amazonas,

no qual não se registra o avanço salino devido à sua alta descarga que empurra as características estuarinas para além de sua foz,chegando à plataforma continental (WELLS, 1995).

4.1.2 Estuário Superior (Marapatá)

O Estuário Superior (ESP) tem sua delimitação geográfica (**z**), de oeste a leste, em Malato (2) e Arienga (8), respectivamente (Fig. 4). Do limite transversal **z**, sentido montante, o Estuário Superior incorpora a foz do Maratauíra e depois se bifurca em dois grandes corpos hídricos, os quais formam o ângulo de ≃ 57° entre si. O primeiro corresponde à própria continuidade do Rio Pará, que transcorre paralelo ao litoral (sentido ENE-WSW) eestende-se até o Estreito de Breves, totalizando aproximadamente 200 km. O segundo corpo hídrico tem orientaçãoNNE-SSW e corresponde ao Rio Tocantins; é através desse rio que as características estuarinas são empurradas ao interior do continente, até às proximidades de Baião (5), somando ≃ 180 km de extensão. Consequentemente, oESP reúne o segmento inicial e mediano do Rio Pará, o baixo Tocantins, o Rio Maratauíra e a vasta drenagem por eles interceptada (Fig. 4-III).

No ESP ocorrem micro e mesomarés semidiurnas; micromarés são registradas próximo ao atracadouro de Breves (3) (Fig. 3a) e a montante de Cametá (4). A jusante desses locais a maré amplifica-se para o tipo mesomaré, alcançando 3,4 m na Ilha Rasa (6) (Fig. 4).

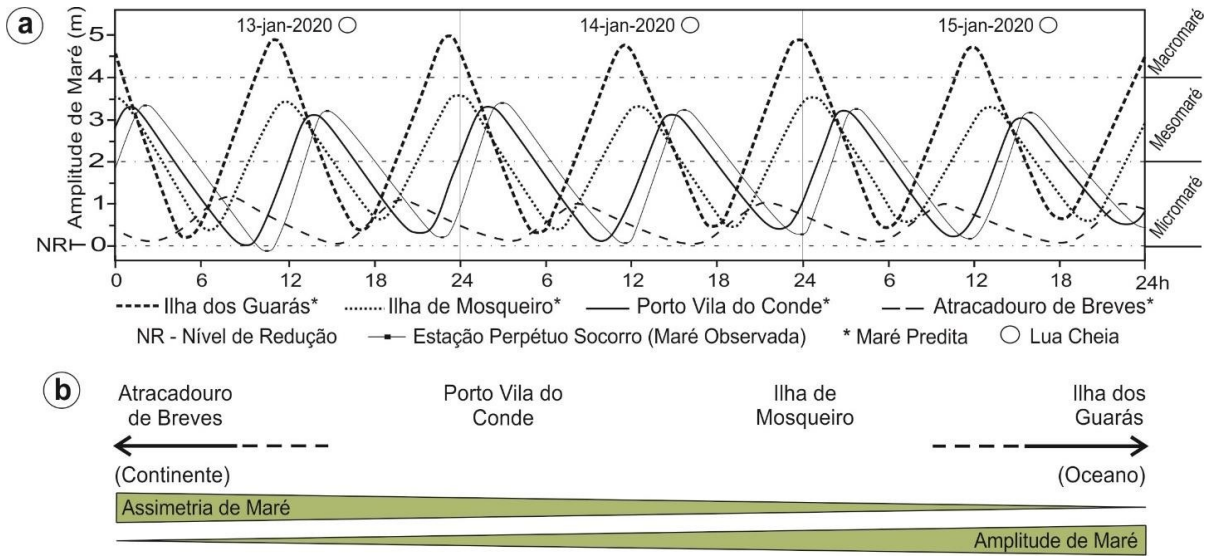

Figura 3. Variação (a) e assimetria de maré ao longo de quatro setores do Estuário do Rio Pará (b) (ver esses locais nafigura 4). Dados de Perpétuo Socorro foram inseridos para comparação.

Dentre as zonas estuarinas, o Estuário Superior exibe a maior assimetria de maré; o tempo de vazante é progressivamente superior ao da enchente a partir do limite transversal **z** (Fig. 4). Nas estações Nazaré e P. Socorroa diferença é de 1,5 e 1,6 h, respectivamente (Figs. 1b e 6). Na foz do Tocantins, Costa (2014) registrou diferença de 2 h (enchente 7,2 e vazante 5,2 h), e isso se reflete na intensidade da corrente que passa a ser maior durante a enchente, alcançando

velocidade máxima de 0,93 m/s *versus* 0,80 m/s de vazante (período chuvoso), e 0,75 m/s (enchente) e 0,67 m/s (vazante) na estação seca. De modo geral, face à assimetria que exibe (Fig. 3b), o ESP pode ser referido como estuário dominado por corrente de enchente (cf. SPEER; AUBREY, 1985).

Concernente à salinidade, no corpo hídrico do ESP ela é praticamente ausente. Dados de modelagem (e.g., ROSÁRIO et al., 2016) atribuem gradiente de salinidade inferior a 0,04 PSU durante a estação seca em trecho do Rio Pará a jusante do limite transversal (**z**). Piratoba et al. (2017) aplicando estudo através de coletas nas estações chuvosa e seca às adjacências de Barcarena, jusante de **z**, registraram água doce (STD < 500 mg L^{-1}) ao longo do ano. Silva et al. (2015) demonstraram valores estáveis de salinidade em torno de 0,02 PSU durante a estação chuvosa nas cercanias de Abaetetuba (7). Portanto, o Estuário Superior pode ser classificado como sendo de água doce ou limnético.

4.1.3 Estuário Médio (Guajará)

O Estuário Médio (EMP), por sua vez, limita-se a jusante com o Estuário Inferior (**y**), e a montante com o Estuário Superior (**z**) e soma aproximadamente 90 km de extensão (Fig. 4-II). Esse estuário é governado pelo regime de meso-macromarés, com ocorrência de mesomarés pouco antes da transição **z**. As mesomarés são registradaspróximo à Vila do Conde, enquanto em Belém (9) ocorrem macromarés, com alcance de 4,3 m durante a sizígia, e assimetria positiva de 20 min (ARAÚJO, 2017) (Fig. 4).

Guajará é o estuário de mistura, convergência e ampla interação entre os processos físico-químicos, resultantes da mistura da água doce transferida pelo Estuário de Marapatá, com a água salobra do Estuário de Marajó. A variação do aporte fluvial guarda relação direta com o regime de precipitação que, por sua vez, é controlado pela movimentação latitudinal da Zona de Convergência Intertropical (ZCIT). A estação chuvosa (dezembro e maio) é influenciada pela ZCIT próxima ao litoral, conferindo maior volume de chuvas. Em agosto a ZCIT volta a se reposicionar a Norte, diminuindo a precipitação (junho a novembro) (SOUZA-FILHO et al., 2009; MORAES et al., 2005). A entrada da estação chuvosa afeta o EMP, pois regula o volume de água doce nos rios a montante, que esvaziam seus fluxos no Rio Pará. Dos rios a montante, o Tocantins é o principal, com 10.900 m^3/s de descarga médiaanual (ANA, 2019).

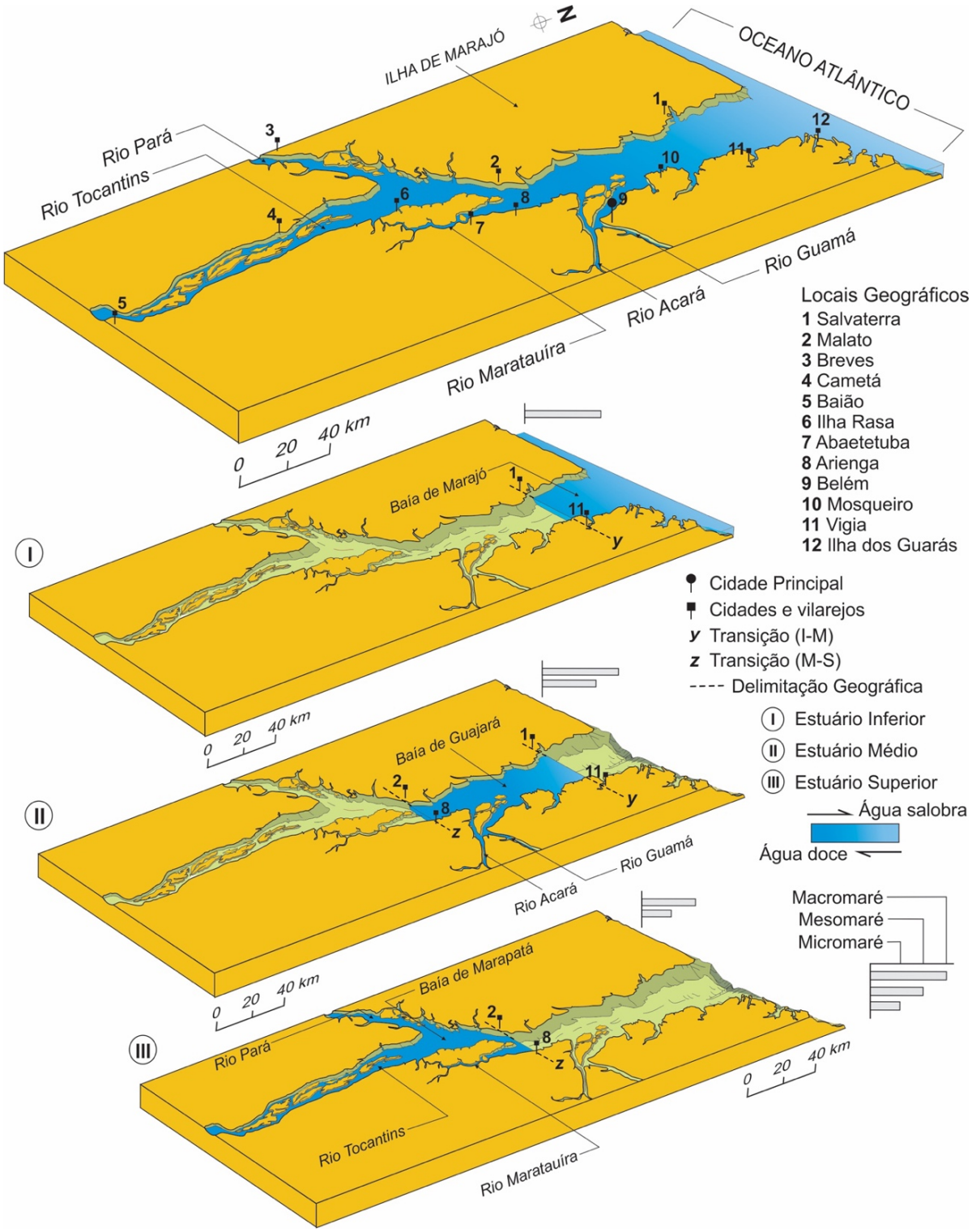

Figura 4. Compartimentos do Estuário do Rio Pará, Norte do Brasil. O diagrama superior fornece a visão geral desse estuário, enquanto os diagramas I, II e III relacionam zonas correspondentes ao Estuário Inferior do Rio Pará (ESP), Estuário Médio do Rio Pará (EMP) e Estuário Superior do Rio Pará (ESP), respectivamente. Baías principais foram listadas e seus nomes emprestados ao estuário correspondente.

O maior volume de precipitação tende a ocorrer no mês de março, todavia o pico máximo de vazão ocorre geralmente do final de abril a maio (ANA, 2019), refletindo em um tempo de retardo (*lag time*) no *input* de água doce ao estuário do Rio Pará de aproximadamente dois

meses (Fig. 5). Além da extensa área coletora, o *lag time* pode ter associação com a topografia modesta e baixa declividade, constando de relevo predominantemente plano,menos favorável ao escoamento superficial (HOOVER; HURSH, 1943). Outro fator relevante à indução de retardodeve estar nos materiais subjacentes, os quais podem requerer tempos diferentes ao processo de infiltração e percolação de águas superficiais (HORTON, 1945; RAWLS et al., 1993). Deve-se ainda levar em conta a cobertura vegetal, face à sua capacidade de interceptação e retardo em diferentes escalas à transferência de água (BOSCH; HEWLETT, 1982).

Durante a estação seca, o gradiente de salinidade no EMP pode apresentar valores locais em torno de 2,4 (GUIMARÃES, 2014). Com a introdução de água doce no período chuvoso, tanto do Rio Tocantins (10.900 m^3/s), quanto do Rio Amazonas, através do Estreito de Breves (6.000 m^3/s [CALLÈDE et al., 2010]), a concentração salina reduz de 2,4 para valores abaixo de 0,2 PSU (ROSÁRIO et al., 2016) ou se torna ausente (MASCARENHAS et al., 2018). Em razão de fenômeno sazonal e tempo de retardo, espera-se que entre os meses de março e junho o Estuário de Guajará apresente o mais baixo gradiente de salinidade, ao passo entre setembro e dezembro, deve ocorrer a maior concentração salina causada pelo enfraquecimento do aporte fluvial.

A sensibilidade e resposta do Estuário Médio às estações do ano implica em sua subordinação sazonal aos parâmetros ambientais das zonas estuarinas adjacentes. Entre os meses de janeiro e junho, o Estuário Médio desenvolve maior interação com estuário de montante (Superior/Marapatá), incorporando mais claramente suas características ambientais (água doce - limnético). De julho a dezembro, o EMP apresenta maior interação com o estuário de jusante (Inferior/Marajó), podendo apresentar água salobra (oligohalino). Tal condição imprime no EMP o caráter essencialmente transicional, pois abriga, de modo alternado, atributos dos estuários Superior ou Inferior que passam a dominar sobre ele. Os estuários Superior e o Inferior, ao contrário do Médio, tendem a apresentar menor perturbação anual em seus parâmetros relativos ao gradiente de salinidade, constituindo-se de água doce e salobra, respectivamente.

Retardo de resposta de bacias de drenagem à precipitação tem sido analisado em diversos estudos usando desde séries históricas (e. g., JIANG; SU; HARTMANN, 2007; KRIAUCIUNIENE et al., 2012) a eventos de menor duração (e. g., KHADDOR et al., 2019). Lesack et al. (2013) detectaram *lag time* de aproximadamente uma semana (6,6 dias) entre o ciclo do degelo no trecho montante do canal de Tsiigehtchic, distante aproximadamente 200 km da costa, e a chegada da água doce ao delta do Estuário do Makenzie, no Canadá. No caso

do Tocantins, a extensão e alcance longitudinal de sua bacia de drenagem, em articulação ao relevo modesto, geologia subjacente, cobertura vegetal e barramentos artificiais devem ser considerados como fatores substanciais quanto ao seu *lag time* de duração aproximada de dois meses (Fig. 5).

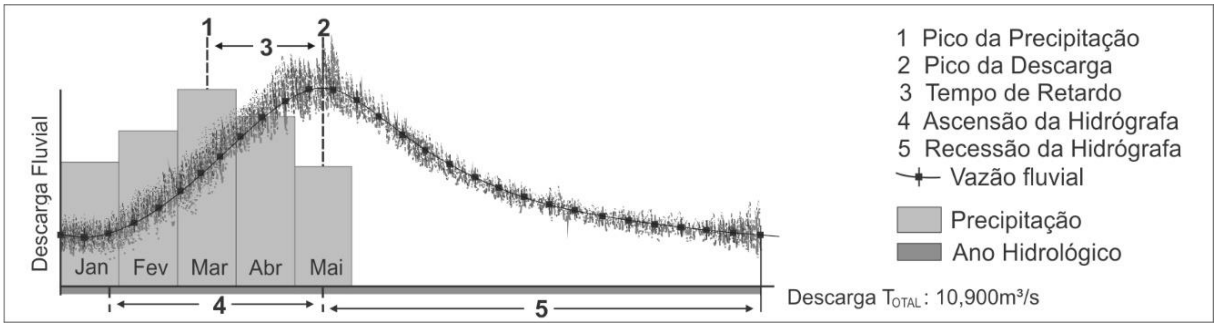

Figura 5. Hidrógrafa do Rio Tocantins baseada em dados de precipitação e descarga fluvial média anual.

4.2 Ambientes inundáveis do Sistema Tocantins-Maratauíra, Estuário Superior

Os ambientes inundáveis do STM estão submetidos ao regime de mesomarés, com altura de Preamar da Maréde Sizígia (PMS) e a Preamar da Maré de Quadratura (PMQ) de 3,35 m e 2,67 m, respectivamente (Fig. 6). Contudo, monitoramento posterior registrou amplitude de maré de 3,78 m e PMS em torno de 3,55 m.

Dos 22 sítios selecionados para o monitoramento, 2 ocupam altimetria abaixo de 1 m, 6 estão no intervalo de 1 a 3 m, 12 situam-se entre 3 e 5 m e 2 ocorrem no intervalo de 5 a 6,5 m (Fig. 7). Com base nos indicadores altimétricos e na interação deles com os diferentes ciclos de marés, três categorias de ambientes inundáveis e um não inundável foram reconhecidos e cartografados em escala de detalhe (1:2,7 km). Os ambientes inundáveis se posicionam no intervalo de 0 a 5 m – planície – e são eles: 1 - Zona de Inframaré (ZIf); 2 - Zona de Intermaré (ZIt) e 3 - Zona de Supramaré (ZSp). O domínio zonal não inundado foi designado de Terra Firme (TFi), termo corrente na descrição do relevo amazônico para áreas não sujeitas à inundação. Os valores de área e porcentagens incluídos na descrição referem-se apenas ao CIOA.

4.2.1 Zona de Inframaré (ZIf)

A zona de Inframaré (ZIf) compreende as superfícies de menor altimetria e mais restrita ocorrência espacial (6,24%), com área de 21,4 km² no CIOA (Fig. 8). Situada no intervalo entre o NR (0 cm) e 1 m, a ZIf é constituída por flancos de margem suave a íngreme, inclinados na direção do rio e tem característica análoga à zona de estirâncio praial. Sua declividade varia entre 2 e 20°, com restritas áreas que atingem localmente até 75°. A cobertura sedimentar da

ZIf é constituída de areia, com textura variada, silte, argila rica em matéria orgânica e turfa, de idade holocênica. Comumente, esses depósitos repousam sobre as coberturas detrito-lateríticas, de idade pleistocênica, que afloram às margens e leitos dos canais.

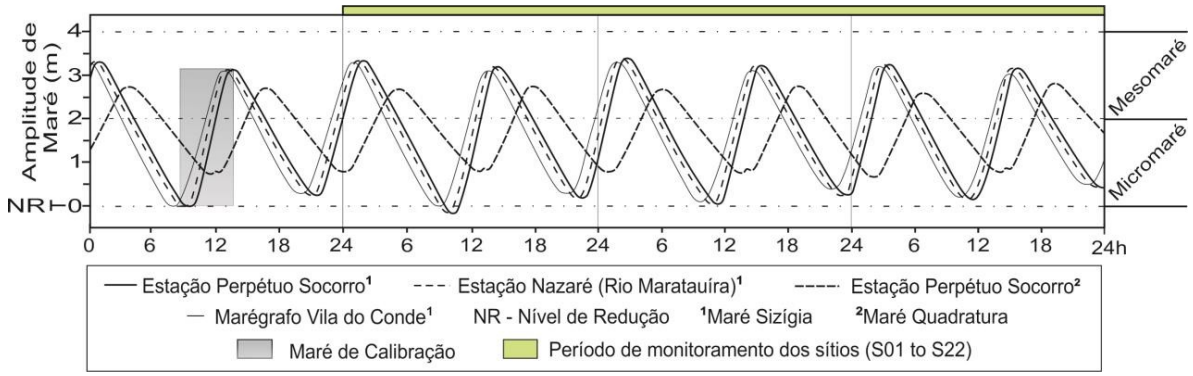

Figura 6. Variação de maré nas estações locais (P. Socorro e Nazaré). Maré de referência (Marégrafo de Vila do Conde) foi inserida para fins de comparação.

Concernente à vegetação, a ZIf exibe contraste entre os setores proximais e os distais ao NR; no primeiro há restrita ocorrência de vegetação, geralmente gramíneas e ervas higrófilas, enquanto o segundo abriga formações pioneiras. Macrófitas aquáticas das espécies *linifera* e *arborescens*, do gênero *Montrichardia*, têm maior ocorrência e comumente formam bosques em associação com *Rhizophora*, e menos frequentemente, com a *Avicennia*.

4.2.2 Zona de Intermaré (ZIt)

A Intermaré (ZIt) constitui a zona de topografia intermediária (1 a 3 m) (Fig. 7). Ela ocupa um terço (32,6%) do CIOA, aproximadamente 133,8 km² (Fig. 8). A ZIt exibe morfologia peculiar, uma vez que em seu intervalo ocorre a transição entre os flancos de margens (ZIf) e o nível de terra plano, denominado de várzea, que se desenvolve a partir dos discretos "diques" marginais. A declividade geral da várzea ocorre entre 1 e 5°, enquanto nos flancos suaves pode variar de 5 a 15°, tendo ainda margens íngremes de contato local com a ZIf de até 67°. A ZIt é constituída por depósitos lamosos, turfosos e arenosos (Holoceno), além de matéria orgânica em decomposição. Esses depósitos geralmente repousam sobre as coberturas detrito-lateríticas pleistocênicas.

Essa zona reúne indivíduos das Formações pioneiras (*Montrichardia linifera* e *arborescens*) e, eventualmente, *Rhizophora* e *Avicennia* nos trechos de contato descendente com a ZIf. A várzea é recoberta por palmeiras (*Mauritia flexuosa* L., *Mauritiella armata* e *Euterpe oleracea* Mart.) e pela floresta aluvial, com espécies arbóreas de *Machaerium lunatum* (L.f.), *Mimosa regnellii* Benth., *Pterocarpus amazonicus* Huber., *Pachira aquatica* Aubl.,

Hevea brasiliensis, Spondias mombin, *Calycophyllum spruceanum*, *Virola surinamensis* Cham., *Swartzia polyphylla*.

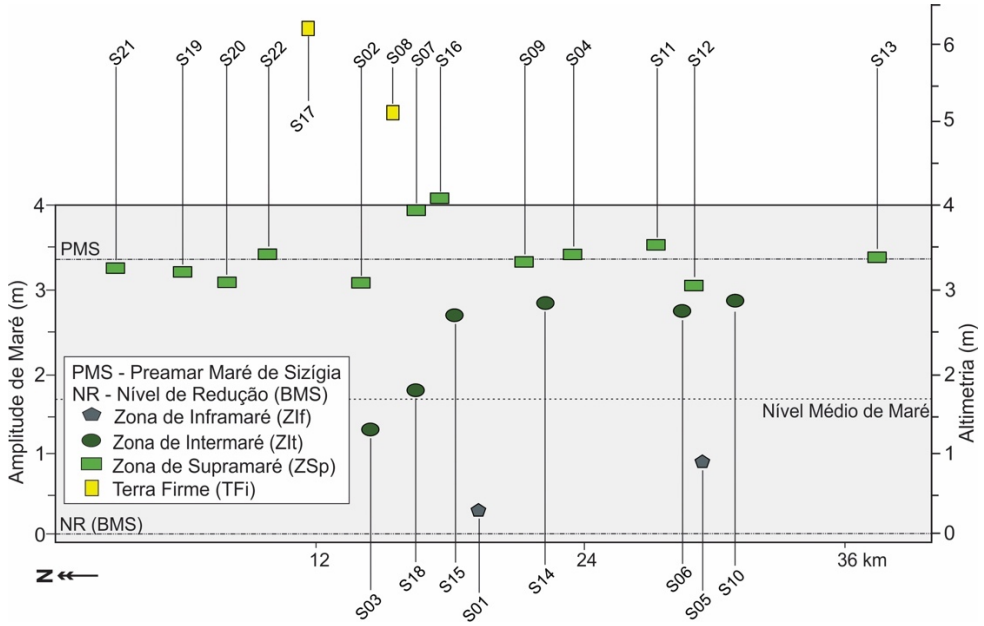

Figura 7. Diagrama hidrotopográfico dos sítios S01 a S22 monitorados no Sistema Tocantins-Maratauíra, Estuário Superior do Rio Pará. O diagrama relaciona os sítios às zonas inundáveis correspondentes, incluindo a altimetria e o nível da PSM obtidos em janeiro de 2020 (conferir a distribuição espacial dos sítios na figura 8).

4.2.3 Zona de Supramaré (ZSp)

O domínio ambiental da Supramaré (ZSp) constitui o intervalo terminal da planície fluviomarinha, limitando-se com Terra Firme. A ZSp ocorre ao longo do intervalo de 3 a 5 m (Fig. 7) e ocupa quase metade da área insular(40,1%), aproximadamente 164,4 km² (Fig. 8). Sua declividade oscila entre 0 e 4° (áreas inundáveis), com ocorrênciarestrita de até 35° nas feições negativas proximais à TFi. A ZSp é constituída por depósitos de idade Pleistoceno-Holoceno e sedimentos recentes nas frações argila e silte, ricos em matéria orgânica, além da areia em textura variada.

A Zona de Supramaré é recoberta por palmeiras (*Mauritia flexuosa* L., *Mauritiella armata*, *Euterpe oleracea* Mart., *Oenocarpus bacaba* e *Acrocomia aculeata*) e pela floresta ombrófila aluvial (*Spondias mombin*, *Virola surinamensis* Cham., *Banara guianensis* Aubl., *Swartzia polyphylla*, *Hevea brasiliensis*, *Calycophyllum spruceanum*, *Swartzia racemosa* Benth., *Pentaclethra macroloba*, *Allamanda gardneriana Blanchetti*, *Himatanthus sucuuba* (Spruce) Woods., *Bombax aquatica* (Aub.) K. Schum., *Symphonia globulifera* Linn., *Eschweilera amara* Mart., *Licania macrophylla* Benth., *Macrolobium multijugum* Benth., *Carapa guianensis* Aubl., *Parkia multijuga* Benth., *Campsiandra laurifolia*, *Vouacapoua*

americana Aubl.). Há também a presença de espécies de palmeiras que normalmente não ocorrem na ZIt (e.g., *Astrocaryum aculeatum* e *Attalea maripa*).

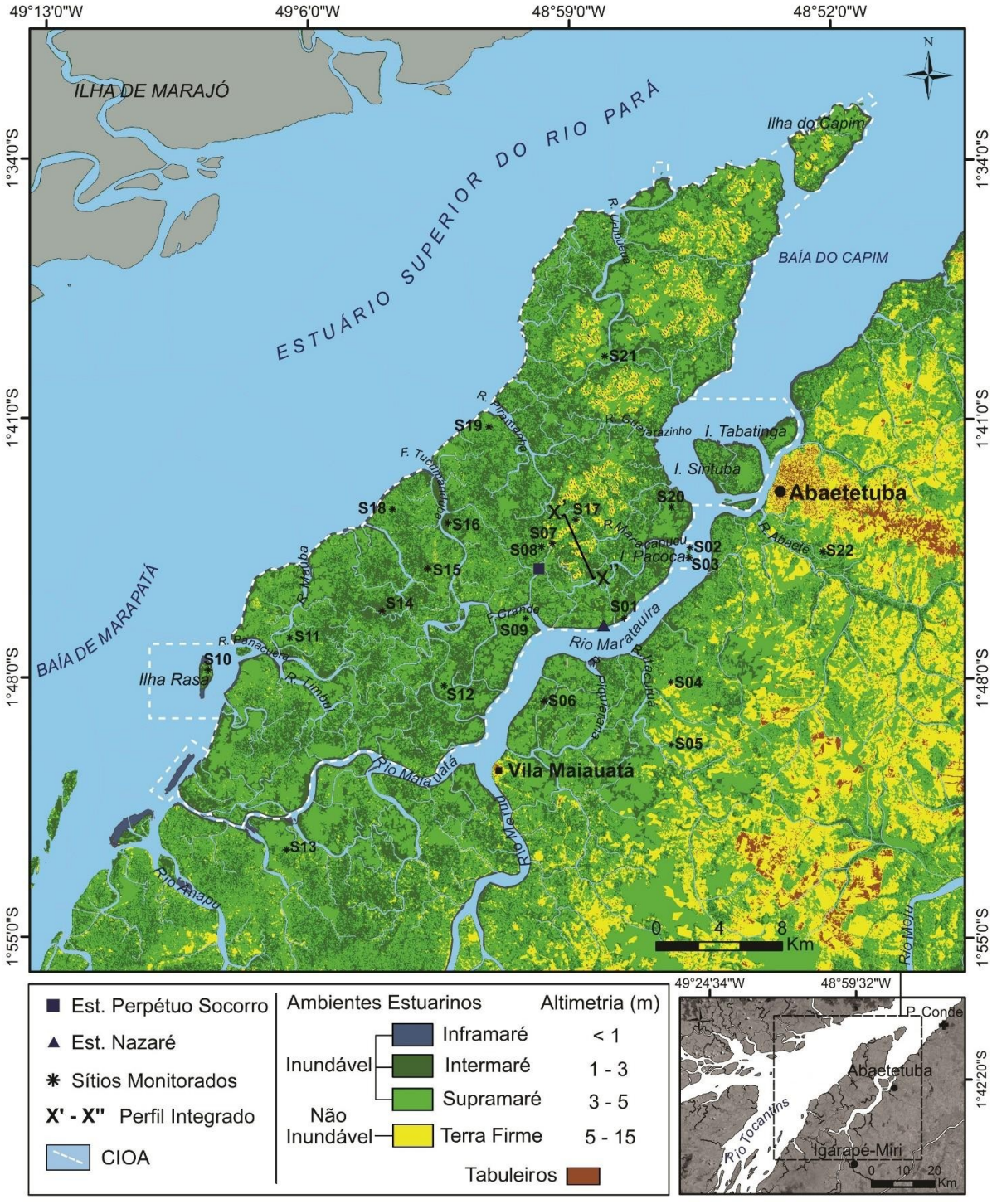

Figura 8. Ambientes inundáveis do Sistema Tocantins-Maratauíra, Estuário Superior do Rio Pará. Os códigos S01 a S22 se referem aos locais dos sítios de monitoramento. Os principais elementos da paisagem, interceptados pelo perfil integrado (X'–X"), constam no tópico seguinte (Fig. 11).

4.2.4 Terra Firme (TFi)

A Terra Firme (TFi), por sua vez, corresponde ao quarto ambiente identificado. Ela pode ser referida como subunidade morfológica parcialmente integrada aos tabuleiros e ocorre no intervalo entre 5 e 15 m. A TFi ocupa apenas 20,4% do CIOA (83,8 km²), comportamento que muda no domínio continental, quando a TFi assume expressiva ocorrência espacial, ao mesmo tempo em que ZIt e ZSp restringem-se às margens dos rios (Fig. 8). Sua cobertura sedimentar compreende sedimentos quaternários de fração fina, média e grossa, incluindo grânulos e seixos e depósitos detrítico-lateríticos. Localmente, a TFi pode apresentar irregularidades morfológicas superficiais formadas por feições negativas suaves de até 0,3 m. Excetuando-se os flancos dessas feições (≤ 35°) a declividade desse ambiente varia entre 4 e 13°. A cobertura ecológica da TFi consiste, principalmente, em *Campsiandra laurifolia*, *Vouacapoua americana* Aubl., *Dipteryx odorata*, *Manilkara huberi*, *Beilschmiedia sulcata* e *Diplotropis brasiliensis* Benth. Ao lado da ZSp, a TFi apresenta maior alteração antrópica, realçada pela presença de floresta secundária em distintos estágios de sucessão ecológica.

5. Interpretações e Discussões

Dados hidrodinâmicos envolvendo amplitude e frequência de marés revelam que a circulação hidrodinâmica do Estuário Superior tem sido conduzida por micro e mesomarés semidiurnas, não obstante sua geografia montante e a intensa descarga fluvial que essa zona estuarina incorpora. A influência da forçante marinha em região intracontinental pode estar associada a um conjunto de fatores, dentre os quais a ausência de variações topográficas positivas no talvegue, ampla desembocadura do Rio Pará e segmento retilíneo até a foz do Tocantins-Maratauíra, e à presença de relevo predominantemente baixo e suave.

Em estuários acomodados em zonas costeiras com geomorfologia caracterizada por costões rochosos, acentuado desnível topográfico e canais sinuosos, a amplitude de maré tende a reduzir-se expressivamente a montante (WRIGHT; COLEMAN; THOM, 1973). O Rio Pará, além de exibir configuração oposta a esses parâmetros fisiográficos e constar de um sistema de drenagem que transcorre sobre relevo predominantemente baixo e plano, mostra-se favorável à propagação de mesomarés por até 180 km da atual linha de costa (micromarés avançam até ≃ 340 km) (Figs. 1a, 3a e 4). Em compensação, esse distanciamento pode ser responsável pela dupla distorção de maré detectada localmente, qual seja; (i) altura da preamar em Nazaré e P. Socorro levemente acima das registradas no Marégrafo do Porto do Conde (MPC) e (ii) nível de baixa-mar em Nazaré e P. Socorro frequentemente inferior ao registrado no MPC.

Marés astronômicas são passíveis de distorções ao adentrarem os sistemas estuarinos, principalmente na altura. De acordo com Nichols e Biggs (1985), a distorção na altura de maré

pode decorrer de efeitos friccionais do leito, resultando na diminuição (hiposíncrono), ou compressionais da margem, causando sua amplificação (hipersíncrono). Marés mais altas no Maratauíra têm possível relação com a sua geometria para-afunilada (Fig. 1b), que induz à compressão lateral do fluxo, resultando em amplificação. É possível também que a morfologia preexistente do leito seja desfavorável ao atrito, propício, portanto, à propagação da maré. Por outro lado, tal distorção parece compatível com a defasagem temporal entre Baía do Capim (MPC) e o Maratauíra (Nazaré e P. Socorro), seguido de inversão de fluxo na planície de inundação.

A defasagem temporal constatada separa em 1,2 h o início da vazante e da enchente no MPC das estações de monitoramento (Fig. 2A). Esse retardo regula contínuos processos de distorção de maré nos estágios de vazante (Maratauíra continua esvaziando-se por ≃ 1,2 h, enquanto no MPC o fluxo de enchente é disparado – redução da baixa-mar) e de enchente (estofo da enchente ocorre primeiro no MPC, disparando a vazante, enquanto no Maratauíra a enchente é conservada por ≃ 1 h – elevação da preamar) (Fig. 6). A respeito dos fluxos de inversão na planície, esses são disparados antes do estofo de maré. Eles indicam a proximidade do estágio vazante (partem dos ambientes inundáveis para os rios) e foram identificados a partir do deslocamento sistemático de fragmentos sobrenadantes, principalmente vegetais.

Fluxos reversos provém da ZIt, ZSp e cursos rasos, e são empurrados, possivelmente, pela descarga fluvial. Esses fluxos sugerem que a água que extravasou a margem e inundou os ambientes começa a ser devolvida, mas eles não correspondem propriamente ao fluxo de vazante, uma vez que nos rios que envolvem tais ambientes ainda ocorre a enchente. Fluxos reversos aumentam à medida que o estofo de maré se aproxima, passando a inverter a circulação nos cursos da planície e cabeceira de drenagem local, reintroduzido a descarga na calha do rio e elevando, dessa maneira, o nível de maré até a preamar (Fig. 9). Enchente conservada e fluxos reversos na planície durante a maré cheia são fatores internos que podem estar causando preamares em P. Socorro (3,35 m) e Nazaré (3,31 m) pouco acima do MPC (3,26 m) (Figs. 6 e 9).

De natureza oposta aos fatores internos, fatores externos, relativos à constituinte orbital (Equinócio) também afetam as marés. Medições recentes em P. Socorro indicaram PMS de 3,55 m e amplitude de 3,78 m (Fig. 10), mas esse estuário já foi atingido por marés maiores. Segundo os moradores, no período anterior (Mar-2019), a maré alcançou ambientes não inundáveis, invadiu moradias e acarretou significativas perdas materiais.

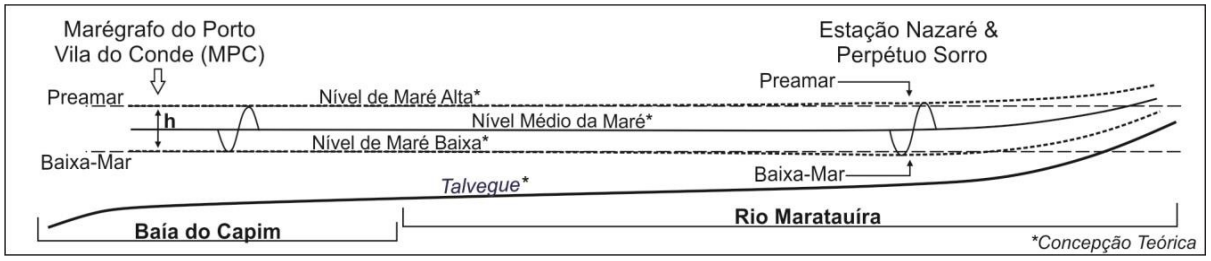

Figura 9. Esboço associando o MPC, na Baía do Capim, com as estações de monitoramento de maré (Nazaré e P. Socorro)e o processo físico de amplificação de maré detectado a partir do Maratauíra.

Face à estratégia da população local em demarcar o nível das marés excepcionais para construir pisos de futuras moradias, a "maré de março" pôde ser mensurada. Sua altura foi de 4,07 m (macromaré), aqui designada de Maior Maré Astronômica (MMA) (Fig. 10). A esse respeito, cabe mencionar a previsão fornecida ao MPC de 3,40 m, isto é, 0,67 m abaixo da observada em P. Socorro. De modo geral, o Maratauíra pode ser descrito como hipersincrônico (cf. NICHOLS; BIGGS, 1985), pois a geometria (constrição marginal, convergência de fluxo, atrito moderado ausente [DYER, 1995]) e processos hidrodinâmicos (esvaziamento mais longo, conservação de enchentee fluxo inverso da planície antes do estofo) se mostram capazes de induzir a amplificação das marés. No caso da MMA, a constituinte meteorológica (período chuvoso – Fig. 5) deve ter se somado aos fatores internos e produzido essa maré excepcional.

A amplificação de maré é um fenômeno comum em estuários próximos à costa; Santos (2010) registrou amplificação máxima de 0,35 e 0,40 m nas marés de quadratura e sizígia, respectivamente, no estuário de Caravelas, a 10 km do litoral da Bahia, Nordeste do Brasil. Aqui foram constatadas a amplificação de 0,21 m (quadratura) e 0,17 m (sizígia). Trata-se de valores baixos, mas expressivos, perante a posição geográfica desse sistema estuarino em relação ao oceano.

Os dados relativos ao gradiente de salinidade demonstram que os efeitos marinhos têm sua influência enfraquecida na composição do parâmetro químico, o qual é regido pela descarga de água doce do Tocantins e seus tributários. Em vista disso, o papel dos mecanismos que influenciam o Estuário Superior pode ser categorizado da seguinte forma: o marinho exerce maior controle no parâmetro físico (micro e mesomarés, oscilação no nível da água, circulação e inversão da corrente fluvial) e o mecanismo fluvial [que em parte imprimea assimetria na corrente] rege o parâmetro químico, isto é, corpo hídrico doce, controlando diretamente a fitoecologia. A descarga fluvial dilui a água salobra a jusante (i. e. Estuário Médio, Fig. 4-II), neutralizando eventuais impactos que a salinidade poderia ter sobre o ESP. Assim, a maré que penetra esse estuário apresenta-se dissociada da salinidade, semelhante ao Rio La Plata, na Argentina (cf. WELLS, 1995). Trata-se, portanto, de ambiente fluviomarinho.

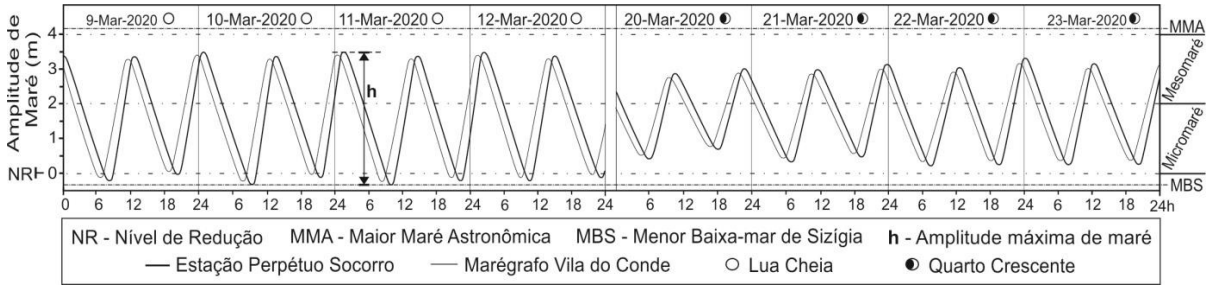

Figura 10. Dados do monitoramento de maré entre 9 e 23 de março de 2020. O valor de h é 3,78 m, amplitude máxima recorrente. Note que a MMA foi plotada para fins de comparação.

O domínio dos ecossistemas de água doce, constituído principalmente por espécies de *Euterpe oleracea* Mart. (açaí), *Mauritia flexuosa* L. (buriti) e *Montrichardia linifera* (aninga) que recobrem a ZIt e a ZSp, reflete o controle fluvial na ecologia da paisagem (Fig. 11). Tipos botânicos do ecossistema transicional de manguezal (*Rhizophora* e *Avicennia*), que paradoxalmente ocorrem a jusante do Tocantins e no Maratauíra, devem estar associados à alta capacidade de adaptação dessas espécies aos parâmetros ecológicos desfavoráveis (e.g., água doce (cf. WANG et al., 2011)) ou, ainda, assinala condições ambientais diversas às do presente.

Estudo prévio sugere que a subida do nível do mar pós-glacial ocorrida no Holoceno Médio propiciou o surgimento de uma franja de manguezal na planície e ilhas proximais do baixo Tocantins (RIBEIRO; VALADÃO, 2020). Apesar da descida e estabilização do nível do mar no Holoceno Tardio, parte da franja desse ecossistema foimantida na paisagem face à sua resiliência, afirmam esses autores. Diversos estudos têm mostrado que a implantação e dinâmica dos manguezais no litoral Norte (COHEN et al., 2012), Nordeste (RIBEIRO et al., 2018) e Sudeste (FRANÇA et al., 2013) do Brasil atenderam às flutuações marinhas holocênicas. De modo geral, o ecossistema de manguezal tem sido usado como bioindicador de mudanças paleoambientais (cf. BLASCO;SAENGER; JANODET, 1996). Em Marapatá seu desenvolvimento encontra-se limitado pela indisponibilidade salina, bem como pela competição com espécies do ecossistema de água doce que prosperam na paisagem moderna. A salinidade não detectável nesse setor controlado por mesomarés confere a seus cursos hídricos uma condição especial que os distingue de rios, bem como de canais de maré. Nesse caso, tais cursos poderiam ser designados de "rios de maré", seguindo Cohen e McCarthy (1963), Wells (1995) e Cook, Sommerfield e Wong (2007). O fato de esvaziarem-se totalmente no estuário do Rio Pará, ao invés do oceano, imprime no Tocantins e Maratauíra a característica introduzida por Emeka et al. (2010) aos rios de maré.

Baseado em uma tríade de critérios ambientais (1 - controle por marés; 2 - salinidade não detectável; 3 - esvaziamento do fluxo no estuário), os rios Maratauíra, Guajarazinho, Urubuéua, Piramanha, Tucumanduba, Maúba, Panacuera, Timbuí, Maiauatá, Furo Grande, Quianduba,

Maracapucu, Piquiarana, Itacuruçá, Abaeté e cursos adjacentes são rios de maré e muitos deles não constituem exatamente rios (sem nascente), mas elo de conexão entre diferentes corpos d'água (Fig. 8). É plausível considerar que parte de toda a rede de drenagem do Estuário Superior seja compatível com rios de maré, formando assim um grande sistema de rios de maré da CostaNorte do Brasil, incluindo o Capim (cf. FREITAS; SILVEIRA; ASP, 2012) e outros rios a jusante do ESP, não obstantesuas particularidades. Em relação ao Tocantins, a designação de rio de maré pode ser aplicável ao seu baixo curso(adjacências de Baião à sua foz; Fig. 4).

Seguindo à altimetria dos ambientes, o mapeamento revela o predomínio de zonas sensíveis à incursão por marés, principalmente no CIOA, onde os ambientes no intervalo de 0 a 5 m representam 78,9% de sua área (Fig.8).Entre os ambientes inundáveis, a ZIf fica submersa com maior frequência (≃ 18 h) ao longo do ciclo diário. A exposição integral dessa zona ocorre na BMS. Durante a BMQ, apenas sua crista fica emersa (Fig. 11). Esse controle diferencial da ZIf por marés reflete na morfodinâmica e heterogeneidade dos depósitos sedimentares que a constitui, quais sejam, os lamosos (mais estáveis) e os arenosos (dinâmicos).

Os depósitos lamosos oferecem condições ideais para o desenvolvimento de bosques de *Montrichardia*, com ocasional presença de *Rhizophora*. Esses bosques têm grande relevância na proteção do substrato quanto aos processos erosivos (THAMPANYA et al., 2006; GILMAN et al., 2008), bem como desempenham papel importantena estabilidade geomorfológica dos ambientes ascendentes (ZIt e ZSp). Os depósitos arenosos, por outro lado, representados por barras transversais e longitudinais nos rios de maré, são constituídos por areia bem selecionada, geralmente de granulometria fina a média, formados em ambientes de alta energia (cf. REINECK; SINGH, 1980). Sua morfodinâmica resulta do atrito causado por fluxos de maré e pela energia das ondas na ausência de vegetação. Em razão do contínuo aporte sedimentar controlado por correntes bidirecionais da maré de sizígia, esses depósitos têm se expandido e migrado, inclusive, avançando sobre trechos lamosos, preenchendo espaços de acomodação pré-existentes e reduzindo a batimetria nos rios de maré.

Contrário à ZIf (sempre inundável), o ambiente da ZIt (várzea) é totalmente inundado apenas por marés de sizígia. Nas marés de quadratura o efeito da inundação é parcial (Figs. 7 e 11). A frequência de inundação da ZIt pode ser definida pela razão entre o percentual de marés de sizígia maior de 3 m *versus* sua altimetria (≤ 3 m). De acordo com a projeção, 55,4% das marés esperadas ao longo do ano causam a inundação total desse ambiente. Apesar de inundável, a ZIt abriga grande parte da ocupação antrópica através do uso de palafitas. Todavia, a população geralmente discrimina superfícies abaixo de 2,5 m.

Gêneros arbóreos lenhosos e palmeiras (Fig. 11) recobrem os depósitos silto-argilosos, ricos em matéria orgânica, com ocasional presença de areia fina da ZIt. Esses depósitos superficiais da ZIt têm continuidade lateral e estendem-se até o limite das áreas inundáveis da ZSp. Nesse limite, ocorre a substituição de depósitos silto-argilosos com lentes de areia fina por depósitos silto-arenosos, areno-siltosos e de areia fina a média, com matéria orgânica. Esse arranjo dos depósitos sedimentares da ZIt e ZSp decorre do trabalho das marés e fornece indícios do mecanismo envolvido no aporte e formação dos sistemas sedimentares. Os sedimentos são distribuídos atendendo ao gradiente de energia, mecanismo de transporte e ambiente de deposição, com sedimentos finos sendo depositados nos ambientes de baixa energia, enquanto os médios a mais grossos são arrastados para os de alta energia (cf. REINECK; SINGH, 1980; GUJAR; ANGUSAMY; RAJAMANICKAM, 2007). Esse gradiente energético está presente nas marés (DYER, 1979) e o suprimento sedimentar decorre da circulação hidrodinâmica que transporta os materiais durante os ciclos de alta energia da maré de sizígia.

Segundo Costa (2014), o transporte de volume instantâneo do Tocantins alcança a ordem 169.677,91 m³/s na enchente, contra -137.694,46 m³/s na vazante durante o período chuvoso, e no período seco, alcança 129.965,39 m³/s (enchente) e -104.585,09 m³/s (vazante), o que reforça a alta capacidade de suprimento de material particulado aos ambientes inundáveis. Quando a maré incursa sobre a ZIt e ZSp, a areia fina é depositada sobretudo na fase máxima de inundação (redução de corrente), enquanto no estofo, com a energia do fluxo anulada, a fração fina (silte e argila) é depositada, originando sucessões silto-argilosas com lentes de areia fina (cf. REINECK; SINGH, 1980). Esse padrão deposicional tem sido registrado também na planície de maré da Ilha de Marajó (cf. SOUZA-FILHO; EL-ROBRINI,1996; FRANÇA; SOUZA-FILHO; EL-ROBRINI, 2007). A respeito dos depósitos silto-arenosos com lentes de areias finas, areias médias e mal selecionadas que passam a ocorrer de modo caótico em trecho não sujeito à inundação da ZSp, sua fonte deve ser ascendente (Terra Firme) e o fornecimento decorre de processos erosivos.

O substrato da Terra Firme é caracterizado por irregularidades suaves (feições negativas de até 30 cm), observadas desde o trecho terminal da ZSp (Fig. 11). Somando-se à cobertura vegetal, tais feições auxiliam na delimitação entre ZSp e TFi, pois realçam a transição, e ao mesmo tempo, destacam os ambientes não inundáveis. A respeito dos mecanismos que controlam essa morfologia, tendo em vista sua ocorrência acima do nível da maré, pode-se atribuí-los a processos erosivos guiados pela precipitação. Entretanto, consideramos que a cobertura vegetal e a baixa declividade dificultariam a formação de fluxos concentrados (cf. HORTON, 1945), tornando essa hipótese um pouco mais complexa. De modo geral, gênese e

evolução sedimentar da TFi exigem investigação morfogenética e abordagem metodológica específicas, não incluídas, portanto, no escopo e objetivo deste trabalho.

As três categorias de ambientes inundáveis (ZIf,ZIt e ZSp) reconhecidas e mapeadas têm seu ciclo de inundação controlado por mesomarés. A ZIf, ZIt e ZSp têm maior ocorrência geográfica no complexo insular, mas nem todo o Complexo Insular forma um grande ambiente inundável (planície fluviomarinha). Oposta à prévia interpretação, o CIOA é constituído também por ambientes acima do nível das marés, como retratado pela TFi.

No âmbito da TFi foram identificadas superfícies topográficas de ≃ 7,6 m no trecho mesocentral do CIOA, as quais formam um corredor com média altimétrica de 6 m, conectando os sítios S07 e S17 (Fig. 8). Além delas, foi reconhecida uma sequência de elevações semelhantes a norte, para a qual não foi possível determinar a altimetria exata pelo método aqui empregado, pois a maré não tinha proximidade lateral. Apesar da sequência de áreas elevadas ao norte (Fig. 8), dificilmente ocorrem superfícies de topografia > 8,5 m no CIOA.

Gradiente altimétrico associado à distribuição geográfica dos ambientes inundáveis revelou particularidades geomorfológicas dificilmente mensuradas em abordagem não detalhada. Dentre essas particularidades do Complexo Insular, pode-se notar a distinção topográfica entre o setor norte (sistema Maracapucu-Piramanha à Ilha do Capim) direcionado ao mar, e o setor sul (sistema Maracapucu-Piramanha ao Rio Maiauatá) direcionado ao continente (Fig. 8). O setor sul é constituído de topografias mais baixas (ZIt e ZSp), com a TFi quase ausente. A norte o comportamento morfológico é inverso; a TFi passa a ocorrer desde o sistema Maracapucu-Piramanha, tornando-se recorrente nas proximidades da crista (Ilha do Capim). Neste setor norte, a TFi ocupa 39,6% dos ambientes, seguido pela ZSp com 38,8%, enquanto as zonas de baixa altimetria (< 3 m) somam menos de 22%. Portanto, mais de 76% da porção norte do CIOA situa-se no intervalo acima de 3 m, enquanto ao sul, os ambientes abaixo de 3 m ocupam quase a metade (40,6%) de sua área (Fig. 8). Esses números fornecem uma visão mais pormenorizada acerca da localização dos ambientes mais suscetíveis à inundação.

As áreas mais afetadas pela hidrodinâmica estão voltadas ao continente, o que reduz relativamente sua suscetibilidade aos impactos induzidos por ondas, correntes de maré e erosão acelerada, geralmente convergente sobre zonas frontais voltadas para o mar, como o norte do CIOA, posicionado na tríplice confluência dos rios Pará-Tocantins-Maratauíra. Contudo, a ocorrência desses ambientes na retaguarda do continente não reduz sua intrínseca suscetibilidade aos efeitos da inundação estuarina. Ao longo do ano, estima-se que 55,4% das marés são capazes de colocar 40% de todo setor sul abaixo do nível da preamar. Para o norte a mesma estimativa projeta inundação total de apenas 21,1% de sua área. Consequentemente, a

sul devem ocorrer as áreas de maior acumulação de sedimentos, menor decomposição da matéria orgânica e maior renovação da água retida em nascentes, depressões superficiais e reservatórios subsuperficiais. Trata-se também do setor com maior ocorrência de sistemas sedimentares modernos, mas isso não permite defini-lo como sendo mais jovem em relação ao setor norte.

Figura 11. Perfil integrado dos ambientes inundáveis do Sistema Tocantins-Maratauíra, no Estuário Superior, considerando a fitoecologia, a altimetria, a declividade e os tipos de marés. Com direção noroeste-sudeste, o perfil se estende do Rio Piramanha ao Rio Maracapucu-Miri (ver localização na figura 8). Pequenos corpos hídricos denominados *igarapés* foram interceptados pelo transecto, mas devido à escala adota, esses *igarapés* não puderam ser plotados.

O setor sul é marcado por intensa dinâmica ambiental, regida por efeitos fluviomarinhos contínuos, enquanto o setor norte exibe menor subordinação, apresentando, portanto, maior estabilidade. Nesse sentido, o fator determinante é a altimetria dos ambientes, fortemente influenciado pela presença da TFi. O reconhecimento e caracterização da TFi ao longo do CIOA resulta em um confiável marcador geomórfico, tanto por discriminar os ambientes não sujeitos

à influência de maré, quanto por evidenciar que nem todo o ambiente estuarino tem sua evolução associada à morfodinâmica moderna.

Conclusões

No estuário do Rio Pará três zonas foram definidas, denominadas Estuário Inferior, Estuário Médio e Estuário Superior. A delimitação dessas zonas atendeu às particularidades que esse rio exibe quanto às interações por marés, descarga fluvial e gradiente de salinidade. Os ambientes do Sistema Tocantins-Maratauíra foram reconhecidos como pertencentes ao Estuário Superior, cujo ciclo de inundação é regido por mesomarés com amplitude de até 3,78 m. Dentre esses ambientes, os mais suscetíveis à inundação estão no intervalo entre 0 e 3 m, os quais representam 39% do CIOA e têm maior ocorrência no setor sul, direcionado ao continente. Apesar da influência de mesomarés, a paisagem ecológica é constituída essencialmente por ecossistemas de água doce, consequência da alta descarga fluvial que neutraliza a salinidade no Estuário Médio, a jusante do STM. Ao Baixo Tocantins, Maratauíra e cursos acoplados à drenagem desses rios foi atribuída a designação de rios de maré, incluindo em suas características a ausência de salinidade e o esvaziamento de seus fluxos no estuário do Rio Pará, ao invés do oceano.

A respeito da constituição ecológica dos ambientes inundáveis, não obstante o gradiente limnético e o domínio de ecossistemas de água doce, foi detectada a presença de tipos botânicos pertencentes ao manguezal, sugerindo que o nível do mar esteve acima do atual em um passado recente. Além disso, a ocorrência da Terra Firme (Tfi) intraplanície fluviomarinha constitui outro marcador temporal na paisagem, tendo em vista sua dinâmica não associada às interações do estuário moderno. Assim, as espacialidades da franja de manguezal remanescente (marcador ecológico) e da Tfi (marcador geomórfico) são heranças que apontam para mecanismos ambientais com magnitude diversa àqueles identificados e atualmente expressos na paisagem.

Agradecimentos: À Coordenação de Aperfeiçoamento de Pessoal de Nível Superior (CAPES), pela concessão de bolsa de Doutorado ao primeiro autor, e ao Programa de Pós-Graduação em Geografia (PPGG-IGC, UFMG), pelo auxílio parcial para a execução dos trabalhos de campo. Os autores agradecem àqueles que deram suporte às atividades executadas em campo, bem como aos proprietários das áreas localizadas ao longo do Sistema Tocantins-Maratauíra, pela permissão de acesso aos sítios de monitoramento.

Referências

ALMEIDA, S. S.; AMARAL, D. D.; SILVA, A. S. L. Análise florística e estrutura de florestas de várzea no estuário amazônico. Acta Amazônica, v. 34, p. 513–524, 2004. DOI: 10.1590/S0044-59672004000400005

ANA. HidroWeb. Sistema de Informações Hidrológicas, 2019. Disponível em: <http://www.snirh.gov.br/hidrotelemetria>.

ARAÚJO, C. V. Tempo de inundação da Ilha de Sirituba (Abaetetuba, PA). Trabalho de Conclusão de Curso (Faculdade de Oceanografia). Instituto de Geociências, Universidade Federal do Pará, Belém. 2017. 36p.

BEZERRA, M. O. M.; FREITAS, P. P.; BALTAZAR, L. R. S.; ROLLNIC, M.; PINHEIRO, L. Estuarine processes in macro- tides of Amazon estuaries: A Study of Hydrodynamics and Hydrometeorology in the Marajó Bay (Pará-Brazil). Journal of Coastal Research, v. 65, p. 1176–1181, 2013.

BLASCO, F.; SAENGER, P.; JANODET, E. Mangroves as indicators of coastal change. Catena, v. 27, p. 167–78, 1996. DOI:10.1016/0341-8162(96)00013-6

BOSCH, J. M.; HEWLETT, J. D. A review of catchment experiments to determine the effect of vegetation changes on water yield and evapotranspiration. Journal of Hydrology, v. 55, p. 3–23, 1982. DOI: 10.1016/0022-1694(82)90117-2

BRYCE, S.; LARCOMBE, P.; RIDD, P. V. The relative importance of landward directed tidal sediment transport versus freshwater flood events in the Normanby River estuary, Cape York Peninsula, Australia. Marine Geology, v. 149, p. 55– 78, 1998. DOI: 10.1016/S0025-3227(98)00013-9

CALLÈDE, J.; COCHONNEAU, G.; RONCHAIL, J.; ALVEZ, F.V.; GUYOT, J.L.; GUIMARES, V.S.; de OLIVEIRA, E. Les apports en eau de l'Amazone à l'Océan Atlantique. Journal of Water Science, v. 23, p. 247–273. 2010. DOI: 10.7202/044688ar

CARR, M. L.; REHMANN, C. R.; STOECKEL, J. A.; PADILLA, D. K.; SCHNEIDER, D. W. Measurements and consequences of retention in a side embayment in a tidal river. Journal of Marine Systems, v. 49, p. 41–53, 2004. DOI: 10.1016/j.jmarsys.2003.05.004

COHEN, B.; MCCARTHY, L. T. Salinity of the Delaware Estuary. Del. Geol. Survey, v. 10, p. 1–41, 1963. DOI: 10.3133/wsp1586B

COHEN, M. C. L.; PESSENDA, L. C. R.; BEHLING, H.; ROSSETTI, D. F.; FRANÇA, M. C.; GUIMARÃES, J. T. F.; FRIAES, Y.; SMITH, C. B. Holocene palaeoenvironmental history of the Amazonian mangrove belt. Quaternary Science Reviews., v. 55, p. 50–58, 2012. DOI: 10.1016/j.quascirev.2012.08.019

COOK, T. L.; SOMMERFIELD, S. K.; WONG, K. C. Observations of tidal and springtime sediment transport in the upper Delaware Estuary. Estuarine, Coastal and Shelf Science, v.72, p. 235–246, 2007. DOI: 10.1016/j.ecss.2006.10.014

CORRÊA, I. S. Aplicação do diagrama de Pejrup na interpretação da sedimentação e da dinâmica do estuário da Baía de Marajó-Pa. Pesquisas em Geociências, v. 32, n. 2, 109–118, 2005. DOI: 10.22456/1807-9806.19551

COSTA, M. S. Aporte Hídrico e do Material Particulado em Suspensão para a Baía do Marajó: contribuição dos rios Jacaré Grande, Pará e Tocantins. Dissertação (Mestrado em Geologia) -

Programa de Pós-Graduação em Geologia e Geoquímica, Universidade Federal do Pará, Belém. 2014. 83p.

DALRYMPLE, R. W.; ZAITLIN, B. A.; BOYD, R. Estuarine facies models: conceptual basis and stratigraphic implications. Journal of Sedimentary Research, v. 62, p. 1130–1146, 1992. DOI: 10.1306/D4267A69-2B26-11D7-8648000102C1865D

DANTAS, M.; TEIXEIRA, S. Origem das Paisagens. In: JOÃO, X., TEIXEIRA, S.; FONSECA, D. (org.) Geodiversidade do Estado do Pará. Belém: CPRM, 2013. p. 23–52.

DAVIES, J. L. A morphogenic approach to world shorelines. Zeitschrift für Geomorphologie, v. 8., p. 27–42, 1964. DOI: 10.1127/zfg/mortensen/8/1964/127

DHN. Tábua das Marés, 2020. Marinha do Brasil. Disponível em: <http://www.mar.mil.br>.

DIONNE, J. C. Towards a more adequate definition of the St. Lawrence estuary. Zeitschrift für Geomorphologie, v. 7, p. 36–44, 1963.

DYER, K. R. Sediment transport processes in estuaries. In: PERILLO, G. M. E. (org.). Geomorphology and Sedimentology of Estuaries. Ed. Amsterdam: Elsevier, 1995. p. 423–449.

DYER, K.R. Estuarine Hydrography and Sedimentation. Cambridge University Press, 1979. 239p.

ELLIOTT, M.; MCLUSKY, D. S. The need for definitions in understanding estuaries. Estuarine, Coastal and Shelf Science, v. 55, p. 815–827, 2002. DOI: 10.1016/j.ecss.2010.01.021

EL-ROBRINI, M.; RANIEIRI, L. A.; SILVA, P. V. M.; GUERREIRO, J. S.; ALVES, M. A. M. S.; OLIVEIRA, R. R. S.; SILVA, M. S. F.; AMORA, P. B. C.; EL ROBRINI, M. H.; FENZL, N. (2018). Pará. In: MUEHE, D. (org.). Panorama da erosão costeira no Brasil. MMA, Brasília: p. 66–166.

EMEKA, N. C.; ANTIA, V. I.; UKPONG, A. J.; AMAH, E. A.; NTEKIM, E. E. U. A study on the Sedimentology of tidal rivers: Calabar and Great Kwa, S. E. Nigeria. Sci. Res. (Seychelles), v. 47, p. 370–386, 2010.

FAPESPA. Fundação Amazônia de Amparo a Estudos e Pesquisas. Estatísticas Municipais Paraenses: Igarapé-Miri. Belém, 2016.

FITZGERALD, D. M.; BUYNEVICH, I. V.; FENSTER, M. S.; MCKINLAY, P. A. Sand dynamics at the mouth of a rock-bound, tide-dominated estuary. Sedimentary Geology, v. 131, p. 25–49, 2000. DOI: 10.1016/S0037-0738(99)00124-4

FRANÇA C. F.; SOUZA-FILHO, P. W. M; EL-ROBRINI, M. Análise faciológica e estratigráfica da planície costeira de Soure (margem leste da ilha de Marajó-PA), no trecho compreendido entre o canal do Cajuúna e o estuário Paracauari. Acta Amazonica, v. 37, p. 261–268, 2007. DOI: 10.1590/S0044-59672007000200013

FRANÇA, M. C.; COHEN, M. C. L.; PESSENDA, L. C. R.; ROSSETTI, D. F.; LORENTE, F. L.; BUSO JUNIOR, A. Á.; GUIMARÃES, J. T. F.; FRIAES, Y.; MACARIO, K. Mangrove

vegetation changes on Holocene terraces of the Doce River, southeastern Brazil. Catena, v. 110, p. 59–69, 2013. DOI: 10.1016/j.catena.2013.06.011

FREITAS, P. T. A.; SILVEIRA, O. F.; ASP, N. E. Tide distortion and attenuation in an amazonian tidal river. Brazilian Journal of Oceanography, v. 60, p. 429–446, 2012. DOI: 10.1590/S1679-87592012000400003

FURTADO, A. M. M.; PONTE, F. C. Mapeamento de Unidades de Relevo do Estado do Pará. Revista GeoAmazônica, v. 2, p. 56–67, 2013. DOI: 10.17551/2358-1778/geoamazonia.n1v2p56-67

GILMAN, E. L.; ELLISON, J.; DUKE, N. C.; FIELD, C. Threats to mangroves from climate change and adaptation options: A review. Aquatic Botany, v. 89, p. 237–250, 2008. DOI: 10.1016/j.aquabot.2007.12.009

GREGÓRIO, A. M. S.; MENDES, A. C. Characterization of sedimentary deposits at the confluence of two tributaries of the Pará River estuary (Guajará Bay, Amazon). Continental Shelf Research, v. 29, p. 609–618, 2009. DOI: 10.1016/j.csr.2008.09.007

GUIMARÃES, R. H. E. Influência da sazonalidade sobre as águas estuarinas dos furos da ilha de Colares (baía do Marajó). Dissertação (Mestrado em Geologia) - Programa de Pós-Graduação em Geologia e Geoquímica, Geociências, Universidade Federal do Pará, Belém. 2014. 114p.

GUJAR, A. R.; ANGUSAMY, N.; RAJAMANICKAM, G. V. Characterization of Opaques off Konkan Coast Maharashtra, Central West Coast of India. Journal of Minerals e Materials Characterization e Engineering, v. 6, p. 53–67, 2007. DOI: 10.4236/jmmce.2007.61005

HARRIS, P.; HEAP, A.; BRYCE, S.; PORTER-SMITH, R.; RYAN, D., HEGGIE, D. Classification of Australian clastic coastal depositional environments based upon a quantitative analysis of wave, tidal, and river power. Journal of Sedimentary Research, v. 72, p. 858–870, 2002. DOI: 10.1306/040902720858

HOITINK, A. J. F.; JAY, D. A. Tidal river dynamics: implications for deltas. Reviews of Geophysics, v. 54, p. 240–272, 2016. DOI: 10.1002/2015RG000507

HOOVER, M. D.; HURSH, C. R. Influence of topography and soil-depth on runoff from forest land. Transactions, American Geophysical Union, v. 24, p. 693–698, 1943. DOI: 10.1029/TR024i002p00693

HORTON, R. E. Erosional development of streams and their drainage basins: hydrophysical approach to quantitative morphology. Geol. Soc. Am. Bufl., v. 56, p. 275–370, 1945.

JAY, D. A.; SMITH, J. D. Circulation, density distribution and neap-spring transitions in the Columbia River Estuary. Progress in Oceanography, v. 25, p. 81–112, 1990. DOI: 10.1016/0079-6611(90)90004-L

JIANG, T.; SU, B.; HARTMANN, H. Temporal and spatial trends of precipitation and river flow in the Yangtze River Basin, 1961–2000. Geomorphology, v. 85, p. 143–154, 2007. DOI: 10.1016/j.geomorph.2006.03.015

KHADDOR, I.; ACHAB, M.; BEN JBARA, A.; ALAOUI, A. H. Estimation of Peak Discharge in a Poorly Gauged Catchment Based on a Specified Hyetograph Model and Geomorphological Parameters: Case Study for the 23–24 October 2008 Flood, KALAYA Basin, Tangier, Morocco. Hydrology, v. 6, p. 1–13, 2019. DOI: 10.3390/hydrology6010010

KJERFVE, B.; MAGILL, K. E. Geographic and hydrodynamic characteristics of shallow coastal lagoons. Marine Geology, v. 88, p. 187–199, 1989. DOI: 10.1016/0025-3227(89)90097-2

KRIAUCIUNIENE, J.; MEILUTYTE-BARAUSKIENE, D.; REIHAN, A.; KOLTSOVA, T., LIZUMA, L.; SARAUSKIENE, D. Variability in temperature, precipitation and river discharge in the Baltic states. Boreal Environment Research, v.17, p. 150–162, 2012.

LESACK, L. F. W.; MARSH, P.; HICKS, F. E.; FORBES, D. L. Timing, duration, and magnitude of peak annual water-levels during ice breakup in the Mackenzie Delta and the role of river discharge. Water Resour. Res., v. 49, p. 8234–8249, 2013. DOI: 10.1002/2012WR013198

LIMA, R. R.; TOURINHO, M. M.; COSTA, J. P. C. Várzeas flúviomarinhas da Amazônia brasileira: características e possibilidades agropecuárias. Belém: FCAP. SDI, 2001. 342p.

MACPHERSON, L.; HAIGH, I.; PATTIARATCHI, C. Coastal flooding in the Peel Harvey Estuary and the effects of mean sea level rise. In: Proceedings of the 20th Australasian Coastal and Ocean Engineering Conference and the 13th Australasian Port and Harbour Conference: diverse and developing. Barton ACT: Australia. 2011. p. 446–451.

MASCARENHAS, A. C. C.; CORREA, A. W. R.; CARNEIRO, A. C.; COSTA, M. S.; ROLLNIC, M.; MEDEIROS, C. Seasonal Exchanges of Salt and Suspended Particulates between the Sol Bay and the Pará River, Amazonian Coast. Journal of Coastal Research, v. 85, p. 111–115, 2018.

MORAES, B. C.; COSTA, J. M. N.; COSTA, A. C. L.; COSTA, M. H. Variação espacial e temporal da precipitação no estado do Pará. Acta Amazônica, v. 35, p. 207–214. 2005. DOI: 10.1590/S0044-59672005000200010

NICHOLS, M. M.; BIGGS, R. B. Estuaries. In: Davis R. A. (org.). Coastal sedimentary environments. New York: Springer-Verlag, 1985. p. 77–186.

PIRATOBA, A. R. A.; RIBEIRO, H. M. C.; MORALES, G. P.; GONÇALVES, W. G. Caracterização de parâmetros de qualidade da água na área portuária de Barcarena, PA, Brasil. Revista Ambiente & Água, v. 12, p. 435–456, 2017. DOI: 10.4136/ambi-agua.1910

PRESTES, Y.O.; ROSÁRIO, R. P.; ROLLNIC, M.; SOUZA, M. Volume transport in the tidal limit of the Pará River, Brazil. Proceedings of the 17th Physics of Estuaries and Coastal Seas (PECS): Porto de Galinhas. 2014. p. 19–24.

QUEIROZ, J. A. L.; MACHADO, S. A.; HOSOKAWA, R. T.; SILVA, I. C. Estrutura e dinâmica de floresta de várzea no estuário amazônico no estado do Amapá. Floresta, v. 37, p. 339–352, 2007.

RAMOS, C. A. R. Qualidade ambiental, distribuição e densidade do Mesozooplâncton do estuário de Guajará-Miri, Vigia de Nazaré, NE do Estado do Pará. Dissertação (Mestrado em Ciência Animal) – Programa de Pós-Graduação em Ciência Animal, Universidade Federal do Pará, Belém. 2007. 126p.

RAWLS, W. J.; AHUJA, L.R.; BRAKENSIEK, D.; SHIRMOHAMMADI, A. Infiltration and soil water movement. In: MAIDMENT, D. (org.), Handbook of Hydrology. New York: McGraw-Hill, 1993. p. 1–5.

REINECK, H-E., SINGH, I. B. Depositional Sedimentary Environments. Second ed. New York: Springer-Verlag, 1980. 543p.

RIBEIRO, S. R.; BATISTA, J. E. L.; COHEN, M. C. L.; FRANÇA, M. C.; PESSENDA, L. C. R.; FONTES, N. A.; ALVES, I. C.C.; BENDASSOLLI, J. A. Allogenic and Autogenic Effects on Mangrove Dynamics from the Ceará Mirim River, North- eastern Brazil, during the Middle and Late Holocene. Earth Surf. Process. Landforms, v. 43, p. 1622–1635, 2018. DOI: 10.1002/esp.4342

RIBEIRO, S. R.; VALADÃO, R. C. Processos fluviomarinhos associados à formação da Ilha Rasa, Sul da Baía de Marapatá, Nordeste do Pará, Brasil. Arquivos de Ciências do Mar, v. 53, p. 110–119, 2020. DOI: 10.32360/acmar.v53iEspecial.42659

ROSÁRIO, R. P.; BORBA, T. A. C.; SANTOS, A.S.; ROLLNIC, M. Variability of Salinity in Pará River Estuary: 2D Analysis with Flexible Mesh Model. Journal of Coastal Research, v. 75, p. 128–132, 2016

SANTOS, L. A. S. Modelagem numérica da dinâmica do sistema estuarino Caravelas-Peruíbe, BA. Dissertação (Doutorado em Oceanografia) - Programa de Pós-Graduação em Oceanografia, Universidade de São Paulo, São Paulo. 2010. 85p.

SCHUBEL, J. R.; HAYES, M. O.; PRITCHARD, D. W. The estuarine environment: estuaries and estuarine sedimentation. Washington: American Geological Institute, 1974.

SOUZA-FILHO, P. W. M., EL-ROBRINI, M. Morfologia, processos de sedimentação e litofácies dos ambientes morfo- sedimentares da planície costeira Bragantina, nordeste do Pará, Brasil. Geonomos, v. 4, n. 2, p. 1–16, 1996. DOI: 10.18285/geonomos.v4i2.197

SILVA, C. S.; VIÉGAS, D. R.; SOUZA, E. C.; BARBOSA, C. C.; SILVA, A. S. Avaliação de salinidade, condutividade elétrica, sólidos totais dissolvidos e potencial de oxidação/redução das águas superficiais do rio Maratauíra-Abaetetuba-PA. In: XIV Encontro de Profissionais da Química da Amazônia, 2015, Belém. Anais... Belém: 2015. p. 1–6.

SOUZA-FILHO, P. W. M.; LESSA, G. C.; COHEN, M. C. L.; COSTA, F. R.; LARA, R. J. The subsiding macrotidal barrier estuarine system of the eastern Amazon coast, Northern Brazil. In: DILLENBURG, S. F.; HESP, P. A. (org.). Geology and Geomorphology of Holocene coastal barriers of Brazil. New York: Springer-Verlag, 2009. p. 347–376.

SPEER, P. E.; AUBREY, D. G. A. study of non-linear tidal propagation in shallow inlet/estuarine systems. Part II: Theory. Estuarine, Coastal and Shelf Science, v. 21, p. 207–224. 1985. DOI: 10.1016/0272-7714(85)90096-4

THAMPANYA, U.; VERMAAT, J. E.; SINSAKUL, S.; PANAPITUKKUL, N. Coastal erosion and mangrove progradation of Southern Thailand. Estuarine, Coastal and Shelf Science, v. 68, n. 1-2, p. 75–85, 2006. DOI: 10.1016/j.ecss.2006.01.011

VRIEND, H. J. Advances in morphodynamics of tidal rivers and estuaries. In: International Conference on Estuaries and Coasts, 2003, Hangzhou. Proceedings… Hangzhou: IRTCES, 2003. p. 3–10. ISBN 7-900662-67-7.

WANG, W.; YAN, Z.; YOU, S.; ZHANG, Y.; CHEN, L.; LIN, G. Mangroves: obligate or facultative halophytes? A review. Trees, v. 25, p. 953–963, 2011. DOI: 10.1007/s00468-011-0570-x

WELLS, J. T. Tide-dominated estuaries and tidal rivers. In: PERILLO, G. M. E. (org.). Geomorphology and Sedimentology of estuaries. Amsterdam: Elsevier, 1995. p. 179–205. DOI: 10.1016/S0070-4571(05)80026-3

WRIGHT, L. D.; COLEMAN, J. M.; THOM, B. G. Process of channel development in a high-tide range environment: Cambridge Gulf–Ord River Delta, Australia. Journal of Geology, v. 81, p. 15–41, 1973. DOI: 10.1086/627805

CHAPTER 2:

SPATIAL AND TEMPORAL PATTERNS OF COASTAL DRAINAGE REARRANGEMENT BY LARGE TROPICAL RIVERS IN A PASSIVE MARGIN SETTING

Abstract – Rearrangements involving tropical fluvial systems sheltered in the passive margin are well documented; however, few studies have investigated rivers whose rearrangement directly affects the coastal landscape. In the coastal environment, the records of sea-level changes and tectonics, may be superimposed by estuarine dynamics, thus hindering the understanding of this phenomenon and its mechanisms. Based on well drilling records, sediment cores, tectonic indicators, and 14C-dating, herein, we approach the paleogeographic mouth history of the Tocantins River, considering it as an opportunity to describe the coastal rearrangements on a spatiotemporal scale and their final products. The results suggest that the Tocantins was an Amazon Basin tributary until the Late Pleistocene, when it diverged from the Amazon River and opened a new eastern pathway towards the Atlantic Ocean. The laterite layer offset overlapping the sedimentary succession was consistent with the subsidence events after fluvial rearrangement. This succession comprises fining-upward sequences assigned to tidal channel infilling, related to the estuarine environment. Tocantins' seaward mouth imposition drove the coastal landscape. First, the Maratauíra incised valley opened; consequently, a land tract that started to detach from the mainland during the middle Holocene was wholly separated after 700 cal a BP. Data indicate that tectonics and sea-level change caused the significant paleogeographic development until ~1490 cal a BP, while estuarine dynamics took the most part in the tardy evolution. These results demonstrate that island building is a product of drainage rearrangement; likewise, they reveal the influence of tectonics until the last millennium affecting late Holocene deposits. Therefore, these findings suggest that the coastal history of the Tocantins, including the onset of new mouths and opening of incised valleys, is possibly distinct among the documented river rearrangements.

Keywords: Estuarine sedimentary records; Holocene tectonics; Island morphogenesis; Sea-level change.

1. Introduction

Rivers are routinely depicted as primary agents of landscape development. The lowering of topography and minor landforms carved over Earth's surface have been ascribed to streams (e.g., Campbell et al., 2006; Caputo and Soares, 2016; Hoorn et al., 2010; Pupim et al., 2015; Valadão, 2009). Fluvial action that drives changes in the landscape has a geomorphic threshold that, when exceeded during high-magnitude events, leads to river adjustments (Lorang and Hauer, 2017). Local adjustments may be shared by the changes generally synchronic – or not – performed along its fluvial course, as several environmental forces regulate the river

equilibrium, such as tectonics (Cunha et al., 2005; Whitfield and Harvey, 2012), climate effects (Preece and Bridgland, 1999; Whittaker, 2012), relative sea-level (RSL) changes (Wenzens and Wenzens, 1997), and estuarine processes (Shimozono et al., 2019). Consequently, an adjusted fluvial system can provide a variety of responses involving channel avulsion, capture, and the lateral migration of meandering.

Conditioned by any of these forces, the river pathway can constantly rearrange over time, irrespective of the setting that shelters itself, as documented from the semiarid and tropical (Neagu et al., 2020; Rossetti and Góes, 2008; Wickert, 2016) upward to temperate and glacial environments (Cienciala et al., 2020; Peña-Monné and Sampietro-Vattuone, 2020), portraying the diffuse character on the surface. Naturally, the rearrangement outcome overreaches the organization of the physical features of the landscape, influencing biogeographical components. For instance, the rearrangements caused by the uplift of hills and vertical movements from eastern South America, which ensued during Africa's break-up, formed river barriers that isolated and refugia aquatic organisms upland. Otherwise, the denudation process and lowering blocks captured the adjacent upland drainage and promoted biotic diversification among fish species (Ribeiro, 2006). In the Amazonian lowlands, drainage rearrangement has been ascribed as a part of the genetic diversity in avian and fish species due to the disconnection of the Atlantic tributaries from the continental realm drainage (Barreto et al., 2022; Lovejoy et al., 2006; Hoorn et al., 2010; Wilkinson et al., 2009). Therefore, if the primary interest in fluvial rearrangement is gathering evidence to enhance paleogeographic reconstructions, secondarily, it may serve as a key to aid in biogeographical and biologic-faunal knowledge evolution at a comprehensive scale.

Along the passive setting margin, many rivers have frequently held an evolutionary past that is barely explained by the design of its contemporary drainage network. These riverine evolutions are associated with relatively dormant mechanisms, revealing that intraplate tectonic reactivation and climate change have depicted the primary forces behind the drainage changes (Antoine et al., 2000; Avşin et al., 2019; McLaren et al., 2011; Schoenbohm et al., 2004; Soria-Jáuregui et al., 2018). However, there are only a few studies related to rivers, whose rearrangements have coastal landscape implications, and a sector in which RSL change coupled with tectonics (allogenic force) designates the trend and mechanism of the rearrangement process. Consequently, understanding the phenomenon has been hampered, further limiting the achievement of analogous potential.

One of the reasons for the lack of investigations may be attributed to the difficulty of integrating the impact transferred to the littoral by fluvial adjustment owing to the dynamic

estuarine (autogenic force) that fosters tidal channel migration on a local scale in a short duration (Ribeiro et., 2018; Shimozono et al., 2019). These local effects may be superimposed on regional effects, challenging the isolation of the consequences of fluvial adjustments from estuarine processes. Another snag lies in the tidal influence, mainly in meso-macrotidal estuaries. The tidal cycle generates a wide range of deposits (such as sand bars, muddy flats, and lateral accretion). Although internally produced, this autogenic influence can drastically change the landscape as a result of allogenic forces (Beerbower, 1964; Cecil, 2013; Kim et al., 2014). Thus, unraveling river rearrangements that reach the coast entails both time-and spatial-scale patterns, processes, and products that must not be disregarded.

In this study, we examined the paleogeographic history of the Tocantins River, focusing on its mouth, lying along the coast. Some studies have suggested that the Tocantins River flows northwestward, instead of northeasterly (e.g., Ab'Sáber, 2000; Bemerguy and Costa, 1991; Costa et al., 2001, 1996; Rossetti and Valeriano, 2007; Soares Júnior et al., 2011), and is likely connected to the Amazon River. The most striking evidence for this interpretation derives from the residual fan-shaped morphology along its lower course; however, no comprehensive study has investigated the development of this structure, and its sedimentary deposit origin remains unknown. In addition, the widespread occurrence of islands in the lower course and mouth is a striking characteristic of this river, leading to a paramount questionnaire about the role of these islands in the drainage rearrangement scope. Therefore, the Tocantins River provides an opportunity to describe coastal rearrangements at different time and spatial scales, with their products preserved alongside their valleys and estuarine mouths. Eleven stratigraphic profiles, including well drilling records (5) and sediment cores (6), were obtained, and several questions were addressed: a) how the Tocantins River affected the coastal eastern Amazon paleogeography draw; b) it formed alluvial fans during its fluvial adjustment; c) the islands alongside its mouth have counterparts in this process; d) the tectonics, sea-level changes, and estuarine process events may be adequately recognized, and if their influence may be isolated in time space.

2. Physiography and Geological background

As a mesocontinental tropical river, the Tocantins extend from the Brazilian Central Plateau to the Pará River on the Amazonian coast, covering approximately 1960 km (MMA, 2006). Its mean discharge is approximately 10,900 $m^3.s^{-1}$ (ANA, 2020; Prestes et al., 2020) with a maximum suspended sediment value of 112.8 $mg.L^{-1}$ during the rainy period, and the flow velocity reaches a peak of 0.93 m/s (Costa, 2014). Extensive island systems occur alongside

littoral zones, mainly between Amazon, Pará, and Tocantins River mouths; that are part of a young geological system, often assigned to the Late Pleistocene-Holocene (Ab'Sáber, 2000; Barbosa et al., 1974. The islands were established on lower Tocantins, with an unknown origin, especially those set alongside its mouth (Fig. 1d), termed the Insular Complex of West Abaetetubense (CIOA) (Ribeiro and Valadão, 2021).

The CIOA occupies an area of 410 km^2 and presents an irregular parallelogram shape attributed to two pairs of rivers running slightly parallel towards it. The Tocantins and Maratauíra rivers comprise the former with the SSW-NNE direction, whereas the Pará and Maiauatá rivers with the SW-NE trending form the latter. This entire sector is inserted in the Pará River Upper Estuary (ESP) (Fig. 1b–d), characterized by semidiurnal micro-to mesotidal, but without saline intrusion (< 0.5%). Due to this characteristic of tidal control and virtually non-existent salinity, water bodies from the ESP are categorized as tidal rivers (Ribeiro and Valadão, 2021).

The Tocantins-Maratauíra mouth morphology is constituted mainly through the fluviomarine plain with elevations up to 5 m (Fig. 1d). It is prone to regular flooding by a mesotidal that may reach 3.78 m during the spring tidal. This area is covered mainly by pioneer vegetation, while "Terra Firme" vegetation is present across the supratidal zone towards the highest topography (Ribeiro and Valadão, 2021). Pleistocene terraces (5-10 m) separate the fluviomarine plain of the highest morphological unit in this sector, termed as the Plateau, whose surface is poorly dissected (Fig. 1d) (Furtado and Ponte, 2013). This landform is widespread over the extensive area of the continental realm and exhibits the tallest geomorphological features up to 30 m elevation. The climate is warm and humid tropical, with a mean annual temperature of 27ºC and a mean annual precipitation of about 2700 mm (FAPESPA, 2016). A drier period of lower rainfall occurs between July and December, followed by a rainy season during January and June, influenced by the Intertropical Convergence Zone (ITCZ) (Souza-Filho et al., 2009).

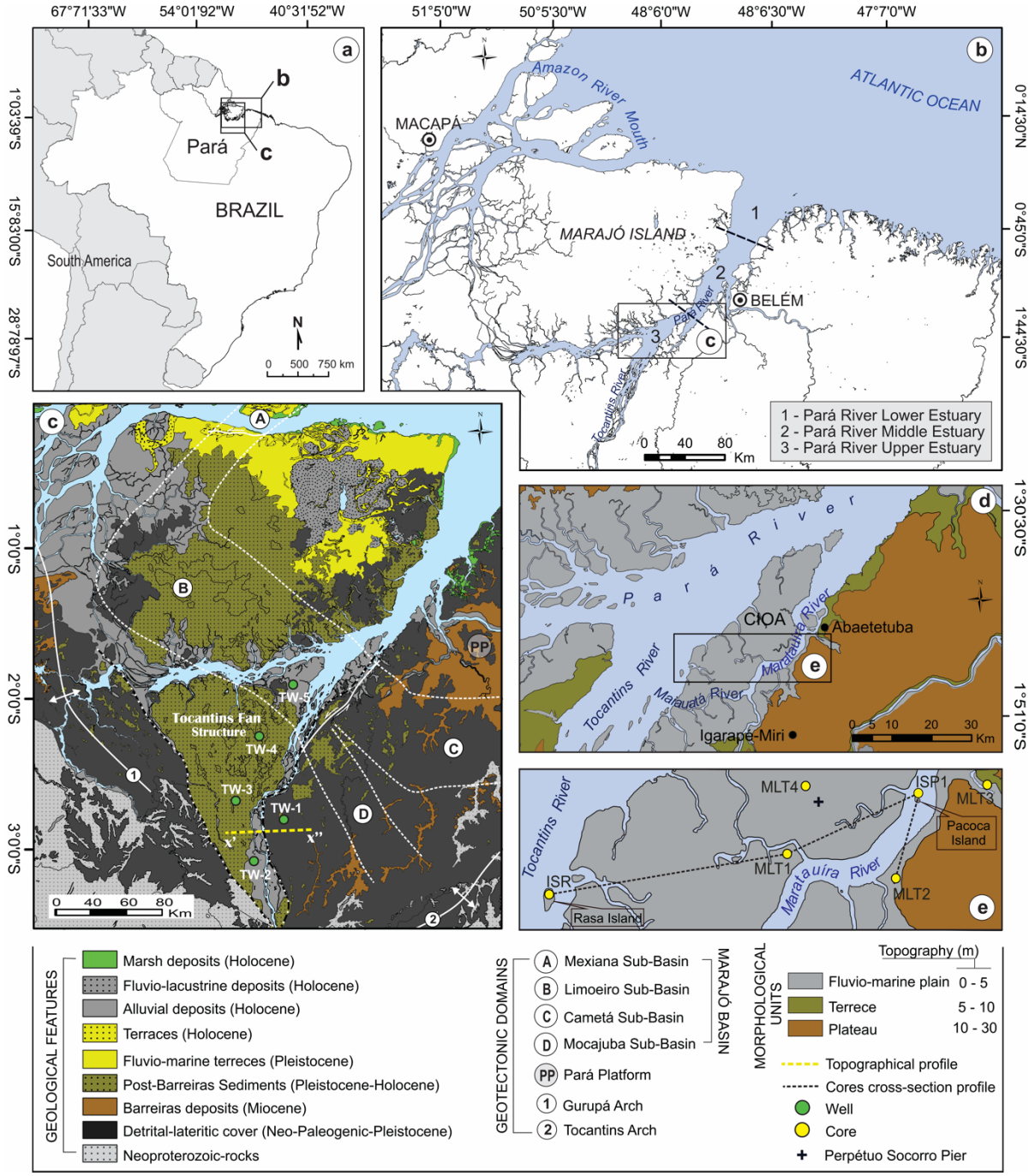

Figure 1. Study area on the northern coast (b) detached from the Brazilian territory (a). The geological context, geotectonic framework, and well drilling location at the Tocantins River valley are indicated, including Marajó Basin limits (dashed white line), and Tocantins Fan (dashed black-white line) (c). Spatial distribution of main morphological features (d) and sampling site alongside the Tocantins and Maratauíra rivers mouths (e).

Geologically, this sector is inserted almost entirely in the Limoeiro sub-basin (LsB), one of the four sub-basins incorporated by the Marajó Basin. The other part lies on the Pará platform (Fig. 1c). The Marajó Basin is limited from Pará platform by the Gurupá arch to the west-southwest and the Tocantins Arch to the northeast (Fig. 1c) (Villegas, 1994). The tectonic structure of the LsB results from the NW-SE trend in the central portion of the Marajó Basin

and its southern and northern boundaries, with the Mexiana and Cametá sub-basins defined by the Arari and Tocantins strike-slip fault zones, respectively. LsB consists of a sedimentary pile approximately 16,000 m thick (Zalán and Matsuda, 2007). Bottom-to-top sandstones, claystones, and shales represent this succession; conglomerates of the Breves/Jacarezinho Formations (Aptian-Cenomanian); sandstones, conglomerates, and claystones of the Anajás Formation (Early Cretaceous); and sandstones, conglomerates, and claystones of the Limoeiro Formation (Late Cretaceous) (Costa et al., 2002). Presence of these units have been attributed to the depositional environments ranging from the fluvial to shallow marine (Villegas, 1994). Deposits overlie this succession, mixed with siliciclastic carbonates of the Marajó Formation (Paleocene-Eocene), followed by sandstones and mudstones of the Tucunaré and Pirarucu Formations (Quaternary) (Rossetti and Góes, 2008). Transitional to shallow marine depositional settings were assigned to these deposits (Costa et al., 2002; Rossetti et al., 2008ab; Rossetti and Góes, 2008).

The northmost CIOA area is inserted in the Pará platform (Fig. 1c), a geotectonic domain, which corresponds to crystalline and Paleozoic rocks with small tectonic subsidence zones, overlaid by Neogene deposits of the Pirabas/Barreiras formations and post-Barreiras sediments. From bottom to top, the Pirabas Formation (Oligocene–Early Miocene) consists of limestones, laminated mudstones, and calciferous sandstones (Ferreira, 1977) attributed to the inner shelf, lagoon, and mangrove depositional environments (Arai et al., 1998; Góes et al., 1990). The Barreiras Formation (Miocene/middle Miocene) consists of deposits of conglomerate, sandstone, and claystone (siliciclastic non-fossiliferous) derived from a transitional environment (estuarine) (Rossetti et al., 1989). The Barreiras Formation is unconformably overlain by aeolian and fluvial-estuarine sand and mud sediments of the Late Pleistocene and Holocene ages, widely termed as post-Barreiras sediments (Tatumi et al., 2008), which infill the Tocantins fan structure, followed by alluvial deposits (Holocene) represented by clay, silt, and sandy. It is noteworthy that for a large part of this regional geology, tops of plateaus are covered by lateritic rock (Paleogene-Early Quaternary) originated from weathering (Costa, 1991). In contrast, on the lower topography, lateritic deposits distributed in riverbank outcrops commonly overlain post-Barreiras sediments, further overlain by the Holocene deposits (Ribeiro and Valadão, 2021).

3. Materials and Methods

3.1 Remote Sensing

This study used stratigraphic and chronological data combined with morphostructural and topographical indicators. Morphostructural and topographic data were obtained from the Advanced Land Observing Satellite (ALOS) through the Alaska Satellite Facility (ASF) (http://search.asf.alaska.edu). The ALOS satellite utilizes the sensor Phased Array L-type band Synthetic Aperture Radar (PALSAR), which collects day-and-night land observations. The PALSAR sensor aids in achieving high-resolution DEM products because its active microwave sensor (L-band 1.27 GHz) can avoid weather barriers, irrespective of day or night. The dataset consisted of radiometric terrain corrected images with polarization mode HH (RT1) at 12.5 m resolution. The DEM was used to extract lineaments based on the visual analysis. These lineaments were correlated with the features previously reported by the Geological Survey of Brazil (CPRM) (http://geobank.sa.cprm.gov.br). DEMs were geometrically corrected, filtered, and patterned using SIRGAS 2000 as the reference datum. After fieldwork, other minor lineaments were manually fixed and vectorized on the DEMs. The spatial distribution of lineaments and their dies was obtained from the Stereonet Program (https://visiblegeology.com/stereonet). Along with these products, cartographic data consisting of shapefiles (hydrography, geology, geomorphology, and vegetation) obtained from the Brazilian Institute of Geography and Statistics (IBGE) (http://www.ibge.gov.br/geociencias/downloads-geociencias) were integrated into the radar database. All analyses were performed using a GIS environment (ESRI ArcGIS software, v. 10.2®).

3.2 Fieldwork and sample processing

Fieldwork was carried out (December-2018, January-2019, and January-2021) to collect six sediment cores: two from the CIOA center (MLT1 and MLT4), two from the CIOA proximal islands (ISP1 and ISR), and two from the mainland sector (MLT2 and MLT3). The core depth ranged from 1.9 to 5.5 m (Table 1) and the cores were collected using a Russian sampler from the estuarine flats. The sediment core topography was defined based on the local reduction level measured in the Perpétuo Socorro Pier, localized in the CIOA (Ribeiro and Valadão (2021) (Fig. 1e). In addition to core samples, data from the five wells drilled at 18 to 60 m depths were also included in the study. The wells were drilled within the inner Tocantins Valley adjacent to its current course. Well geological profiles were obtained from the Geological Survey of Brazil and the Groundwater Information System. In this study, well drilling records complement the sediment cores. The well drilling records may help to

understand the long-term features of the sedimentary infill of the lower Tocantins River, whereas the sediment cores are the basis for the study related to its mouth (Fig. 1c–d).

Table 1. Summary of sediment cores and well drilling with their respective geographical coordinates and depth.

Core	Geographical Coordinate	Depth (cm)	Well	Geographical Coordinate	Depth (m)
MLT1	S1°47'10.57"/W49°0.10'6"	550	WT-1	S2°42'53"/W49°36'23"	18
MLT2	S1°48'11.47"/W48°56'39"	550	WT-2	S3°00'59"/W49°44'57"	45
MLT3	S1°45'4.06"/W48°52'28"	250	WT-3	S2°45'00"/W49°46'52"	34
MLT4	S1°45'21.86"/W49°0.2'40"	195	WT-4	S2°14'24"/W49°03'33"	40
ISP1	S1°45'22.06"/W48°55'48"	550	WT-5	S1°53'46"/W49°23'10"	60
ISR	S1°48'33.58"/W49°8'43.9"	410			

3.3 Facies description core and well drilling

Facies analysis was undertaken, including a description of color (Munsell Soil Color Charts, 2009), texture, and structure, following the methods reported by Walker (1992). Similarly, macroscopic analysis of surface sediments was performed, recording sandy sediment size, sorting, and rounding. Concerning the well drilling, the lithofacies were defined based on the drillers' lithology descriptions, including type, sample texture, color, and grain size and architectures. According to Miall (1978), sedimentary facies were grouped into facies associations. These facies associations are genetically related and have identical environmental significance; thus, they are diagnostic of a particular sedimentary environment (Reading, 1996). Therefore, facies integration and their architectural elements, emphasizing strata distribution and bounding surfaces, represent a widely used technique (Miall, 1994). This helps to deduce the depositional scenarios, including their interconnections in space and time, and hence achieve more realistic paleoenvironmental reconstructions**.**

3.4 Radiocarbon dating

Six bulk samples (approximately 10 g each) along the MLT1 (CIOA) and MLT2 (Mainland) sediment cores were selected for dating. This selection was based mainly on the deposit discontinuity, sediment nature, texture, and color. The samples were subjected to DirectAMS. A chronological framework for the sedimentary samples was provided by accelerator mass spectrometry (AMS) dating at DirectAMS Laboratory (Bothell). Radiocarbon ages were normalized to a $\delta^{13}C$ value of 25‰ VPDB and reported as calibrated years (cal yr BP, 2σ) using CALIB 8.2 and the SHCal20 curve (Hogg et al., 2020). The dates are reported in the text as the median of the range of calibrated ages (Table 1).

4. Results

4.1 Radiocarbon dates and sedimentation rates

The radiocarbon dates are presented in Table 2. No age inversions were observed. The estimated sedimentation rates were determined based on the thickness of the deposits and their numerical ages, revealing nonlinear rates of accumulation (millimeter/year) between the dated points. Sedimentation rates were relatively higher in the CIOA (0.7 mm/yr) than in the eastern mainland sector (0.6 mm/yr). For the CIOA, accumulation rates are 0.2 mm/yr (550–413 cm), 3 mm/yr (413–213 cm), and 2.7 mm/yr (213–0 cm) core MLT1. In turn, the mainland exhibits accumulation rates of 0.6 mm/yr (550–447), 0.4 mm/yr (447–287 cm) and 1.8 mm/yr (287–0 cm) at the core MLT2 (Fig. 3).

Table 2. Sediment samples selected for radiocarbon dating with laboratory number, code core/depth, 14C yr BP and calibrated (cal) ages.

Laboratory Number (D-AMS)	Sample	Depth (cm)	Age BP	Ages (Cal yr BP, 1σ)	Ages (Cal yr BP, 2σ)	Median Probabilily
038503	MLT1–peat	213	854 ± 25	686–699	680–709	700
038502	MLT1–peat	413	1591 ± 31	1405-1428	1401–1483	1430
038501	MLT1	550	7215 ± 34	7970–8011	7944–8022	7990
044419	MLT2–peat	287–290	1633 ± 30	1475-1526	1448-1530	1490
046399	MLT2	447	5902 ± 28	6693-6732	6630–6747	6690
038504	MLT2	550	7661 ± 38	8389–8419	8374–8452	8410

4.2 Core facies description

The six sediment cores consisted of muddy, sandy, and peat deposits. In general, sandy deposits present a heterolithic internal structure. In contrast, the mud-dominated portions are heterolithic with sand lenses, followed by the parts without any clear sedimentary structures. Peat deposits mainly consisted of well-decomposed fibers rather than younger vegetable roots. These deposits are partially organized into fining-upward deposits (MLT3, MLT4, and ISR; Fig. 3). Eight facies were identified along the cores based on the internal sedimentary structures, organic content, sediment texture and color, and contact relationships. They were grouped into three facies associations namely Tidal channel (FAC), Tidal flat (FAF), and Swamp mix estuarine flat (FAS). The overall characteristics are summarized in the Table 3.

4.2.1 Facies Association Tidal channel (FAC)

This unit was sand-dominated and occurred at the intervals of 250–190 cm (MLT3), 195–158 cm (ISP1), and 410–330 cm (ISR). It consisted of massive sand (Sm), cross-stratified sand (Scs), flaser heterolithic bedding (Hf), and inclined heterolithic stratification (HIS) facies (Figs. 2 and 3). These deposits often occur at the base of these cores and are organized into fining-

upward successions. The moderately sorted massive sand (Fig. 2g) supports the well-sorted cross-stratified, inclined sand interbedded by mud, overlain by flaser bedding, or minor components of the wave-drape structures (Fig. 3). The continuous sand layer retarded the sampling process, with the equipment penetrating to a maximum thickness of 1.9 m (MLT4), 2.5 m (MLT 3), and 4.1 m (ISR). Locally, some facies structures of unidirectional cross-low angles have millimetric mud films inside (Fig. 2a). Likewise, on the mud interbedded in variable proportions, with thicknesses ranging from millimeter to 1.6 centimeter thick beds, there is no clear indication of the erosional surface between sand and mud bed (Fig. 2b). The typical facies of this association have bed forms linked to the migration of ripples by unidirectional flows (Scs) and high-energy alternation in a subaqueous (IHS) bed migration environment. Diagnostic low flow regime, with the absence of energy for the deposition in portion lenses of muds (Hf) (Fig. 2c) and drapes muddy wave (Hw) into the sand succession were found in the FAC (Figs. 2e and 3; Table 3).

4.2.2 Facies Association Tidal flat (FAF)

Comprised mainly by mud dominance, the FAF occurred between 550–413 cm and 212 –0 cm (MLT1), 550–292 cm and 93–0 cm (MLT2), 135–0 cm (MLT3), 109–31 cm (MLT4), 550–350 cm and 155–0 cm (ISP1), and 260–0 cm (ISR) (Fig. 3). The facies group consists of massive mud (Mm), lenticular heterolithic bedding (Hl), and wavy heterolithic bedding (Hw). Massive facies (structureless) may occasionally present plane-parallel muddy features (Fig. 2f). This contrasts with a succession comprising interbedded organic mud with sand, forming a wide variety of intercalation rhythmites varying from millimeter-thick beds (Hw) and laminae mud drapes (Hl) (Fig. 2e). These bedform facies are linked with the energy flow environment to deposition from suspension and alternating traction force to sand deposition. In the cores in which FAT also occurs in the uppermost part, as such MLT1, MLT2, MLT3, ISP1 and ISR, the mud often presents oxidized, with a dark yellow color and brown spots. The profile of bioturbation increasing upwards is characteristic of these deposits. The FAF is laterally extensive and occurs across the sampled sectors. Because of the stacked sequences in such a bedding rhythmic type, this facies group was assessed to be genetically related to the tidal flats (Fig. 3; Table 3).

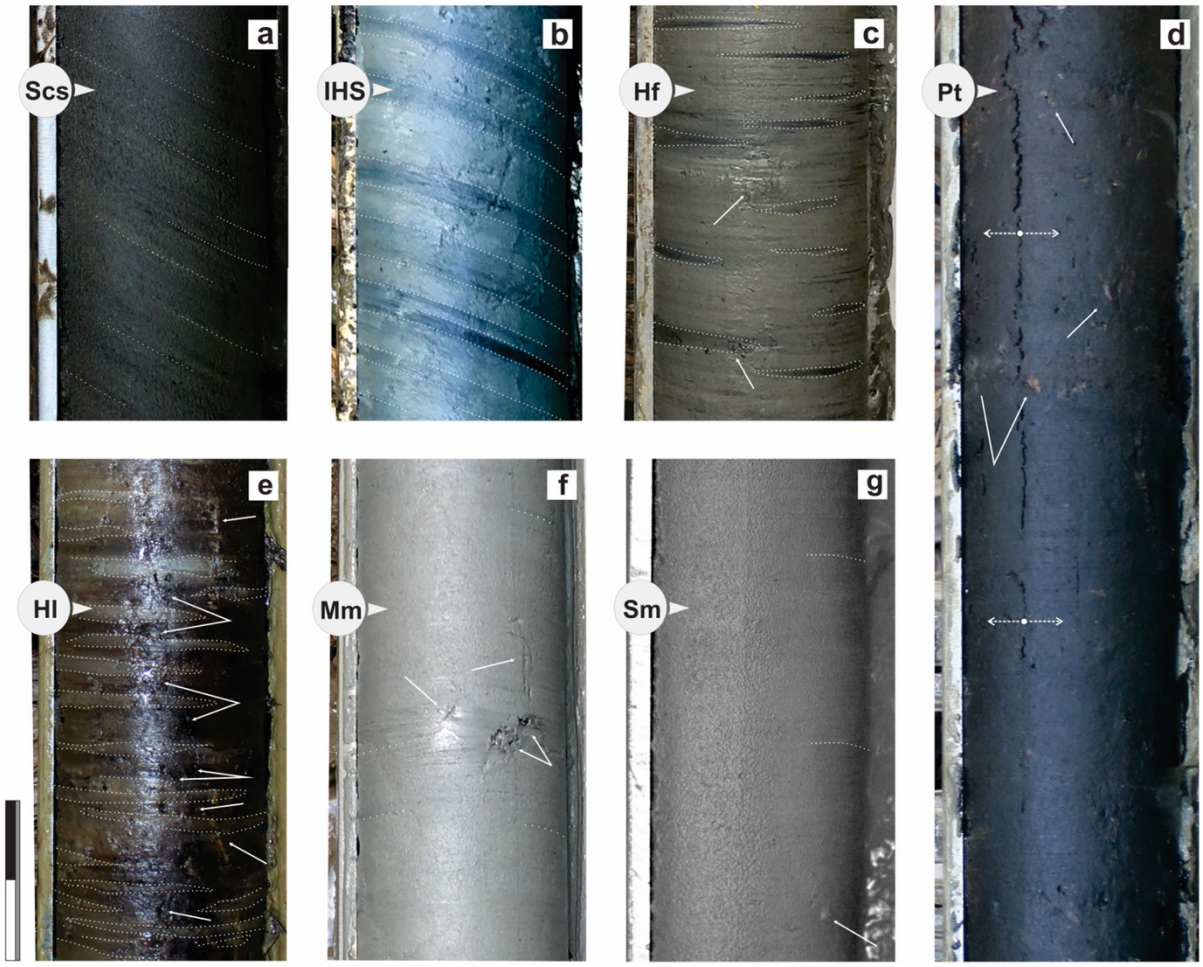

Figure 2. Holocene sedimentary beddings and internal structures from the estuarine deposits sampled alongside the Insular Complex, at the Tocantins and Maratauíra rivers mouths. (a) Unidirectional cross-stratified sand (Scs) presenting relative symmetry, reaching 25º angle. This sandy deposit exhibits from medium to fine grain size, with parallel lamination in muddy films (white line dashed). (b) Sand and mud alternation forming inclined heterolithic stratification (IHS), with low-angle (~14º). Dashed white lines contour indicated mud strata. (c) Flaser facies comprises millimetric muddy lenses (white line contour) within the sediments packages sand-dominated very fine. (d) Peat deposits preserved, occasionally contend younger roots (arrow). A crack propagates from the top to bottom (arrow divergent), indicating the less cohesive character upwards due to increasing partially decomposed fibrous network. (e) Succession deposits variant from lenticular structure (Hl) to wavy (Hw) tidal rhythmic forms interbedded in variable proportions. Predominant black mud-organic contrasts with a very fine sand bed were found in these facies (outline by the dashed white line). (f) Massive mud (Mm) and (g) Massive sand (Sm) facies. Locally, these massive deposits may present some plan-parallel structure (dashed white line). White arrows indicate features assigned to bioturbation regardless of the processes (roots marks, benthonic dwelling, roots, or leaves).
Vertical scale-bar: 4 cm. Sample diameter: 5 cm

4.2.3 Facies Association Swamp mixed estuarine flat (FAS)

This facies association consists mainly of a thick peat layer with abundant woody roots and root marks, present at MLT1 (413–212 cm), MLT2 (292–93 cm), and ISP1 (530–155 cm) (Fig. 3). Facies heterolithic bedding with sandy lenses that reach 40 cm in thickness between the peat deposits at core MLT2 completes this succession. The peat layer appears to have a relatively similar thickness among these three core sectors (Fig. 3). Although the present peat

is well-decomposed, fibers and younger roots may be recognized (Fig. 2d). The FAP has a wide geographical range (Supplementary Data), which makes the peat deposit an indicator of a common depositional setting, often saturated, and characterized by low oxygen content (anaerobic conditions), resulting in a thick peat layer due to the accumulation of organic matter. This can be related to swamp mixed estuarine flats resulting from similar genetic links and environmental processes. Remarkably, their organic content lacks palynological analysis to be undertaken in the future work that might resolve the issue related to peat origin and its paleoenvironmental significance.

4.3 Well drilling description

The sediment consisted mainly of the very fine to medium sand, followed by clay. In contrast with cores, the degree of detail in well-drilling records is variable as there is no handbook for lithological descriptions to which water well drillers must adhere. Thus, the textural lithology provides a more reliable degree of the details. Frequently mentioned colors included ‘reddish-white’ to ‘reddish-yellow,’ ‘greenish-yellow,’ ‘variegated,’ and ‘dark gray.’ The descriptions of clay and sand were standardized, irrespective of the absence of sedimentary structures. Clayey sand and sandy clay are referred to as silts. Soils and laterite rocks characterized the uppermost succession of the wells, and sand and muddy rocks comprised the lower portion.

Distinguishing sandy bodies between the tidal channels or transgressive sandbars by the sand texture described in the report, for example, “sand fine,” is not as easy as it seems. Thus, indicators such as lithological units and stacking patterns are critical for interpreting their systems and relating them to the depositional environment. Considering the main characteristic involving, the fining-upward cycles consisting of the presence of a base sustained by mainly medium-sized sand gradually capped by the fine texture until clay at the top (Fig. 4), alongside sedimentological and architectural elements, three facies associations were identified as Tidal Channel (A), Tidal Flat (B), and Paleosol (C) (as summarized in Table 3). The Facies Association considers geological mapping, correlations between lithological units, and their implications for the regional stratigraphy.

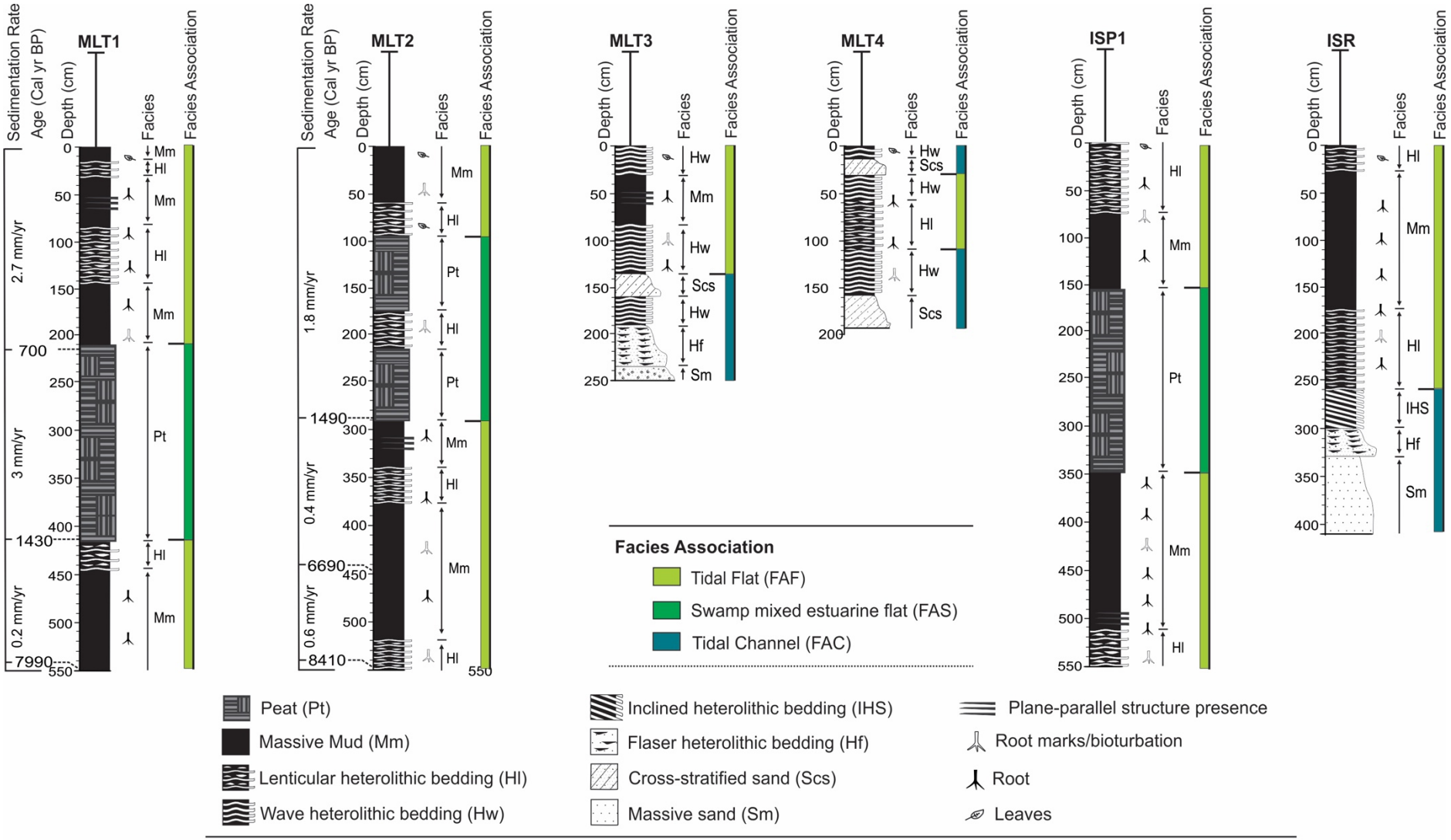

Figure 3. Sediment cores summary, considering their sedimentary facies and facies associations as a function of depth. The profile included chronological ages and accumulation rates.

4.3.1 Facies Association A (Tidal Channel)

This association occurs along the intervals 16–9 m (WT-1), 37–25 m, 17–14 m (WT-2), 24–8 m (WT-3), 36–26 m, 18–9 m (WT-4), 56–44 m, and 32–25 m (WT-5). It consists of a thick sandy layer arranged into medium sand, always present as the lowermost deposits at the base of each complete fining upward cycle. This medium-sand base texture gradually decreases, reaching very fine-grained sand at the top of the unit (Fig. 4). Facies association (A) extends laterally from the south-to-north trend downstream of the Tocantins Valley. Over most of the study area, the preservation of this unit described by well drillers occurs with thicknesses that are generally similar along the geological profiles. This unit was assessed as the representation of the tidal channel deposits; both having a common geometry and their internal organization into fining-upward successions.

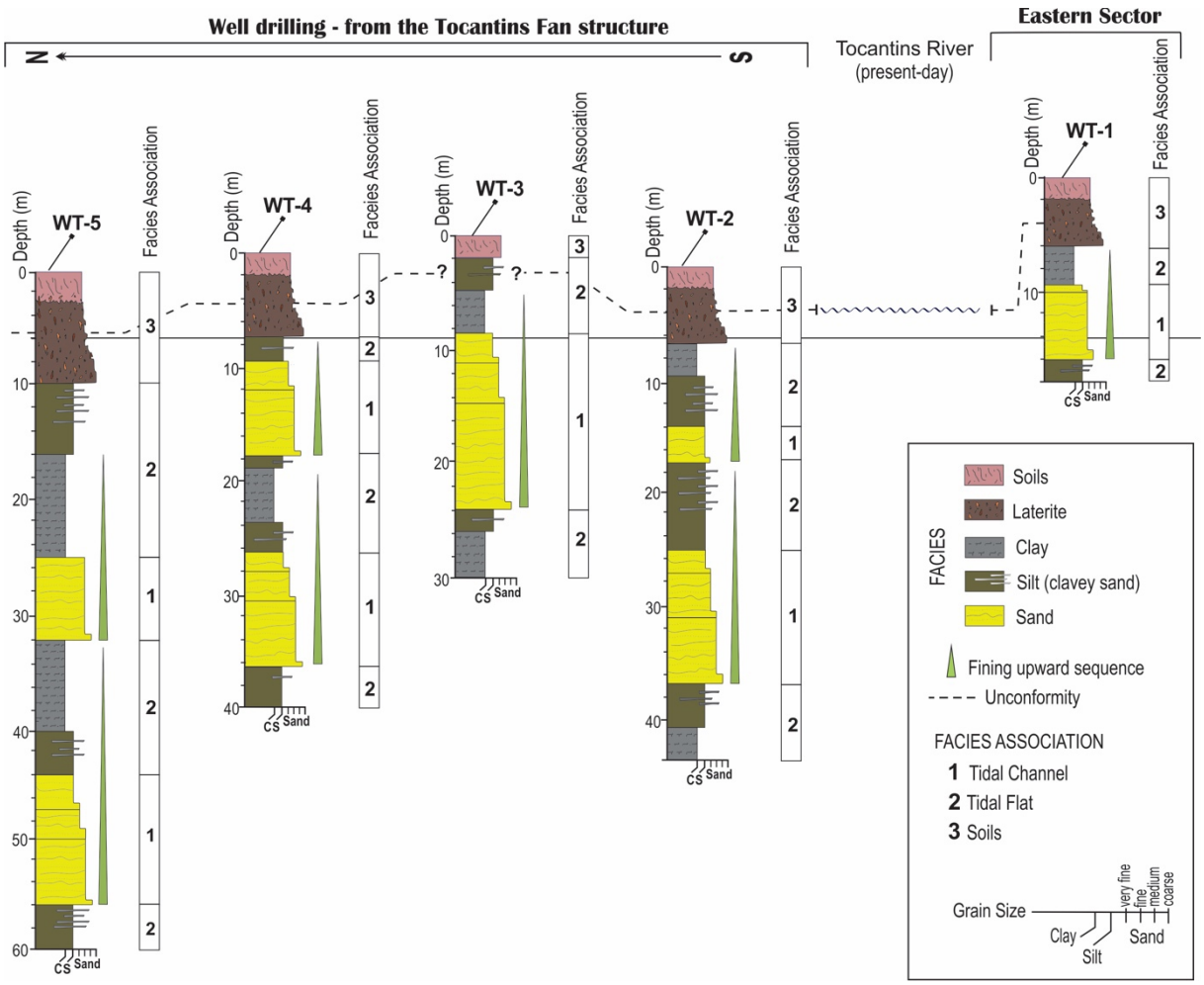

Figure 4. Summary of the wells drilling lithological profiles with sedimentary facies, textural character, and facies associations. The wells distribution is according to the Tocantins River geographical position and upstream-downstream occurrence relation.

4.3.2 Facies Association B (Tidal Flat)

This unit lithology from well drilling recorded in the Tocantins valley is typically muddy. It may be recognized along the intervals 18–16 m, 9–6 m (WT-1), 44–37 m, 25–17 m, 14–7m (WT-2), 30–24 m, 8–2 m (WT-3), 40–36 m, 26–18 m, 9–7 m (WT-4), 60–56 m, 44–32 m, 25–10 m (WT-5). This deposit commonly consisted of clay, clayey sand, sandy clay, and occasionally very fine sand. Into WT-5 muddy layer was nearly 16 m thick (Fig. 4). Facies association (B) extends laterally from the south-to-north direction downstream of the Tocantins Valley. In the western part of the study area, this unit has less occurrence (4 m), whereas in the northward-most west sector, the muddy layer reaches a thickness of 15 m. Silt and clay facies exhibit genetically similar lithological characteristics, overlying the sandy deposits of the tidal channel. Such characteristics led to the assessment of this unit as a tidal flat deposit.

4.3.3 Facies Association C (Paleosol)

This uppermost unit occurred at the intervals of 6–0 m (WT-1), 7–0 m (WT-2), 2–0 m (WT-3), 7-0 m (WT–4), and 10–0 m (WT-5) (Fig. 4). It represents the top of the wells and consists of laterite rocks with iron oxides (lower deposits) and soils (upper deposits). The lower deposit overlies the tidal flat facies association at the WT-1, WT-2, WT-4, and WT-5 wells, where it exhibits a sharp basal contact, suggesting a striking change in the sedimentation processes. Owing to its distribution along almost all sites, locally ranging from approximately 4 to 7 m in thickness, the laterite rocks conceivably correspond to the same stratigraphic unit, with stratigraphic importance in time and space. Thus, the lower unit is interpreted as a paleosol (Fig. 4). The paleosol is recognized as a chronostratigraphic boundary, playing the role of an unconformity. The upper unit of this facies association encompasses a pedogenic profile well development of red-yellow latosol overlapping the laterite layer present in all the wells. In WT-3, the latosol overlapped directly with tidal flat deposits.

4.4 Lineaments

The lineaments were plotted in Rosetta diagrams to analyze their spatial distributions and directions. As shown in the graphs, the NE–SW trend prevailed across the region, followed by the NW–SE corresponding to subordinate preference. Five distinct sets of structures were generated; the four most frequent of them are shown in the diagrams: normal fault, normal oblique dextral fault, dextral strike-slip fault, and sinistral strike-slip fault. (1) The normal fault tendency is mainly NW–SE with an azimuth of 346°, a NE–SW trend, and a subordinate azimuth of 37 °. (2) Concerning the normal oblique dextral fault, the most directional frequency

Table 3. Cores and well drilling Facies Association and their sedimentary characteristics.

Sampled	Facies Association	Description	Interpretation
Cores	FAC	Sand with fine-grained and fine to medium-grained texture and light yellow color. A well-sorted sand occasionally having fine clast disperse-supported. Parallel lamination can be present. Fine-grained cross-stratified slightly-symmetric greenish to gray color; millimetric lamination in muddy levels can occur internally. Inclined stratification and Flaser heterolithic bedding with a muddy portion of gray to very dark gray and black color, varying from 2 mm to 1.7 cm thickness.	Tidal channel
	FAF	Muddy and heterolithic deposits show olive-brown to dark gray and black color. Their intercalations are millimetric formed by fine-grained sand, gray to gray dark, reddish-brown color, and varies from wavy to lenticular bedding in millimetric thickness. Massive mud, olive-brown, gray to very dark gray; parallel lamination can be present. Many plant fragments are distributed alongside this succession. Its bioturbations include many woody roots, root marks, and dwelling structures. Oxidized mud with a dark yellow color, and brown spots.	Tidal flat
	FAS	Peat deposits (Pt) are black, occasionally varying from greenish to brown-reddish-black color. Although it can present younger fibers and roots, this peat is typically well-decomposed, having organic muddy drapes internal resulting from its decomposition process. This facies association's small interval (40 cm) encompass lenticular heterolithic bedding facies. Bioturbations features in this facies include woody roots, root marks, and structures produced by the benthic fauna.	Swamp mixed estuarine flat
Well drilling	A	Sand matrix-supported medium-coarse, overlap by moderately to well-sorted sand, upward fine to very fine-grained, reddish-white to reddish-yellow, reddish-yellow colors, with locally present variegated clay.	Tidal Channel
	B	Silty and clay deposits whitish-gray colors, reddish-white, reddish-yellow, greenish-yellow, occasionally occurrence of very fine sand in yellow to reddish-yellow colors. These arranged muddy deposits complete the fining upward sequence.	Tidal Flat
	C	Deposits comprise a laterite rocks profile having iron and aluminum oxides, mottling reddish-brown, yellow color, and gray. The upper unit encompasses soils of reddish-yellow and yellow colors, with mottling rooting reddish-brown color.	Paleosol

of this set is the NE–SW trend with an azimuth of 40°, and the NW–SE trend and azimuth 339° correspond to subordinate preference. (3) The dextral strike-slip fault, in turn, tended to be NE–SW with an azimuth of 38°, and the E–W trend and azimuth of 85° corresponded to subordinate preference. (4) Completing the most directional frequency of lineaments, the sinistral strike-slip fault, the E–W-trend with the 93° azimuth is the principal, while the NE–SW trend with an azimuth of 39° is subordinate, and they comprise the most directional trend of the morphostructures.

5. Discussion and Interpretations

5.1 Western Tocantins River: hierarchy, sedimentary records, and regional scale fluvial rearrangement

Morphostructural data combined with remote sensing have been used to investigate the drainage rearrangement on a regional scale, and their application includes satellite image analysis to identify paleochannels. The technique generally uses multi-band images to show subtle differences in the surface moisture and related land cover (e.g., Davidson and Watson, 1995), leading to the infers of paleochannels (Nandini et al., 2013). Nonetheless, this widely used technique may be unsuitable for the investigation and trackback paleodrainage in the areas where weathering occurs continuously over long durations, resulting in the deep weathering profiles, as for the present study area.

Well drilling records show deeply weathered profiles marked by a lateritic layer in the Tocantins valley (TW-1, TW-2, WT-4, and WT-5) (Fig. 4). Weathering must have been of sufficient intensity to modify the sedimentary deposits infilled in the depressions and abandoned channel segments after fluvial capture. This lateritic profile may better explain why the rearrangement of Tocantins did not preserve its former fluvial pathway. If the Tocantins drained northwestward towards the Amazon River, we estimated that a fluvial course of up to ~200 km was left behind (Fig. 5). Nevertheless, the identified paleochannels based on the satellite image interpretations (e.g., Lima et al., 2017; Rossetti et al., 2007; Rossetti and Valeriano, 2007) poorly represent the improved reconstruction of the fluvial history of the Tocantins. Beyond obliterated infill-deposits and amalgamated scars by weathering, the few recognized paleochannels perhaps indicate that Western Tocantins consisted of a relatively straight channel instead of a distributary network typical of the calescent alluvial fan system, as previously envisaged by Lima et al. (2017).

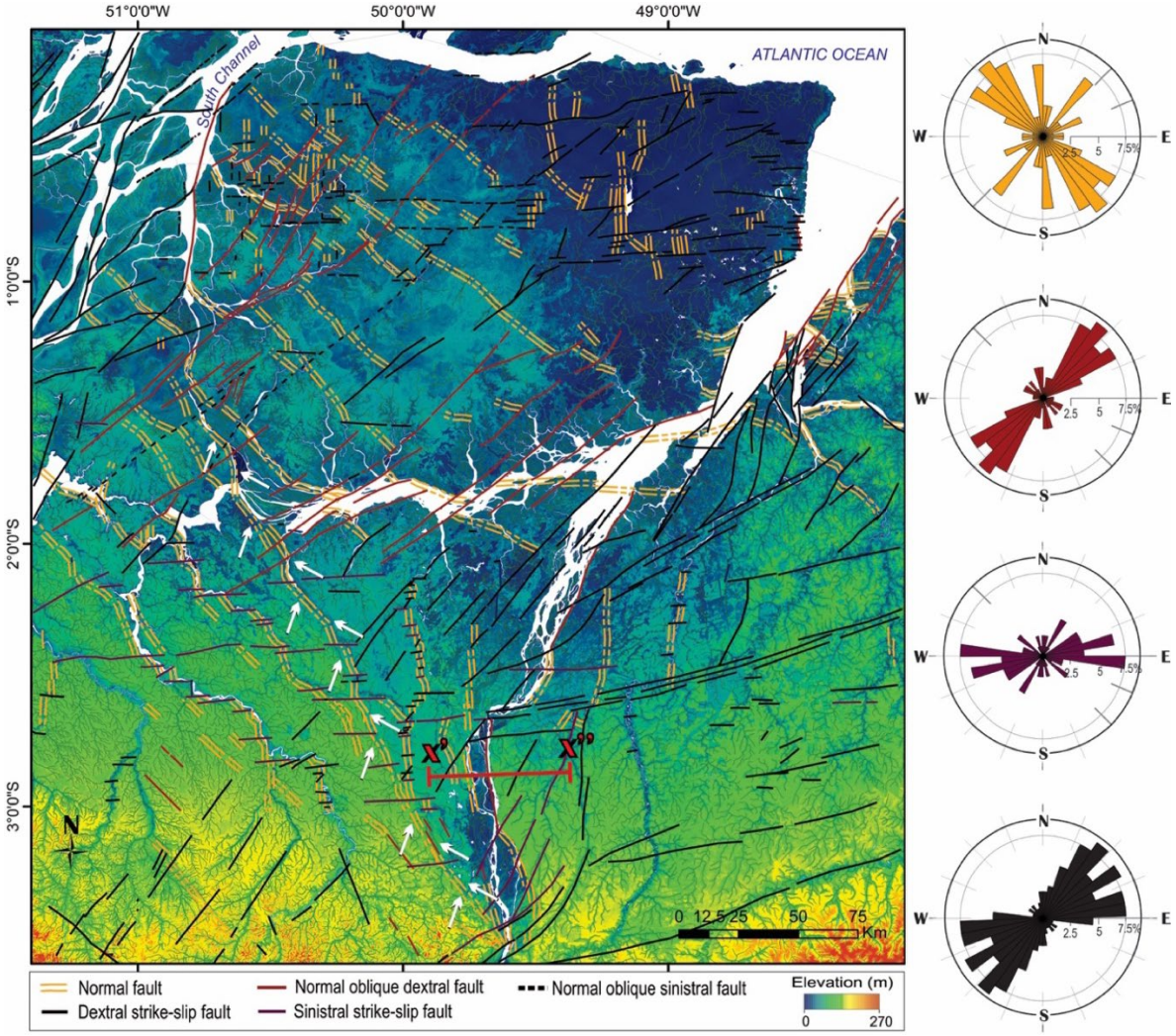

Figure 5. Morphostructural overview of the region. The contemporary network drainage presents rivers that project directly to the east, some forming bays continental, owing to the blocking of the channels modeled by elbow anomalies (see left). According to the normal NW-SE-trend structure, the white arrows suggest the course probable of the ancient Tocantins. The geologic profile (X'–X") is illustrated in the text ahead. The Rosette diagrams show the frequency trend of the regional lineaments. The strike-slip faults represent the highest density of structures. (See the area in Fig. 1c).

Based on the lineaments results, it is possible to consider the existence of a structured paleo-drainage by normal faults with a NW–SE trend (almost NNW–SSE) (Figs. 5 and 7). This structure would result in the slightly straight Tocantins course without obstacles running towards the Amazon River, emptied nearly at its mouth. The PaleoTocantins River was probably one of the largest tributaries of the Neogene Amazon basin. The normal faults NW–SE trend could have been developed within a transtensive regime related to the main event of transcurrent displacement within the Pará state northeastern region, whose normal faults NW–SE were active from the Miocene to Pliocene (Fig. 8a) Costa et al., 1996). Furthermore, these faults correspond to the main components of the regional neo tectonic framework; they favored landward sea advance, allowing deposition of shallow-marine sediments corresponding to Pirabas/Barreiras Formation (Costa et al., 2002).

Data-oriented integration to clarify the origin of the Tocantins River, paleogeographic history of its riverine connections, and time when the course was active as an Amazon tributary remains unavailable. However, sedimentary records can provide elements that suggest either quick shifting or capture of this river eastward instead of slow diversion fluvial or distributary drainage formation.

The facies formed by sand (medium-to fine-grained size), subsequently overlain by a muddy deposit composed of silt and clay facies, and observed along WT-2, WT-3, WT-4, and WT-5 (Fig. 4) reflect the net transport of sediment with a gradual loss of depositional energy (James and Walker, 1992) named fining upwards. The fining upward multistory suggests a mode of deposition that is repeated in the system. Traditionally, this stack comprises the bulk of fluvial deposits; therefore, repeated fining upward cycles have been typically assigned to ancient fluvial sequences (Allen, 1965; Johnson, 1984). Although fining upward succession is widely employed to identify fluvial systems, products formed through lateral migration of meandering, and consequently infills by muddy deposits (Miall, 2006; Walker and Cant, 1979), it is not necessarily diagnostic for the unique depositional system. In contrast, different depositional systems can produce similar architectural elements. Fining upward can be formed in virtually any depositional environment, with a decline in energy levels over the time and availability of the fine-textured sediments. Thus, it may be found in fluvial and estuarine plains and inner shelf to deep-water (slope to basin-floor) settings (Catuneanu, 2006). Because of the natural variability of these products, facies organized into fining upwards must be coupled with regional stratigraphy to better understand the depositional environment and its controls.

Within this approach, the depositional environment may be related to the transitional estuarine environment under marine transgression. Sand facies were interpreted as products of the deposited tidal channel (Facies Association A). In contrast, mud facies consisted of tidal flats formed on the inner estuarine systems (Facies Association B). The channel deposits, including sandbars, were gradually deposited landward due to sea-level rise, overlapping former muddy sediments with the development of sedimentation cycles. As a trigger to the in-channel deposition, each cycle would have commenced because of the transgressive setting, wherein the tidal channel incised its course after an initial period of erosion over the former tidal flat. The redistribution of energy and materials controlled by the tidal forces leads channels to adjust gradually, migrate laterally, or become blocked after the avulsion event (Hughes, 2012; Terwindt 1988; van Straaten, 1954). Consequently, with the reduced tidal prism, as the cross-sectional channel area reduced, the flow strength decreased, favoring the filling of the abandoned channel by fine-grained sand passing through silt and clay sediments, thus

exhibiting upward fining deposits over an erosional base (Davis and Dalrymple, 2010; Hayes, 1975; Rieu et al., 2005; Symonds and Collins, 2007). Over time, these processes may result in a well-preserved parasequence tidal-channel infill.

The correlation of wells WT-2, WT-3, WT-4, and WT-5 suggests that the tidal channel fill is probably multistory (Fig. 7), wherein deposits are superimposed on each other, developing the repeating fining-upward cycles. Dalrymple et al. (1992) indicated that estuarine tidal channels continuously infill during rising sea levels under the adequate sediment supply. Analogous cases from multistory tidal channel infills have been reported in surveys by Hardley et al. (2006) and Morgans-Bell and Mcllroy (2015).

Likely, during the deposition of these sequences related to the estuarine setting, the Western Tocantins River may have played a secondary role in the depositional systems control and stratigraphic evolution. Thus, sand and mud facies are related mainly to the retrogradation coastal settings that receive sediments from marine and transitional sources, which does not imply the absence of a fluvial deposition influence. Likewise, it is worth mentioning that the fluvial influence is not disregarded herein. Our interpretation considers the fluvial role, but it must have been subordinate due to more intense estuarine controls involving long-term stratigraphy. As discussed below, we present three brief arguments that reinforce our interpretation. First, the repetitive pattern of the fining-upward cycle is present in almost all profiles, allowing presumes overall sedimentation mechanism, whose effects were shared regionally, suggesting an allogenic character, such as the base level. Nascimento (2003), utilizing well records logging taken from the Barreiras Formation (~150 km downstream of this area), documented some sedimentary successions with cycles fining upward based on the shape pattern. Such sequences comprise sandstone and claystone, and their occurrence was recognized between the surface and a depth of 160 m, mainly attributed to sea-level highstand conditions. The succession shown here is similar to that reported by the author, suggesting a syndepositional correlation.

Second, the stratigraphic units from the study area encompass Miocene rocks and younger ages. This unit is chrono-related to the Barreiras Formation (Late Miocene/Early Pliocene), consisting of massive and stratified sandstone, laminated and massive mudstone, and heterolithic-bedded deposits. Although the Barreiras Formation has already been considered continental in origin, Arai et al. (1988) and Rossetti et al. (1989) emphasized various sedimentary features related to the tidal processes through facies analysis, ascribing the source of these deposits to transitional estuarine environments. Finally, the development of an

unconformity on the top of these successions is represented by a laterite layer (WT-1, WT-2, WT-4, and WT-5; Figs. 4 and 6), whose profile reaches up to 7 m thickness.

Laterite is a ferruginous and siliceous accumulation that forms concrete oxidation horizons associated with a tropical climate with well-defined dry and wet seasons. Oxidation resulting from seasonal anaerobic conditions leads to the reduction of iron (Fe) oxides due to sediment microorganism activity (Bighan et al., 2002; Szymański and Skiba, 2013). Fe-reduced (Fe^{+2}) can readily migrate within the profile and thus re-oxidize and precipitate (Fe^{+3}), forming nodules and mottles (Bighan et al., 2002). In the Amazon, laterite has widespread occurrence, and generally marked an unconformity at the top of the Barreiras Formation, interpreted as a paleosol resulting from the sea level drop that started in the Tortonian, combined with a period of tectonic stability (Rossetti, 2006; 2004). Here, the laterite occurrence in the uppermost sedimentary profile may correlate with the paleosol overlying the Barreiras Formation recognized by those authors. The horizon overlying the tidal deposits (WT-1, WT-2, WT-4, and WT-5) indicates the probable end of estuarine sedimentation cycles (Fig. 5). This change, followed by the entrance of environmental conditions that favored its development, was long-term, due to its thickness and distribution across the area, giving the significance of regional unconformity. While the channel infill deposits occurred during a sea-level rise, the laterite layer implies fluvial conditions prevalence after RSL fall, with prolonged stages of supply sediment cut-offs.

Textural characteristics with fine-grained to medium-grained predominance and good sorting, followed by silt and clay, may be critical as an efficient tool for assessing the mechanisms responsible for delivering sediments to the sampled locals (Fig. 4). For instance, some studies have reported that deposits preserved alongside this sector comprise alluvial fans (e.g., Furtado and Ponte, 2013; Lima et al., 2017), owing to the evident fan-shaped morphology (Rossetti and Valeriano, 2007). Nevertheless, the versions of architectural facies that occur here, followed by an absence of the coarsest deposits typical of the proximal zones in the alluvial fan [for example, conglomerates, gravelly with sandy or muddy supported matrix, pebbly and fine pebble conglomerates, and medium-grained sands moderately to poorly sorted, make these deposits and their features poorly analogous to facies from fans and their models, (Miall, 2006; 1992; 1985) regardless of the model employed, such as the distributive fluvial systems (DFS) (e.g., Weissmann et al., 2013, 2010), fluvial distributary systems (e.g., Nichols and Fisher, 2007), terminal fans (e.g., Kelly and Olsen, 1993), and megafan (e.g., Shukla et al., 2001). Furthermore, the sedimentary stacking does not correlate with the generally expected deposits for either unstable streams or rivers having flow transitions alongside the surface with

significant energy loss (Alexander et al., 2001; Gao et al., 2020). Therefore, such additional remarks reinforce the rearrangement caused by neotectonics force (allogenic) rather than internal dynamics, either alluvial or fluvial.

NE–SW trend strike-slip faults must have been responsible for developing the northward-new fluvial course, a zone whereby the modern Tocantins would flow until the Atlantic Ocean (Costa et al., 1996; Rossetti and Valeriano, 2007; Soares Júnior et al., 2011) (Fig. 7). The NE–SW trend is part of the framework of this area active since the Plio-Pleistocene, including a set of E–W trending dextral strike-slip faults, which respond by shifting several rivers abruptly to eastward-linked NW–SE trending normal faults (Costa et al., 2001, 1996). The NE–SW trend is consistent with the orientation of tectonic lineaments prevailing in the Amazon developed from the Neocretaceous (Bezerra, 2003; Vilegas, 1994), which underwent reactivation pulses during the Cenozoic, mainly Quaternary (Fig. 8b) (Costa et al., 1996; 2002; Rossetti et al., 2008a). Later, this NE–SW trend strike-slip fault must have acquired an oblique kinematic component, because its effect produced an important subsidence event.

Topographic analysis showed a striking difference between the east (highest) and west (lower) (Figs. 6 and 7). Although secondary structures have developed, forming adjacent geometry blocks, the major fault coincident with the current river course induced a dip that reached 14 m west, as recorded via laterite east (Figs. 4, 6 and 8). Subsidence explains the vertically lowered fan-shaped structure well-accommodated in the lower Tocantins valley, whose morphology probably borders between the current (NE–SW) and the former (NW–SE) courses (Fig. 7). It can be suggested that while the Tocantins River quickly opened its pathway to the east (towards the Atlantic) through erosion over the tectonic crack with NE–SW-trend, the fan-shaped structure underwent subsidence caused by the slow tectonic pulses (Figs. 6 and 7).

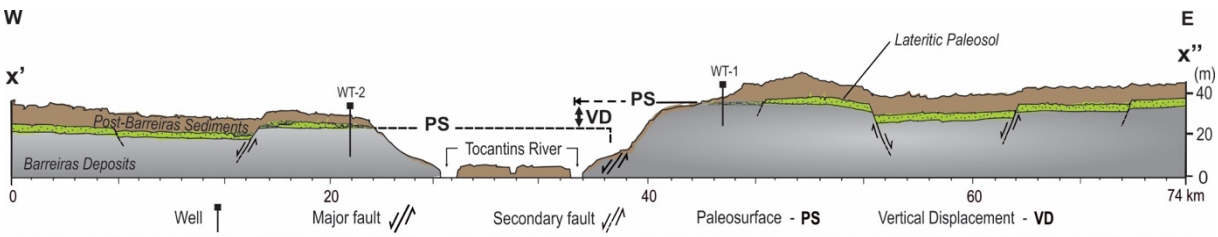

Figure 6. Topographical and geologic setting. The central displacement that affects the geological layers between the eastern and western sectors is assigned to the subsidence process. The lateritic layer suggests a regional paleosurface. (See Figs. 1c and 5 for profile-line localization).

The Tocantins incision started upstream and gradually propagated north-north-eastern until its course was connected to a small shoreline valley (Pará River mouth). The age of this valley is uncertain as its geometry is compatible with the NE–SW zone, which was active during

the Pliocene and reactivated in the Quaternary (Fig. 8a–b). This event probably occurred during the Late Pleistocene because the current Tocantins River cuts through the laterite paleosol (unconformity) on the top Barreiras Formation (WT-1 and WT-2; Fig. 6). Over time, this laterite underwent intense pedogenetic processes, resulting in one red-yellow latosol characterized in the upper part of the sedimentary succession. Although the well-developed latosol is assigned to materials/sediments altered from the laterite crust, the well-sorted, medium-grained aeolian sands, with sharp basal contact encompassed in this pedogenic profile, are also correlated with the Post-Barreiras-Barreiras deposits of Pleistocene–Holocene age (Tatumi et al., 2008).

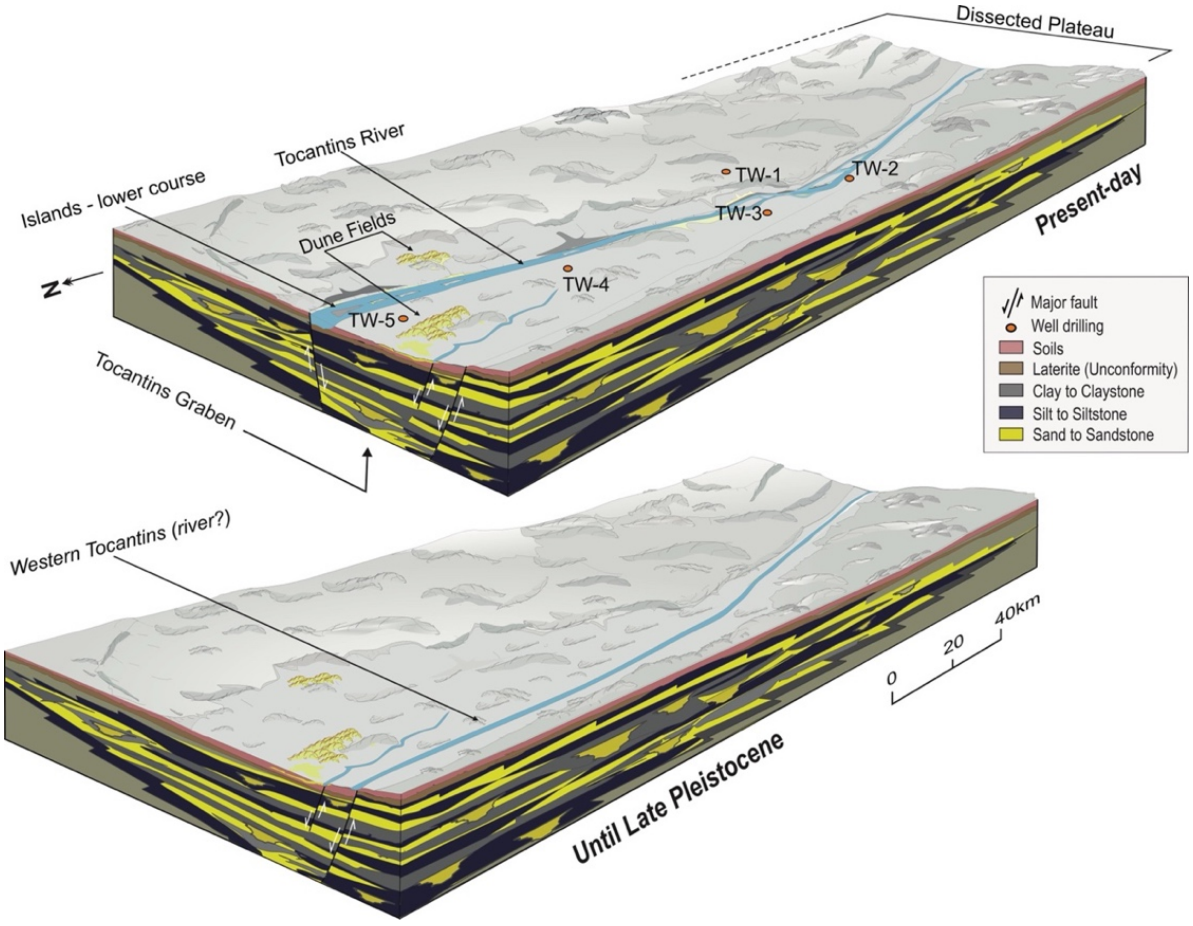

Figure 7. Current paleogeographic sketch of the Tocantins River valley, including its geological framework setting and depositional systems. The correlation of strata is based on wells drilling facies (see their sites plotted). The strata comprise sandy deposits reaching to sandstone (Tidal channel) covered by muddy bodies variant from mudstone to claystone (Tidal flats) (mid-Miocene and Pliocene). This succession is bound by an unconformity characterized lateritic layer (Pleistocene), in turn, overlaying by soils (Post-Barreiras sediments - Late Pleistocene-Holocene). Note the Tocantins Late Pleistocene-position at the bottom graphic.

After the Tocantins shift, almost all drainage networks from the northeastern region with fluvial connection, or emptying into the Tocantins River, must have opened or undergone tectonic adjustment. The most striking effects on modern drainage are anomalies forced on

channels, represented by elbow morphology, embayment, and straight fluvial segments controlled by E–W trending strike-slip zones (Fig. 5) (Costa et al., 2001; Rossetti, 2014). In this context, the fan-shaped structure confined by NNW–WWE, NE–SW, and E–W trending faults, according to the data presented here, corresponds to a depression resulting from the tectonic subsidence that may be termed as 'Tocantins Graben' (Fig. 7). Subsequently, its depocenter received sediment yielded by a dissected plateau, in addition to olian processes and flood-generated fluvial deposits over the Holocene.

5.2 Coastal implications from the river adjustment: incised valley and island-morphogenesis through the Holocene

We assigned the lower Tocantins' present-day position to the fluvial rearrangement process (Figs. 7 and 9). The newly opened eastern, favored by the slope relation continent-coast topographic gradient, strongly implicating the evolved paleogeography throughout the Late Pleistocene. Minor normal faults with a NW–SE trend interacted with the strike-slip fault having NE–SW trend (Fig. 5), forming a sizable tectonic zone in the NE–SW direction that precisely occupied the area between Baião and Abaetetuba (Fig. 8c). Rhombic-shaped islands in this zone are likely developed and controlled by conjugated normal faults having N-S trends with the strike-slip fault with a NE–SW structure (Fig. 8c–d).

These generally wide and elongated islands are marked by a slightly straight northward edge, limited by a small channel network that forms an anastomosing fluvial sub-pattern into lower Tocantins (Fig. 8d). Perhaps some of these islands correspond to continental tracts remaining within the fluvial system, while the Tocantins opened their course towards the Atlantic. In contrast, the sedimentary features from the cores revealed the tidal influence on the deposition system. This indicates that some of these islands evolved due to sea-level rise during the middle Holocene. Therefore, the evidence suggests that tectonic and sea-level change forces may have simultaneously shared their influences in time and space.

The cores have dominantly muddy to sandy structures, frequently interbedded with layers and lenses of well-sorted sand or mud, and containing a spectrum of heterolithic bedding structures reflect the alternating bedload and suspension deposition in tidal conditions (cf. Reineck and Wunderlich, 1968; Hughes, 2012) (Fig. 3). Such sedimentary features and their indicators, integrated to framework tectonic and 14-C chronology, allowed the recognition of landscape evolution in four phases in the Tocantins River mouth. First, the Maratauíra incised valley opened (Late Pleistocene–Early Holocene), which drowned during sea-level rise between 8410 and 1490 cal yr BP (second phase). The sea-level drop and estuarine

hydrodynamics controlling peatland deposition from 1490 to 700 cal yr BP delimited the third phase. The last phase implies intense tidal channel activity, leading to complete separation of the CIOA from the mainland after ~700 cal yr BP.

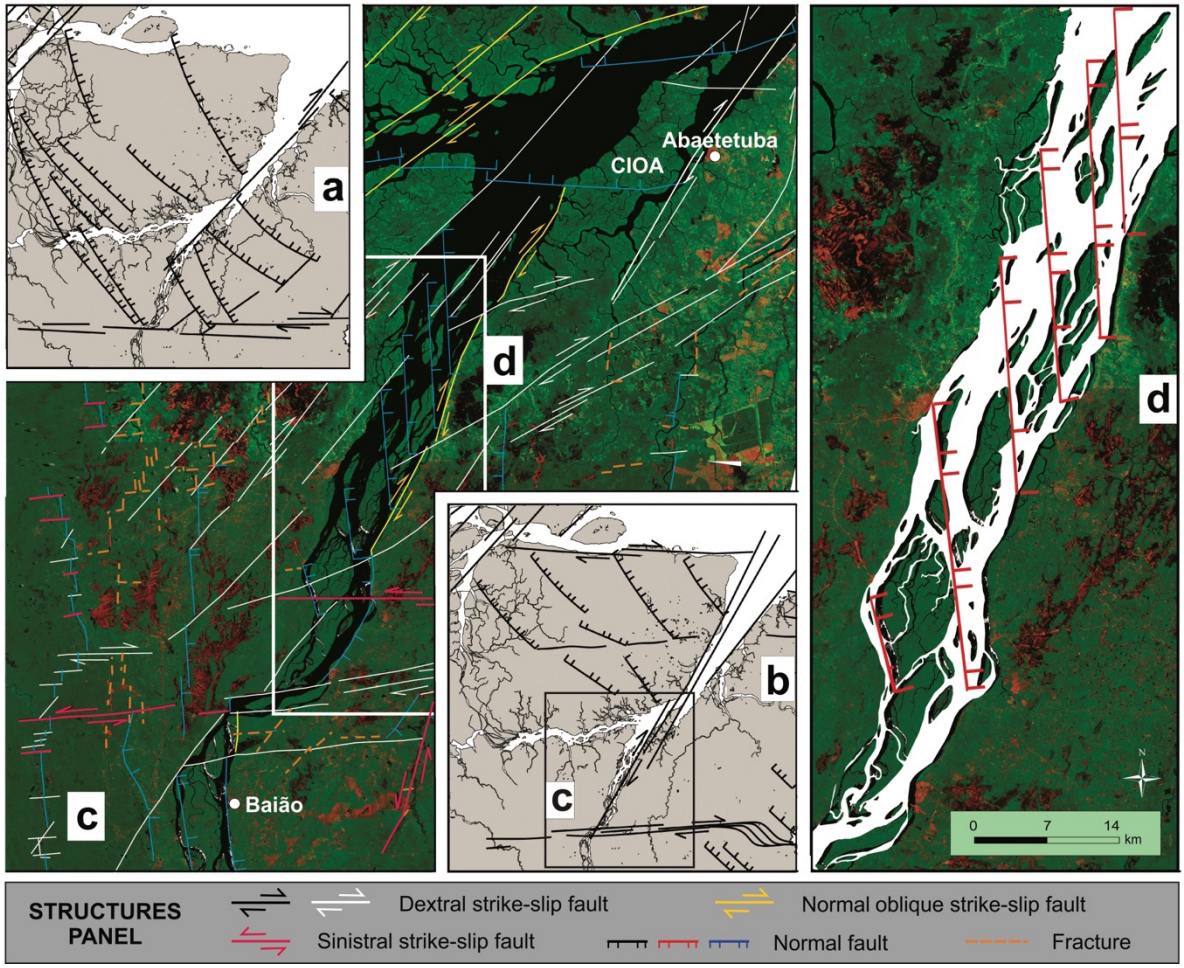

Figure 8. Major features of the regional tectonics framework developed during the (a) Neogene and (b) Quaternary (after Costa et al., 1996). The structural Baião-Abaetetuba zone, including contemporary faults, is presented in the figure principal (c). Highlight for islands in the lower course of Tocantins, with straight edges, suggesting structural control (d).

5.2.1 Phase I: The Maratauíra incised valley - Early Holocene

At some time near the Last Glacial Maximum (20,000 and 18,000 BP), when the sea level was 100–120 m below the present-day level in the Amazonian littoral zone, the flat surface of the eastern part of the mainland has been deeply eroded by a small drainage system (Maslin et al., 2006). During sea-level lowstand, the gradient difference between the exposed shelves triggered rapid fluvial erosion that connected the Tocantins River to the ocean, leading to incised valley formations. Incised valley is a geomorphological fluvially eroded feature in response to sea-level fall, which cause rivers to incise their beds in an attempt to reach a new profile equilibrium (Boyd et al., 2006; Holbrook et al., 2006; Qiang and Qiang, 2019). During this period, the Maratauíra River was still non-existent.

A small and shallow incised valley opened immediately downstream of the eastern part, corresponding to the seaward-most portion of the Early Holocene. This valley later became the Maratauíra River (Fig. 9–1). Its position was established by a normal fault NE–WS trend originating within the Quaternary tectonic framework (e.g., Costa et al., 1996). This fault controls the eastern mainland edge, resulting in a straight border seaward, as well as the Pará Estuary position (Fig. 8b). The sea-level lowstand and neotectonic effects governed the Maratauíra valley geometry and physiography.

5.2.2 Phase II: The peninsular morphology – Mid-late Holocene

The post-glacial sea level rise drowned the Maratauíra incised valley, leading to the development of a ria (cf. Evans and Prego, 2003) (Fig 9–2). As transgression proceeded, marine sediments progressively overlaid older fluvial deposits exposed by previous erosion, resulting in widespread best-developed tidal flats occurring alongside estuarine sub-systems and small embayment. These flats (FAF) encompass massive mud and lenticular heterolithic bedding facies (MLT1, MLT2, and ISP1; Fig. 3), which are formed by energy rhythmites and are assigned to a tidal-dominant environment (cf. Davis, 2010) (Fig. 2e). Even though these beddings, called heterolithic, may also form in non-marine environments, characterized by relatively high-energy episodes, when bedding appears in stacked sequences, they strongly suggest tidal phenomena as modes of accumulation owing to their cyclicity (Daidu et al., 2013; Davis, 2010). Therefore, stacked facies sequences, such as those occurring among cores (Fig. 3), are evidence of the sea level reaching this sector since 8410 cal yr BP (Fig. 9).

During this sea-level rise, the Maratauíra did not undergo a sedimentary evolution analogous to incised valleys infilled due to the greater availability of sediments (Wang et al., 2019); contrariwise, Maratauíra was broadened over time became unfilled incised valley (Catuneanu, 2019) (Fig. 9–3). Because this second phase has the longest time among the phases, from 8.5 to ~1.5 cal yr BP, several transformations occur over this 7 ka BP. For instance, the dextral zone strike-slip NNE-SSW trend (NE–SW) emerged in the tectonic framework (Fig. 8c).

The dextral zone NNE-SSW trend likely originated during the middle Holocene, or may even be a result of a reactivation pulse from the Tocantins lineament (cf. Villegas, 1994). This lineament defines Limoeiro and Cametá sub-basin boundaries, and their development occurred alongside the system of normal faults that controlled the Marajó Basin geometry (Fig. 1c) during the Neogene (Fig. 8a). Irrespective of the origin of this dextral strike-slip fault, if by development within the tectonic framework from the middle Holocene that started to control

the lower course of the Tocantins River, or by Tocantins lineament reactivation, this zona has articulated with a normal fault in the NE-SW direction (Fig. 9–3).

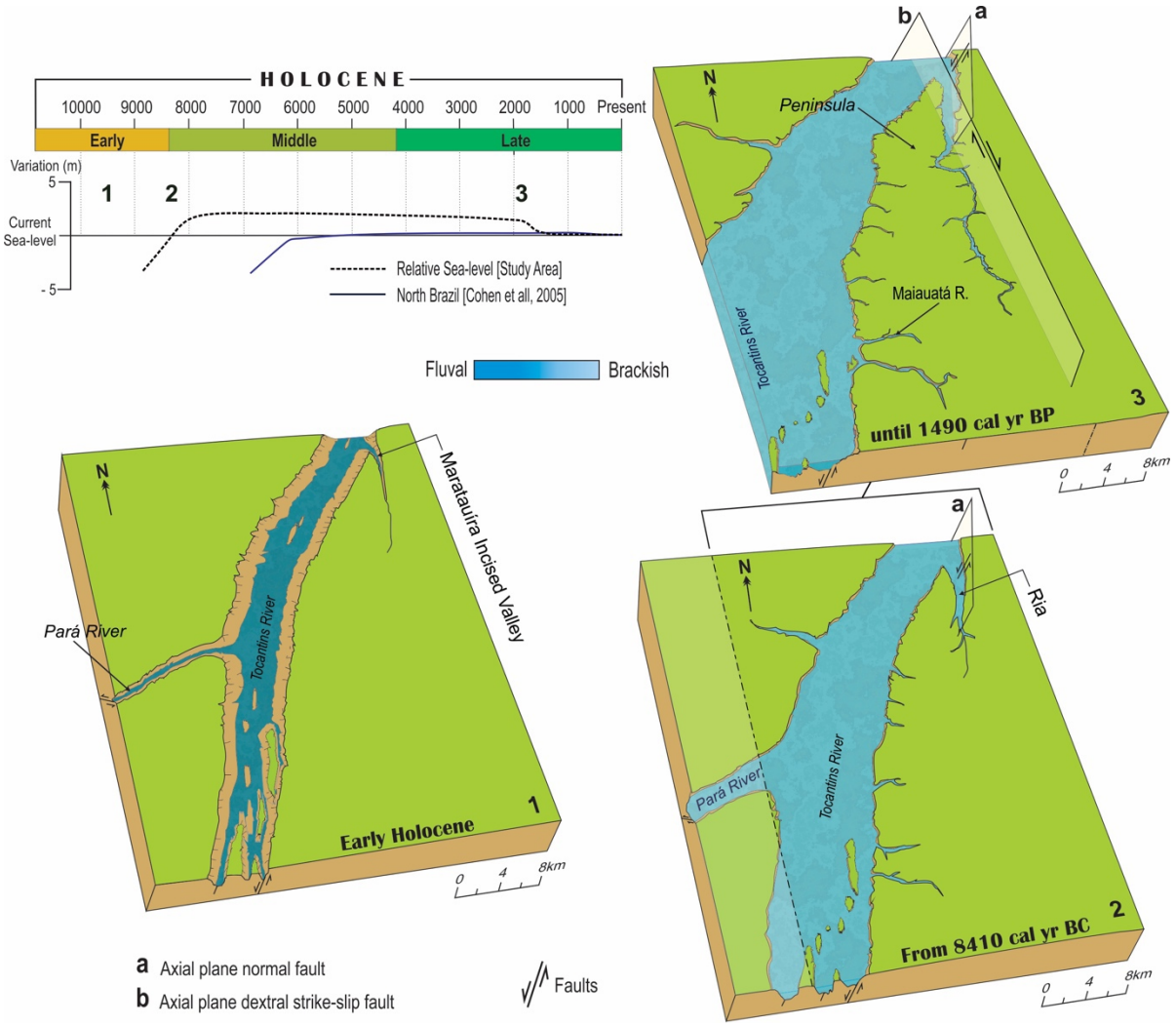

Figure 9. The conceptual summary sequence of CIOA evolution. Block-1: Sea-level lowstand (Last Glacial Maximum) and the normal tectonic regime led to incised-valley development (Fisty Phase). Block-2: Post-glacial sea-level rising drowned Maratauíra incised valley. At the same time, the dextral strike-slip fault NNE–SSW trend has emerged. Block-3: Detachment pronounced from the mainland, followed by most significant penetration of the Maratauíra river to land-ward and the peninsula setting are responses to the tectonic interplay (2 and 3 blocks encompass the Second Phase). The top shows the relative sea-level curve proposed for the study area.

The interplay between these structures resulted in a zone favorable for Maratauíra evolution. This zone propagated from the sea landward, implying both the broader opening valley-mouth and its penetration to the south-southwest, which resulted in peninsular morphology development (Fig. 9–3). Concomitant with mainland fringe detachment, the brackish influence advanced over this region owing to the NNE–SSW effects. Consequently, a variety of estuarine sub-environments were formed with more expansive tidal flats.

5.2.3 Phase III: The peatland development – Late Holocene

The third phase comprises ~1490 and 700 cal yr BP, characterized by a striking environmental change (Fig. 10–4). Its signature in the depositional system is expressed through stratigraphic discontinuity. Such discontinuity is related to the aggradation by the sediment of organic nature, forming peats (FAS), accumulated in an intermediate position in the MLT1, MLT2, and ISP1 cores (Fig. 3; Supplementary Data). Peat is formed due to accumulation of the plant remains in waterlogged conditions that inhibit the process of decomposition (e.g., intertidal zone, salt marsh, mangrove, transition to freshwater habitats, wetlands, and bogs) (Shennan 2019; Shennan et al., 1996). In Natal littoral, northeastern Brazil, peat deposits were related to the demise of coastal vegetation due to accelerated sea-level rise during the mid-Holocene (Boski et al., 2015). Here, the formation of peat deposits began at about ~1490 cal yr BP (Fig. 3), which is inconsistent with the sea-level rise period in the Amazonian region. In contrast to Natal, the occurrence of these peats may be associated with RSL falls.

Studies in the Amazonian littoral zone have reported that the RSL reached its current position around 7000 cal yr BP (Behling and da Costa, 2000; Cohen et al., 2005), with no significant change during the Holocene (Behling et al., 2001; Cohen et al., 2005; Rossetti et al., 2008b; Vedel et al., 2006). Although these studies emphasize that RSL has been relatively stable, this peat deposit can provide new insights to consider that RSL could have exceeded the current level. The chief element to be considered in this hypothesis is the interpretation that these plant debris accumulated alongside the stratigraphic column results from the wetland forest represented by a paleomangrove, although this sector is currently a freshwater environment (Ribeiro and Valadão, 2021; 2020). In this context, the RSL rise would have favored the establishment of paleomangrove strips as a forthright of the brackish influence caused by marine incursion. It is likely that the RSL rapidly dropped to the current level before 1490 cal yr BP, decreasing brackish input and culminating in the demise of this halophyte vegetation. Its organic debris accumulated and formed a layer of peatland (Fig. 2d) that reaches 2.1 m (MLT1), 1.9m (MLT2), and 1.8m (ISP) (Figs. 4 and 11). Recently, Ribeiro et al. (*submitted*) applied the multiproxy method, including palynology, to a muddy deposit underlain by this peat layer, identified a high mangrove pollen frequency related to the middle Holocene.

The undisturbed deposits and the absence of erosive contact between peat and muddy succession suggest that the RSL drop did not force geomorphologic confinement; on the contrary, this sector remained under estuarine inundation (*várzea*). The inundation frequency helps to clarify why the peat rapidly accumulated at 3 mm/yr (Fig. 3). Further, the RSL falling to its present-day position gave rise to a freshwater environment (Fig. 10). Due to the processes and significance that comprise this phase, it has a threshold character because the sea-level

changes and strength tectonics, which play a crucial role in the genesis of these islands, have weakened influence after 1490 cal yr BP forward (Fig. 10–4).

5.2.4 Phase IV: The CIAO separation – over the past 700 cal yr BP

In the last phase, the entire peninsula detached from the mainland (Fig. 10–5). We speculated that its separation and rise in the CIOA setting must have taken place in recent time scales after 700 cal yr BP. The main geomorphic event that resulted in its detachment is related to upstream erosion in the Maiauatá River, accompanied by a dextral strike-slip fault NNE-SSW trend, which has acquired an oblique kinematic component. This explains the muddy succession thickness that overlaps the peat layer in MLT1 compared to the MLT2 core (Fig. 11). Based on the historical reports, Maiauatá was a narrow and shallow river, possibly running towards the west and emptying in the Tocantins in past (Fig. 10–4). Maiauatá incised its headwaters and opened a pathway to connect to the Maratauíra River. The connecting of Maiauatá and Maratauíra led to separation and drift from this mainland tract in the estuarine zone (Fig. 10–5). Likewise, it is considered a significant event in the implication framework of coastal drainage rearrangements. Other tidal channels must have also shared the estuarine dynamics attributed to Maiauatá, as shown in the sedimentary records presented below.

Judging by the correlation cores, the activity assigned to the tidal channel (FAC) is indicated mainly by the facies cross-stratified sand (Scs) and inclined heterolithic stratification (IHS) in cores MT3, MLT4, and ISR (see Fig. 3). Scs facies display low-angle stratification (18−25°) and locally contain mud drapes on the foresets, occasionally paired (Fig. 2a). Cross-stratified is predominantly unidirectional, probably forming low-angle-inclined fronts of bars within the ebb-dominated channel (Thomas et al., 1987). This structure suggests bedform migration, which generally involves tidal bars within estuarine channels (Davis, 2010). In turn, the IHS exhibits almost evenly inclined sand and mud, either flood-or-ebb-oriented, and its preservation is probably due to tidal asymmetry in this estuary, where subordinate flow cannot entirely obliterate existing bedforms (cf. Choi, 2010). Because of the dips with inclinations of ~14° (Fig. 2b), these facies may be assigned to the lateral accretion of point bars in the meandering tidal channel (de Mowbray, 1983; Dott, 1983), after lateral migration.

The succession gradually becomes interbedded and muddy-dominated at the top, as the channel energy decreases during its gradual infill. As described in numerous cases, tidal channel migration comprises a fining upward sequence, starting with sand, cross-stratified, or heterolithic inclined facies, which grade into heterolithic intertidal mud-sand couplets (Dalrymple, 2010). This pattern is present in sedimentary stacking in the MLT3, MLT4, and

ISP cores (Fig. 3). In this case, we assessed these lateral migrations as an autogenic process owing to their local-scale events related to the internal dynamics of the estuarine environment during the last millennium, completing the CIOA genesis.

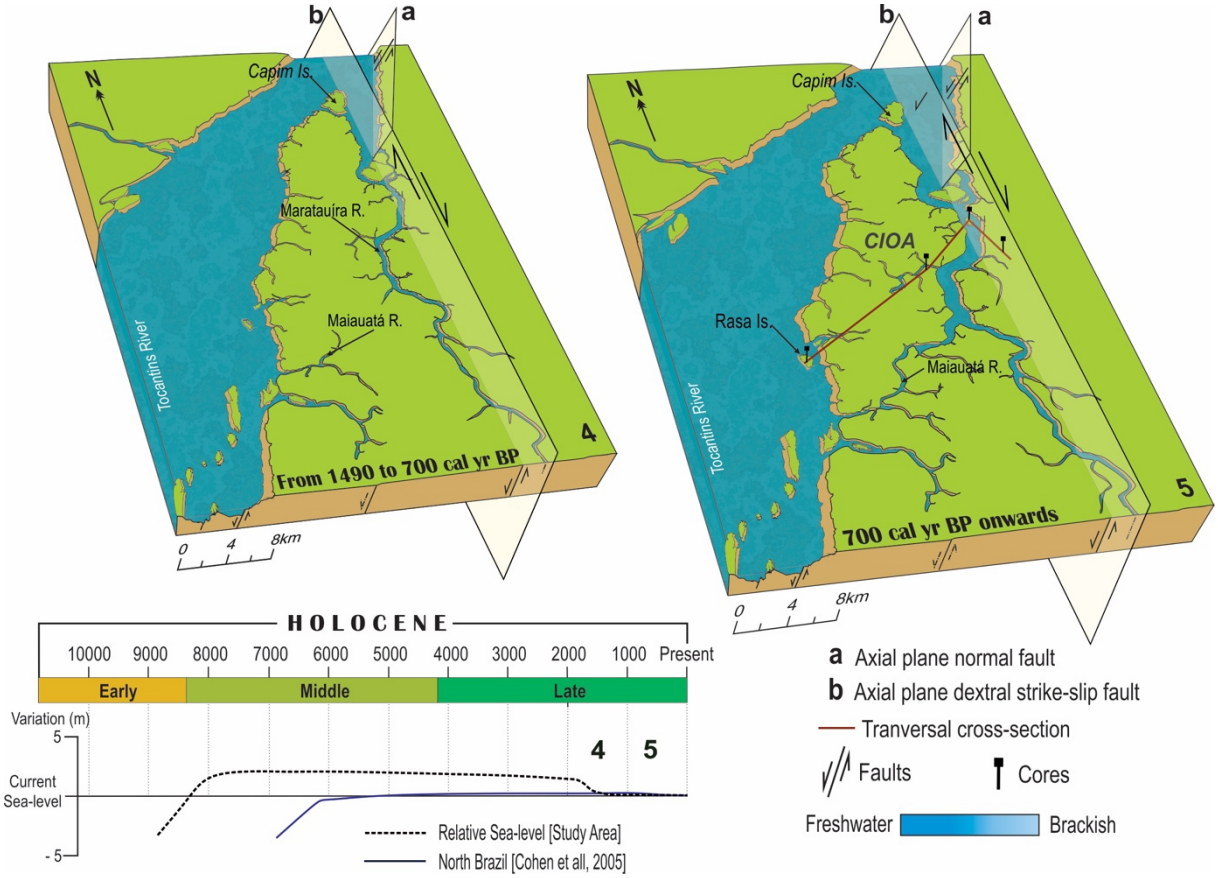

Figure 10. Block-4: Progressive peninsular detachment from the mainland because of the dextral strike-slip fault NNE–SSW trend, combined with RSL attaining its present-day level and intense estuarine hydrodynamics (Third Phase). Block-5: Maiauatá headwater erosion opened the pathway to the Maratauíra river, resulting in the CIOA's complete separation from the mainland (Fourth Phase). Note RSL falling to present day-position at the bottom graphic.

5.3 Tectonic evidence in the passive margin - signals from the Amazonian islands

Along with the data presented above, brief clarifications to underpin the Insular Complex structure formed via detachment from the mainland are also provided. First, the CIOA exhibits a morphological feature whose eastern geometry still holds the lateral shape, compatible with the mainland edge from where this island complex was separated. Additionally, their lateral displacement northward entirely coincides with the neotectonic framework represented by dextral strike-slip faults that are active along the study area (Fig. 8c). In addition to the river layout and riverbanks defined by minor faults, currently this zone expresses its control through the Capim Is., which has undergone gradual separation from the northward most from the CIOA (Fig. 10–5).

Second, the Maratauíra River has a wide mouth, considering its longitudinal profile (Figs. 1d and 8c). Furthermore, its drainage basin area and discharge volume are low and have a relatively stable annual volume, suggesting that the neotectonic process responsible for opening this valley, with consequent separation of the CIOA from the mainland, remains active. Thus, its wider mouth must be related to tectonic movements instead of erosion combined with peaks from a higher discharge fluvial. Third, widespread peat deposits are distributed in the mainland, Pacoca Island, and CIOA, which exhibit lateral and chronological correlations at the bottom between 1490 and 1430 cal yr BP (Fig. 11; Supplementary Data). These deposits are similar in thickness in the cores, suggesting a unique formation process within the same spatial context (Figs. 11 and 12).

Finally, the peat layers exhibited a vertical displacement, gradually increasing from the mainland, Pacoca Island, to the CIOA. Considering the continent as a reference until the Pacoca Islands, it is 96 cm, reaching up to 131 cm of vertical offset in the CIOA (Fig. 11). This downward movement points to slight subsidence of the CIOA after, or concurrent to, its detachment from the mainland, creating accommodation space progressive to the muddy deposits overlapping the peat layer (Fig. 11). The subsidence event was consistent with the high accumulation rate of 2.7 mm/yr of estuarine infill (Figs. 3 and 11). The oblique kinematic com ponent of the strike-slip fault NNE-SSW is invoked to explain the accommodation space creation. The CIOA block dip is due to the normal tension component indicating that this sector underwent subsidence simultaneously with its horizontally northward movement (Figs. 11 and 12).

The Maratauíra Valley opened and outstretched parallel to the Tocantins' mouth, giving the Insular Complex genesis. Both geomorphic features seem consistent with the coastal river rearrangement episode, with its main evolutionary stage occurring during the middle-late Holocene. Within this relatively short duration a variety of processes such as tectonic movement, sea-level changes, and dynamic intense entail channeled the estuaries. These forces imprinted their signature and generated a range of products preserved at the Tocantins River mouth. Despite being a partially mesotidal estuary, a character that would hamper the recognition of those signatures, and coastal rearrangement can be well investigated and reconstructed.

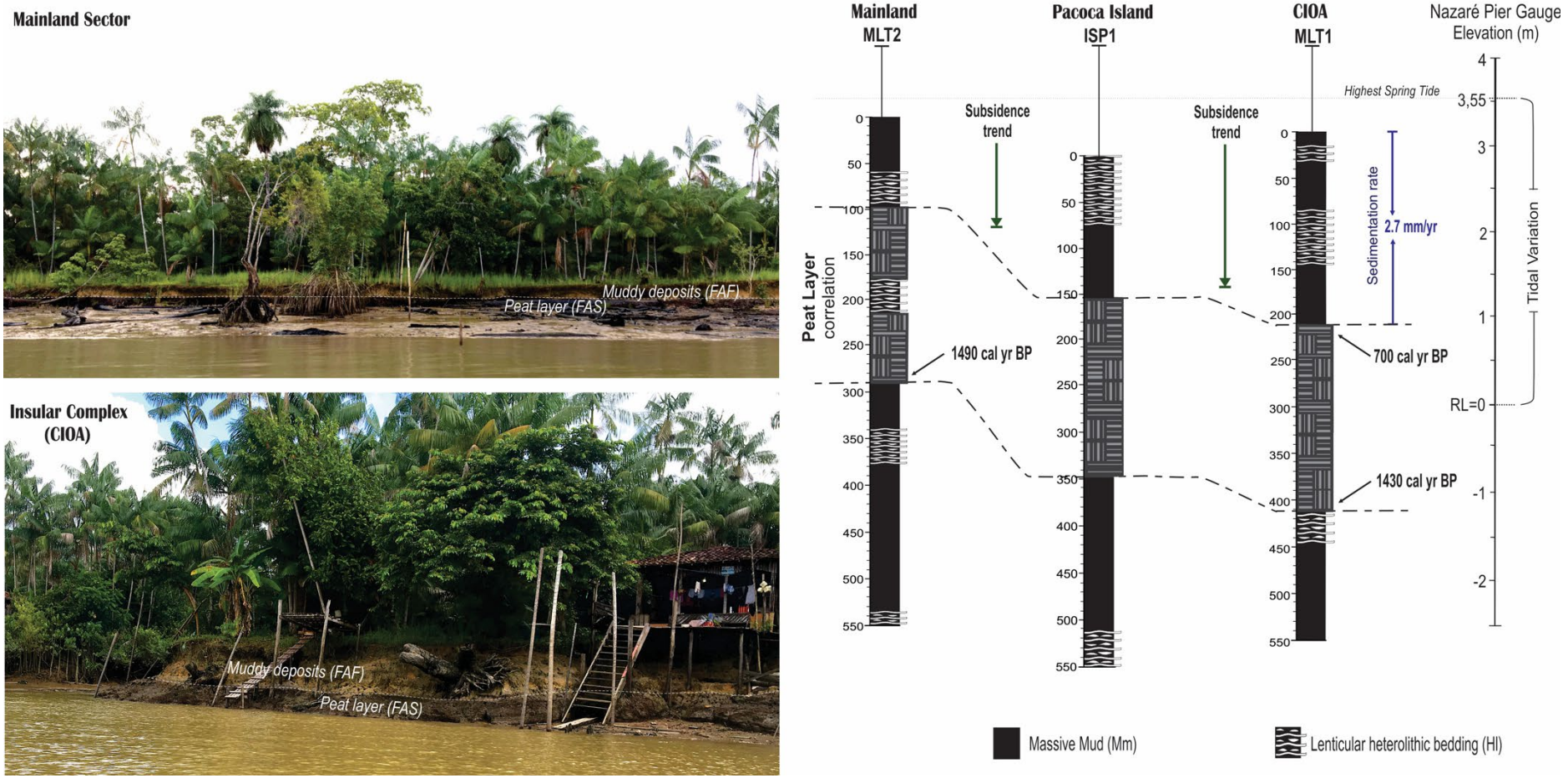

Figure 11. The peat layer correlation among the cores sedimentary features, considering the local Reduction Level (RL). This correlation among the MLT1, MLT2, and ISP1 reveal peat layer vertical offset, consistent with the subsidence from Pacoca island and CIOA after detachment from the mainland. Photo showing the thickness of the muddy sediment piles overlapping the peat layer in the insular sector (CIOA), compared to the mainland, both accumulated in the last 700 years.

The CIOA emphasizes that islands may have a complex geomorphology, resulting in a transitional nature. Overall, our data suggest that the trigger for the island's building exceeds the mechanisms that drove recent changes. The genesis is connected to the rearrangement of the Tocantins, which equates to the central stage of regional paleogeography. Thus, it is reasonable to propose that islands represent a product derived from river rearrangement, regardless of the coupled mechanism. These islands did not just invoke the archive of the Tocantins' mouth past but were also key to understanding the formation and evolution of Maratauíra.

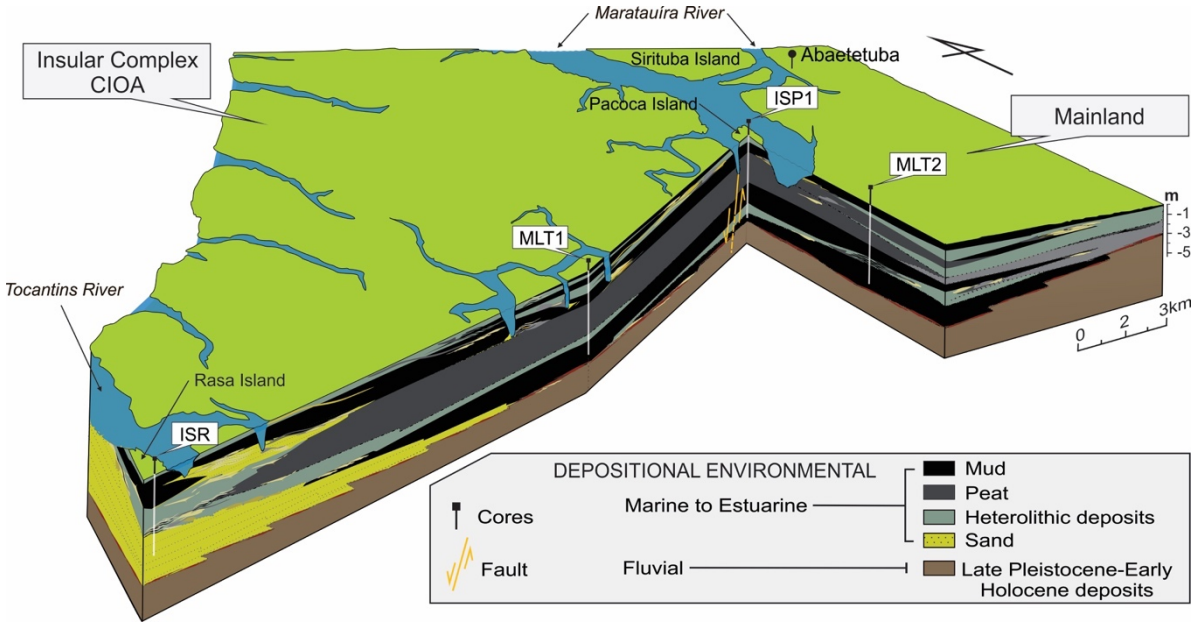

Figure 12. Stratigraphical transversal correlation of Holocene succession obtained from the sediment cores, from east to westward. Four sites were included with distinct geomorphological setting: mainland (MLT2), Pacoca Is. (ISP1), CIOA (MLT1), and Rasa Is. (ISR). Peat deposits accumulate with thickness similar in the center portion, laterally continuous, with depths of some meters overlapping mud and sand packets. Heterolithic deposits overlie the peat layer. Altogether, this package encompasses depositional marine to estuarine environments. Late Pleistocene-Early Holocene deposits, assigned to the fluvial environment, support that package. Note the effect of the oblique strike-slip fault NE-SW trend, which coincides with the course of the Maratauíra River, slightly displacing the peat layer. (See Figs. 1e and 10 for profile-line localization, and Fig. 3 for cores deposits).

Considering the documented rearrangements, such phenomena generally shift the upstream river systems, often addressing any tributaries. In contrast, the factor that causes the Tocantins' rearrangement has implied drastic tectonic changes until its new mouth; an east course, conjoined with an unfilled parallel incised valley is opened towards the Atlantic Ocean, weakening and inactivating the older one. Although these activities from strong tectonic control are generally assumed to be inherent to active margins, they may be equally associated to passive margins with subordinate intensities, as displayed herein (an extensive drainage system was connected to the Amazon outlet until the timing of intraplate tectonics led to its

decoupling). The passive geotectonic domain did not restrain the role of tectonic rearrangement, forcing the setting mouth to be distinct for these river systems. Moreover, joint data suggests that the tectonic pulses persisted, affecting even the last millennium-deposited strata. These findings reinforce that passive margin studies must carefully investigate recent tectonics. In this sense, different spatial-temporal patterns are helpful as they allow availability of the high-resolution data, usually with sensitive adherence on a shorter scale, thereby providing more reliable drainage reconstruction.

Conclusions

Integrated data provided an overview of the Tocantins riverine transition from western to eastern. This work recognized two key episodes, and its coastal impacts. The Tocantins River was an Amazon basin tributary until the Late Pleistocene, when it abandoned its ancient drainage net and migrated eastward. Infilled-valley sedimentary sequences were assigned to the estuarine environment and they likely deposited a transgressive setting. The west-to-east transition depicts a long-term evolutionary history, influencing more than 200 km of the strip region affected by the river. The second episode refers to the Holocene paleogeography that evolved alongside the coastal mouth. During this time, the Maratauíra incised valley opened, and as it penetrated its bed landward, an extensive tract of land detached from the margin of the eastern mainland. Tectonics and sea-level change compounded the tendency force behind the paleogeographic development until the last millennium. Afterward, the coastal evolution witnessed the estuarine dynamics becoming the main force.

This study revealed a history of rearrangement closely linked to tectonic control, despite the geography involving the passive margin of South America. By originating from an estuarine mouth, followed by incised valley and islands, having processed temporality and diverse mechanisms, the Tocantins River gathers unique products. Generally, rearrangement studies show tributaries diverted upstream without affecting their mouths, with fluvial shifts often encompassing the long term. Based on these characteristics, we indirectly underpin this rearrangement as a little analog among the reported cases. Lastly, our findings reinforce that passive margin addressed studies must have one outlook carefully while tracking tectonic activity, adopting a space-temporal hierarchy pattern favorable to examine and dialogue with recent and long-term geomorphic facts.

References

Ab'Saber, A.N., 2000. Fundamentos da geomorfologia costeira no Brasil atlântico inter e subtropical. Rev. Bras. Geomorfol. 1, 27–43. https://doi.org/10.20502/rbg.v1i1.67

Alexander, J., Bridge, J.S., Cheel, R.J., Leclair, S.F., 2001. Bedforms and associated sedimentary structures formed under supercritical water flows over aggrading sand beds. Sedimentology 48, 133–152. https://doi.org/10.1046/j.1365-3091.2001.00357.x

Allen, J.R.L., 1965. Fining-upwards cycles in alluvial successions. Geological Journal 4, 229–246. https://doi.org/10.1002/gj.3350040201

ANA (National Waters Agency), 2020. Accessed: January 2020. Available: http://www.snirh.gov.br/hidrotelemetria/Mapa.aspx

Antoine, P., Lautridou, J.P., Laurent, M., 2000. Long-term fluvial archives in NW France: response of the Seine and Somme rivers to tectonic movements, climatic variations and sea-level changes. Geomorphology 33, 183–207. https://doi.org/10.1016/S0169-555X(99)00122-1

Arai, M., Uesugui, N., Rossetti, D.F., Góes, A.M., 1988. Considerações sobre a idade do grupo Barreiras no nordeste do estado do Pará. 35 Cong. Bras. Geol., vol. 2. S.B.G., Belém, Brazil, 738–752.

Avşin, N., Vandenberghe, J., van Balen, R., Klyak, N.G., Oztürk, T., 2019. Tectonic and climatic controls on Quaternary fluvial processes and river terrace formation in a Mediterranean setting, the Göksu River, southern Turkey. Quaternary Research 91, 533–547. https://doi.org/10.1017/QUA.2018.129

Barbosa, G.V., Rennó, C.V., Franco, E.M.S., 1974. Geomorfologia da Folha SA-22 Belém. In: DNPM (Ed.). Folha SA.22 Belém: geologia, geomorfologia, solos, vegetação, uso potencial da terra, Rio de Janeiro, pp. 70–130.

Barreto, S.B., Knowles, L.L., Mascarenhas, R., Affonso, P.R.A. de M., Batalha-Filho, H., 2022. Drainage rearrangements and in situ diversification of an endemic freshwater fish genus from north-eastern Brazilian rivers. Freshwater Biology. https://doi.org/10.1111/FWB.13879

Beerbower, J.R., 1964. Cyclothems and cyclic depositional mechanisms in alluvial plain sedimentation. In: D.F. Merriam (Ed.), Symposium on Cyclic Sedimentation. Kansas Geological Survey Bulletin 169:31–42.

Behling, H., Cohen, M.C.L., Lara, R.J., 2001. Studies on Holocene mangrove ecosystem dynamics of the Bragança Peninsula in north-eastern Pará, Brazil. Palaeogeography, Palaeoclimatology, Palaeoecology 167, 225–242. https://doi.org/10.1016/S0031-0182(00)00239-X

Behling, H., da Costa, M.L., 2000. Holocene environmental changes from the Rio Curua record in the Caxiuana region, Eastern Amazon Basin. Quaternary Research 53, 369–377. https://doi.org/10.1006/qres.1999.2117

Bemerguy, R.L., Costa, J.B.S., 1991. Considerações sobre o sistema de drenagem da Amazônia e sua relação com o arcabouço tectono-estrutural. Bol. Museu Paraense Emílio Goeldi, Série Ciências da Terra 3, 75–97.

Bigham, J.M., Fitzpatrick, R.W., Schulze, D.G., 2018. Iron Oxides. Soil Mineralogy with Environmental Applications 7, 323–366. https://doi.org/10.2136/SSSABOOKSER7.C10

Boski, T., Bezerra, F.H.R., de Fátima Pereira, L., Souza, A.M., Maia, R.P., Lima-Filho, F.P., 2015. Sea-level rise since 8.2ka recorded in the sediments of the Potengi-Jundiai Estuary, NE Brasil. Marine Geology 365, 1–13. https://doi.org/10.1016/j.margeo.2015.04.003

Boyd, R., Dalrymple, R.W., Zaitlin, B.A., 2006. Estuarine and Incised-Valley Facies Models. Facies Models Revisited 171–235. https://doi.org/10.2110/PEC.06.84.0171

Bezerra, P.E.L., 2003. Compartimentação Morfotectônica do Interflúvio Solimões−Negro. Doctoral Thesis, Univ. Fed. Pará, Belém.

Catuneanu, O., 2019. Model-independent sequence stratigraphy. Earth-Science Reviews 188, 312–388. https://doi.org/10.1016/J.EARSCIREV.2018.09.017

Catuneanu, O., 2006. Principles of Sequence Stratigraphy. Elsevier, Amsterdam.

Campbell, K.E., Frailey, C.D., Romero-Pittman, L., 2006. The Pan-Amazonian Ucayali Peneplain, late Neogene sedimentation in Amazonia, and the birth of the modern Amazon River system. Palaeogeography, Palaeoclimatology, Palaeoecology 239, 166–219. https://doi.org/10.1016/j.palaeo.2006.01.020

Caputo, M.V., Soares, E.A.A., 2016. Eustatic and tectonic change effects in the reversion of the transcontinental Amazon River drainage system. Brazilian Journal of Geology 46, 301–328. https://doi.org/10.1590/2317-4889201620160066

Cecil, C.B., 2013. An overview and interpretation of autocyclic and allocyclic processes and the accumulation of strata during the Pennsylvanian-Permian transition in the central Appalachian Basin, USA. International Journal of Coal Geology 119, 21–31. https://doi.org/10.1016/j.coal.2013.07.012

Choi, K.S., 2010. Rhythmic climbing-ripple cross-lamination in inclined heterolithic stratification (IHS) of a macrotidal estuarine channel, Gomso Bay, west coast of Korea. Journal of Sedimentary Research 80, 550–561. https://doi.org/10.2110/jsr.2010.054

Cienciala, P., Nelson, A.D., Haas, A.D., Xu, Z., 2020. Lateral geomorphic connectivity in a fluvial landscape system: Unraveling the role of confinement, biogeomorphic interactions, and glacial legacies. Geomorphology 354, 107036. https://doi.org/10.1016/J.GEOMORPH.2020.107036

Cohen, M.C.L., Souza Filho, P.W.M., Lara, R.J., Behling, H., Angulo, R.J., 2005. A Model of Holocene Mangrove Development and Relative Sea-level Changes on the Bragança Peninsula (Northern Brazil). Wetlands Ecology and Management 2005 13:4 13, 433–443. https://doi.org/10.1007/S11273-004-0413-2

Color, M., 2009. Munsell Soil Color Charts, New Revised Edition. Macbeth Division of Kollmorgen Instruments, New Windsor, NY.

Costa, M. da S. da, 2014. Aporte Hídrico e de Material Particulado em Suspensão para a Baía do Marajó: contribuições dos Rios Jacaré Grande, Pará e Tocantins. Master Thesis, Univ. Fed. Pará, Belém.

Costa, J.B.S., Bemerguy, R.L., Hasui, Y., Borges, M. da S., Ferreira Júnior, C.R.P., Bezerra, P.É.L., Costa, M.L. da, Fernandes, J.M.G., 1996. Neotectônica Da Região Amazônica: Aspectos Tectônicos, Geomorfológicos e Deposicionais. Geonomos 4, 23–43. https://doi.org/10.18285/geonomos.v4i2.199

Costa, J.B.S., Hasui, Y., Bemerguy, R.L., Soares Júnior, A. v., Villegas, J.M.C., 2002. Tectonics and paleogeography of the Marajó Basin, northern Brazil. Anais da Academia Brasileira de Ciencias 74, 519–531. https://doi.org/10.1590/S0001-37652002000300013

Costa, J.B.S., Léa Bemerguy, R., Hasui, Y., da Silva Borges, M., 2001. Tectonics and paleogeography along the Amazon river. Journal of South American Earth Sciences 14, 335–347. https://doi.org/10.1016/S0895-9811(01)00025-6

Costa, M.L., 1991. Aspectos Geológicos dos Lateritos da Amazônia. Revista Brasileira de Geociências 21, 146–160. https://doi.org/10.25249/0375-7536.1991146160

Cunha, P.P., Martins, A.A., Daveau, S., Friend, P.F., 2005. Tectonic control of the Tejo river fluvial incision during the late Cenozoic, in Ródão - Central Portugal (Atlantic Iberian border). Geomorphology 64, 271–298. https://doi.org/10.1016/j.GEOMORPH.2004.07.004

Daidu, F., Yuan, W., Min, L., 2013. Classifications, sedimentary features and facies associations of tidal flats. Journal of Palaeogeography 2, 66–80. https://doi.org/10.3724/SP.J.1261.2013.00018

Dalrymple, R.W., Choi, K., 2007. Morphologic and facies trends through the fluvial-marine transition in tide-dominated depositional systems: A schematic framework for environmental and sequence-stratigraphic interpretation. Earth-Science Reviews 81, 135–174. https://doi.org/10.1016/j.earscirev.2006.10.002

Dalrymple, R.W., Zaitlin, B.A., Boyd, R., 1992. Estuarine facies models; conceptual basis and stratigraphic implications. Journal of Sedimentary Research 62, 1130–1146. https://doi.org/10.1306/D4267A69-2B26-11D7-8648000102C1865D

Davidson, D.A., Watson, A.I., 1995. Spatial variability in soil moisture as predicted from airborne thematic mapper (ATM) data. Earth Surface Processes and Landforms 20, 219–230. https://doi.org/10.1002/esp.3290200304

Davis, R.A., 2010. Tidal Signatures and Their Preservation Potential in Stratigraphic Sequences. Principles of Tidal Sedimentology 35–55. https://doi.org/10.1007/978-94-007-0123-6_3

Davis, R.A., Dalrymple, R.W., 2010. Principles of tidal sedimentology. Principles of Tidal Sedimentology 1–621. https://doi.org/10.1007/978-94-007-0123-6

de Mowbray, T., 1983. The genesis of lateral accretion deposits in recent intertidal mudflat channels, Solway Firth, Scotland. Sedimentology 30, 425–435. https://doi.org/10.1111/J.1365-3091.1983.TB00681.X

Dott, R.H., 1983. Episodic sedimentation; how normal is average? How rare is rare? Does it matter? Journal of Sedimentary Research 53, 5–23. https://doi.org/10.1306/212F8148-2B24-11D7-8648000102C1865D

Evans, G., Prego, R., 2003. Rias, estuaries and incised valleys: is a ria an estuary? Marine Geology 196, 171–175. https://doi.org/10.1016/S0025-3227(03)00048-3

FAPESPA. Amazon Foundation for Studies and Research Support. Pará Municipal Statistics: Igarapé-Miri. Belém, 2016. Accessed: June 2019. Available: https://www.fapespa.pa.gov.br/node/201

Ferreira, C.S., 1977. Fácies da Formação Pirabas (Mioceno Inferior): Novos conceitos e ampliações. (Projeto específicos ABe. FINEP) - Anais Academia Brasileira de Ciências, 49: 353.

Furtado, A.M.M., Ponte, F.C., 2013. Mapeamento de Unidades de Relevo do Estado do Pará. Revista Geoamazônia 2, 56–67. https://doi.org/10.17551/2358-1778/geoamazonia.n1v2p56-67

Gao, C., Ji, Y., Wu, C., Jin, J., Ren, Y., Yang, Z., Liu, D., Huan, Z., Duan, X., Zhou, Y., 2020. Facies and depositional model of alluvial fan dominated by episodic flood events in arid conditions: An example from the Quaternary Poplar Fan, north-western China, Sedimentology. https://doi.org/10.1111/sed.12684

Góes, A.M., Rossetti, D. de F., Nogueira, A.C.R., Toledo, P.M. de, 1990. Modelo deposicional preliminar da Formação Pirabas no Nordeste do Estado do Pará. Boletim do Museu Paraense Emílio Goeldi, Ciências da Terra 2, 3–15.

Hadley, D.F., Arochukwu, E.C., Nishi, K., Sarginson, M.J., Md Salleh, H., Omar, M., 2006. Depositional Modelling of Champion Field, Brunei: Assessing the Impact of Reservoir Architecture on Secondary Recovery. All Days. https://doi.org/10.2118/101033-MS

Hayes, M.O., 1975. Morphology of sand accumulation in estuaries: an introduction to the Symposium. Geol and Eng 2, 3–22. https://doi.org/10.1016/B978-0-12-197502-9.50006-X

Hogg, A.G., Heaton, T.J., Hua, Q., Palmer, J.G., Turney, C.S.M., Southon, J., Bayliss, A., Blackwe Boswijk, G., Bronk Ramsey, C., Pearson, C., Petchey, F., Reimer, P., Reimer, R., Wacker, L., 2020. SHCal20 Southern Hemisphere Calibration, 0–55,000 Years cal BP. Radiocarbon 62, 759–778. https://doi.org/10.1017/RDC.2020.59

Holbrook, J., Scott, R.W., Oboh-Ikuenobe, F.E., 2006. Base-Level Buffers and Buttresses: A Model for Upstream Versus Downstream Control on Fluvial Geometry and Architecture Within Sequences. Journal of Sedimentary Research 76, 162–174. https://doi.org/10.2110/JSR.2005.10

Hoorn, C., Wesselingh, F.P., ter Steege, H., Bermudez, M.A., Mora, A., Sevink, J., Sanmartín, I., Sanchez-Meseguer, A., Anderson, C.L., Figueiredo, J.P., Jaramillo, C., Riff, D., Negri, F.R., Hooghiemstra, H., Lundberg, J., Stadler, T., Särkinen, T., Antonelli, A., 2010. Amazonia through time: Andean uplift, climate change, landscape evolution, and biodiversity. Science 330, 927–931. https://doi.org/10.1126/science.1194585

Hughes, Z.J., 2012. Tidal Channels on Tidal Flats and Marshes. Principles of Tidal Sedimentology 269–300. https://doi.org/10.1007/978-94-007-0123-6_11

James, N.P., Walker, R.G., 1992. Facies Models: response to sea-level changes. Geol. Assoc. Canada 407. https://doi.org/10.1097/00000433-198206000-00020

Johnson, S.Y., 1984. Cyclic fluvial sedimentation in a rapidly subsiding basin, northwest Washington. Sedimentary Geology 38, 361–391. https://doi.org/10.1016/0037-0738(84)90086-1

Kelly, S.B., Olsen, H., 1993. Terminal fans-a review with reference to Devonian examples. Sedimentary Geology 85, 339–374. https://doi.org/10.1016/0037-0738(93)90092-J

Kim, W., Petter, A., Straub, K., Mohrig, D., 2014. Investigating the autogenic process response to allogenic forcing: Experimental geomorphology and stratigraphy. From Depositional Systems to Sedimentary Successions on the Norwegian Continental Margin 9781118920, 127–138. https://doi.org/10.1002/9781118920435.ch5

Lima, M.I.C., Barbosa, A.M., Alvarenga, M.M., Guimarães, H.G., Menezes, E.O., 2017. Evidências de movimentos neotectônicos no interflúvio Baixo Rio Xingu – Baixo Rio Tocantins, Nor-Nordeste do Estado do Pará, com base em imagens SRTM e PALSAR. In: Simp. Bras. Sens. Rem. São Paulo, Proceedings, pp. 1–8. Accessed: December 2020. Available: https://abre.ai/eb07

Lorang, M.S., Hauer, F.R., 2017. Fluvial Geomorphic Processes, Methods in Stream Ecology: Third Edition. Elsevier Inc. https://doi.org/10.1016/B978-0-12-416558-8.00005-6

Lovejoy, N.R., Albert, J.S., Crampton, W.G.R., 2006. Miocene marine incursions and marine/freshwater transitions: Evidence from Neotropical fishes. Journal of South American Earth Sciences 21, 5–13. https://doi.org/10.1016/J.JSAMES.2005.07.009

Maslin, M., Knutz, P.C., Ramsay, T., 2006. Millennial-scale sea-level control on avulsion events on the Amazon Fan. Quaternary Science Reviews 25, 3338–3345. https://doi.org/10.1016/j.quascirev.2006.10.012

McLaren, S., Wallace, M.W., Gallagher, S.J., Miranda, J.A., Holdgate, G.R., Gow, L.J., Snowball, I., Sandgren, P., 2011. Palaeogeographic, climatic and tectonic change in southeastern Australia: the Late Neogene evolution of the Murray Basin. Quaternary Science Reviews 30, 1086–1111. https://doi.org/10.1016/J.QUASCIREV.2010.12.016

Miall, A.D., 2006. The Geology of Fluvial Deposits. The Geology of Fluvial Deposits. https://doi.org/10.1007/978-3-662-03237-4

Miall, A.D., 1994. Reconstructing fluvial macroform architecture from two-dimensional outcrops; examples from the Castlegate Sandstone, Book Cliffs, Utah. Journal of Sedimentary Research 64, 146–158. https://doi.org/10.1306/D4267F78-2B26-11D7-8648000102C1865D

Miall, A.D., 1992. Alluvial Models. In: Walker, R.G. and James, N.P. (Ed.), Facies Models Response to Sea Level Change, Geological Association of Canada, St. John's, pp. 119–142.

Miall, A.D., 1985. Architectural-element analysis: A new method of facies analysis applied to fluvial deposits. Earth Science Reviews 22, 261–308. https://doi.org/10.1016/0012-8252(85)90001-7

Miall, 1978. Facies types and vertical profilemodels in braided river deposits: a summary. In: Miall, A.D. (Ed.), Fluvial Sedimentology. Canadian Society of Petroleum Geologists, Calgary, pp. 597–604

Morgans-Bell, H.S., McIlroy, D., 2005. Palaeoclimatic implications of Middle Jurassic (Bajocian) coniferous wood from the Neuquén Basin, west-central Argentina. Geological Society, London, Special Publications 252, 267–278. https://doi.org/10.1144/GSL.SP.2005.252.01.13

Nandini, C. v., Sanjeevi, S., Bhaskar, A.S., 2013. An integrated approach to map certain palaeochannels of South India using remote sensing, geophysics, and sedimentological techniques. International Journal of Remote Sensing 34, 6507–6528. https://doi.org/10.1080/01431161.2013.803629

Nascimento, M.H.D'O., 2003. Identificação de ambientes de sedimentação na área metropolitana de Belém a partir de perfis de poço. MS Dissertation, Univ. Fed. Pará, Belém.

Neagu, N., Matmon, A., Enzel, Y., Porat, N., 2020. Quaternary evolution of a hyperarid drainage under climatic fluctuations and rift-margin base-level fall, NE Negev, Israel. Geomorphology 354, 107042. https://doi.org/10.1016/J.GEOMORPH.2020.107042

Nichols, G.J., Fisher, J.A., 2007. Processes, facies and architecture of fluvial distributary system deposits. Sedimentary Geology 195, 75–90. https://doi.org/10.1016/j.sedgeo.2006.07.004

Peña-Monné, J.L., Sampietro-Vattuone, M.M., 2020. Fluvial piracies in the NE sector of the Sierra de Aconquija (Tafí Valley, NW Argentina). Cuadernos de Investigación Geográfica 46, 285–301. https://doi.org/10.18172/CIG.4204

Preece, R.C., Bridgland, D.R., 1999. Holywell Coombe, Folkestone: A 13,000 year history of an English Chalkland Valley. Quaternary Science Reviews 18, 1075–1125. https://doi.org/10.1016/S0277-3791(98)00066-3

Prestes, Y.O., Borba, T.A. da C., Silva, A.C. da, Rollnic, M., 2020. A discharge stationary model for the Pará-Amazon estuarine system. Journal of Hydrology: Regional Studies 28. https://doi.org/10.1016/j.ejrh.2020.100668

Pupim, F. do N., Bierman, P.R., Assine, M.L., Rood, D.H., Silva, A., Merino, E.R., 2015. Erosion rates and landscape evolution of the lowlands of the Upper Paraguay river basin (Brazil) from cosmogenic 10Be. Geomorphology 234, 151–160. https://doi.org/10.1016/J.GEOMORPH.2015.01.016

Qiang, W., Qiang, W., 2019. Incised valley of Last Glacial Maximum stage in the drilling strata on the Tianjin-Hebei Coastal Plain. Journal of Geomechanics 25, 877–888. https://doi.org/10.12090/J.ISSN.1006-6616.2019.25.05.072

Reineck, H. -E, Wunderlich, F., 1968. Classification and Origin of Flaser and Lenticular Bedding. Sedimentology 11, 99–104. https://doi.org/10.1111/j.1365-3091.1968.tb00843.x

Ribeiro, A.C., 2006. Tectonic history and the biogeography of the freshwater fishes from the coastal drainages of eastern Brazil: An example of faunal evolution associated with a divergent continental margin. Neotropical Ichthyology 4, 225–246. https://doi.org/10.1590/S1679-62252006000200009

Ribeiro, S.R., Valadão, R.C., Gomes, M.O.S., Bittencourt, J.S., Alves, R.A. (Submitted). Paleoecological indicators of the highstand sea level on the Amazonian supralittoral until the last two millennia. Journal of South American Earth Sciences.

Ribeiro, S.R., Batista, E.J.L., Cohen, M.C.L., França, M.C., Pessenda, L.C.R., Fontes, N.A., Alves, I.C.C., Bendassolli, J.A., 2018. Allogenic and autogenic effects on mangrove dynamics from the Ceará Mirim River, north-eastern Brazil, during the middle and late Holocene. Earth Surface Processes and Landforms 43, 1622–1635. https://doi.org/10.1002/esp.4342

Ribeiro, S.R., Valadão, R.C., 2021. Efeitos marinho e fluvial na dinâmica dos ambientes inundáveis do Estuário Superior do Rio Pará, Norte do Brasil. Revista Brasileira de Geomorfologia 22. https://doi.org/10.20502/rbg.v22i4.2017

Ribeiro, S.R., Valadão, R.C., 2020. Processos fluviomarinhos associados à formação da Ilha Rasa, Sul da Baía de Marapatá, Nordeste do Pará, Brasil. Arquivos de Ciências do Mar 53, 110–119. https://doi.org/10.32360/acmar.v53iEspecial.42659

Rieu, R., van Heteren, S., van der Spek, A.J.F., de Boer, P.L., 2005. Development and Preservation of a Mid-Holocene Tidal-Channel Network Offshore the Western Netherlands. Journal of Sedimentary Research 75, 409–419. https://doi.org/10.2110/JSR.2005.032

Rossetti, D.F., 2014. The role of tectonics in the late Quaternary evolution of Brazil's Amazonian landscape. Earth-Science Reviews 139, 362–389. https://doi.org/10.1016/j.earscirev.2014.08.009

Rossetti, D.F., Góes, A.M., 2008. Late Quaternary drainage dynamics in northern Brazil based on the study of a large paleochannel from southwestern Marajó Island. Anais da Academia Brasileira de Ciencias 80, 579–593. https://doi.org/10.1590/s0001-37652008000300017

Rossetti, D.F., Góes, A.M., Valeriano, M.M., Miranda, M.C.C., 2008a. Quaternary tectonics in a passive margin: Marajó Island, northern Brazil. Journal of Quaternary Science 23, 121–135. https://doi.org/10.1002/JQS.1132

Rossetti, D.F., Valeriano, M.M., Góes, A.M., Thales, M., 2008b. Palaeodrainage on Marajó Island, northern Brazil, in relation to Holocene relative sea-level dynamics. Holocene 18, 923–934. https://doi.org/10.1177/0959683608091798

Rossetti, D.F., Valeriano, M.M., 2007. Evolution of the lowest amazon basin modeled from the integration of geological and SRTM topographic data. Catena 70, 253–265. https://doi.org/10.1016/j.catena.2006.08.009

Rossetti, D.F., Valeriano, M.M., Thalês, M., 2007. Remote sensing applied to decipher the origin of the Marajó Island, northern Brazil. In: Simp. Bras. Sens. Rem. Florianópolis, Proceedings, pp. 2133–2141. Accessed: December 2020. Available: https://abre.ai/eb51

Rossetti, D.F., 2006. The Role of Tectonics on the Preservation of Incised-Valley Estuaries in Areas with Low Accommodation Rates: Examples From Upper Scretaceous and Miocene Successions in Northern Brazil. Incised Valleys in Time and Space 199–217. https://doi.org/10.2110/PEC.06.85.0199

Rossetti D. F., 2004. Paleosurfaces from northeastern Amazonia as a key for reconstructing paleolandscapes and understanding weathering products. Sedim. Geol. 169: 151–174. https://doi:10.1016/j.sedgeo.2004.05.003

Rossetti, D.F., Truckenbrodt, W., Góes, A.M., 1989. Estudo paleoambiental e estratigráfico dos Sedimentos Barreiras e Pós-Barreiras na região Bragantina, nordeste do Pará. Boletim do Museu Paraense Emílio Goeldi, Série Ciências da Terra 1, 25–74.

Shennan, I., 2019. Peat. In: Charles W.F., Christopher, M. (Eds.), Encyclopedia of Coastal Science. Springer Nature Switzerland AG, pp. 1364–1367.

Shennan, I., Long, A.J., Rutherford, M.M., Green, F.M., Innes, J.B., Lloyd, J.M., Zong, Y., Walker, K.J., 1996. Tidal marsh stratigraphy, sea-level change and large earthquakes, I: A 5000 year record in Washington, U.S.A. Quaternary Science Reviews 15, 1023–1059. https://doi.org/10.1016/S0277-3791(96)00007-8

Schoenbohm, L.M., Whipple, K.X., Burchfiel, B.C., Chen, L., 2004. Geomorphic constraints on surface uplift, exhumation, and plateau growth in the Red River region, Yunnan Province, China. GSA Bulletin 116, 895–909. https://doi.org/10.1130/B25364.1

Shimozono, T., Tajima, Y., Akamatsu, S., Matsuba, Y., Kawasaki, A., 2019. Large-Scale Channel Migration in the Sittang River Estuary. Scientific Reports 2019 9:1 9, 1–9. https://doi.org/10.1038/s41598-019-46300-x

Shukla, U.K., Singh, I.B., Sharma, M., Sharma, S., 2001. A model of alluvial megafan sedimentation: Ganga Megafan. Sedimentary Geology 144, 243–262. https://doi.org/10.1016/S0037-0738(01)00060-4

Soares Júnior, A.V., Hasui, Y., Costa, J.B.S., Machado, F.B., 2011. Evolução do rifteamento e paleogeografia da margem Atlântica Equatorial do Brasil: Triássico ao Holoceno. Geociencias 30, 669–692.

Soria-Jáuregui, Á., Jiménez-Cantizano, F., Antón, L., 2019. Geomorphic and tectonic implications of the endorheic to exorheic transition of the Ebro River system in northeast Iberia. Quaternary Research 91, 472–492. https://doi.org/10.1017/QUA.2018.87

Souza-Filho, P.W.M., Lessa, G.C., Cohen, M.C.L., Costa, F.R., Lara, R.J., 2009. The Subsiding Macrotidal Barrier Estuarine System of the Eastern Amazon Coast, Northern Brazil. Lecture Notes in Earth Sciences 107, 347–375. https://doi.org/10.1007/978-3-540-44771-9_11

Symonds, A.M., Collins, M.B., 2007. The establishment and degeneration of a temporary creek system in response to managed coastal realignment: The Wash, UK. Earth Surface Processes and Landforms 32, 1783–1796. https://doi.org/10.1002/ESP.1495

Syvitski, J.P.M., Cohen, S., Kettner, A.J., Brakenridge, G.R., 2014. How important and different are tropical rivers? — An overview. Geomorphology 227, 5–17. https://doi.org/10.1016/J.GEOMORPH.2014.02.029

Szymański, W., Skiba, M., 2013. Distribution, Morphology, and Chemical Composition of Fe-Mn Nodules in Albeluvisols of the Carpathian Foothills, Poland. Pedosphere 23, 445–454. https://doi.org/10.1016/S1002-0160(13)60037-5

Tatumi, S.H., Silva, L.P. da, Pires, E.L., Rossetti, D.F., Góes, A.M., Munita, C.S., 2008. Datação de Sedimentos Pós-Barreiras no Norte do Brasil: implicações paleogeográficas. Revista Brasileira de Geociências 38, 514–524. https://doi.org/10.25249/0375-7536.2008383514524

Terwindt, J.H.J., 1988. Palaeo-tidal reconstructions of inshore tidal depostional environments. In: de Boer PL, van Gelder A, Nio SD (eds) Tide-influenced sedimentary environments and facies, sedimentology and petroleum geology. D. Reidel Publishing, Dordrecht, pp 233–263

Thomas, R.G., Smith, D.G., Wood, J.M., Visser, J., Calverley-Range, E.A., Koster, E.H., 1987. Inclined heterolithic stratification—Terminology, description, interpretation and significance. Sedimentary Geology 53, 123–179. https://doi.org/10.1016/S0037-0738(87)80006-4

van Straaten, L.M.J.U., 1954. Composition and structure of recent marine sediments in the Netherlands. Leidse Geol Mededel 19, 1–110.

Valadão, R.C., 2009. Geodinâmica de superfícies de aplanamento, desnudação continental e tectônica ativa como condicionantes da megageomorfologia do Brasil oriental. Revista Brasileira de Geomorfologia 10, 77–90. https://doi.org/10.20502/rbg.v10i2.132

Vedel, V., Behling, H., Cohen, M., Lara, R., 2006. Holocene mangrove dynamics and sea-level changes in northern Brazil, inferences from the Taperebal core in northeastern Pará State. Vegetation History and Archaeobotany 15, 115–123. https://doi.org/10.1007/s00334-005-0023-9

Villegas, J.M., 1994. Geologia estrutural da Bacia de Marajó. Belém (PA). MS Dissertation, Univ. Fed. Pará, Belém.

Walker, R.G., 1992. Facies, facies models and modern stratigrahic concepts. In Facies Models – Response to Sea Level Change, Walker RG, James NP (eds). Geological Association of Canada: Ontario; 1–14.

Walker, R.G., Cant, D.J., 1979. Sandy Fluvial Systems. In: Walker, R.G. (Ed.), Facies Models Geoscience, Geological Association of Canada, St. John's, 23-31.

Wang, R., Colombera, L., Mountney, N.P., 2019. Geological controls on the geometry of incised-valley fills: Insights from a global dataset of late-Quaternary examples. Sedimentology 66, 2134–2168. https://doi.org/10.1111/sed.12596

Weissmann, G.S., Hartley, A.J., Nichols, G.J., Scuderi, L.A., Olson, M., Buehler, H., Banteah, R., 2010. Fluvial form in modern continental sedimentary basins: Distributive fluvial systems. Geology 38, 39–42. https://doi.org/10.1130/G30242.1

Weissmann, G.S., Hartley, A.J., Scuderi, L.A., Nichols, G.J., Davidson, S.K., Owen, A., Atchley, S.C., Bhattacharyya, P., Chakraborty, T., Ghosh, P., Nordt, L.C., Michel, L., Tabor, N.J., 2013. Prograding distributive fluvial systems-geomorphic models and ancient examples. SEPM Special Publications 104, 131–147. https://doi.org/10.2110/sepmsp.104.16

Wenzens, E., Wenzens, G., 1997. The influence of tectonics, sea-level fluctuations and river capture on the Quaternary morphogenesis of the semi-arid Pulpi Basin (southeast Spain). Catena 30, 283–293. https://doi.org/10.1016/S0341-8162(97)00016-7

Whitfield, E., Harvey, A.M., 2012. Interaction between the controls on fluvial system development: Tectonics, climate, base level and river capture - Rio Alias, Southeast Spain. Earth Surface Processes and Landforms 37, 1387–1397. https://doi.org/10.1002/esp.3247

Whittaker, A.C., 2012. How do landscapes record tectonics and climate? Lithosphere 4, 160–164. https://doi.org/10.1130/RF.L003.1

Wickert, A.D., 2016. Reconstruction of North American drainage basins and river discharge since the Last Glacial Maximum. Earth Surface Dynamics 4, 831–869. https://doi.org/10.5194/ESURF-4-831-2016

Wilkinson, M.J., Marshall, L.G., Lundberg, J.G., Kreslavsky, M.H., 2010. Megafan Environments in Northern South America and their Impact on Amazon Neogene Aquatic Ecosystems. Amazonia, Landscape and Species Evolution: A Look into the Past 162–184. https://doi.org/10.1002/9781444306408.CH10

Zalán, P.V., Matsuda, N.S., 2007. Bacia do Marajó. Boletim de Geociências da Petrobras, 15, 311–319.

Supplementary Data

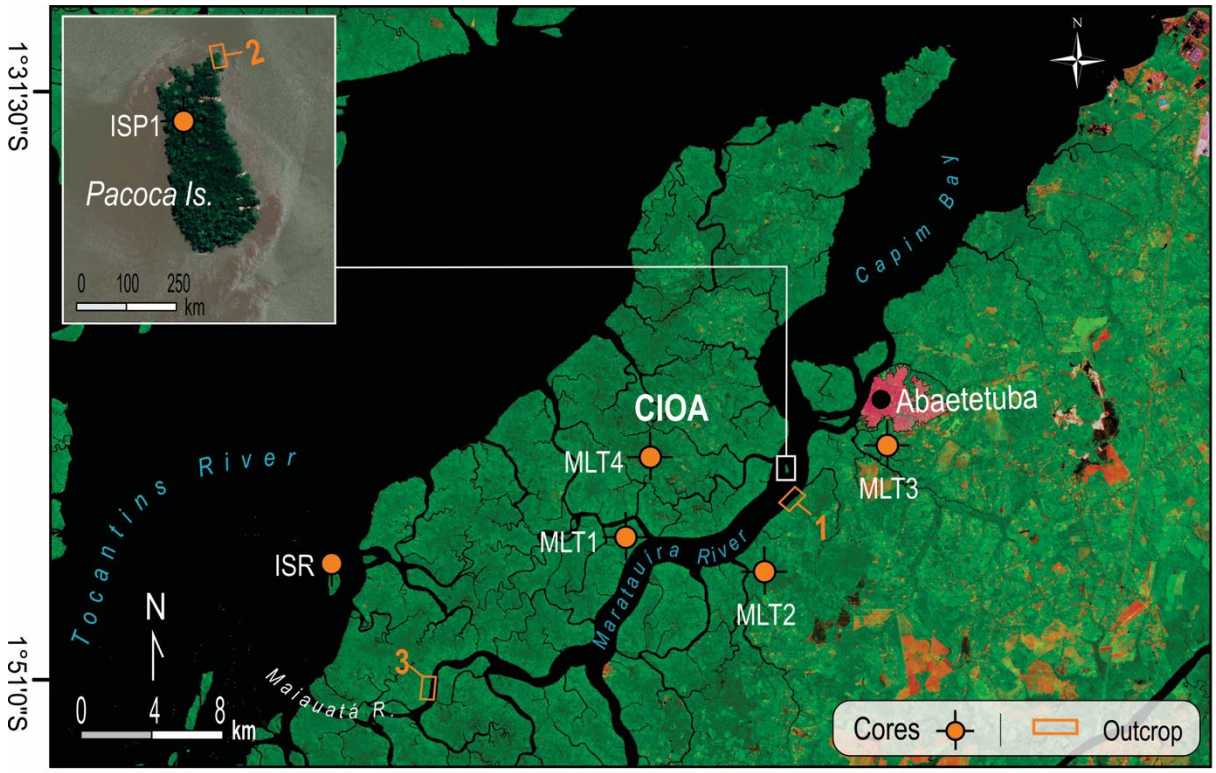

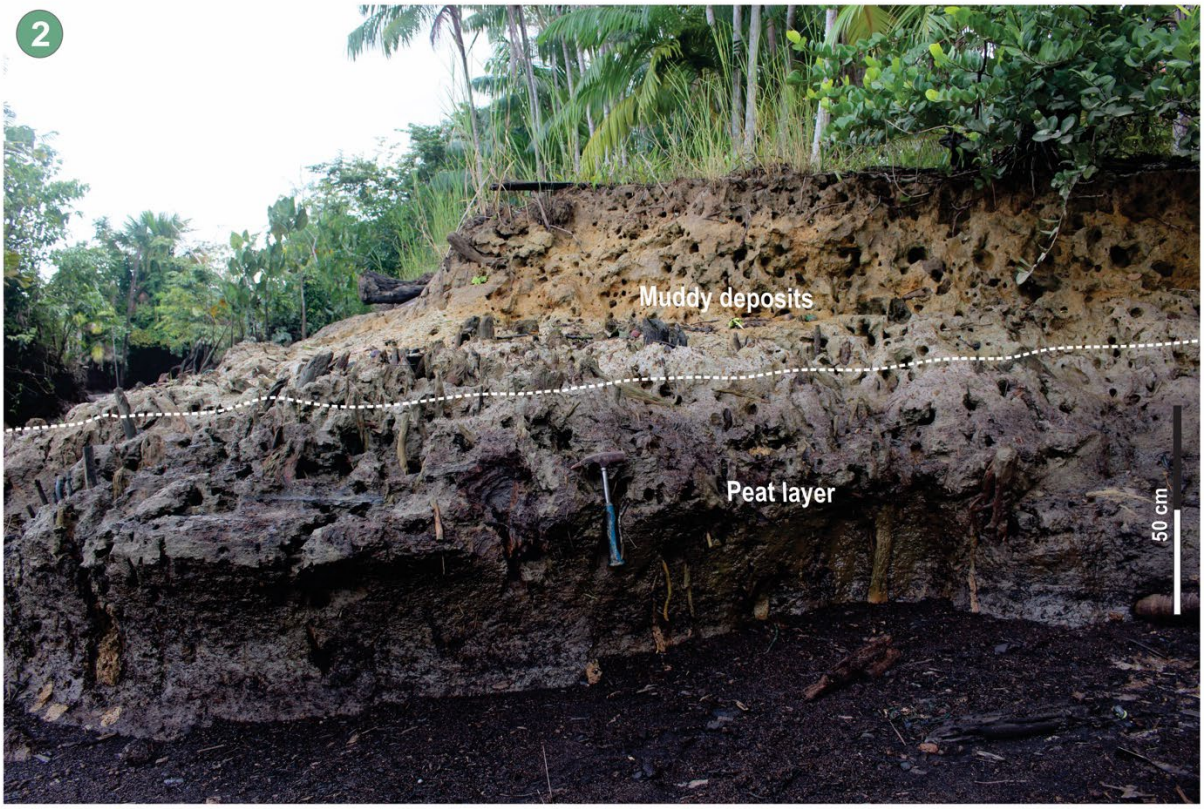
2
Muddy deposits
Peat layer
50 cm


3
Muddy deposits
Peat layer
50 cm

CHAPTER 3:

PALEOECOLOGICAL INDICATORS OF THE HIGHSTAND SEA LEVEL ON THE AMAZONIAN SUPRALITTORAL UNTIL THE LAST TWO MILLENNIA

Abstract – Holocene sea-level changes are ubiquitous worldwide. The relative sea levels (RSL) of the Northeast and Southeast littoral zones of Brazil were higher than the current level during the middle Holocene. It has been assumed that the RSL was stable since 7 ka BP in the North Brazilian littoral, particularly in the Amazonian coast. Based on a multiproxy approach (pollen content, $\delta^{13}C$, 14C-dating, and sedimentary and geomorphological features) applied to a sediment core obtained from the Amazonian supralittoral zone (> 50 km away from the modern coastline), our study investigated the signatures of the RSL highstand in this region. The results show that the marine influence was more intense from 6459 cal yr BC to 466 CE than that of the present. During this period, a mangrove community represented by *Rhizophora* and *Avicennia* established and thrived on the Itacuruçá tidal flat, probably due to post-glacial sea-level rise, which surpassed the present level during the middle Holocene. The mangrove population declined after 466 CE, while freshwater vegetation developed, with the dominance of various associations of taxa. The sudden deposition of organic debris in the sedimentary record is consistent with the decrease in mangrove communities. This pronounced environmental change is possibly related to the reduction of the RSL, which reached the present-day position before the last millennium. Climate influence has not been recognized as significant in this process. Irrespective of the curve model showing the position or values from the RSL and related causes, this investigation addresses the indicators of this phenomenon. The results presented here suggest that understanding the variable trends of the Late Holocene RSL and their influence on paleoecological dynamics and paleogeographical evolution requires further advancement.

Keywords: Holocene sea-level change; Paleo-mangrove; Freshwater vegetation; Palynology; Itacuruçá flats.

1. Introduction

Sea-level changes occur worldwide over a broad range of spatiotemporal scales. As a ubiquitous phenomenon in coastal regions, these changes have been recognized through geomorphology (Kelletat, 2019), strata stacking patterns of the sedimentary rocks (Allen and Posamentier, 1993; Dalrymple et al., 1994; Ghandour et al., 2021), systems of coastal valley drowning and river connectivity (Evans and Prego, 2003; Galili et al., 2005), and littoral spatial dynamics of ecosystems (Cameron and Palmer, 1995; Yao and Liu, 2017). The growing interest in sea-level changes has fostered technical (e.g., satellite-based radar altimeter and tidal gauge of high-precision) and methodological advances in the study and interpretation of paleo-sea

levels. Gathering evidence of these events helps to understand the structure of shore landscapes under distinct characteristics (geological, biological, and hydrological), which allows for the development of a more realistic paleogeographic framework. This provides support for the accuracy of modeling predictions of relative sea level (RSL) rise from a future perspective (Dayan et al., 2021; Sampath et al., 2015).

Systematic investigations focusing on reconstructing the paleo-sea level along the Brazilian coast have been conducted based on organic content, topographical indicators, and 14C chronology of the seashore sediments (Angulo et al., 2006; Bezerra et al., 2003; Boski et al., 2015; Castro et al., 2014; Martin et al., 2003; Suguio et al., 2013; Tomazelli, 1990). For example, in the eastern and southeastern littoral zones, these investigations revealed that the sea level was previously higher than that of the present because of the influence of the interglacial period (middle Holocene), with a late-Holocene trend of RSL decline until the current level (Angulo et al., 2006; Angulo and Lessa, 1997; Bezerra et al., 2003; Boski et al., 2015; Dominguez et al., 1990; Suguio et al., 2013). The paleo-sea level of the Amazon has been studied in terms of pollen analysis and sedimentary facies, as well as with $\delta^{13}C$, $\delta^{15}N$, C/N, and Holocene radiocarbon chronology. These multi-proxy investigations have identified that RSL reached its current level between 7000 and 5000 yr BP and has remained stable since then (e.g., Behling et al., 2001; Behling and da Costa, 2000; Cohen et al., 2005; Rossetti et al., 2008; Vedel et al., 2006).

The interglacial sea level of the Amazon could have exceeded the present level during the middle Holocene, which is supported by the peat deposits cropping out at the Maratauíra riverbank, 180 km from the coastline. The development of peat deposits could be attributed to paleo-mangrove demise after the RSL declined to the current level. In addition, a present-day mangrove fringe represented mainly by *Rhizophora* on the estuarine landscape, otherwise dominated by freshwater vegetation, can be evidence of the post-glacial sea-level rise that affected this region (Ribeiro and Valadão, 2021; 2020). If mangroves previously occupied this region, then it is plausible that the relative sea level could have been higher than that of the present-day in northern Brazil.

Mangrove forests are unique ecosystems because of their physiological adaptations to harsh saline environments (Mukherjee et al., 2015; Spalding et al., 2010). Mangroves grow on mudflats between mean sea level and high spring tide in tropical and sub-tropical shorelines worldwide (Polidoro et al., 2010). Their growth depends on temperature, tidal inundation frequency, and mud sediment supply (Lugo and Snedaker, 1974). Kodikara et al. (2018) demonstrated that optimal growth and productivity rates in this forest can occur at

concentrations ranging from 15 to 17 PSU due to the regulation of leaf water, osmotic potentials, and stomatal conductance, which present better physiological performances under moderate salinity.

Mangrove community dynamics are also related to changes in sea level, as they migrate landward with a rise in sea level, and seaward when the level declines (Blasco et al., 1996; Gilman et al., 2008). Some investigations have demonstrated the complex relationship among the growth, spatial, and temporal fluctuations and demise of mangroves on coastal interfaces conditioned by freshwater (Aziz and Khan, 2001; Naidoo, 1985). Considering the mangrove responses to sea-level changes, the marine influence can be traced based on the spatiotemporal dynamics, in this case, using a field away from the shoreline.

In northern Brazil, outside the Amazonian coast, there is little evidence of the effects of Holocene marine incursion on the supralittoral sector (> 50 km from the modern shoreline). The most expressive is based on the geomorphological features of the drowned valleys on the sheltered coast of Marajó Island, approximately 250 km west of our study area (e.g., Barbosa et al., 1974). However, despite some geomorphological relevance, such evidence has been criticized because of the absence of physical significance, lack of analogous proximal indicators for correlation, and mainly the scarcity of chronological and bio-stratigraphical data. Therefore, these issues contributed to assigning the possible Holocene transgression to a hypothetical scenario.

To date, no comprehensive study has examined the micropaleontological content of the Amazonian supralittoral to detect possible Holocene marine influences (or constrain the sea-level rise), although this area is a sensitive and potentially untapped region that could explain the RSL trends based on ecological history. Its distant location enables the tracing of marine incursion influences outside the modern coastline, which is typically well-researched. Therefore, we studied a core retrieved from a supratidal environment of southeast Abaetetuba city, Pará River Upper Estuary, northern Brazil, to detect marine transgressive events. The pollen content and sedimentary features of the MLT2 core were combined with $\delta^{13}C$, ^{15}N, organic matter C/N, and chronological data to propose a paleoenvironmental overview of the Amazonian supralittoral evolution occurring between the middle and late Holocene.

2. Study Area

The Itacuruçá estuarine plain river is located in the south-southwest part of Abaetetuba, 180 km from the modern coastline. This sector comprises the Pará River Upper Estuary (ESP), classified as semidiurnal micro-to mesotidal (Ribeiro and Valadão, 2021). The Tocantins River

is the main fluvial body of the ESP (Fig. 1a), which has an approximate discharge of 12900 $m^3.s^{-1}$ (ANA, 2019; Prestes et al., 2020). This high fluvial discharge prevents the ESP from experiencing saline influence (< 0.5); thus, Itacuruçá and other water bodies from the ESP have been defined as tidal rivers, that is, their hydrodynamics are controlled by the tide. However, the large freshwater input results in virtually non-existent salinity levels (Ribeiro and Valadão, 2021).

The geomorphology of the area consists mainly of lowlands that shelter wide valleys and numerous estuaries, resulting in a jagged inshore setting (Fig. 1a). Extensive islands occur alongside the littoral zone, mainly between the Amazon, Pará, and Tocantins river mouths, which are part of a geologically young system, often assigned to the Late Pleistocene-Holocene (Barbosa et al., 1974). These fluviomarine plains constitute the main local morphological units, with elevations of up to 5 m above the local reduction level (Fig. 1c). The region is subdivided into three zones: subtidal (< 1 m), intertidal (1–3 m), and supratidal (3–5 m). However, because of the spatial scale adopted in this study, only the central unit, that is, the fluviomarine plain, can be represented by mapping. The fluviomarine plain is partially prone to regular flooding by the mesotidal regime, with spring tides reaching up to 3.78 m (Ribeiro and Valadão, 2021).

The vegetal cover includes pioneer formations in the subtidal zone, composed mainly of *Montrichardia linifera*, *Mauritia flexuosa*, *Machaerium lunatum*, and *várzea* vegetation, dominated by terrestrial trees that are tolerant to flooding, such as *Euterpe oleracea* and *Pterocarpus amazonicus*, which occupy the intertidal zone. In contrast, the supratidal zone is mainly covered by *Virola surinamensis*, *Swartzia polyphylla*, *Hevea brasiliensis*, and *Calycophyllum spruceanum*. The Terra Firme, a morphological unit not subjected to tidal influence, occurs upstream of the study area. This unit varies between 5 and 15 m, but in the insular complex (Figs. 1b, c), the Terra Firme does not exceed 8 m. Its vegetation cover consists mainly of *Vouacapoua americana*, *Dipteryx odorata*, and *Manilkara huberi* (Ribeiro and Valadão, 2021; 2020). These vegetation groups are related to dense alluvial ombrophilous forests (Fig. 1b). The climate is classified as typical warm and humid tropical. The influence of seasonality of the Intertropical Convergence Zone (ITCZ) results in a characteristic climate with two seasons (Souza-Filho et al., 2009), a rainy season that occurs between January and July and a drier season prevailing for the rest of the year (July to December). The total precipitation averages 2700 mm per year, and the mean annual temperature is 27 °C (FAPESPA, 2016).

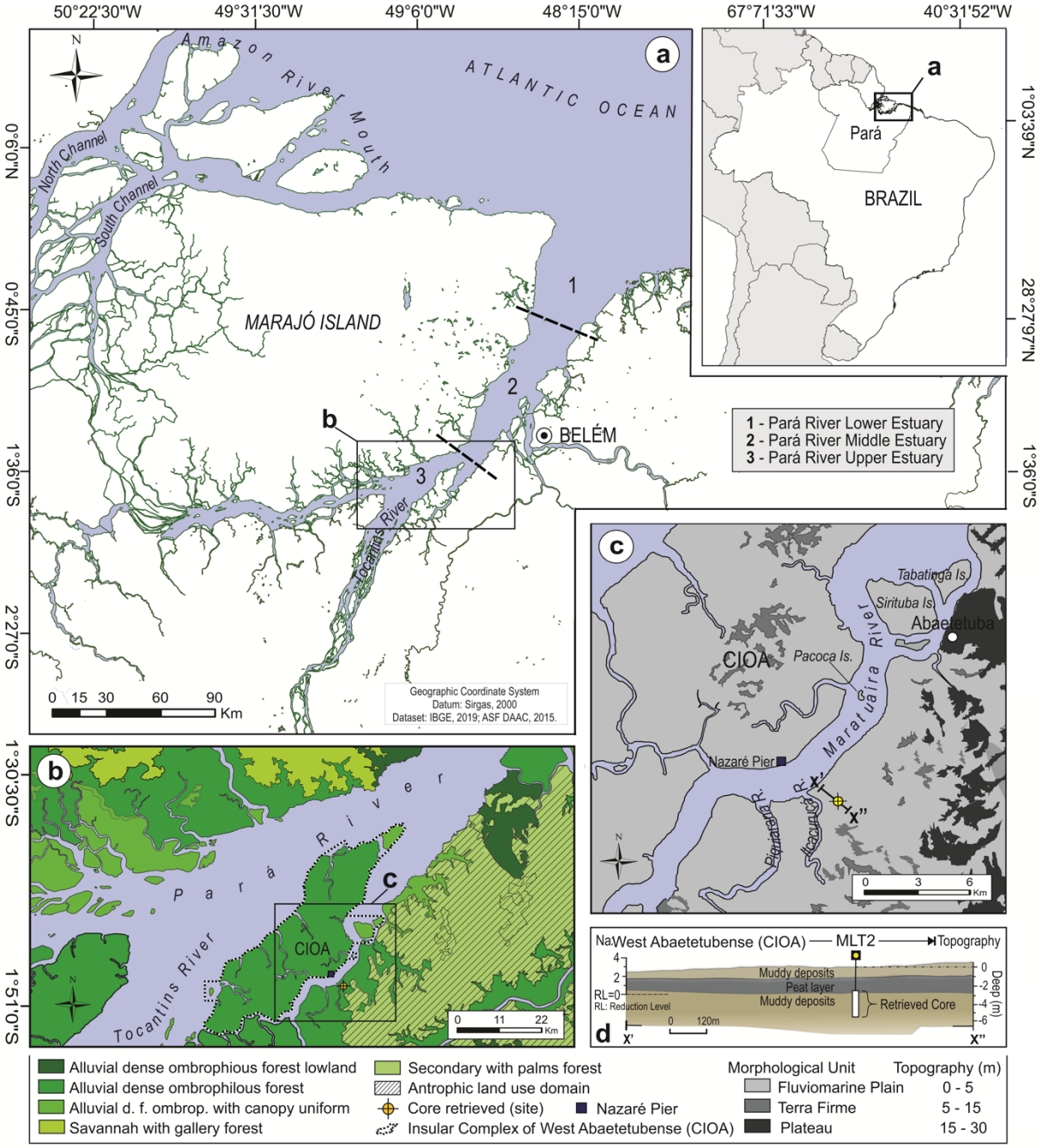

Figure 1. Study area on the northern coast of the state of Pará detached from Brazilian territory (a). Regional distribution of vegetation (b) followed by main morphological features and sampling site at the Itacuruçá estuarine plain (c). Note the integrated profile sketch (sedimentary setting, topography, and reduction level), illustrating the MLT2 core position beneath the present-day surface (d).

Miocene rocks and quaternary sedimentary deposits characterize the geology of the area. The Pirabas/Barreiras formations consist of Miocene limestones, laminated mudstones, and calciferous sandstones (Ferreira, 1977). The Barreiras Formation (Miocene/Middle Miocene) consists of conglomerates, sandstones, and claystones (siliciclastic non-fossiliferous) (Góes et al., 1990; Rossetti et al., 1989). Eolian and fluvial-estuarine sandy and muddy sediments of the Late Pleistocene and Early Holocene overlie the Barreiras Formation. These sediments are

termed post-Barreira deposits (Tatumi et al., 2008). Regionally, a large part of this sequence is capped by debris-lateritic deposits (?Pleistocene) distributed in riverbank outcrops of the study area (Ribeiro and Valadão, 2021).

3. Materials and methods

3.1 Remote Sensing

The cartographic database was obtained from the Brazilian Institute of Geography and Statistics (IBGE) (http://www.ibge.gov.br/geociencias/downloads-geociencias). The integrated approach of this study consisted of combined morphostructural and topographic data, which were analyzed using remote sensing products, including images from ALOS-PALSAR radar data (http://search.asf.alaska.edu). The dataset obtained consisted of radiometric terrain corrected (RTC) images with HH polarization mode (RT1) and 12.5 m resolution, to produce a high-resolution digital elevation model (DEM). The DEM was geometrically corrected, filtered, and patterned using SIRGAS 2000 as the reference, and used to generate the local topographical profile. In addition to radar data, cartographic datasets consisting of shapefiles from the natural environment (hydrography, geology, geomorphology, and vegetation) were obtained from the same IBGE repository. After fieldwork, the remote sensing products were manually interpreted and vectorized in detail. All processing and analyses were performed in a GIS environment (ESRI ArcGIS software v. 10.2®).

3.2 Fieldwork and sample processing

One sediment core was retrieved during fieldwork in January 2019. The sampling site consisted of a supratidal flat near the entrance of the Itacuruçá River. The MLT2 core (1°48′11.47″S, 48°56′39.66″W) was approximately 463 m from this river (Fig. 1c). The drilling reached a depth of 550 cm, and the retrieved core corresponded to the deepest part of the sample. The MLT2 had a depth of 280 cm and was collected using Russian corer equipment. The top of the MLT2 core (0 cm depth) was 2.70 cm beneath the surface (see sketch illustrating the MLT2 sampling position in the sedimentary context, Fig. 1d). The core topography was defined based on the local reduction level measured in the Nazaré Pier, localized on the insular complex of West Abaetetubense (CIOA), following the procedures of Ribeiro (2021) (Fig. 1c, d). The Global Position System (GPS) determined the core geographical coordinates using SIRGAS 2000 as the reference. In addition to MLT2 core, at different locations along the study area, visual analysis of outcrops was performed, including morphological and geobotanical unit descriptive surveys.

3.3 Facies description core

Facies analysis was performed, including a description of color (Munsell Soil Color Charts, 2009), texture, and structure, following the methods of Walker (1992). Macroscopic analysis of sediments was also conducted by recording sandy sediment size, sorting, and rounding. The sedimentary facies were codified according to Miall (1978). Finally, the MLT2 core profile was integrated into pollen data and divided into facies associations that were genetically related and had identical environmental significance; therefore, they were indicative of a particular sedimentary environment (Reading, 1996). This is critical for achieving paleoenvironmental evolution models (Dalrymple and Choi, 2007).

3.4 Pollen and spore analysis

Fifty-six 1 cm^3 samples were retrieved at 5 cm intervals throughout the MLT2 core for pollen analysis. All samples were prepared using standard pollen analytical techniques, including KOH-10% and acetolysis (Erdtman, 1960). The sample residues were mounted on slides in a glycerin gelatin medium. Pollen and spores were identified by comparison with reference collections of approximately 4000 Brazilian forest taxa and various pollen keys (Colinvaux et al., 1999; Absy, 1975; Roubik and Moreno, 1991), based on the reference collection of the Paleontology and Macroevolution Laboratory, Federal University of Minas Gerais. Pollen and spore data were presented as percentages of the total terrestrial pollen sum in pollen diagrams. The taxa were grouped according to the source: mangroves, trees, shrubs, palms, herbs, and ferns. The software TILIA and TILIAGRAF were used to calculate and plot the pollen diagram (Grimm, 1987). CONISS was used for cluster analysis of pollen taxa, permitting the zonation of the pollen diagram.

3.5 Isotopic and elemental analysis

Isotopic analysis ($\delta^{13}C$, $\delta^{15}N$) has the potential to identify changes in the sources of Organic Matter (OM) for each depositional environment, including the relationship between C/N (Meyers, 1997, 1994). For instance, the C3 terrestrial plants show $\delta^{13}C$ values between −32‰ and −21‰ and C/N ratio >12, while C4 plants have $\delta^{13}C$ values ranging from −17‰ to −9‰ and C/N ratio >20. In C3-dominated environments, freshwater algae and marine algae have $\delta^{13}C$ values between −25‰ and −30‰ and −24‰ to −16‰, respectively, while algae present $\delta^{13}C$ values ≤16‰ on the C4-dominated environments (Haines, 1976; Deines, 1980; Meyers, 1994). On the other hand, $\delta^{15}N$ is used as an indicator of organic matter sources and paleoproductivity; $\delta^{15}N$ >10.0‰ indicate aquatic OM as the source (phytoplankton), while

terrestrial vascular plants present an average of 0‰ (Meyers, 1994; Thornton and McManus, 1994). Hence, the preserved elemental and isotopic compositions from sediments used in tandem ($\delta^{13}C$, $\delta^{15}N$, and C/N) allow tracing of the sources of MO in coastal deposits.

A total of 18 samples (2–20 mg) were collected at intervals of ~ 15 cm from the core. The samples were analyzed for carbon-13 (^{13}C) nitrogen-15 (^{15}N) by isotope ratio mass spectrometry at the Laboratory for Biotechnology and Bioanalysis (LBB2), the DirectAMS Laboratory (Bothell, WA, USA), and the Stable Isotope Laboratory of the CENA/USP. The $\delta^{13}C$ and $\delta^{15}N$ results were expressed per mil (‰) concerning the VPDB and N2 standards, respectively. The TOC and TN were measured from a same parcel and provided data to calculate C/N (w/w) value for all samples. The determination of organic matter sources, such as C3 and C4 terrestrial plants and marine and freshwater algae, will be environmental-dependent with a specific $\delta^{13}C$, $\delta^{15}N$, and C/N composition (Lamb et al., 2006; Meyers, 1997; Thornton and McManus, 1994).

3.6 Radiocarbon dating

Three bulk samples (approximately 10 g each) along the MLT2 core were selected for dating. This selection was based mainly on the deposit discontinuity, sediment nature, texture, and color. The samples were examined and subjected to DirectAMS. A chronological framework for the sedimentary samples was provided by accelerator mass spectrometry (AMS) dating at DirectAMS Laboratory (Bothell). Radiocarbon ages were normalized to a $\delta^{13}C$ value of 25‰ VPDB and reported as calibrated years (cal yr BC, 2σ) using CALIB 8.2 and the SHCal20 curve (Hogg et al., 2020). The dates are reported in the text as the median of the range of calibrated ages (Table 1).

4. Results

4.1 Radiocarbon dates and sedimentation rates

The radiocarbon ages calibrated are shown in Table 1 and Figures 2 and 3. The sample from the core bottom (280 cm) registered 6503–6425 cal yr CE, followed by 4798–4681 cal yr CE at a depth of 177 cm, and 420–502 CE near the MTL2 top (35–37 cm). The rates of sedimentation were estimated from the thickness of the deposits and their numerical ages, presenting 0.6 (280–177 cm) and 0.4 mm/yr (177–0 cm) (Fig. 2). No age inversions were observed.

Table 1. Sediment samples selected for radiocarbon dating with laboratory number, code core/depth, ^{14}C yr BP and calibrated (cal) ages.

Laboratory number (D-AMS)	Sample	Depth beneath surface (cm)	Depth Core (cm)	Age BP	Ages (Cal yr BC, 1σ)	Ages (Cal yr BC, 2σ)	Median Probabilily
044419	MLT2	287–290	35–37	1633 ± 30	424–476	420–502	466 CE
046399	MLT2	447	177	5902 ± 28	4782–4744	4798–4681	4743
038504	MLT2	550	280	7661 ± 38	6470–6440	6503–6425	6459

4.2 Core facies description

The sediment MLT2 core consisted primarily of mud with internal structures that include a heterolithic lenticular, and peat deposits. The peat deposits were mainly well-decomposed fibers rather than younger vegetable roots. Facies were identified based on internal sedimentary structures, organic content, sediment texture and color, and contact relationships. Pollen and spore records, and $\delta^{13}C$, $\delta^{15}N$, and C/N values were added to the facies structures, allowing for two facies associations: tidal flat (A) and swamp mixed estuarine flat (B). The characteristics of each of these associations are summarized in Table 2.

4.2.1 Facies Association A (Tidal flat)

This unit was almost fully cored into the MLT2. It occurs along the interval 280–38 cm in the core studied and comprises deposits of organic-rich mud with fine sands well sorted. Radiocarbon dates indicate that accumulation occurred between 6459 cal yr BC and 466 CE (Fig. 2). Their facies element structures consist of massive mud (Mm) and lenticular heterolithic bedding (Hl). The latter has a subordinate (31%) without continuous occurrence, representing 75 cm of 242 cm in this succession (Figs. 2 and 3). The Mm (structureless), may occasionally present planar and parallel laminated mud. Locally, this deposit exhibits gray scattered pigmented mottles and bioturbation features such as woody roots and root marks (Fig. 5b). The heterolithic lenticular-bedding facies, in turn, is characterized by oscillation ripples of millimeter-thickness fine sand lenses, which may gradually enlarge to form sand waves. Altogether, these bedforms are linked with a low energy flow environment to deposition from suspension (Mm), with alternating traction force to sand lens deposition (Hl) (Fig. 2).

Pollen assemblages of Association A allowed the identification of 21 pollen taxa. This zone was dominated by mangrove pollen (62–88%) and was composed of *Rhizophora* (42–86%) and *Avicennia* (4–16%). The pollen spectra also included ecological groups of trees (6–22%) and shrubs (4–9%), mainly Euphorbiaceae (3–7%), Fabaceae (2–6%), Malpighiaceae (1–5%), *Mimosa* (3–11%), Rubiaceae (0–9%), Bignoniaceae (0–4%), and Burseraceae (0–4%). The palm ecological group appeared with percentages < 18%, and herb pollen comprised <

11%. Palms are represented by *Euterpe oleraceae* (0–15%) and *Mauritia flexuosa* (0–8%), while Poaceae (3–8%), Cyperaceae (2–6%), and *Borreria* (0–3%) represent the herbs. Trilete and monolete ferns formed between 1 and 11%, and foraminifera between 3 and 10% in this zone (Figs. 2 and 3). Organic matter $\delta^{13}C$ ranged from –26.8 and to –25.5‰ (mean –26.2‰), whereas $\delta^{15}N$ varied between –1 and 4‰ (mean 2.5‰). Minimum and maximum C/N values are 15 and 45, respectively (Figs. 2 and 3).

4.2.2 Facies Association B (Swamp mixed estuarine flat)

Association B occurred between 38 and 0 cm in the uppermost part of the core, representing 13.6% of the MTL2 (Fig. 2). It was formed of well-decomposed peat deposits with internal organic muddy drapes. This unit was deposited after 466 CE. Besides the sample at the core (Supplementary Data, P1), this peat presented good quality outcrops on the river bank, yielding almost continuous exposure through the Maratauíra and Maiauatá Rivers (Supp. P2). In addition, the presence of rivers that enter estuarine tidal flats allow for the analysis and inference of their spatial distribution, such as the records at the Furo Grande and Maracapucu-Miri localities of the CIOA. Accordingly, the upper contact of the peat with muddy deposits (not retrieved) has been recognized as abrupt to gradual, mainly based on the outcrop scale (Supplementary Data, P1).

The lowest contact relation was inferred from cores drilled previously (Supplementary Data, P1). The drilled cores revealed a predominantly abrupt contact between the peat and the underlying unit (Fig. 2). The latter is often muddy but encompasses heterolithic deposits consisting of fine sand. The advancement of the survey in this region suggests a correlation between peat layers, indicating a widespread geographical distribution throughout the supralittoral sector. Such elements lead us to assume that peat formation is related to common depositional processes, with a paleoenvironmental significance assigned to swamp mixed estuarine flats.

Pollen analysis revealed the predominance of trees (22–45%), palms (18–38%), and mangroves (19–55%). Trees mainly consisted of Euphorbiaceae (4–14%), *Pachira aquatica* (4–11%), *Machaerium lunatum* (2–9%), *Spondias mombin* (1–7%), Malpighiaceae (0–7%), and *Calycophyllum spruceanum* (0–5%), whereas the palm group as mainly characterized by *Euterpe oleraceae* (15–20%), *Mauritia flexuosa* (8–19%), and Arecaceae (4–8%). Mangrove pollen was represented by *Rhizophora* (9–35%) and *Avicennia* (4–8%). Herb groups had low percentages (< 9%). Ferns (1–10%) were represented by monolete and psilate triletes, and foraminifera ranged from 3 to 6% (Figs. 2 and 3). The $\delta^{13}C$ and $\delta^{15}N$ values are between –27.2

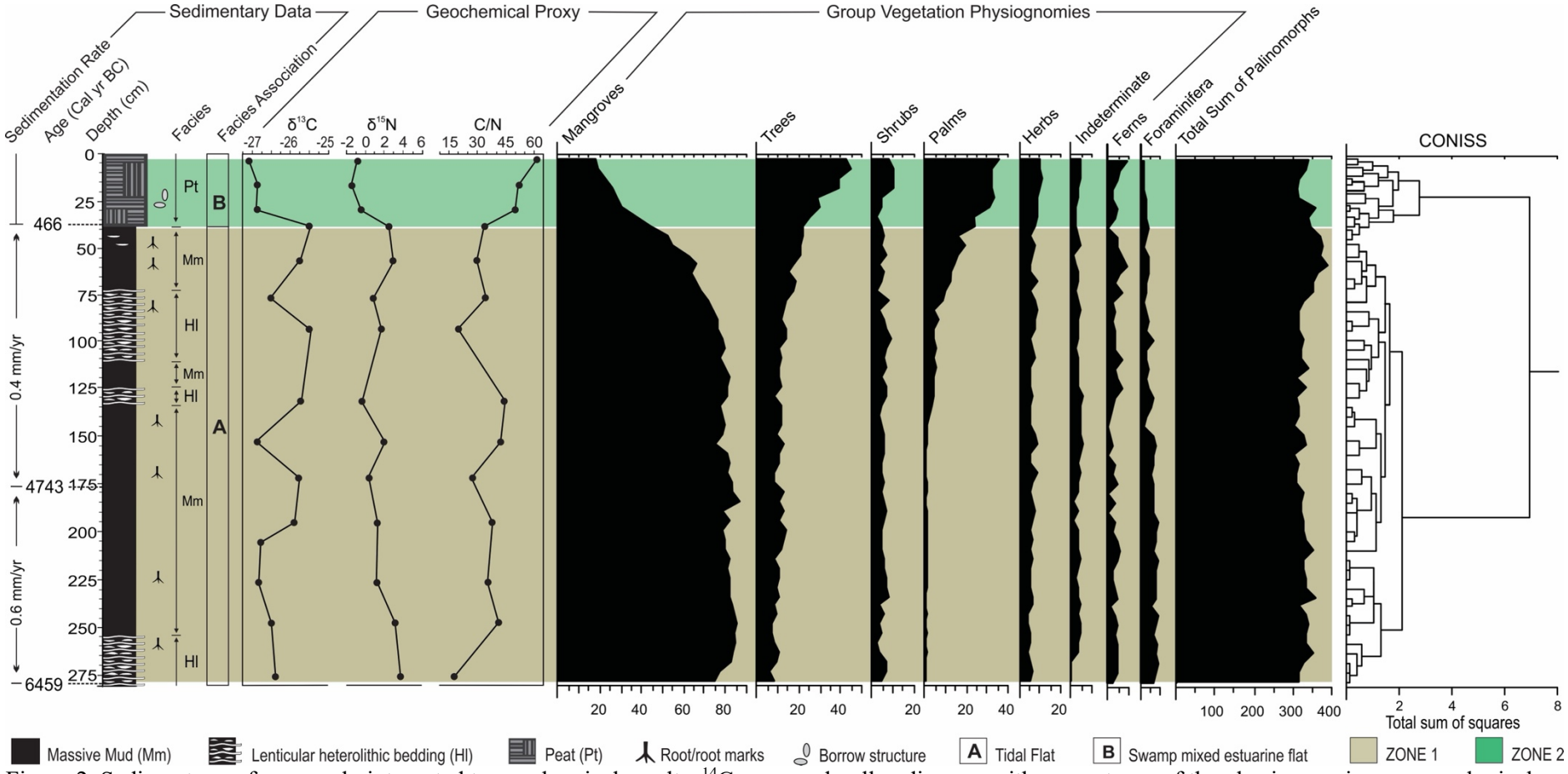

Figure 2. Sediment core framework, integrated to geochemical results, ^{14}C ages, and pollen diagram with percentages of the physiognomic group ecological.

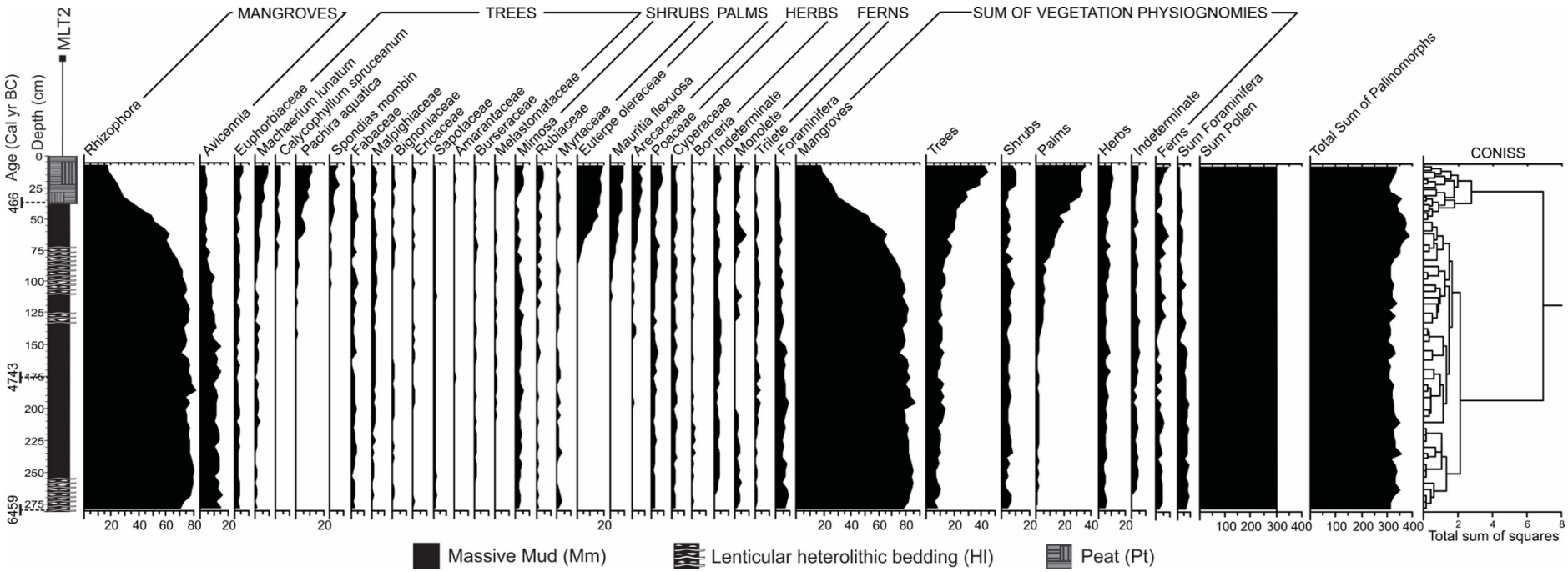

Figure 3. Pollen diagram of the core MLT2, with percentages of the most frequent pollen taxa, samples age, and cluster analysis.

and approximately –25.5‰ (mean –26.4‰) and –0.9 and 2.7‰ (mean 1.8‰), respectively. The C/N values occur between 30 and 62 (Fig. 2, Tab. 2).

Table 2. Facies associations identified along the MLT2 core according to sedimentary characteristics, pollen and geochemical data.

Facies Association	Facies description	Pollen dominance	Geochemical data	Paleoenvironment
A	Massive mud (Mm), olive-brown, gray to very dark gray and black; parallel lamination mud can be present. Heterolithic lenticular deposits (Hl) olive-brown, greenish to gray to dark gray and black. Lenticular structures rhythmic interbedded in variable proportions of sand; these deposits contain	Mangrove	$\delta^{13}C$= –25.5 to –26.8 ‰ $\delta^{15}N$= –1 to 4‰ C/N= 15 – 45	Tidal Flat
B	woody roots and root marks. Peat deposits (Pt), black, brown-reddish, and black to dark-gray, well-decomposed, with mud drapes. Locally, they present abundant bioturbations and dwelling structures produced by the benthic fauna, which are easily recognized.	Trees and palms	$\delta^{13}C$= –25.5 to –27.2‰ $\delta^{15}N$= –0.9 to 2.7‰ C/N= 30 – 62	Swamp mixed estuarine flat

5. Discussion

5.1 The history of mangrove establishment in the supralittoral region

Pollen preserved in the lower part of the MLT2 core indicated an intertidal environment occupied by mangroves. This ecosystem has a growth performance in brackish water, tolerating high salinity (Ball, 1998; Spalding et al., 2010). For example, *Avicennia* demonstrates extreme salt tolerance, and *Rhizophora* exhibits relatively high salt tolerance (Jayatissa et al., 2008; Kodikara et al., 2018). The trigger for the initial conditions for mangrove development in this sector was likely the post-glacial sea level rise through saline input. The dominance of *Rhizophora*, with the genus *Avicennia* subordinate along the 268 cm (280–40 cm), suggests a brackish estuary with a biologically consolidated halophyte community (Figs. 2, 3, 4–I and 5a).

According to Panapitukkul et al. (1998), *Avicennia* represents a pioneer species; it develops first on mudflats that provide resistance to waves and currents. Consequently, successional colonization by other species, especially *Rhizophora* and *Brugeria*, which occupy available space, results in a mangrove zonation pattern (Thampanya, 2006). Thus, this mangrove is represented mainly by *Rhizophora*, while *Avicennia* suggests a climax stage of mangrove forest in the estuarine landscape. In addition, the frequent presence of the foraminifera genus *Ammonia,* which is typically related to shallow nearshore areas, estuaries, and tidal swamps (e.g., Murray and Alve, 1999; Long et al., 2006), indicates that these conditions existed and followed alongside the mangrove community. The radiocarbon dates show that mangrove has been established in the supralittoral region for the last 6459 cal yr CE (Figs. 2 and 4–I).

The mechanism for the shoreside landscape setting was mainly sea-level changes. Estuarine bodies along global coastlands altered in relation to Holocene sea-level rise (Wolanski and Elliott, 2015). The marine incursion affected these morphologies and produced embayments within pronounced valleys inherent to the Pleistocene sea-level fall (Evans and Prego, 2003). The estuaries of this region probably share an analogous palaeogeographical history, in which the Maratauíra River is an unfilled incised valley that opened during the Late Pleistocene-Early Holocene, driven by tectonic mechanisms coupled with glacial sea-level decline. Consequently, the marine incursion reached the supralittoral region, producing rias and forming a variety of estuarine sub-environments with more expansive tidal flats. The transgressive event marks the gradual drowning of numerous fluvial features landward, extending the marine realm 180 km beyond the modern coastline (Fig. 4–I–II)

Deposits are dominantly muddy and frequently interbedded with layers and lenses of well-sorted, very fine-grained sands constituting MLT2 core Zone 1 (Fig. 2). Sedimentary structures with alternating beds/laminae of sand and mud are primarily formed in tidal settings (Daidu et al., 2013) because slack tides favor mud deposition in very fine-grained sands (Dalrymple et al., 2012; Reineck and Wunderlich, 1968). This vertical pattern of facies on the base of the core suggests an estuarine environmental setting established 6459 cal yr BC when the sea level had already reached this sector (Facies Association A).

Isotopic data are consistent with the ecological conditions developed in an estuarine setting, with paleoproductivity influenced by terrestrial plants (Fig. 6). For example, the $\delta^{13}C$ value indicates productivity associated with the arrival of C3-plants within the watershed (Meyers, 1994; Qiu et al., 1997), such as mangrove. The binary $\delta^{13}C$ (≥ -25.5) and C/N (≥ 12) suggest OM enrichment by this plant group (Cloern et al., 2002; Meyers, 1997). In addition,

the low $\delta^{15}N$ value reinforces the OM of terrestrial plants influencing the Zone 1 infill (Lamb et al., 2006; Meyers, 1994) (Fig. 3 and 6).

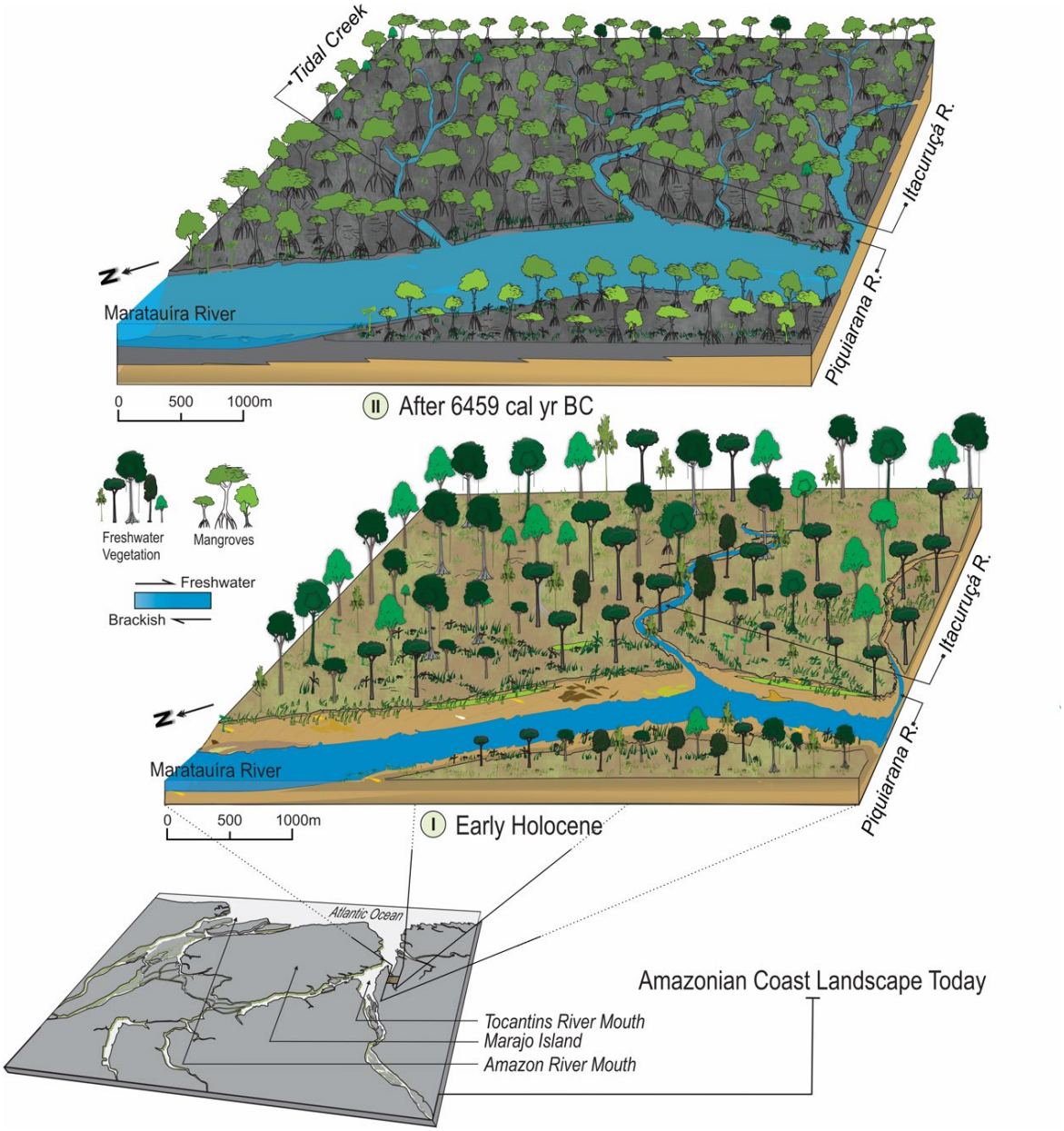

Figure 4. Conceptual evolution of the landscape from the Itacuruçá plain, at the Amazonian supralittoral, between the early and middle Holocene. The first significant change occurred during post-glacial sea-level rise. The emergence of brackish conditions in a previously fluvial environment (Phase I) led to the establishment of the mangrove swamp, which began to dominate the estuarine landscape since ~6.5 ka BP (Phase II).

As *Rhizophora* grew and colonized the intertidal flats, their complex roots generated strong turbulence, resulting in more sediment traps to expand mudflats horizontally (Bird, 1971; Friess et al., 2012). Mangrove development reshaped the ecological landscape from the dominant fluvial-ecosystem inherited from the Late Pleistocene (Fig. 4–I) to the brackish forest (Fig. 4–II). Thus, this RSL rise has played a crucial role in the dynamics of the Late Quaternary

on the Amazonian coast. Despite its poorly understood effects on inner sub-estuarine systems in the supralittoral region due to the lack of sufficient data to create a model, it can be speculated that the RSL was at least 2 ± 0.5 m higher than the current level.

The emerging change from brackish estuary to estuary with the greatest fluvial control on chemistry parameters, that is, the freshwater environment, occurred near the late Holocene (Fig. 7–III). The pollen spectra showed an increase in both trees, *Pachira aquatica* and *Machaerium lunatum*, and freshwater palms, represented mainly by *Euterpe oleracea* and *Mauritia flexuosa* species. Simultaneously, the mangrove began to decrease at 57 cm in the MLT2 core (Figs. 3 and 5a). From 30 cm upward (Zone 2), the pollen percentages suggested both the decline of mangroves and expansion of forests typical of freshwater conditions (Fig. 3).

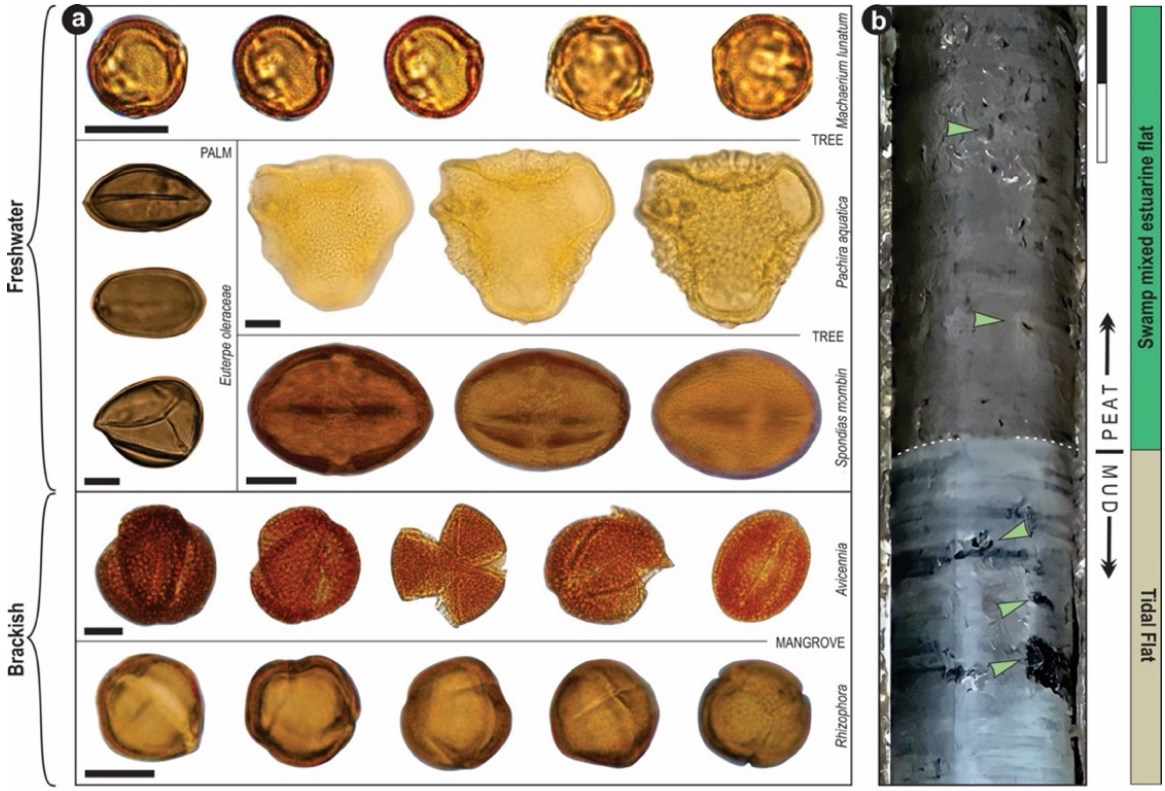

Figure 5. Photomicrographs of the most representative pollen grains from the mid-late Holocene of the Itacuruçá tidal flat, Amazonian supralittoral, Brazil. The pollen plate is organized as the environmental evolution from the mangroves (brackish) upward to "*várzea*" (freshwater vegetation) (a). The ecological change signature preserved in the sedimentary record (b) indicates abrupt contact between the lower muddy deposit and the uppermost peat deposit. Note overlapping peat conformity to the muddy succession (dashed white line). Bioturbation attributed to woody root as well as dwelling structures produced by the benthic organisms has been pointed with arrows (light green). Pollen scale bar: 10 μm. Core scale bar: 4 cm.

The RSL likely started to fall, and the saline gradient decreased at approximately ~ 400 CE because freshwater vegetation raised its pollen frequency from the various associations of taxa. This vegetation, which had refugia in the upstream sector since the middle Holocene,

began the migration process downstream, growing on former tidal flats previously occupied by mangroves. The freshwater ecosystems became prevalent after 466 CE (Fig. 7–IV). Coupled with pollen, the sedimentary system also provides reliable records of this pronounced environmental change and suggests an RSL fall.

The abrupt contact between the lower mangrove (Zone 1) and peat deposits (Zone 2) on the uppermost portion of MLT2 without erosion provides evidence of paleoenvironmental transition (Fig. 5b), indicating that the depositional system did not undergo significant physical changes, such as subaerial exposition. This interpretation is supported by other previously drilled cores (Supplementary F1), which clearly show the contact relation between these two units. Although the age is lacking for these, the analysis of the components, such as the geographical occurrence, thickness, and co-depth, suggests that these peatlands correspond to the same unit, which allows for their correlation. The abrupt basal transition, linked to a lack of erosive contact, indicates that the RSL decline did not force geomorphologic confinement, but instead induced maintenance under tidal inundation frequency (*várzea*), resulting in the present estuarine hydrodynamics.

The organic debris deposition and peat formation along Zone 1 is consistent with both mangrove decline and inundation frequency because peat demands saturated conditions, such as low oxygen contents, to inhibit decomposition, in-depth burial, and preservation in the stratigraphic record (Facies Association B) (Long et al., 2006; Shennan et al., 1996). Presumably, peat is autochthonous and directly related to the paleo-mangrove demise (Fig. 2). The organic-terrestrial character of the C3 plants is supported by geochemistry data, whose $\delta^{13}C$ values presented a mean of –26.4‰ (Meyers, 1997).

The $\delta^{15}N$ average value of 1.8‰ is related to land vascular plants and C/N values increasing from 30 to 62 are also consistent with terrestrial plants as primary organic sources (Meyers, 1997; Thornton and McManus, 1994) (Figs. 2 and 6). The spectral behavior between foraminifera and ferns in the pollen diagrams also helps demonstrate the ecological evolution from brackish to freshwater environments. The fern frequency increased upward in Zone 2, whereas foraminifera decreased (Fig. 3). The behavior of the ferns suggests a mostly freshwater influence (ferns typically occupy streams or lowland regions near the continental swamp) (Berreda et al., 2009), and the foraminifera can be assigned to the diminished brackish water effect, as they are predominantly shallow marine organisms (Long et al., 2006).

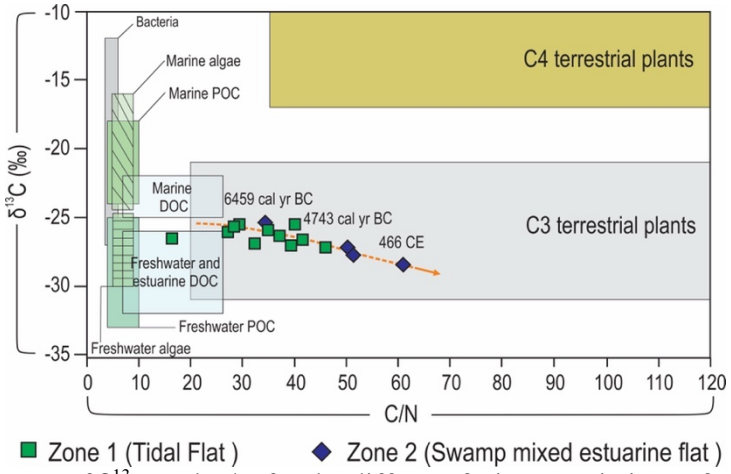

Figure 6. Binary diagram of $\delta^{13}C$ and C/N for the different facies associations of Tidal flat and Swamp mixed estuarine flat, with interpretation according to data presented by Lamb et al. (2006) Meyers (1997; 1994), Thornton and McManus (1994). The trendline (orange arrow) indicates the increasing paleoproductivity enriched by terrestrial organic matter from the C3 plants from the Zone 1 to Zone 2.

5.2 Mangroves on Itacuruçá tidal flat: new signals regarding the sea-level rise in the Amazon

Palynological studies on littoral areas worldwide have been critical for assessing paleoecological setting relations at the land-sea interface in tropical and subtropical regions. Many of these have demonstrated that mangrove dynamics are driven by sea-level fluctuations (Ellison, 2005; Engelhart et al., 2007; Hait and Behling, 2009; Punwong et al., 2018; Sloss et al., 2007; Tossou et al., 2008; Woodroffe and Grindrod, 1991). Previous studies on the Amazonian littoral zone reported that the RSL reached its current position near 7000 cal yr BP (Behling and da Costa, 2000; Cohen et al., 2005), with no significant change during the Holocene (Behling et al., 2001; Cohen et al., 2005; Rossetti et al., 2008; Vedel et al., 2006). The mangrove establishment in Itacuruçá is consistent with sea-level rise affecting the supralittoral zone. The age obtained from the MLT core base of approximately 7.6 ka BP was similar to that observed in previous studies (Tab. 1). Nevertheless, the decline of this mangrove is not consistent with the environmental conditions indicated for the last 7 ka BP years of a relatively steady RSL (Fig. 8A).

Mangroves are resilient and tolerate environmental stress, which means that they can survive even high-magnitude changes. In addition to climate change, mangroves are inhibited by nutrient-poor (sandy) soil or higher freshwater inflow (Alongi, 2009). The reduction of muddy sediment input may have a more significant impact if the mangroves span areas subject to sea-level rise (Furukawa and Wolanski, 1996). These conditions can cause asphyxiation from the increase in mean tide level because the lack of sediment supply may limit the vertical accretion of the occupied substrate (Bird, 1971). Moreover, a high input of sand to mangrove

substrates can lead to stagnancy or demise of the vegetation, which depends on muddy sediments for root fixation, trunk stability, and ecological growth (1996; Toorman et al., 2018).

The analysis of the MLT2 indicated that the input of muddy sediments was steady over time, including upward gradations by organic debris that developed peat. Peatland is an excellent substrate for this vegetation (cf. Mckee et al., 2007), typically formed due to the root system that traps the own organic matter produced (Cameron and Palmer, 1995). Considering these ecological relationships, peat bogs likely did not restrain mangrove maintenance. However, contrary to mangrove expansion in relation to organic debris deposition, Itacuruçá peats coincide with mangrove pollen reduction frequency. Thus, these are probably the "fingerprint" of mangrove demise (Figs. 2, 7–III and IV).

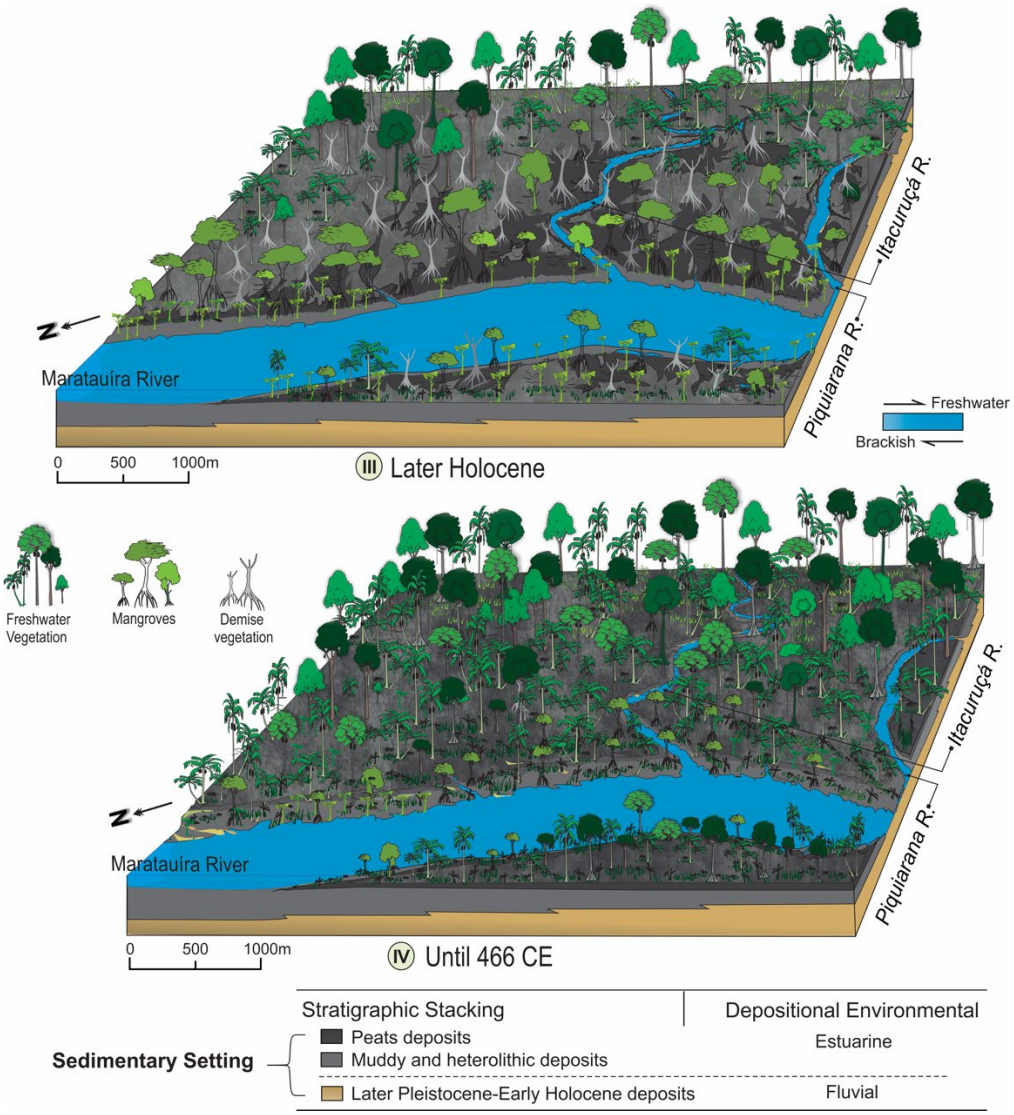

Figure 7. The mangrove community endured significant spatial loss, while freshwater ecosystems, represented mainly by trees and palms, occupied these areas during the late Holocene (Phase III). In the last phase, freshwater forests nearly completely replaced the mangroves. This environmental change likely resulted from the RSL decline and its stabilization at the current position, which reduced the saline influence and favored the freshwater vegetation domain along the Itacuruçá flat (Phase IV).

The pollen spectrum of the peat bed revealed botanical types related to new environmental conditions (Figs. 2 and 3). For example, *Euterpe oleracea*, *Mauritia flexuosa*, *Machaerium lunatum*, *Spondias mombin,* and *Pachira aquatica* were the most representative species (Fig. 5a). This set is typical of freshwater ecosystems, described in several environments with hydrological regimes controlled by freshwater availability (Gomes et al., 2017; Hofmann, 2002). This floodplain vegetation began to thrive over the estuarine plain from 466 CE, while the mangrove forest contracted (Fig. 7–III and IV).

In the Amazon, mangroves occurred from the western to eastern littoral sector during the middle Holocene and underwent dynamics that involved spatial disruption. Western mangrove communities were established in tidal flats associated with the Amazon River mouth as a direct consequence of marine incursion after 5560–5470 cal yr BP (Guimarães et al., 2012). In the late Holocene, freshwater input caused the mangrove area to shrink (Cohen et al., 2012). In the central sector of Marajó Island, ~140 km downstream from the study area, a more substantial marine influence caused the mangroves to occupy the intertidal zone between 7328–7168 and 2306–2234 cal yr BP. Subsequently, the mangrove was replaced by freshwater herbs due to increased fluvial discharge (Smith et al., 2011). The eastward mangrove communities at Bragança, in turn, underwent reduction and migration to lowland areas during the mid-Holocene; however, the authors suggest an accentuated RSL decline as the main driving force (Cohen et al., 2021; Vedel et al, 2005).

Except for the eastward mangrove, the dynamics of these wetlands have been assigned to Holocene climate changes (Cohen et al., 2012; Guimarães et al., 2012; Smith et al., 2011). The wet phase and high rainfall conditions increased the Amazon River discharge after 4.2 ka BP, influencing the zone occupied by halophyte vegetation, reducing the saline gradient within the context of sea-level stability, and providing conditions for freshwater forest vegetation (*várzea*) to replace the mangrove (Cohen et al., 2012). Despite this pattern, the estuarine flat from Itacuruçá provides some indicators suggesting that the brackish-to-fluvial environmental shift could have been driven by a natural/forced “cut” of the most high-magnitude mechanism, that is, the decline in the RSL.

The data still do not indicate that the RSL suffered small oscillations during the middle Holocene after exceeding the current level (Fig. 8A). Nonetheless, based on pollen frequency, geochemistry, and ages, it is possible to infer that the RSL was sufficiently higher than the present level from the middle to late Holocene, providing conditions for this paleo-mangrove to thrive for more than 6 ka. Furthermore, the RSL as an outward control for the ecological

landscape would be indicated by its “mirrored” characteristic: it influenced mangrove development while restraining the growth of freshwater vegetation (Fig. 3).

Without competition, mangroves prosper in Itacuruçá because of favorable environmental variants, such as seawater influence, and the protection from high-frequency erosive processes such as storms, waves, and tidal currents. Based on the results, it can be concluded that Itacuruçá offers an enhanced opportunity for determining the paleo-sea level rise on the Amazonian inner coast, and this knowledge can help in understanding the flooded embayment setting on the south side of the island of Marajó that was previously attributed to tectonic causes (cf. Barbosa et al., 1987). The RSL decline would also help reinforce the mangrove dynamics/contraction during the late Holocene along north-northwest littoral Amazonian, which is assigned mainly to climate change and freshwater outflow, causing an environmental imbalance in these wetlands.

5.3 Mangrove dynamic trends in the context of climate change and RSL

Pollen data shows a mangrove occurrence at the supralittoral from ~6500 cal yr BC to 466 CE. Since then, the halophyte community nearly disappeared, and was replaced by the freshwater forest in the late Holocene (Figs. 2, 4 and 7). The understanding of the mechanisms behind the mangrove *versus* freshwater vegetation dynamics in the region has indicated precipitation regime changes driven by climate change as an important force. Considering that mangroves develop over mudflats along large river mouths that are sensitive to fluvial discharge variations, the role of climate change cannot be disregarded. Assessment is required to isolate the climatic influence from the non-climatic factors controlling mangroves.

Drier climate trends mark the advance of the saline influence into estuaries due to less fluvial discharge (cf. Potter et al., 2010), which favors the mangrove migration to mudflats landward. This scenario would help understand the Itacuruçá mangroves; however, a drier climate is not consistent with the recent paleoclimatic history of the Amazon. For example, in the Carajás region, upstream of the study area, the pollen spectrum was evaluated by Absy et al. (2012), who gauged the impact of drier conditions in the early and mid-Holocene on the expansion of the open savannah. However, this savannah gave way to a forest complex due to increasing precipitation after 4.4 ka BP. Subsequently, based on geochemical organic and petrographic analyses of sediments from lakes in the same region, Sifeddine et al. (2001) identified that the hydrological regime prevailed from approximately 4.5 ka BP, indicating wetter conditions associated with the development of tropical rainforests (Fig. 8B).

Recently, Guimarães et al. (2021) recognized evidence of a wet climate in this region, in which shallow lakes developed into swamps with herbs and shrubs. Subsequently, at

approximately 3 ka BP, the vegetation of the plateaus acquired a structure that marked the establishment of wetter environmental conditions after the drier phase. In general, studies have demonstrated wet climate establishment from the Serra Sul dos Carajás (cf. Absy et al., 1991; Guimarães et al., 2019; Reis et al., 2017; Sifeddine et al., 2001) and other sectors across the continental Amazon (cf. Behling and da Costa, 2000; da Silva et al., 2020; Pessenda et al., 2004; 2001; 1997) to its coastal region (Guimarães et al., 2012; Toledo and Bush, 2008), which have formed a "wetter arch" around this study area since the early-late Holocene (Fig. 8B).

These studies provide a synthesis of past climates on a regional scale and compose a reliable body of evidence that indicates that a wet climate, with a higher rainfall regime similar to current conditions, was present in the region, sharing space and time with mangrove expansion. Thus, the beginning of these climates followed by increased discharge, which is suggested as the trigger to replace mangroves with freshwater vegetation in the Amazon River mouth during the early mid-Holocene, does not explain the paleo-mangrove decline in the Itacuruçá tidal flat. In the Itacuruçá mudflats, the mangroves thrived until the Late Holocene, even under the direct influence of the Tocantins River, with higher freshwater inflow caused by increased rainfall.

The palynological approach provides high-resolution local detection of changes in vegetation (Ellison, 2005) either by external (e.g., Decker et al., 2021) or internal forces (e.g., Ribeiro et al., 2018). If opposing climatic phases affected those wetlands, with freshwater advancing over the halophyte environment, its record should have been well preserved in the pollen, with an increased frequency of the freshwater genera, rather than mangroves. However, the present study did not recognize these signals imprinted at the MLT2 core through pollen content, and thus isolated climate noise. In contrast, the pollen representativeness from the mangrove indicate their forest dominance in this estuary. Thus, the hypothetical scenario of a long-lasting dry climate is inconsistent with the data presented here as well as those of other studies performed along the wetter arch (Fig. 8B). The eventual wet conditions were not sufficient to affect the paleo-mangrove, probably because the magnitude of the brackish influence caused by the RSL rise exceeded the site of occupation.

These findings link the paleo-mangrove and its dynamics to a trending RSL change. The RSL highstand since ~6459 cal yr BC probably helped develop and expand the paleo-mangroves. In contrast, its decline over the last two millennia represents the main force behind its reduction and area loss, and the subsequent appearance of freshwater vegetation on tidal flats at approximately 466 CE (Fig. 8A). We are not suggesting that there was no high input or increase in the drainage network's fluvial discharge due to wetter climates. Based on the

analysis of our data, we argue that the influence of increased freshwater discharge, which could impact mangrove dynamics, may have been weakened by a more intense marine effect from the mid-late Holocene in this estuary.

The RSL highstand signals from the supralittoral allow for reevaluation of the marine incursion in the region, in this case, characterized by a probable rapid rise during the middle Holocene, followed by stabilization and an equally rapid fall in the late Holocene (Fig. 8A). Such data will help to gather evidence to improve the curve model for the north Brazilian coast in different time-space scales. Similarly, considering the paleo-incursion peak at 2 ± 0.5 m above the present-day level, the curve of the RSL for the Amazonian coast would probably become more analogous to that of the northeastern and south-southeastern Brazil littoral zones, reflecting a general trend instead of the contrast previously suggested (Fig. 8A). Several authors agree that the sea-level rise attained a peak 2–5 m above the present level over the Holocene, before decreasing during the late Holocene to the present level (Angulo et al., 2006; Bezerra et al., 2003; Boski et al., 2015; Castro et al., 2014; Martin et al., 2003; Suguio et al., 2013; Tomazelli, 1990). The mangroves nearly disappeared as they migrated seaward during the Late Holocene in the Espírito Santo littoral zone in the southeastern region (França et al., 2015) and at Bahia on the northeastern coast in response to relative sea-level decline (Fontes et al., 2017; Moraes et al., 2017) (Fig. 8A).

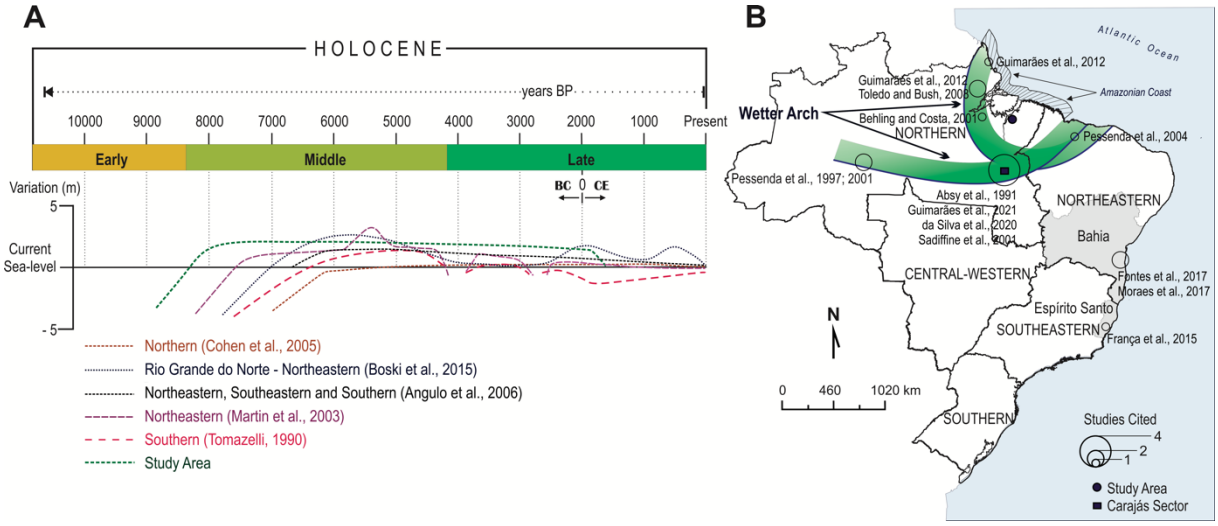

Figure 8. Summary of sea-level rise curves for Brazilian regions during the Holocene (A). The sea level curve proposed for the study area is plotted in the diagram. According to several studies, wet climates were present in several sectors of the Amazon region during the Late Holocene. These sectors comprise a wetter climate arch upstream of the study area (B).

Conclusions

This study evaluated the pollen content of a sediment core retrieved from the Itacuruçá flat in the Amazonian supralittoral region. Pollen data integrated with sedimentary features, chronological ages, and elementary data ($\delta^{13}C$, $\delta^{15}N$, and C/N) showed that the marine influence in this sector was more intense than that presently. A mangrove community occupied the muddy flats 180 km from the shoreline for over 6 ka BP, between ~6500 cal yr BC and 466 CE. It is likely that this halophyte community was established because of post-glacial sea-level rise, which exceeded the current level. After 466 CE, the landscape witnessed mangrove contraction, and freshwater vegetation became the dominant forest. Organic debris deposition in the sedimentary record was consistent with mangrove decline, and such environmental changes may be related to the RSL decline instead of the influence of climate change.

Our results suggest that the RSL rapidly increased during the middle Holocene, followed by stabilization and an equally rapid decrease to its present-day position near the two last millennia; this finding is inconsistent with previous investigations addressing the Amazonian coast. Accordingly, advances are necessary to understand the causes and trends of RSL variables in the late Holocene and gather evidence to improve the RSL curve model for the north Brazilian coast. Here, the paleo-mangrove is the leading benchmark of marine incursion, primarily because of its establishment in a field far from the coastline. These distant fields provide reliable archives for understanding RSL oscillations, allowing for the unraveling of ecological dynamics and, consequently, the development of the most robust paleogeographic models.

References

Absy, M.L., Cleef, A., Fournier, M., Martin, L., Servant, M., Sifeddine, A., Silva, M.F. da, Soubies, F., Suguio, K., Turcq, B., van der Hammen, T., 1991. Mise en évidence de quatre phases d'ouverture de la forêt dense dans le sud-est de l'Amazonie au cours des 60000 dernières années: Première comparaison avec d'autres régions tropicales. Comptes Rendus de L"Academie des Sciences, Serie II.

Absy ML. 1975. Polen e esporos do Quaternário de Santos (Brasil). Hoehnea 5: 1–26.

Allen, G.P., Posamentier, H.W., 1993. Sequence stratigraphy and facies model of an incised valley fill; the Gironde Estuary, France. Journal of Sedimentary Research 63, 378–391. https://doi.org/10.1306/D4267B09-2B26-11D7-8648000102C1865D

Alongi, D.M., 2009. The energetics of mangrove forests. The Energetics of Mangrove Forests 1–216. https://doi.org/10.1007/978-1-4020-4271-3

ANA (National Waters Agency), 2019. Accessed: November 2019. Available: http://www.snirh.gov.br/hidrotelemetria

Angulo, R.J., Lessa, G.C., 1997. The Brazilian sea-level curves: a critical review with emphasis on the curves from the Paranaguá and Cananéia regions. Marine Geology 140, 141–166. https://doi.org/10.1016/S0025-3227(97)00015-7

Angulo, R.J., Lessa, G.C., Souza, M.C. de, 2006. A critical review of mid- to late-Holocene sea-level fluctuations on the eastern Brazilian coastline. Quaternary Science Reviews 25, 486–506. https://doi.org/10.1016/j.quascirev.2005.03.008

Aziz, I., Khan, M.A.M., 2001. Effect of Seawater on the Growth, Ion Content and Water Potential of Rhizophora mucronata Lam. Journal of Plant Research 114, 369–373. https://doi.org/10.1007/PL00013998

Ball, M., 1998. Mangrove species richness in relation to salinity and waterlogging: a case study along the Adelaide River floodplain, northern Australia. Global Ecology & Biogeography Letters 7, 73–82. https://doi.org/10.1111/J.1466-8238.1998.00282.X

Barbosa, G.V., Rennó, C.V., Franco, E.M.S., 1974. Geomorfologia da Folha SA-22 Belém. In: DNPM (Ed.). Folha SA.22 Belém: geologia, geomorfologia, solos, vegetação, uso potencial da terra, Rio de Janeiro, pp. 70–130.

Behling, H., Cohen, M.C.L., Lara, R.J., 2001. Studies on Holocene mangrove ecosystem dynamics of the Bragança Peninsula in north-eastern Pará, Brazil. Palaeogeography, Palaeoclimatology, Palaeoecology 167, 225–242. https://doi.org/10.1016/S0031-0182(00)00239-X

Behling, H., da Costa, M.L., 2000. Holocene environmental changes from the Rio Curua record in the Caxiuana region, Eastern Amazon Basin. Quaternary Research 53, 369–377. https://doi.org/10.1006/qres.1999.2117

Berreda, V., Palazzesi, L., Marenssi, S., 2009. Palynological record of the Paleogene Río Leona Formation (southernmost South America): Stratigraphical and paleoenvironmental implications. Review of Palaeobotany and Palynology 154, 22–33. https://doi.org/10.1016/j.revpalbo.2008.11.005

Bezerra, F.H.R., Barreto, A.M.F., Suguio, K., 2003. Holocene sea-level history on the Rio Grande do Norte State coast, Brazil. Marine Geology 196, 73–89. https://doi.org/10.1016/S0025-3227(03)00044-6

Bird, E.C.F., 1971. Mangroves as land-builders. The Victorian Naturalist 88, 189–197.

Blasco, F., Aizpuru, M., Besnehard, J., 2019. Mangroves, Ecology 1108–1114. https://doi.org/10.1007/978-3-319-93806-6_203

Blasco, F., Saenger, P., Janodet, E., 1996. Mangroves as indicators of coastal change. Catena 27, 167–178. https://doi.org/10.1016/0341-8162(96)00013-6

Boski, T., Bezerra, F.H.R., de Fátima Pereira, L., Souza, A.M., Maia, R.P., Lima-Filho, F.P., 2015. Sea-level rise since 8.2ka recorded in the sediments of the Potengi-Jundiai Estuary, NE Brasil. Marine Geology 365, 1–13. https://doi.org/10.1016/j.margeo.2015.04.003

Cameron, C.C., Palmer, C.A., 1995. The mangrove peat of the Tobacco Range islands, Belize Barrier Reef, Central America.

Castro, J.W.A., Suguio, K., Seoane, J.C.S., da Cunha, A.M., Dias, F.F., 2014. Sea-level fluctuations and coastal evolution in the state of Rio de Janeiro, southeastern Brazil. Anais da Academia Brasileira de Ciências 86, 671–683. https://doi.org/10.1590/0001-3765201420140007

Church, J.A., Woodworth, P.L., Aarup, T., Wilson, W.S., 2010. Understanding Sea-Level Rise and Variability. Understanding Sea-Level Rise and Variability, 428. https://doi.org/10.1002/9781444323276

Church, J.A., White, N.J., Aarup, T., Wilson, W.S., Woodworth, P.L., Domingues, C.M., Hunter, J.R., Lambeck, K., 2008. Understanding global sea levels: past, present and future. Sustainability Science 2008 3:1 3, 9–22. https://doi.org/10.1007/S11625-008-0042-4

Cloern, J.E., Canuel, E.A., Harris, D., 2002. Stable carbon and nitrogen isotope composition of aquatic and terrestrial plants of the San Francisco Bay estuarine system. Limnology and Oceanography 47, 713–729. https://doi.org/10.4319/LO.2002.47.3.0713

Cohen, M.C.L., Behling, H., Lara, R.J., 2005. Amazonian mangrove dynamics during the last millennium: The relative sea-level and the Little Ice Age. Review of Palaeobotany and Palynology 136, 93–108. https://doi.org/10.1016/j.revpalbo.2005.05.002

Cohen, M.C.L., Camargo, P.M.P., Pessenda, L.C.R., Lorente, F.L., de Souza, A. v., Corrêa, J.A.M., Bendassolli, J., Dietz, M., 2021. Effects of the middle Holocene high sea-level stand and climate on Amazonian mangroves. Journal of Quaternary Science 36, 1013–1027. https://doi.org/10.1002/jqs.3343

Cohen, M.C.L., Pessenda, L.C.R., Behling, H., de Fátima Rossetti, D., França, M.C., Guimarães, J.T.F., Friaes, Y., Smith, C.B., 2012. Holocene palaeoenvironmental history of the Amazonian mangrove belt. Quaternary Science Reviews 55, 50–58. https://doi.org/10.1016/j.quascirev.2012.08.019

Colinvaux, P., De Oliveira, P.E., Patiño, J.E.M., 1999. Amazon Pollen Manual and Atlas. Harwood Academic Publishers, Dordrecht.

Color, M., 2009. Munsell Soil Color Charts, New Revised Edition. Macbeth Division of Kollmorgen Instruments, New Windsor, NY.

da Silva, E.F., Lopes, K. da S., Alves, R., Carreira, L.M.M., Silva, D.F. da, Romeiro, L. de A., Batista Júnior, W.F., Rodrigues, T.M., Secco, R. de S., Guimarães, J.T.F., 2020. Hydroclimate influences on modern pollen rain of upland southeastern Amazonia. The Holocene 30: 721–732. https://doi.org/10.1177/0959683619895586

Daidu, F., Yuan, W., Min, L., 2013. Classifications, sedimentary features and facies associations of tidal flats. Journal of Palaeogeography 2, 66–80. https://doi.org/10.3724/SP.J.1261.2013.00018

Deines, P., 1980. The isotopic composition of reduced organic carbon. In: Fritz P and Fontes JC (eds) Handbook of Environmental Isotope Geochemistry. The Terrestrial Environment, Vol.1. Amsterdam: Elsevier, 329–406.

Dalrymple, R.W., Boyd, R., Zaitlin, B.A., 1994. Incised-Valley Systems: Origin and Sedimentary Sequences. Incised-Valley Systems<subtitle>Origin and Sedimentary Sequences</subtitle>. https://doi.org/10.2110/PEC.94.12

Dalrymple, R.W., Choi, K., 2007. Morphologic and facies trends through the fluvial-marine transition in tide-dominated depositional systems: A schematic framework for environmental and sequence-stratigraphic interpretation. Earth-Science Reviews 81, 135–174. https://doi.org/10.1016/j.earscirev.2006.10.002

Dalrymple, R.W., Mackay, D.A., Ichaso, A.A., Choi, K.S., 2012. Processes, Morphodynamics, and Facies of Tide-Dominated Estuaries. Principles of Tidal Sedimentology 79–107. https://doi.org/10.1007/978-94-007-0123-6_5

Dayan, H., le Cozannet, G., Speich, S., Thiéblemont, R., 2021. High-End Scenarios of Sea-Level Rise for Coastal Risk-Averse Stakeholders. Frontiers in Marine Science 8, 514. https://doi.org/10.3389/fmars.2021.569992/bibtex

Decker, V., Falkenroth, M., Lindauer, S., Landgraf, J., Al-Lawati, Z., Al-Rahbi, H., Franz, S.O., Hoffmann, G., 2021. Collapse of Holocene mangrove ecosystems along the coastline of Oman. Quaternary Research 100, 52–76. https://doi.org/10.1017/qua. 2020.96

Dominguez, J.M.L., Bittencourt, A.C.S.P., Leão, Z.M.A.N., Azevedo, A.E.G., 1990. Geologia do Quaternário costeiro do estado de Pernambuco. Revista Brasileira de Geociências 20, 208–215.

Ellison, J., 2005. Holocene palynology and sea-level change in two estuaries in Southern Irian Jaya. Palaeogeography, Palaeoclimatology, Palaeoecology 220, 291–309. https://doi.org/10.1016/J.palaeo.2005.01.008

Engelhart, S.E., Horton, B.P., Roberts, D.H., Bryant, C.L., Corbett, D.R., 2007. Mangrove pollen of Indonesia and its suitability as a sea-level indicator. Marine Geology 242, 65–81. https://doi.org/10.1016/J.margeo.2007.02.020

Erdtman, G., 1960. The acetolysis method: in a revised description. Svensk Botanisk Tidskrift Lund 54: 561–564.

Evans, G., Prego, R., 2003. Rias, estuaries and incised valleys: is a ria an estuary? Marine Geology 196, 171–175. https://doi.org/10.1016/S0025-3227(03)00048-3

FAPESPA. Amazon Foundation for Studies and Research Support. Pará Municipal Statistics: Igarapé-Miri. Belém, 2016. Accessed: June 2019. Available: https://www.fapespa.pa.gov.br/node/201

Ferreira, C.S., 1977. Fácies da Formação Pirabas (Mioceno Inferior): novos conceitos e ampliações. Natl. Acad. Brás. Ciênc. 49, 353.

Fontes, N.A., Moraes, C.A., Cohen, M.C.L., Alves, I.C.C., França, M.C., Pessenda, L.C.R., Francisquini, M.I., Bendassolli, J.A., Macario, K., Mayle, F., 2017. The impacts of the middle holocene high Sea-Level stand and climatic changes on mangroves of the jucuruçu river, southern Bahia-Northeastern Brazil. Radiocarbon 59, 215–230. https://doi.org/10.1017/rdc.2017.6

França, M.C., Alves, I.C.C., Castro, D.F., Cohen, M.C.L., Rossetti, D.F., Pessenda, L.C.R., Lorente, F.L., Fontes, N.A., Junior, A.Á.B., Giannini, P.C.F., Francisquini, M.I., 2015. A multi-proxy evidence for the transition from estuarine mangroves to deltaic freshwater marshes, Southeastern Brazil, due to climatic and sea-level changes during the late Holocene. Catena 128, 155–166. https://doi.org/10.1016/J.catena.2015.02.005

Friess, D.A., Krauss, K.W., Horstman, E.M., Balke, T., Bouma, T.J., Galli, D., Webb, E.L., 2012. Are all intertidal wetlands naturally created equal? Bottlenecks, thresholds and knowledge gaps to mangrove and saltmarsh ecosystems. Biological Reviews 87, 346–366. https://doi.org/10.1111/J.1469-185X.2011.00198.X

Furukawa, K., Wolanski, E., 1996. Sedimentation in Mangrove Forests. Mangroves and Salt Marshes 1996 1:1 1, 3–10. https://doi.org/10.1023/A:1025973426404

Galili, E., Zviely, D., Weinstein-Evron, M., 2005. Holocene sea-level changes and landscape evolution on the northern Carmel coast (Israel). Méditerranée 79–86. hhttps://doi.org/10.4000/mediterranee.1912

Ghandour, I.M., Al-Zubieri, A.G., Basaham, A.S., Mannaa, A.A., Al-Dubai, T.A., Jones, B.G., 2021. Mid-Late Holocene Paleoenvironmental and Sea Level Reconstruction on the Al Lith Red Sea Coast, Saudi Arabia. Frontiers in Marine Science 0, 744. https://doi.org/10.3389/FMARS.2021.677010

Gilman, E.L., Ellison, J., Duke, N.C., Field, C., 2008. Threats to mangroves from climate change and adaptation options: A review. Aquatic Botany. https://doi.org/10.1016/j.aquabot.2007.12.009

Góes, A.M., Rossetti, D. de F., Nogueira, A.C.R., Toledo, P.M. de, 1990. Modelo Deposicional preliminar da Formação Pirabas no Nordeste do Estado do Pará. Boletim do Museu Paraense Emílio Goeldi, Ciências da Terra 2, 3–15.

Gomes, M.O.S., Meyer, K.E.B., Pessenda, L.C.R., 2017. Reconstituição paleoambiental da Vereda Carrasco da Raposa, Parque Estadual da Serra do Cabral, MG, Brasil, por meio de estudos palinológico e isotópico. Pesquisas em Geociências 44, 41–62. https://doi.org/10.22456/1807-9806.79586

Grimm, E.C., 1987. CONISS: a FORTRAN 77 program for stratigraphically constrained cluster analysis by the method of incremental sum of squares. Computers & Geosciences 13, 13–35. https://doi.org/10.1016/0098-3004(87)90022-7

Guimarães, J.T.F., Cohen, M.C.L., Pessenda, L.C.R., França, M.C., Smith, C.B., Nogueira, A.C.R., 2012. Mid- and late-Holocene sedimentary process and palaeovegetation changes near the mouth of the Amazon River. Holocene 22, 359–370. https://doi.org/10.1177/0959683611423693

Guimarães, J.T.F., Sahoo, P.K., de Figueiredo, M.M.J.C., da Silva Lopes, K., Gastauer, M., Ramos, S.J., Caldeira, C.F., Souza-Filho, P.W.M., Reis, L.S., da Silva, M.S., Pontes, P.R., da Silva, R.O., Rodrigues, T.M., 2021. Lake sedimentary processes and vegetation changes over the last 45k cal a bp in the uplands of south-eastern Amazonia. Journal of Quaternary Science 36, 255–272. https://doi.org/10.1002/jqs.3268

Haines, E.B., 1976. Stable carbon isotope ratios in the biota soils and tidal water of a georgia USA salt marsh. Estuarine and Coastal Marine Science 4, 609–616.

Hait, A.K., Behling, H., 2009. Holocene mangrove and coastal environmental changes in the western Ganga-Brahmaputra Delta, India. Vegetation History and Archaeobotany 18, 159–169. https://doi.org/10.1007/S00334-008-0203-5

Hofmann, C.C., 2002. Pollen distribution in sub-Recent sedimentary environments of the Orinoco Delta (Venezuela) – an actuo-palaeobotanical study. Review of Palaeobotany and Palynology 119, 191–217. https://doi.org/10.1016/S0034-6667(01)00141-5

Hogg, A.G., Heaton, T.J., Hua, Q., Palmer, J.G., Turney, C.S.M., Southon, J., Bayliss, A., Blackwe Boswijk, G., Bronk Ramsey, C., Pearson, C., Petchey, F., Reimer, P., Reimer, R., Wacker, L., 2020. SHCal20 Southern Hemisphere Calibration, 0–55,000 Years cal BP. Radiocarbon 62, 759–778. https://doi.org/10.1017/RDC.2020.59

Jayatissa, L.P., Wickramasinghe, W.A.A.D.L., Dahdouh-Guebas, F., Huxham, M., 2008. Interspecific Variations in Responses of Mangrove Seedlings to Two Contrasting Salinities. International Review of Hydrobiology 93, 700–710. https://doi.org/10.1002/iroh.200711017

Kelletat, D.H., 2019. Holocene Coastal Geomorphology 977–980. https://doi.org/10.1007/978-3-319-93806-6_171

Kodikara, K.A.S., Jayatissa, L.P., Huxham, M., Dahdouh-Guebas, F., Koedam, N., 2018. The effects of salinity on growth and survival of mangrove seedlings changes with age. Acta Botanica Brasilica 32, 37–46. https://doi.org/10.1590/0102-33062017ABB0100

Lamb, A.L., Wilson, G.P., Leng, M.J., 2006. A review of coastal palaeoclimate and relative sea-level reconstructions using δ13C and C/N ratios in organic material. Earth-Science Reviews 75, 29–57. https://doi.org/10.1016/J.earscirev.2005.10.003

Long, A.J., Waller, M.P., Stupples, P., 2006. Driving mechanisms of coastal change: Peat compaction and the destruction of late Holocene coastal wetlands. Marine Geology 225, 63–84. https://doi.org/10.1016/j.margeo.2005.09.004

Lugo, A.E., Snedaker, S.C., 1974. The Ecology of Mangroves. Annual Review of Ecology and Systematics 5, 39–64. https://doi.org/10.1146/annurev.ES.05.110174.000351

Martin, L., Dominguez, J.M.L., Bittencourt, A.C.S.P., 2003. Fluctuating Holocene sea levels is eastern and southeastern Brazil: evidence from a multiple fossil and geometric indicators. Journal of Coastal Research 19, 101–124.

Macintyre, I.G., Toscano, M.A., Lighty, R.G., Bond, G.B., 2004. Holocene history of the mangrove islands of Twin Cays, Belize, Central America. Atoll Research Bulletin 1–16. https://doi.org/10.5479/SI.00775630.510.1

Mckee, K.L., Cahoon, D.R., Feller, I.C., 2007. Caribbean mangroves adjust to rising sea level through biotic controls on change in soil elevation. Global Ecology and Biogeography16, 545–556. https://doi.org/10.1111/J.1466-8238.2007.00317.X

Meyers, P.A., 1997. Organic geochemical proxies of paleoceanographic. Organic Geochemistry 27, 213–250.

Meyers, P.A., 1994. Preservation of elemental and isotopic source identification of sedimentary organic matter. Chemical Geology 114, 289–302. https://doi.org/10.1016/0009-2541(94)90059-0

Miall, 1978. Facies types and vertical profilemodels in braided river deposits: a summary. In: Miall, A.D. (Ed.), Fluvial Sedimentology. Canadian Society of Petroleum Geologists, Calgary, pp. 597–604

Moraes, C.A., Fontes, N.A., Cohen, M.C.L., França, M.C., Pessenda, L.C.R., Rossetti, D.F., Francisquini, M.I., Bendassolli, J.A., Macario, K., 2017. Late Holocene mangrove dynamics dominated by autogenic processes. Earth Surface Processes and Landforms 42, 2013–2023. https://doi.org/10.1002/ESP.4167

Mukherjee, N., Dahdouh-Guebas, F., Koedam, N., Shanker, K., 2015. An interdisciplinary framework to evaluate bioshield plantations: Insights from peninsular India. Acta Oecologica 63, 91–100. https://doi.org/10.1016/J.ACTAO.2014.01.005

Murray, J.W., Alve, E., 1999. Natural dissolution of modern shallow water benthic foraminifera: taphonomic effects on the palaeoecological record. Palaeogeography, Palaeoclimatology, Palaeoecology 146, 195–209. https://doi.org/10.1016/S0031-0182(98)00132-1

Naidoo, G., 1985. Effects of waterlogging and salinity on plant-water relations and on the accumulation of solutes in three mangrove species. Aquatic Botany 22, 133–143. https://doi.org/10.1016/0304-3770(85)90042-7

Panapitukkul, N., Duarte, C.M., Thampanya, U., Kheowvongsri, P., Srichai, N., Geertz-Hansen, O., Terrados, J., Boromthanarath, S., 1998. Mangrove Colonization: Mangrove Progression Over the Growing Pak Phanang (SE Thailand) Mud Flat. Estuarine, Coastal and Shelf Science 47, 51–61. https://doi.org/10.1006/ECSS.1998.0343

Pessenda, L.C.R., Ribeiro, A. de S., Marques Gouveia, S.E., Aravena, R., Boulet, R., Bendassolli, J.A., 2004. Vegetation dynamics during the late Pleistocene in the Barreirinhas region, Maranhão State, northeastern Brazil, based on carbon Isotopes in soil organic matter. Quaternary Research 62, 183–193. https://doi.org/10.1016/J.yqres.2004.06.003

Pessenda, L.C.R., Boulet, R., Aravena, R., Rosolen, V., Gouveia, S.E.M., Ribeiro, A.S., Lamotte, M., 2001. Origin and dynamics of soil organic matter and vegetation changes during the Holocene in a forest-savanna transition zone, Brazilian Amazon region. The Holocene 11, 250–254. https://doi.org/10.1191/095968301668898509

Pessenda, L.C.R., Gouveia, S.E.M., Aravena, R., Gomes, B.M., Boulet, R., Ribeiro, A.S., 1997. 14C Dating and Stable Carbon Isotopes of Soil Organic Matter in Forest–Savanna Boundary Areas in the Southern Brazilian Amazon Region. Radiocarbon 40, 1013–1022. https://doi.org/10.1017/S0033822200018981

Polidoro, B.A., Carpenter, K.E., Collins, L., Duke, N.C., Ellison, A.M., Ellison, J.C., Farnsworth, E.J., Fernando, E.S., Kathiresan, K., Koedam, N.E., Livingstone, S.R.,

Miyagi, T., Moore, G.E., Nam, V.N., Ong, J.E., Primavera, J.H., Salmo, S.G., Sanciangco, J.C., Sukardjo, S., Wang, Y., Yong, J.W.H., 2010. The Loss of Species: Mangrove Extinction Risk and Geographic Areas of Global Concern. PLOS ONE 5, e10095. https://doi.org/10.1371/journal.pone.0010095

Potter, I.C., Chuwen, B.M., Hoeksema, S.D., Elliott, M., 2010. The concept of an estuary: A definition that incorporates systems which can become closed to the ocean and hypersaline. Estuarine, Coastal and Shelf Science 87, 497–500. https://doi.org/10.1016/J.ECSS.2010.01.021

Prestes, Y.O., Borba, T.A. da C., Silva, A.C. da., Rollnic, M., 2020. A discharge stationary model for the Pará-Amazon estuarine system. Journal of Hydrology: Regional Studies 28. https://doi.org/10.1016/j.ejrh.2020.100668

Punwong, P., Selby, K., Marchant, R., 2018. Holocene mangrove dynamics and relative sea-level changes along the Tanzanian coast, East Africa. Estuarine, Coastal and Shelf Science 212, 105–117. https://doi.org/10.1016/J.ecss.2018.07.004

Qiu, L., Williams, D.F., Gvorzdkov, A., Karabanov, E., Shimaraeva, M., 1993 Biogenic silica accumulation and paleoproductivity in the northern basin of Lake Baikal during the Holocene. Geology 21, 25–28. https://doi.org/10.1130/0091-7613(1993)021<0025:BSAAPI>2.3.CO;2

Reineck, H.E, Wunderlich, F., 1968. Classification and Origin of Flaser and Lenticular Bedding. Sedimentology 11, 99–104. https://doi.org/10.1111/j.1365-3091.1968.tb00843.x

Reading, H.G., 1996. Sedimentary Environments: Processes, Facies and Stratigraphy. 3rd Edition, Blackwell, Oxford, 689 p.

Reis, L.S., Guimarães, J.T.F., Souza-Filho, P.W.M., Sahoo, P.K., de Figueiredo, M.M.J.C., de Souza, E.B., Giannini, T.C., 2017. Environmental and vegetation changes in southeastern Amazonia during the late Pleistocene and Holocene. Quaternary International 449, 83–105. https://doi.org/10.1016/J.quaint.2017.04.031

Ribeiro, S.R., Valadão, R.C., 2021. Efeitos marinho e fluvial na dinâmica dos ambientes inundáveis do Estuário Superior do Rio Pará, Norte do Brasil. Revista Brasileira de Geomorfologia 22, 76–98. https://doi.org/10.20502/rbg.v22i4.2017

Ribeiro, S.R., Valadão, R.C., 2020. Processos fluviomarinhos associados à formação da Ilha Rasa, Sul da Baía de Marapatá, Nordeste do Pará, Brasil. Arquivos de Ciências do Mar 53, 110–119. https://doi.org/10.32360/acmar.v53,supl.,42659

Ribeiro, S.R., Batista, E.J.L., Cohen, M.C.L., França, M.C., Pessenda, L.C.R., Fontes, N.A., Alves, I.C.C., Bendassolli, J.A., 2018. Allogenic and autogenic effects on mangrove dynamics from the Ceará Mirim River, north-eastern Brazil, during the middle and late Holocene. Earth Surface Processes and Landforms 43, 1622–1635. https://doi.org/10.1002/esp.4342

Ribeiro, S.R., Valadão, R.C. (Submitted) Spatial and temporal patterns of coastal drainage rearrangement by large tropical rivers in a passive margin setting. Geomorphology.

Rossetti, D.F., Valeriano, M.M., Góes, A.M., Thales, M., 2008b. Palaeodrainage on Marajó Island, northern Brazil, in relation to Holocene relative sea-level dynamics. Holocene 18, 923–934. https://doi.org/10.1177/0959683608091798

Rossetti, D.F., Truckenbrodt, W., Góes, A.M., 1989. Estudo paleoambiental e estratigráfico dos Sedimentos Barreiras e Pós-Barreiras na região Bragantina, nordeste do Pará. Boletim do Museu Paraense Emílio Goeldi, Série Ciências da Terra 1, 25–74.

Roubik, D.W., Moreno, J.E., 1991. Pollen and Spores of Barro Colorado Island. Missouri Botanical Garden: St Louis.

Sampath, D.M.R., Boski, T., Loureiro, C., Sousa, C., 2015. Modelling of estuarine response to sea-level rise during the Holocene: Application to the Guadiana Estuary–SW Iberia. Geomorphology 232, 47–64. https://doi.org/10.1016/J.geomorph.2014.12.037

Shennan, I., Long, A.J., Rutherford, M.M., Green, F.M., Innes, J.B., Lloyd, J.M., Zong, Y., Walker, K.J., 1996. Tidal marsh stratigraphy, sea-level change and large earthquakes, I: A 5000 year record in Washington, U.S.A. Quaternary Science Reviews 15, 1023–1059. https://doi.org/10.1016/S0277-3791(96)00007-8

Sifeddine, A., Martin, L., Turcq, B., Volkmer-Ribeiro, C., Soubiès, F., Cordeiro, R.C., Suguio, K., 2001. Variations of the Amazonian rainforest environment: a sedimentological record covering 30,000 years. Palaeogeography, Palaeoclimatology, Palaeoecology 168, 221–235. https://doi.org/10.1016/S0031-0182(00)00256-X

Sloss, C.R., Murray-Wallace, C. V., Jones, B.G., 2007. Holocene sea-level change on the southeast coast of Australia: a review. undefined 17, 999–1014. https://doi.org/10.1177/0959683607082415

Smith, C.B., Cohen, M.C.L., Pessenda, L.C.R., França, M.C., Guimarães, J.T.F., Rossetti, D.F., Lara, R.J., 2011. Holocene coastal vegetation changes at the mouth of the Amazon River. Review of Palaeobotany and Palynology, 168, 21–30. https://doi.org/10.1016/j.revpalbo.2011.09.008

Souza-Filho, P.W.M., Lessa, G.C., Cohen, M.C.L., Costa, F.R., Lara, R.J., 2009. The Subsiding Macrotidal Barrier Estuarine System of the Eastern Amazon Coast, Northern Brazil. Lecture Notes in Earth Sciences 107, 347–375. https://doi.org/10.1007/978-3-540-44771-9_11

Spalding, M., Kainuma, M., Collins, L., 2010. World atlas of mangroves 319.

Suguio, K., Barreto, A.M.F., Oliveira, P.E. de, Bezerra, F.H.R., Vilela, M.C.S.H., 2013. Indicadores de variações holocênicas do nível do mar ao longo da costa dos estados de Pernambuco e Paraíba, Brasil. Geologia USP. Série Científica 13, 141–152. https://doi.org/10.5327/Z1519-874X201300040008

Tatumi, S.H., Silva, L.P. da, Pires, E.L., Rossetti, D.F., Góes, A.M., Munita, C.S., 2008. Datação de Sedimentos Pós-Barreiras no Norte do Brasil: implicações paleogeográficas. Revista Brasileira de Geociências 38, 514–524. https://doi.org/10.25249/0375-7536.2008383514524

Thampanya, U., 2006. Mangroves and sediment dynamics along the coasts of Southern Thailandd. Dissertation. URL https://edepot.wur.nl/39452 (accessed 12.30.21).

Thornton, S.F., McManus, J., 1994. Application of Organic Carbon and Nitrogen Stable Isotope and C/N Ratios as Source Indicators of Organic Matter Provenance in Estuarine Systems: Evidence from the Tay Estuary, Scotland. Estuarine, Coastal and Shelf Science 38, 219–233. https://doi.org/10.1006/ecss.1994.1015

Toledo, M.B., Bush, M.B., 2008. Vegetation and hydrology changes in Eastern Amazonia inferred from a pollen record. Anais da Academia Brasileira de Ciências 80, 191–203. https://doi.org/10.1590/S0001-37652008000100014

Tomazelli, L.J., 1990. Contribuição ao estudo dos sistemas deposicionais Holocênicos do Nordeste da Província Costeira do Rio Grande do Sul, com Ênfase no Sistema Eólico. PhD thesis, Porto Alegre, Universidade Federal do Rio Grande do Sul, 270 pp.

Toorman, E.A., Anthony, E., Augustinus, P.G.E.F., Gardel, A., Gratiot, N., Homenauth, O., Huybrechts, N., Monbaliu, J., Moseley, K., Naipal, S., 2018. Interaction of Mangroves, Coastal Hydrodynamics, and Morphodynamics Along the Coastal Fringes of the Guianas. Coastal Research Library 25, 429–473. https://doi.org/10.1007/978-3-319-73016-5_20

Tossou, M.G., Akoègninou, A., Ballouche, A., Sowunmi, M.A., Akpagana, K., 2008. The history of the mangrove vegetation in Benin during the Holocene a palynological study. Journal Of African Earth Sciences 52, 45167–174. https://doi.org/10.1016/J.jafrearsci.2008.07.007

Vedel, V., Behling, H., Cohen, M., Lara, R., 2006. Holocene mangrove dynamics and sea-level changes in northern Brazil, inferences from the Taperebal core in northeastern Pará State. Vegetation History and Archaeobotany 15, 115–123. https://doi.org/10.1007/s00334-005-0023-9

Walker RG. 1992. Facies, facies models and modern stratigrahic concepts. In Facies Models – Response to Sea Level Change, Walker RG, James NP (eds). Geological Association of Canada: Ontario; 1–14.

Wolanski, E., Elliott, M., 2015. Estuarine Ecohydrology: An Introduction: Second Edition. Estuarine Ecohydrology: An Introduction: Second Edition 1–321.

Woodroffe, C.D., Grindrod, J., 1991. Mangrove Biogeography: The Role of Quaternary Environmental and Sea-Level Change. Journal of Biogeography 18, 479. https://doi.org/10.2307/2845685

Yao, Q., Liu, K.B., 2017. Dynamics of marsh-mangrove ecotone since the mid-Holocene: A palynological study of mangrove encroachment and sea level rise in the Shark River Estuary, Florida. Plos One 12, e0173670. https://doi.org/10.1371/journal.pone.0173670

Supplementary Data

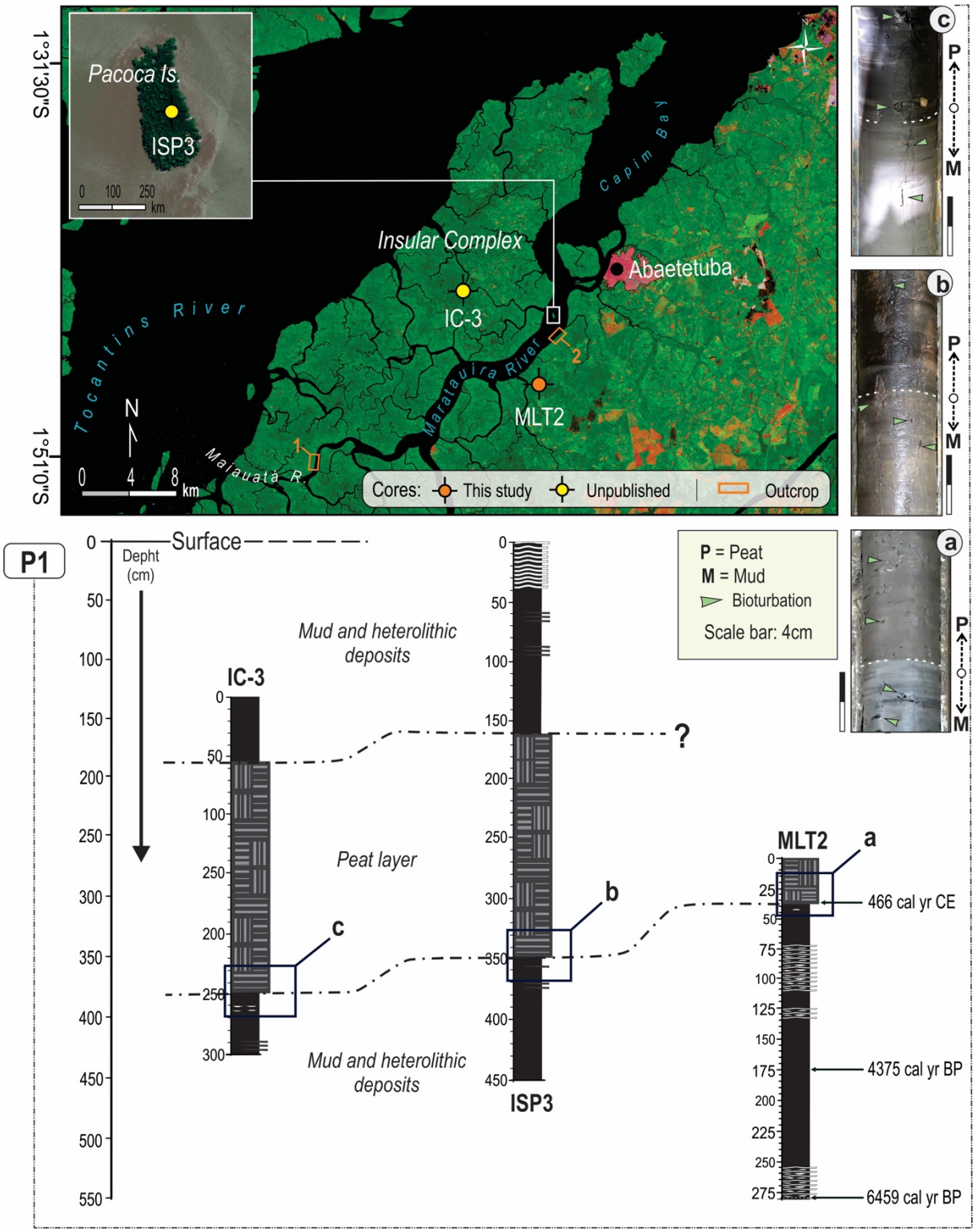

Outcrop 1 - Maiauatá River

P2

Outcrop 2 - Maratauíra River

CHAPTER 4:

FROM BRACKISH TO FRESHWATER ENVIRONMENT: IMPACTS OF THE HOLOCENE RELATIVE SEA LEVEL CHANGE ON THE TOCANTINS MOUTH LANDSCAPE TRANSITION, NORTH BRAZILIAN COASTAL AREA

Abstract – Inter-proxy (pollen, sedimentary features, geomorphology, and geochemistry) data from the Tocantins and Maratauíra river mouths, supported by C14 dating, provides records of processes that drive striking changes in the landscape during the Holocene. The development of the paleo-brackish environment upstream of the Amazon coastline was followed by mangrove establishment between 7990 cal yr BP and 1430 cal yr BP. From 1430–700 cal yr BP, this ecosystem underwent sudden spatial disruption and almost reached extinction. The organic debris accumulated and developed into peatlands. In conjunction, freshwater vegetation was established and an extensive system of tidal rivers carving their way through the Maratauíra flat was formed. This environmental transition, followed by tidal rivers morphogenesis, reflects a possible drop in relative sea level (RSL). After 700 cal yr BP, mangrove pollen frequency slightly increased, along with freshwater vegetation species prone to flooding, suggesting that the RSL rise attained its present-day position thus engulfing the tidal rivers. The estuarine landscape setting with its flooded features as seen today has counterparts mainly in the trend of RSL rise, locally favored by tectonic subsidence. The inter-evidence morphological, ecological, and sedimentary data gathered in this study may improve data for reconstructing the Amazonian paleogeography across the land-seaward interface alongside the Holocene, including new signals to enhance the paleo sea-level curves in northern coastal Brazil.

Keywords: Amazonian paleoenvironment; Maratauíra flat; Peat deposit; Mangrove pollen; Tidal river.

1. Introduction

Long-term ecological history allows the inference that coastal ecosystems are more prone to changes by natural induced stress than those settled in the continental domain, because the former undergo tension generated by continuous processes (tidal current, brackish influence, wave, and tidal erosion) and periodicals (sea-level change) that do not occur in the environment of the latter. At the Late Pleistocene–Holocene boundary, sea-level changes reshaped littoral paleoecology. The ecological archives demonstrate the evolution from ancient continental fluvial settings to estuarine systems, brackish lagoons, and tidal flats suitable for developing halophyte vegetation (Cameron and Palmer, 1995; Cohen et al., 2014; Cordero-Oviedo et al., 2019; França et al., 2015; Yao and Liu, 2017).

Although studies point to slight divergence regarding timing, magnitude of impacts, and products resulting from a fluvial to marine-dominated transition, they maintain a pattern of the almost global tropical zone during the early Holocene transgression; the shrinking ecosystems

unable to adapt to saltwater and nutrient availability and the frequency of brackish tidal oscillations, such as freshwater vegetation, in conjunction to the widespread mangrove expansion (Alongi, 2008; Blasco et al., 1996; Cohen et al., 2012; Ellison, 2008; Lugo and Snedaker, 1974; Lacerda et al., 1995).

In the mid-late Holocene, adverse conditions were gradually established in several regions; former brackish habitats relocated shoreward, followed by fluvial advance, both centrally assigned to relative sea level (RSL) drop. In Brazil's north-eastern and south-eastern coastal zones, loss of mangrove areas has been the primary outcome, including the seaward migration of this forest (Fontes et al., 2017; França et al., 2015). In the northern littoral zone, where the role of RSL change has been scarcely significant, the halophyte vegetation seated on tidal flats near large rivers, such as Amazon, experienced fragmentation forced mainly by increased fluvial discharge due to higher precipitation caused by the commencement of a wet climate (Guimarães et al., 2012; Smith et al., 2011; Cohen et al., 2012). This knowledge of the ecology of the middle Holocene strongly suggests that in mangrove-dominated coastal landscapes, climate change and the RSL drop represent a trend-mechanism that causes its ecological dynamics.

Here, we focus on a freshwater environment that lies 180 km away from the shoreline, at the Amazonian supralittoral, which is populated with freshwater vegetation with narrow mangrove fringes. Our aim is to elucidate whether this mangrove strip is related to an ancient brackish environment from the mid-Holocene or whether it is a response to RSL rise in the recent timescale. Although this field has received attention concerning island formation (Ribeiro and Valadão, 2020), the lack of palaeoecological records limits the development of a palaeogeographical model of this region. To present the Holocene history of the Tocantins-Maratauíra mouth landscape, this study employed palynology integrated with geomorphic indicators, sedimentary features, radiocarbon dating, $\delta^{13}C$, $\delta^{15}N$, and C/N analyses from organic matter applied to one sediment core from the flat Maratauíra in northern Brazil.

2. Study Area

The Maratauíra River is part of the Pará River Upper Estuary (ESP), a semidiurnal estuarine zone that ranges from microtidal to mesotidal zones (Fig. 1b). It is influenced mainly by the Tocantins River, which discharges an annual outflow of 12,900 $m^3.s^{-1}$ (ANA, 2019; Prestes et al., 2020). The ESP boundary is ~ 150 km from the modern shoreline. The downstream ESP lies in the Pará River Middle Estuary followed by the Pará River Lower Estuary. In addition to geographical position, the higher fluvial discharge of Tocantins,

Maratauíra, and numerous other rivers contributes to the freshwater gradient of the ESP (< 0.5). Consequently, the bodies of water in this estuarine zone were classified as tidal rivers, which implies that tides hydrodynamically control them, while the saline influence is non-existent (Ribeiro and Valadão, 2021).

The net interconnection channels across this sector give rise to an island setting that is typical in this region. Altogether, the islands comprise an area of 410 km^2, named the Insular Complex of West Abaetetubense (CIOA). Its morphology is characterized by low topography, mainly fluviomarine flats (0–5m), thus distributed from the lower to highest elevation zones: subtidal (< 1 m), corresponding 6.24% (21.4 km^2), followed by intertidal (1–3 m), with occurrence 32.6% (133.8 km^2), followed by supratidal zone (3–5 m), with 40.1% (164.4 km^2) (Fig. 1d). The Terra Firme, a secondary unit, occurs in 20.4% (83.8 km^2). Although the latter unit comprises intervals between 5 and 15 m, its maximum elevation does not surpass 8 m in the CIAO (Ribeiro and Valadão, 2021).

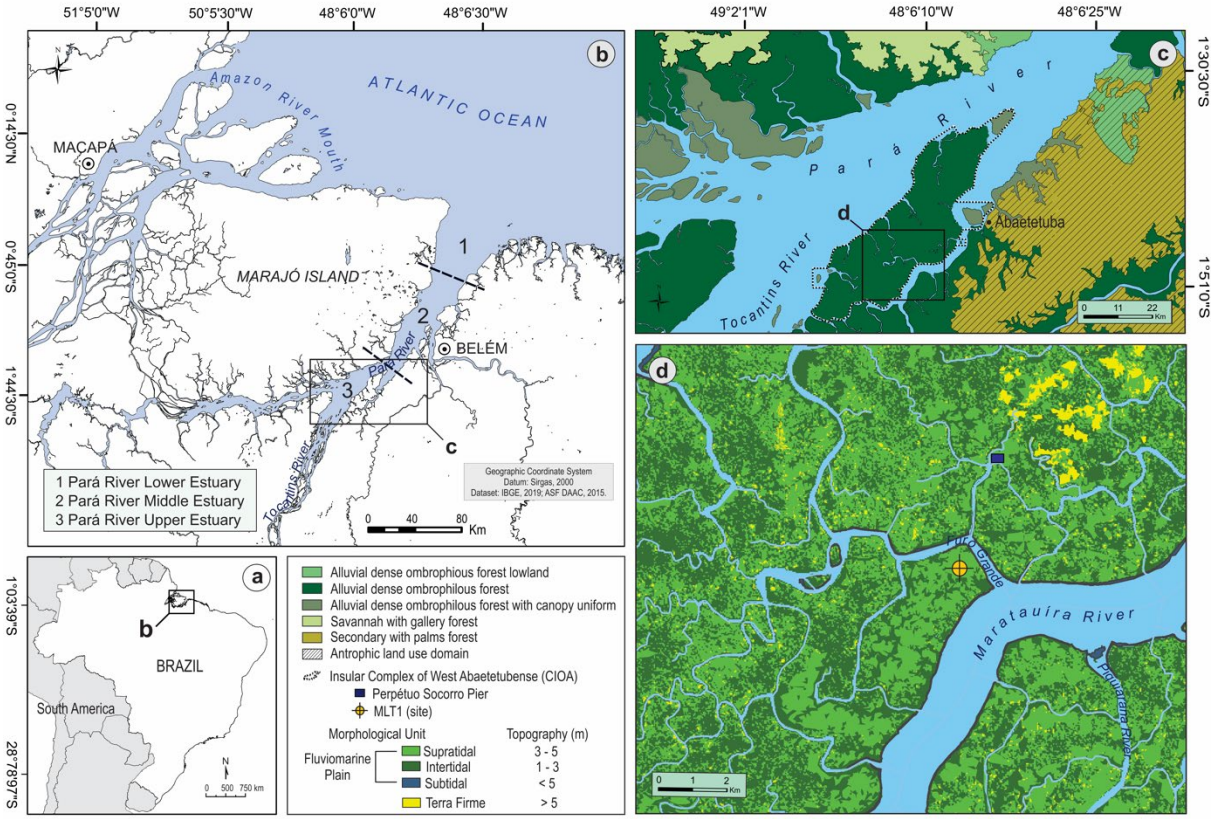

Figure 1. General north coastal location (b) detached from Brazilian territory (a). Distribution of vegetation, land use, and morphological units across the Tocantins and Maratauíra River mouths (c). Elevation of sub-environments encompassed by the fluviomarine plain on a detailed scale and sampled site (d).

The interplay of estuarine freshwater-dominated conditions, with a spring tide that may reach 3.78 m and low elevation (< 8 m), resulted in a complex mosaic of physiognomies (Fig.

1c). The alluvial dense ombrophilous forest shares space with pioneer vegetation, with the occasional presence of mangroves. The alluvial forest consisted mainly of *Pterocarpus amazonicus*, *Virola surinamensis*, *Swartzia polyphylla*, *Hevea brasiliensis*, *Calycophyllum spruceanum*, *Vouacapoua americana*, *Dipteryx odorata*, *Manilkara huberi*. In contrast, pioneer formations are represented mainly by *Montrichardia linifera*, *Mauritia flexuosa*, and *Machaerium lunatum*. In addition, narrow-fringe mangroves, mainly characterized by *Rhizophora,* are presen. The pioneer formation group, including mangroves, occurs in the lowest zone with more frequent flooding (Ribeiro and Valadão, 2020). The climate is typically warm, humid, and tropical. Given the seasonal influence of the Intertropical Convergence Zone (ITCZ), two seasons were recognized (Souza-Filho et al., 2009); a rainy season that occurs between January and July and a drier (less rainy) season that prevails for the rest of the year (July and December). The total precipitation averages 2700 mm per year, and the mean annual temperature is 27 ºC. (FAPESPA, 2016).

The area consists of Miocene and Quaternary sedimentary rocks within the geological framework. Limestones, laminated mudstones, and calciferous sandstones belonging to the Miocene have encompassed the Pirabas Formation (Ferreira, 1977), followed by conglomerates, sandstones, and claystones (siliciclastic non-fossiliferous) from the Miocene/Middle Miocene ages related to the Barreiras Formation (Rossetti et al., 1989).. These deposits reach marine to estuarine depositional environments (Góes et al., 1990; Rossetti et al., 1989). In turn, Quaternary deposits comprising eolian and fluvial-estuarine sandy and muddy sediments termed as post-Barreiras deposits (Late Pleistocene and Early Holocene) overlap with the Barreiras Formation (Tatumi et al., 2008). Post-Barreira deposits are often capped by debris-lateritic deposits (?Pleistocene), distributed in riverbank outcrops in the study area, related to the fluvial environment, and further overlain mainly by estuarine Holocene deposits (Ribeiro and Valadão, 2021).

3. Materials and Methods

3.1 Remote Sensing

The cartographic database encompasses radar images and shapefiles to morphological, topographical, and land-use characterization. Topographic data result from remote sensing products obtained from Advanced Land Observing Satellite (ALOS) through the Alaska Satellite Facility (ASF) (http://search.asf.alaska.edu). ALOS-satellite utilizes the sensor PALSAR (Phased Array L-type band Synthetic Aperture Radar (PALSAR) facing day-and-night land observation. PALSAR-sensor aid in achieving high-resolution DEM products

because its active microwave sensor (L-band - 1.27 GHz) avoids weather barriers, irrespective of day or night. The dataset obtained consists of imagens radiometric terrain corrected, polarization mode HH (RT1), and 12.5 m resolution. DEMs were geometrically corrected, filtered, and pattern to SIRGAS 2000 as the reference datum. Along with these products, cartographic data consisting of shapefiles (hydrography, geology, geomorphology, and vegetation), obtained from the Brazilian Institute of Geography and Statistics - IBGE (http://www.ibge.gov.br/geociencias/downloads-geociencias) were integrated into the radar database. Altogether analyses were performed in a GIS environment (ESRI ArcGis software, v. 10.2®).

3.2 Fieldwork and sample processing

The sample site is located ~180 km from the coastline, locally adjacent to the Furo Grande River (Supplementary Data) (Fig. 1d). Fieldwork was conducted in January 2019 to collect one sediment core. MLT1 (S1°47'10.57"/W49°0.10'6") with a depth of 550 cm was obtained using a Russian Sampler. The sampled site includes a supratidal setting, with an elevation of 3.22 ± 2 cm above the local reduction level, wherein flooding occurred during the spring tide. This topography was obtained based on the Perpétuo Socorro Pier, localized at the CIOA. Further details follow the procedures described in Ribeiro and Valadão (2012). Global Position System (GPS) determined the core geographical coordinates using SIRGAS 2000 as the reference. Visual analyses of vegetation and outcrop settings in the study area were also performed.

3.3 Facies description core

Facies analysis was undertaken following the methods of Walker (1992), wherein the texture, and structure represent the main elements. Macroscopic examination sediments was taken out, recording sandy sediments' size, sorting, and rounding, including a description of color, this latter based on Munsell Soil Color Charts (2009). Followed to Miall's (1978) codified, the facies identified were integrated into pollen data and grouped into facies association, in which each group has a significant diagnostic related to a particular sedimentary environment (Reading, 1996). The study based on facies associations allows one to understand the time and the space-connected depositional' system. Such parameters are critical to achieving the most realistic paleoenvironmental reconstructions (Dalrymple and Choi, 2007).

3.4 Pollen and spore analysis

One-hundred ten 1 cm^3 samples were taken at 5 cm intervals through the core MLT1 for pollen analysis. All samples were prepared using standard pollen analytical techniques, including KOH-10% and acetolysis (Erdtman, 1960). Sample residues were mounted on slides in a glycerin gelatin medium. Pollen and spores were identified by comparison with reference collections of about 4000 Brazilian forest taxa and various pollen keys (Colinvaux et al., 1999; Absy, 1975; Roubik and Moreno, 1991), and based on the reference collection of the Paleontology and Macroevolution Laboratory, Federal University of Minas Gerais. Pollen and spore data were presented as percentages of the total terrestrial pollen sum in pollen diagrams. The taxa were grouped according to the source: mangroves, trees, shrubs, palms, herbs, and ferns. The software TILIA and TILIAGRAF were used to calculate and plot the pollen diagram (Grimm, 1987). CONISS was used for cluster analysis of pollen taxa, permitting the zonation of the pollen diagram. CONISS is a stratigraphically constrained cluster analysis program by the total sum of squares (Grimm, 1987).

3.5 Isotopic and elemental analysis

Considering the analysis of $\delta^{13}C$ and $\delta^{15}N$ has the potential to identify changes in the sources of Organic Matter (OM) in the depositional environment, including the relationship between C/N, for example: In C3-dominated environments, the plants show δ13C values between −32‰ and −21‰, having C/N ratio >12, while C4 plants have δ13C values ranging from −17‰ to −9‰ and C/N ratio >20 (Meyers, 1997; Thornton and McManus, 1994), such indicators are employed in this work. Moreover, freshwater algae and marine algae have $\delta^{13}C$ values between −25‰ and −30‰ and −24‰ to −16‰, respectively in C3-enviroment, and $\delta^{13}C$ values ≤16‰ on the C4-dominated environments (Haines, 1976; Deines, 1980; Meyers, 1994). Thus, the preserved elemental and isotopic compositions from sediments allow tracing of the sources of MO in coastal zones.

Twenty-four samples (20 mg) were collected alongside palynological content at the core, as distributed; 7 samples were collected from 550 to 412 cm, 8 between 412 and 213 cm (due to increased MO seen in the peat layer) and 9 from the 213 to top the MLT1 core. The samples were analyzed for carbon-13 (^{13}C) nitrogen-15 (^{15}N) by isotope ratio mass spectrometry at the Laboratory for Biotechnology and Bioanalysis (LBB2), Washington State University, at DirectAMS Laboratory (Bothell), and the Stable Isotope Laboratory of the CENA/USP. The $\delta^{13}C$ and $\delta^{15}N$ results were expressed per mil (‰) concerning the VPDB and N2 standards, respectively. The TOC and TN were measured from a same parcel and provided data to calculate C/N (w/w) value for all samples. The determination of organic matter sources, such

as C3 and C4 terrestrial plants and marine and freshwater algae, will be environmental-dependent with a specific $\delta^{13}C$, $\delta^{15}N$, and C/N composition (Lamb et al., 2006; Meyers, 1997; Thornton and McManus, 1994).

3.6 Radiocarbon dating

Three bulk samples (~10 g each) were selected for dating along the MLT1 core. This selection considered main the discontinuity, sediment nature, texture, and color. The samples were checked, physically cleaned under the microscope, and conducted to DirectAMS. A chronologic framework for the sedimentary samples was provided by an Accelerator Mass Spectrometer (AMS) dating at DirectAMS Laboratory (Bothell, US). Radiocarbon ages were normalized to a $\delta^{13}C$ value of 25‰ VPDB and reported as calibrated years (cal yr BP, 2σ) using CALIB 8.2 and the SHCal13 curve (Hogg et al., 2020). The dates are reported in the text as the median of the range of calibrated ages (Table I).

4. Results

4.1 Radiocarbon dates and sedimentation rates

Radiocarbon dating of the core at depths of 550 cm, 413, and 213 cm display ages of 7990 cal yr BP, 1430 cal yr BP and 700 cal yr BP, respectively. No shows age inversions (see in Table 1 and Fig. 2). Based on the ratio between the depth intervals (mm) dating and the numerical ages obtained, the sedimentation rates calculate to MLT1 core are about 0.2 mm/yr (550–430 cm), 3 mm/yr (430–213 cm), and 2.7 mm/yr (213–0 cm) (Fig. 2).

Table 1. Sediment samples selected for radiocarbon dating with laboratory number, code core/depth, 14C yr BP and calibrated (cal) ages.

Lab. Number (D-AMS)	Sample	Depth (cm)	Age BP	Ages (Cal yr BP, 1σ)	Ages (Cal yr BP, 2σ)	Median Probabilily
038503	MLT1–peat	213	854 ± 25	686–699	680–709	700
038502	MLT1–peat	413	1591 ± 31	1405-1428	1401–1483	1430
038501	MLT1	550	7215 ± 34	7970–8011	7944–8022	7990

4.2 Core facies description

The sediment MLT1 core consisted primarily of mud and peat deposits. The peat deposits were mainly well-decomposed fibers rather than younger vegetable roots. Facies were identified based on their internal sedimentary structures, organic content, sediment texture and color, and contact relationships. Pollen and spore records and $\delta^{13}C$, $\delta^{15}N$, and C/N values were added to the facies structures, allowing for two facies associations: tidal flat (A) and swamp

mixed estuarine flat (B) and estuarine flat (C). The characteristics of each association are summarized in Table 2.

4.2.1 Facies Association Tidal flat (A)

This unit comprised the bottom of MLT2, and it occurred along the interval 550–413 cm and represented 25.1% of this core. Radiocarbon dates indicated accumulation over 6.5 ka (7990–1430 cal yr BP) (Figs. 2 and 3). Facies Association A included deposits of organic-rich mud with well-sorted fine sand. Their facies element structures consisted of lenticular heterolithic bedding (Hl) and massive mud (Mm). The latter may have contained internal planar and parallel-laminated mud. In contrast, heterolithic lenticular-bedding facies were characterized by oscillation ripples of millimeter-thick fine sand lenses. These bedforms were linked with a low-energy flow environment of deposition from suspension (Mm), with alternating traction force to sand lens deposition (Hl), typically related to tidal flat settings (Figs. 2 and 3; Tab. 2).

Pollen assemblages of Association A were dominated by mangrove pollen (38–72%) composed of *Rhizophora* (35–72%) and *Avicennia* (4–16%) followed by arboreal pollen (18–22%) composed mainly by Euphorbiaceae (3–8%), Fabaceae (3–7%), Rubiaceae (2–8%), *Mimosa* (3–7%), Malpighiaceae (0–4%). The herbs group (6–17%) was represented mainly by Poaceae (2–9%) and Cyperaceae (2–9%). Trilete and monolete ferns formed between 3 and 9%, and foraminifera between 4 and 9% in this zone (Figs. 2 and 3). Organic matter $\delta^{13}C$ ranged from –27.9 and to –26.4‰ (mean –27.2‰), whereas $\delta^{15}N$ varied between 6.1 and 2.8‰ (mean 4.5‰). Minimum and maximum C/N values are 12 and 49, respectively (Fig. 2; Tab. 2).

4.2.2 Facies Association Swamp mixed estuarine flat (B)

Association B was recognized at the interval from 412–213 cm and corresponded to the middle part of the core, representing 36.4% of MTL2, which was formed mainly by peat deposits from 1430 to 700 cal yr BP (Figs. 2 and 3). Its content was mostly decomposed; however, locally, fibers, roots, and trunks were easily distinguishable. Locally, they may contain organic muddy swathes. Besides the sample from the core, the peat exhibited good quality outcrops on the riverbank, yielding exposure due to the Furo Grande River (Fig. 1d and Supplementary data). Several rivers that enter estuarine tidal flats also yield outcrops with almost continuous exposure, allowing inferences to be made about their spatial distribution. Based on this vast subregional occurrence, where the peat deposit is an indicator of a common depositional setting, its unit can be related to a swamp mixed estuarine flat (Fig. 2; Tab. 2).

Pollen analysis revealed the predominance increase of trees (18–42%), palms (15–48%), while mangroves decrease (33 to 2%.) Trees mainly consisted of Euphorbiaceae (3–12%), Fabaceae (3–9%), Meliaceae (3–8%), *Pachira aquatica* (0–6%), *Machaerium lunatum* (1–6%), *Spondias mombin* (1–5%), Myristicaceae (0–5%), and Malpighiacaeae (0–5%), whereas the palm group as mainly characterized by *Euterpe oleraceae* (3–38%), Arecaceae (1–16%) and *Mauritia flexuosa* (2–11%). Mangrove pollen was represented by *Rhizophora* (33–2%) and *Avicennia* (8–4%). Shrub characterized by Rubiaceae (3–8%), *Mimosa* (3–7%) and Myrtaceae (1–5%) presented low percentages, as well the herb group characterized by Poaceae (3–9%), Cyperaceae (2–9%), and *Borreria* (0–4%). Ferns (4–13%) were represented by monolete and psilate triletes, and foraminifera ranged from 5 to 18% (Figs. 2 and 3). The $\delta^{13}C$ and $\delta^{15}N$ values are between –27.5 and approximately –25.4‰ (mean –26.5‰) and 1.3 and 3.8‰ (mean 2.6‰), respectively. The C/N values occur between 23 and 68 (Fig. 2; Tab. 2).

4.2.3 Facies Association Estuarine flat (C)

Facies Association C occurred between 213–0 cm in the uppermost part of the core, representing 38.5%, which accumulated over the past 700 cal yr PB (Figs. 2 and 3). The profile of bioturbation increasing upwards was characteristic of these deposits. Their facies encompassed lenticular heterolithic bedding (Hl) and massive mud (Mm). The Mm facies revealed a main organic layer, often oxidized with a dark yellow color and brown spots. This massive mud layer contrasts with a succession formed by various intercalation rhythmites, varying from beds to laminae composed of mud and fine sand (Hl). Such aspects reflect alternating bedload and suspension deposition in tidal conditions, which were assessed to be genetically related to estuarine flat setting (Fig. 2; Tab. 2).

Pollen assemblages of Association C allowed the identification of 29 pollen taxa. This zone was dominated by palm pollen (39–59%) and was composed of *Euterpe oleraceae* (22–39%), Arecaceae (5-17%) and *Mauritia flexuosa* (3–12%). The pollen spectra also included ecological groups of trees (24–46%) and shrubs (6–10%), mainly Euphorbiaceae (6–15%), Fabaceae (5–12%), Meliaceae (4–12%), *Spondias Mombin* (5–9%), *Mechaerium lunatum* (5–9%), Malpighiaceae (1–5%), *Mimosa* (3–8%) and Rubiaceae (1–6%). Poaceae (2–7%), Cyperaceae (2–5%), and *Borreria* (1–3%) represent the herbs. The mangrove ecological group appeared with percentages < 11% represented by *Rhizophora* (2–10%) and *Avicennia* (0–6%). Trilete and monolete ferns formed between 3 and 8%, and foraminifera between 0 and 9% in

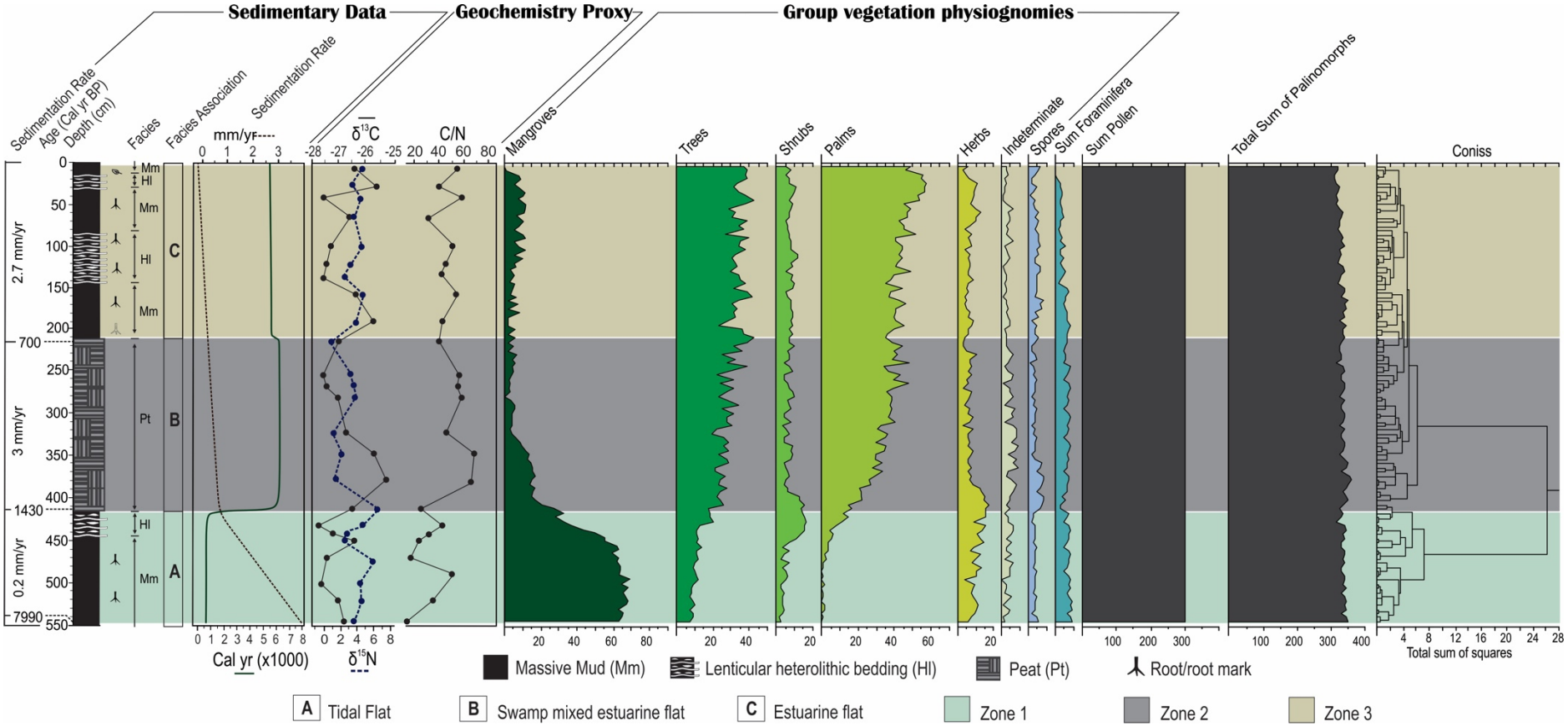

Figure 2. Sediment core framework, integrated to geochemical results, C14 ages, and pollen diagram with percentages of the physiognomic group ecological.

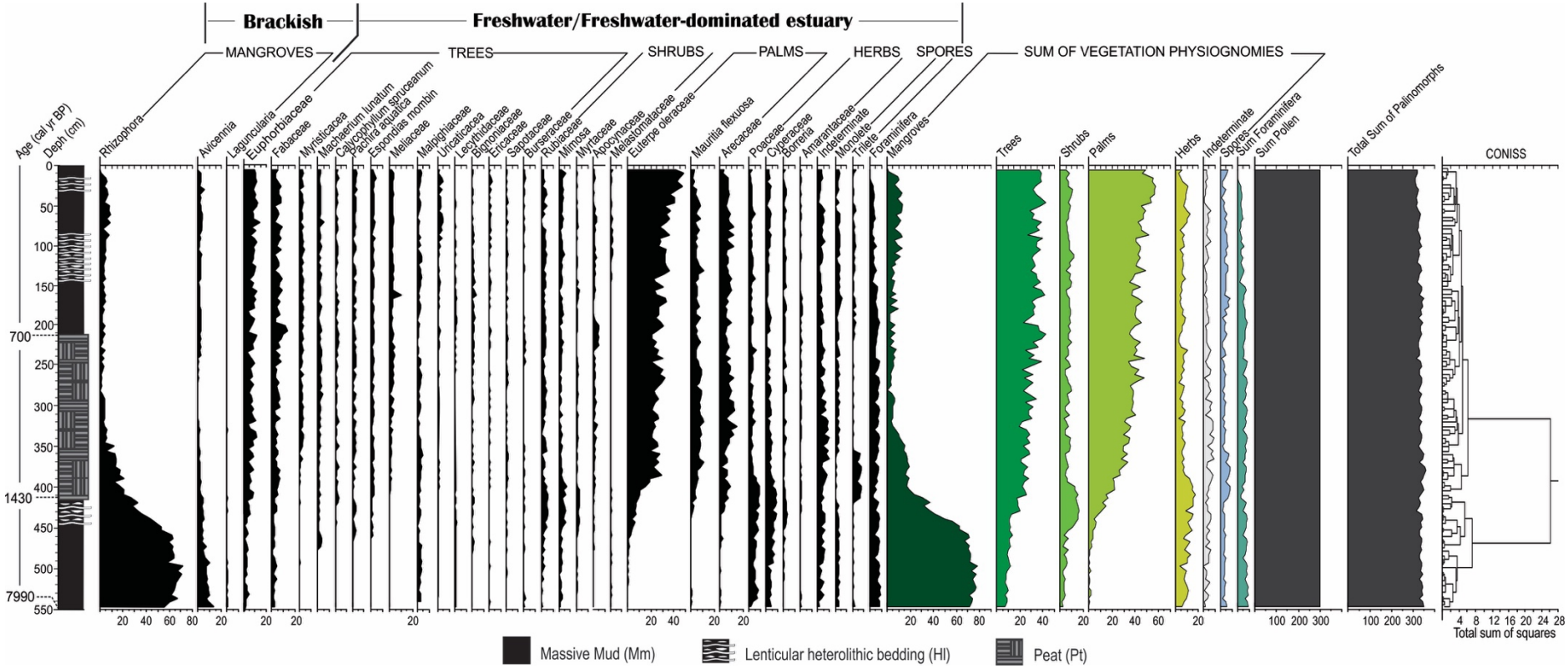

Figure 3. Pollen diagram of the core MLT1, with percentages of the most frequent pollen taxa, samples age, and cluster analysis.

this zone (Figs. 2 and 3). Organic matter $\delta^{13}C$ ranged from –27.8 and to -25.6‰ (mean –26.7‰), whereas $\delta^{15}N$ varied between 2.1 and 5‰ (mean 3.5‰). Minimum and maximum C/N values are 31 and 60, respectively (Figs. 2; Tab. 2).

Table 2. Summary of facies association, predominance of pollen groups and geochemical data.

Facies Association	Facies description	Pollen dominance	Paleoenvironment and Geochemistry data
A	Massive mud (Mm), olive-brown, gray to very dark gray and black; parallel lamination mud can be present. Heterolithic lenticular deposits (Hl) olive-brown, greenish to gray to dark gray and black. These deposits contain woody roots and root marks.	Mangrove	Tidal Flat $\delta^{13}C$= –27.9 to –26.4 ‰ $\delta^{15}N$= 2.8 to 4.5‰ C/N= 12 – 49
B	Peat layer (Pt), black, brown-reddish, and black to dark-gray, well-decomposed, with mud drapes. It revels roots and trunks woods locally present, fibers and organic debris easily recognizable.	Trees and palms	Swamp mixed estuarine flat $\delta^{13}C$= –27.5 to –25.4‰ $\delta^{15}N$= 1.3 to 3.8‰ C/N= 23 – 68
C	Massive mud (Mm), olive-brown and gray and Heterolithic lenticular deposits (Hl) greenish to gray color. Presence of oxidized with a dark yellow color and brown spots. Bioturbation caused by roots, mark roots are easily recognized.	Palms and trees	Estuarine flat $\delta^{13}C$= –27.8 to –26.7‰ $\delta^{15}N$= 2.1 to 5‰ C/N= 31 – 60

5. Discussion

5.1 The middle Holocene terrestrial brackish environment – from 7990 to 1430 cal yr BP

Brackish environments depict bodies with salinities between those of fresh and marine water, which are found in estuarine zones (Rich and Maier, 2015). The Holocene history of estuarine environments is often archived in the sedimentary systems developed by brackish tidal influences, favoring or limiting ecology. The ecology of a region is among the most reliable indices; it provides the key to unraveling paleoenvironmental history. Based on the MLT1 core, some components have been recognized that lead to inferences about establishing a paleo-brackish zone. The first indicator is related to the presence of mangroves, which, together with foraminifera (Kuraman et al., 2004; Shennan et al., 1996), implies an estuarine setting since 7990 cal yr BP.

The Holocene marine influence emergence on the Amazon started around 7 ka BP according to multi-proxy evidence (e.g., Behling et al., 2001; Behling and da Costa, 2000; Cohen et al., 2005; Vedel et al., 2006). This timing is relatively synchronous with that of the

mangroves from Maratauíra. The transgression crossed the paleo-shoreline, ultimately reactivating valleys previously incised over the fluvial deposits on the continental shelf under low-stand sea level during the Late Pleistocene. Maratauíra is one of the valleys that runs down to the sea, which was scoured out by a riverine environment in the past. This unfilled valley was immediately flooded, followed by ria formation, with the latter producing several estuarine subsystems with extensive mudflats where mangroves developed. The pollen frequency across Zone 1 indicates brackish conditions suitable for expanding this vegetation into the late Holocene (Facies Association Tidal Flat – Fig. 2).

Under the influence of saline conditions, flooding-tidal frequency, and mud supply, *Rhizophora*, *Avicennia*, and eventually *Laguncularia* were established in the landscape. Considering the position of this zone, which is 182 km away from the modern shoreline, one plausible explanation concerning mechanism control to the development and maintenance of this halophyte community along ~ 6.5 ka is the rise and stabilization of the sea level, which implies that the RSL could have surpassed ~ 2 ± 0.5 m of the present-day position during the middle Holocene.

Geomorphological evidence of the highstand sea level may be provided by the Terra Firme (Tfi) domain, classified as a sector not prone to inundation or hydrodynamic interplay (Ribeiro and Valadão, 2021). The Tfi environment comprises a unit above the fluviomarine plain between 5 and 8 m, which occurs mainly northward of the insular sector (Fig. 1d). This unit may have developed during this stage, driven by marine sedimentation. In this case, the Holocene transgression emerges as a plausible mechanism to explain why a morphological and depositional product with a tidal signature is present in the inner part of the Tfi domain, where contemporary tidal influence is not detected.

In addition to the rise in the RSL, drier climatic conditions with a deficit pluvial regime may have generated decreased fluvial input and intensified marine conditions upstream, mainly during the Northgrippian (8.2–4.2 ka BP). For instance, a drier climate with minor rainfall occurred across South America compared with the late Holocene (Novello et al., 2017), reducing the exorheic fluvial effect.

Littoral zones affected by drier conditions are prone to the increased saline influence due to less fluvial discharge (Decker et al., 2021; Potter et al., 2010). If the littoral geomorphological setting presents a low topographical slope, the latter driving low fluvial energy, the brackish zone migrates upriver and develops a saline environment inland (Ridd and Stieglitz, 2002). Likely, the Amazonas hydrographic region experienced this phenomenon over the early Holocene due to the drier period (cf. Irion et al., 2010). The subsequent sea-level rise caused a

backwater effect far upstream, silting up the Amazon valley with its tributaries outflow into large estuaries with mudflats. This combination allowed the establishment of mangroves over tidal flats between 5560–5470 and 5290–5150 cal yr BP around the city of Macapá, in the inner Amazon valley (Guimarães et al., 2012). França et al. (2015) and Fontes et al. (2017) suggested behavior similar to that of the Doce River delta (south-eastern), and Jucuruçu River coastal plain (northeastern), Brazilian littoral regions, respectively, when mangroves occupied the most landward position of mudflats in the middle Holocene.

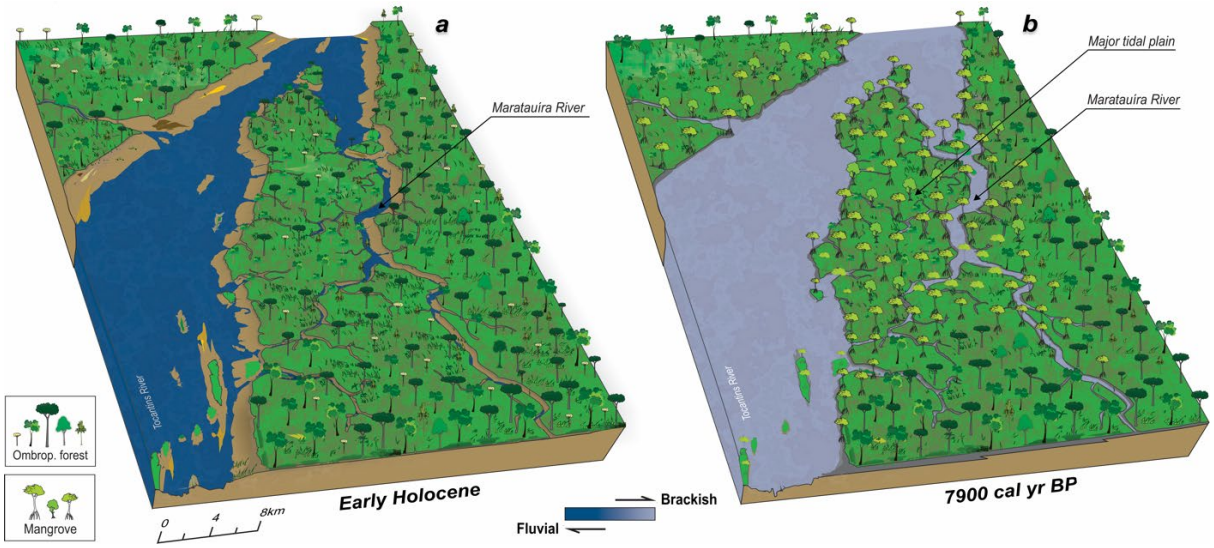

Figure 4. Conceptual presentation for landscape transition in the Tocantins and Maratauíra rivers mouth, north coastal Brazilian. The overall setting was fluvial due to the sea-level lowstand, with depth valleys incised during the Late Pleistocene-Early Holocene. (**a**) Proximal region of the rivers was dominated by ombrophilous forest with open vegetation. (**b**) Mid-Holocene sea-level rise took place, and its effect on former valleys and vegetation is prompt: ria formation and mangroves development over mudflats. The brackish condition dominated this environment until the late Holocene.

Pollen, $\delta^{13}C$, and C/N data from the study area revealed that estuarine organic matter was influenced by C3 terrestrial plants accumulated during this phase. Mangroves and herbs occupied tidal flats on the margin of the estuarine/tidal channels, while the trees and shrubs related to the freshwater ecosystem settled in the upstream highlands. The percentage of trees and shrubs of pollen in Zone 1 may be associated with the pollen inflow of ombrophilous forest from the neighboring plateau. In addition, the isotopic data is consistent with the MO paleoproductivity influenced by terrestrial plants. The $\delta^{13}C$ value is associated with this dominance, as represented here by mangroves. Likewise, the binary C/N ratios suggest organic matter from land C3 plants (Meyers, 1997; Cloern et al., 2002). Consequently, $\delta^{15}N$, with low percentages (2.8 to 6.1‰), also agrees with the OM sources of terrestrial plants. Typically, this plant group takes up dissolved atmospheric N (0‰), which is isotopically less enriched in 15N (< 10 ‰) relative to inorganic nitrogen (Lamb et al., 2006; Meyers, 1997) (Figs. 2 and 5).

In terms of sediment influx to the depositional system (i.e., sediment supply), sedimentation rates were low (0.2 mm/yr). During the RSL rise, more space is typically created to accommodate new sediments (Posamentier et al., 1988), resulting in higher sedimentation rates which is mediated by the energy of the transport agents that distribute the sediment across the basin (Catuneanu, 2019). The relatively low sedimentation rates suggest that the sampled zone corresponds to an interval topographically above the depositional products developed during the post-glacial sea-level rise. Consequently, Zone 1 would encompass sedimentary deposits that originated during the scenario of relatively stable RSL, instead of the lower strata [outside of the interval sampled, formed simultaneously with the rising sea level]. These lower strata may present the highest sedimentation rates.

5.2 Emergence of the freshwater environment – from 1430 to 700 cal yr BP

The estuary dominated by freshwater emerged around 1430 cal yr BP. The sedimentary deposits in Zone 2 consisted of a high accumulation of well-decayed roots from forests, and mud, presenting an increasing trend of pollen producing trees (18–42%) and palms (15–48%), which are diagnostic of freshwater environments, including *Euterpe oleraceae* (3–38%), *Mauritia flexuosa* (2–11%), *Pachira aquatica* (0–6%), *Machaerium lunatum* (1–6%), and *Spondias mombin* (1–5%). Despite this deposit being promising for the preservation of palynomorphs, mangrove pollen exhibited an enormous decrease (from 33% to 2%). Such a decrease suggests much less pollen was available to be preserved within the organic matter. It should be noted that the sedimentation rate increased by fifteen times compared with the lowest Zone, now reaching 3 mm/y. The $\delta^{13}C$ values from −25.6‰ to −27.8‰, indicate C3 plant sources, and the relationship between $\delta^{13}C$ and C/N higher than 45 was consistent with continental organic matter, predominantly composed of C3 plants infilling the sedimentary deposit (Fig. 2) (Deines, 1980; Lamb et al., 2006; Meyers, 1997).

Sedimentary stacking represents by peats and pollen reflects an abrupt change in the palaeoecological framework around 1430 cal yr BP. This age is similar to the base of peat deposits that occur at the Itacuruçá Tidal flat, on the mainland side, which revealed 1490 cal yr BP. Such chronological correlation suggests a similar formation process within the same spatial context. Our interpretation is consistent with the mangrove retreat, simultaneous with *várzea* forest blossoming.

Although mangroves comprise a resilient ecosystem, they show a sensitive threshold regarding the saline–freshwater balance; if this threshold is reached, the ecosystem is drastically affected (Ratajczak et al., 2018). Some studies have demonstrated that optimal growth and

productivity rates in mangrove forests could occur at concentrations ranging from 15–17 PSU owing to the regulation of leaf water and stomatal conductance, which present better physiological performances under moderate salinity (Aziz and Khan, 2001; Jayatissa et al., 2008; Kodikara et al., 2018). The natural/forced reduction of the saline influence, combined with the highest available freshwater, likely represents an environmental stressor that affected this forest in the late Holocene.

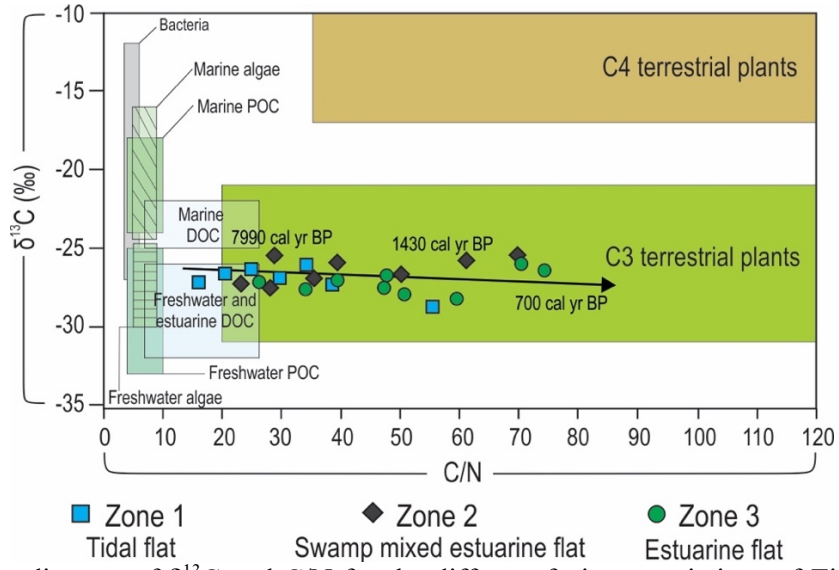

Figure 5. Binary diagram of $\delta^{13}C$ and C/N for the different facies associations of Tidal flat, Swamp mixed estuarine flat and Estuarine flat with interpretation according to data presented by Lamb et al. (2006) Meyers (1997; 1994), Thornton and McManus (1994). The trendline indicates the paleoproductivity influenced by terrestrial organic matter from the C3 plants alongside of the three zones.

Based on the pollen spectrum, it is plausible to suggest that peatland formation resulted directly in mangrove demise, yielding trunks, roots, and organic debris to the depositional system accumulated between 1430 and 700 cal yr BP, resulting in the highest sedimentation rate along the zones studied (3 mm/yr) (Figs. 2, 3 and 7c). Moreover, some characteristics, such as decomposition level, macroparticle content, and thickness, which reach 2 m-thick, suggest that only drastic changes at a broader scale and high magnitude would explain the massive death rate of halophyte plants. Changes of this order of magnitude are typically related to allogenic forces (Beerbower, 1964; Cecil, 2013; Kim et al., 2014), such as sea-level fall and climate changes (cf. Blasco et al., 1996; Decker et al., 2021; Prabakaran, 2020). Therefore, this pair of driving forces must be considered in the interpretation of the transition from fluvial to the brackish system.

The highest available freshwater in the drainage net tends to push brackish features towards the coast, e.g., the Amazon River (cf. Wells, 2006). In this sense, speculate that the

probably increased riverine paleodischarge by Tocantins River during wet periods could turn the marine influence backwards toward the sea, hampering the survival of mangroves. However, paleoclimatic investigations upstream of this area demonstrate the arrival of a humid climate, with a rainfall regime like the current one since ~ 3.5 ka BP (Absy et al., 1991; Reis et al., 2017; Sifeddine et al., 2001). This implies that the Tocantins freshwater runoff has been relatively stable since then; however, the Maratauíra's mangrove disruption occurred after ~ 1.425 cal yr BP. This asynchronous timing is inconsistent with the transition from brackish to freshwater environments, and therefore, the decline of mangroves through climate change. In this case, an RSL drop could be an allogenic mechanism that drove the ecological disruption.

Along with mangrove decline, geomorphological indicators such as the presence of tidal rivers can have a morphogenetic history with a counterpart directly related to the RSL drop. The Maratauíra Plain is incised by an extensive network of channels running down to the river of major hierarchy (Fig. 8). Likely, the most of these channels were nonexistent during the RSL high stand setting, and Maratauíra consisted of a continuous surface. Its rivers were generally represented by marginal drainage, flowing towards Maratauíra and Tocantins. The inner connection that extends from east to west, linking these two rivers, was not yet formed.

As the RSL dropped, numerous channels were formed owing to erosion. Evolution, in terms of incision, and consequently, width, could be driven by topographic imbalance. The increased flow energy during ebbs and rainfall due to wet conditions caused these shallow features to carve out their beds until the mouth reached base-level (cf. Holbrook et al., 2006) when transferring the net load (Fig. 8). The scale, processes, and products turn these channels into a special morphogenetic case; however, the trends that describe incised valley formation are maintained (cf. Allen and Posamentier, 1993; Blum et al., 2013; Catuneanu, 2019). On the other hand, this erosional phase, which entailed the Maratauíra plain, helps to understand of the irregular surface origin encompassed by the Tfi unit.

Locally, the Tfi surface revealed negative features up to a depth of 30 cm. These pervasive features result in a slightly incised topographical substrate, further described as the most striking morphological component of this environment (Ribeiro and Valadão, 2021), which is usually covered by plant biomass such as branches and broad leaves (Supplementary Data). It is likely that such morphological components were carved over the surface during this marine retraction stage combined with the effect of the heaviest rain during the late Holocene. However, it is plausible to suppose that some of these features correspond to former channels or active headwater drainage along the highstand sea level stage.

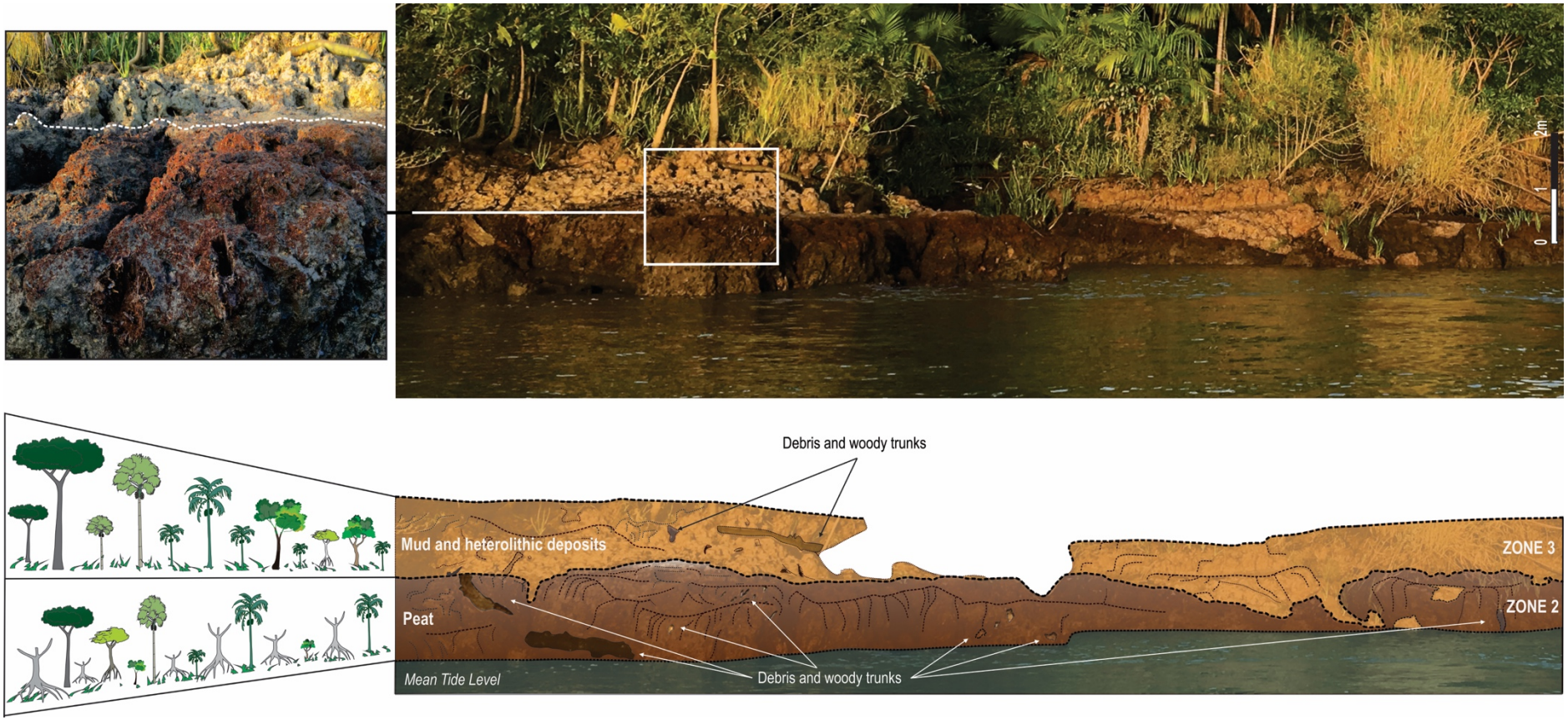

Figure 6. Peat outcrop on the banks of the Furo Grande River, south of the city of Abaetetuba, northern Brazil. The exposure occurs during the ebb tide, revealing the discontinuity between the peat bog (Zone 2) and the overlying muddy deposits (top main image) (Zone 3). In detail, trunks, fibers, and remaining organic debris are exposed due to the erosion process. At the bottom, a schematic graph with thick lines demarcates the boundary between these units, and on its left, it highlights the pollen content preserved in these two zones

This RSL fall implied the progradation of the Amazonian supralittoral, with the translation of the brackish environment towards the shoreline. Due to drastic environmental changes and the death of mangroves, rapid RSL regression was estimated, which reached 1 ± 0.5 m below the current level. Nevertheless, flooding caused by the daily tidal cycle, but without saline influence, persisted alongside the sector. This tidal frequency provided a longer hydroperiod inundation, limiting the microbiological decomposition rate of organic matter and favoring its accumulation (Fig. 6) (cf. Pepper and Gentry, 2015; Shennan, 2019).

5.3 The contemporary estuarine landscape – 700 cal yr BP onwards

The commencement time scale for this phase is based on the sedimentary discontinuity age. The debris supply for peat was cut off, while mud and portions of very fine sand moved into the system overlapping the peat layer after 700 cal yr BP. The 213 cm thick layer, with major mud accumulation, resulted in a mean sedimentation rate of 2.7 mm/yr. The sedimentary features revealed that mud was followed by lenticular bedding with uneven thickness, which is inherent in a tidal process according to periodic cycles. The alternating bedding indicated frequent reworking of sediments influenced by tidal currents of varying strength and direction, where sand and mud lenses were deposited during periods of high (ebb or flood tidal current) and low (slack water) energy flows, respectively (Daidu et al., 2013).

This facies is an unambiguous characteristic of estuarine settings, mainly consisting of tidal processes during deposition of Zone 3 (Fig. 2) (cf. Dalrymple et al., 2012; Reineck and Wunderlich, 1968). Moreover, the pervasive presence of layer mud oxidized in this zone points to drainage fluctuations that are likely linked to tidal cycles. The oxidation resulting from seasonal anaerobic conditions leads to the reduction of iron (Fe) oxides due to sediment microorganism activity (Bigham et al., 2002; Szymański and Skiba, 2013). Fe-reduction (Fe^{+2}) can readily migrate within the profile and thus reoxidize and precipitate, forming nodules and mottles (Bigham et al., 2002).

Trees and palms dominate Zone 3 (Figs. 2 and 3). The majority was established after 1430 cal yr BP, and have prospered since then in the landscape (Fig. 6); in contrast, some elements, such as the increased frequency of mangroves (2–11%), point to their return, suggesting a slightly more favorable environment for them. In this context, it should be questioned whether the estuarine influence has increased in the supralittoral, or freshwater input has decreased.

At the centennial timescale, little evidence is available to assess the existence and intensity of short-term climatic fluctuations in Amazonia over the past millennia, particularly around this sector. On a broader scale, some investigations indicate a dry period in the record

in several localities across South America, in Yasuni National Park, Equador (Weng et al., 2002), in the Pampa Plain, Venezuela (Iriondo, 1999), and the Andes (Malagnino and Strelin, 1996) where it is assigned to glacier advances. In the Brazilian littoral zone, in the Bragança coastal plain, 290 km northeast of the study area, based on mangrove pollen frequency and sedimentary record, Cohen et al. (2005) recognized two periods characterized by low inundation frequency that took place between 1130–1510 AD and after 1560 AD and was completed at the end of the 19th century. The authors suggested a correlation with the Little Ice Age. The drier conditions are reflected in a sea-level regression and less rainfall; consequently, mangrove spatial reduction occurred over the past 500 cal yr BP. In contrast, the return of a wetter period was followed by mangrove development and regular tidal inundation over mudflats.

Here, the abundant arboreal pollen followed by isotopic ^{13}C data occurrence between –27.8 and –25.6‰ related to C3 plants (Lamb et al., 2006; Meyers, 1997) offers a reliable index regarding wet conditions. Likewise, the C/N present mean value of around 38 implies C3 plants (Haines, 1976; Thornton and McManus, 1994) as source matter to infill Zone 3 (Fig. 5). Both proxies suggest those short-scale drier conditions do not was influenced Maratauíra's ecological composition over the past 700 cal yr BP. Pollen from the grass or herb and species diagnostic of the drier climate is absent in sampled sedimentary records (Figs. 2 and 3). In contrast, freshwater species prone to flooding have prospered, sharing space and time with a narrow mangrove strip (Fig. 7d). Given such a setting, is plausible to assume a return to more intense estuarine conditions, which perhaps are linked to relative sea-level rise, coupled with local effects of tectonics.

Current investigations have demonstrated that the Maratauíra Plain has undergone strong neo tectonic controls assigned to subsidence events. For instance, the peat outcrop correlation from the continental area shows that it is positioned 131 cm above the study area in some sites. This suggests that the Maratauíra Plain was affected by tectonic subsidence over the last millennium, displacing this peat layer. The sedimentation rate revealed by the sedimentary succession, which overlaps peat at 2.7 mm/yr, is related to the creation of accommodation space (Fig. 2).

The subsidence CIOA block has been linked to the dextral strike-slip fault, which controls the Maratauíra River and produces a vertical offset between the CIOA and the mainland. According to Emery and Aubrey (1991), tectonic movements can produce significant subsidence of the coastal zone on a local or regional scale, which generates relative sea-level changes. Consequently, rates of sea-level rise are on an increasing trend (Church and Coe,

2003). Therefore, the CIAO block subsidence would culminate in enlarging the marine influence in this region via tidal flooding.

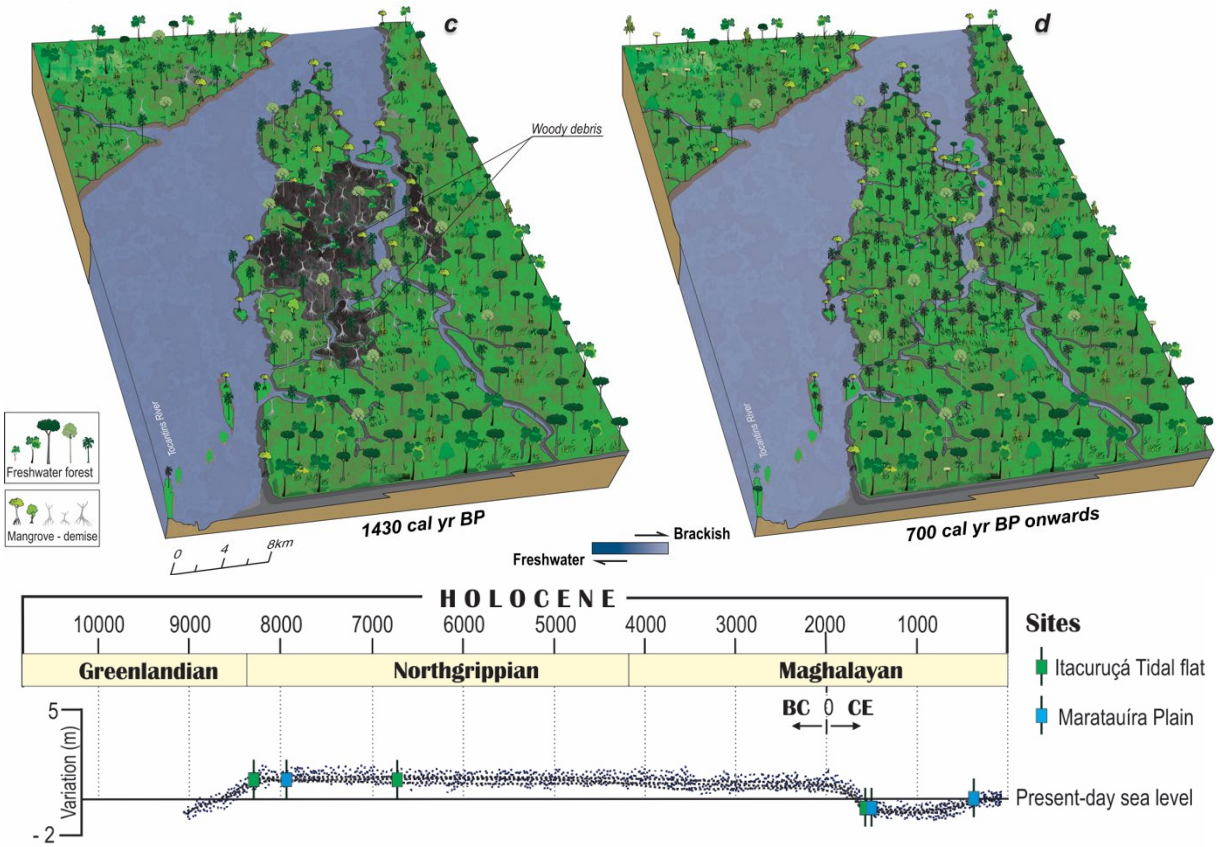

Figure 7. Conceptual landscape evolution during the late Holocene. (**c**) The transition from brackish to a freshwater environment directly affected mangrove survival after 1430 cal yr BP. This vegetation underwent a sudden decline, while peat deposits began formation between 1430 and 700 cal yr BP. Freshwater vegetation arrived and dominated the peatland. The relative sea-level fall drove this transition environmental. (**d**) After 700 cal yr BP, mangroves exhibit a return besides the freshwater forest domain. The contemporary landscape is related to RSL's rise, which reached its current position over the past seven centuries. Mud deposits overlap peatland. Note the supralittoral RSL curve graph after the dataset in this study.

The interplay between the local effects of subsidence and the trend of RSL rise that reaches between 1.8 and 2.4 mm/yr by the end of this century is related to glaciers melting globally (Church et al., 2013), which must be controlling the migration of the mangroves towards the supralittoral zone. On the contrary, the Euterpe oleracea freshwater species that also exhibits an increase near the top of the sample can be related to cultivation by the riverside population. Its commercial promotion in recent decades has led to the reforesting and expansion of its farm cultivation alongside this sector, whereas native freshwater forests have been subjected to environmental pressure (cf. Freitas et al., 2021). Therefore, concerning the modern mangroves that are blossoming here, although some may be relics from the post-glacial sea-level rise inherent to the early Holocene, the inter evidence suggests that they designate a new

plant generation favored by the RSL rise trend, which has reached its present-day position over the past 700 cal yr BP. This event led to the flooding of the tidal rivers that opened in the previous phase, forming a regional estuarine system, which attributes the multi-island setting to the Maratauíra flat as observed today (Figs. 1d and 8).

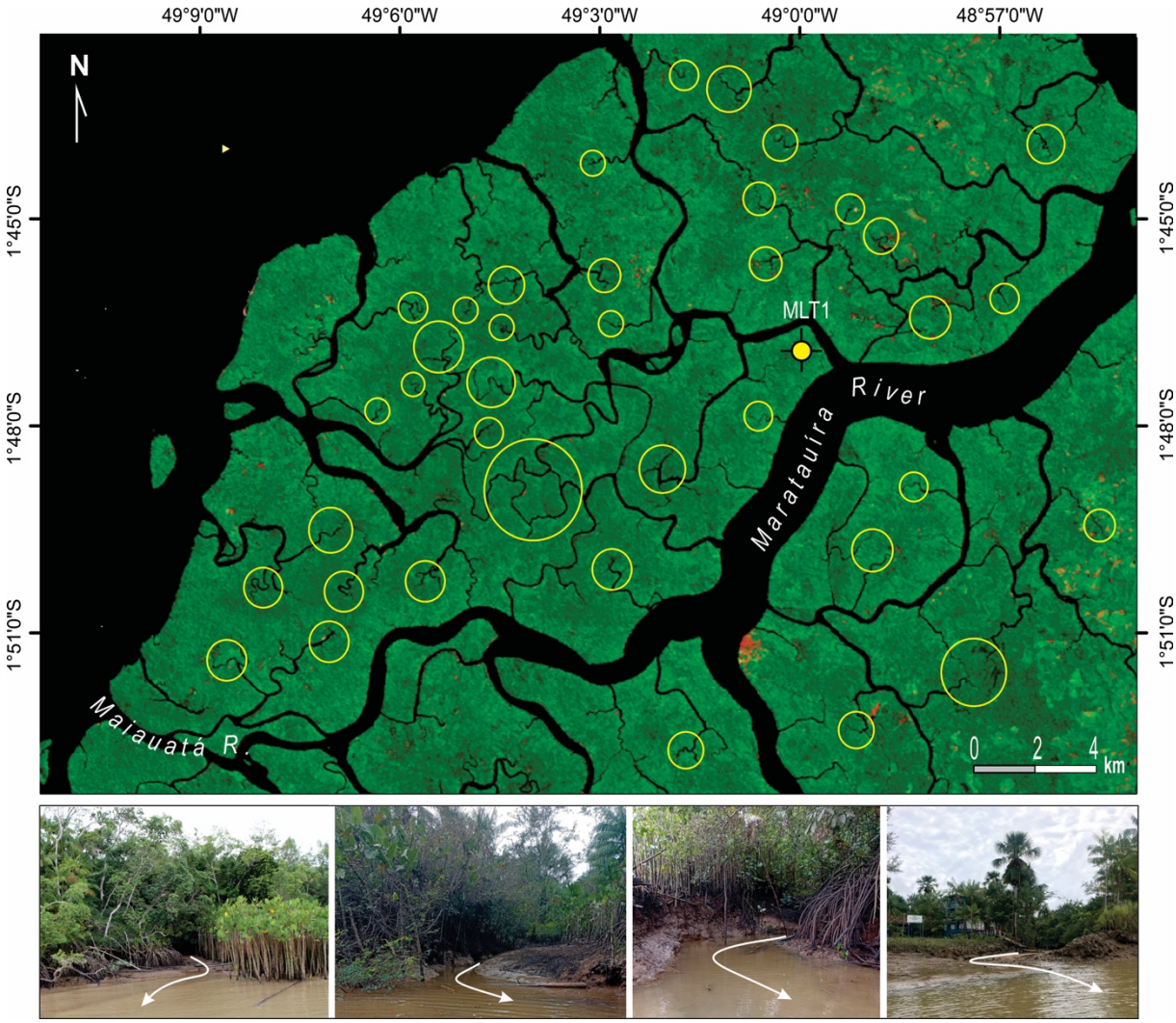

Figure 8. The extensive system of tidal rivers constitutes the drainage network southward of the Maratauíra plain, including head washed (yellow circle). The formation of these numerous and narrow channels is assigned to RSL fall around 1430 cal yr BP. Note that such channels incised their valleys over the late Holocene muddy deposits. Later, they were drowned, attributing the insular design to this region. Pictures below exemplify some of these systems, showing their mouths during the lower tide period. The white arrow indicates the ebb tidal current direction.

Conclusions

The records obtained at the Maratauíra tidal flat in northern Brazil demonstrate significant environmental changes over the Holocene. Three main periods of landscape evolution between 7990 and 1430 cal yr BP, 1230 and 700 cal yr BP, and 700 cal yr BP onwards (contemporary) were recognized. The first invoked a brackish environment marked by sub-estuaries, extensive mudflats, and mangrove forests. This component set was related to post-

glacial sea-level rise above the present-day level. The mangrove area underwent spatial disruption after 1430 cal yr BP, whereas freshwater vegetation grew on the mudflats. A continuous peat layer that reached 200 cm-thick organic debris deposited into the sedimentary system was attributable to its demise. This environmental phase was depicted by freshwater control favored by the RSL drop. After 700 cal yr BP, in addition to the established vegetation, pollen indicated an increase in mangroves, resulting in the physiognomy of the *várzea* observed today. Such a setting may be assigned to the RSL rise trend combined with subsidence effects, which favor the sea-level advance reaching its current position.

Focusing on a region with scarce paleoenvironmental investigations, the inter-evidence morphological, ecological, and sedimentary data gathered in this study may improve data for reconstruction of the palaeogeographical framework across the land-seaward interface throughout the Holocene for this supralittoral region, including new signs to add to the discussion regarding the paleo-sea level in northern coastal Brazil.

References

Absy, M.L., Cleef, A., Fournier, M., Martin, L., Servant, M., Sifeddine, A., Silva, M.F. da, Soubies, F., Suguio, K., Turcq, B., van der Hammen, T., 1991. Mise en évidence de quatre phases d'ouverture de la forêt dense dans le sud-est de l'Amazonie au cours des 60000 dernières années: Première comparaison avec d'autres régions tropicales. Comptes Rendus de L"Academie des Sciences, Serie II.

Absy ML. 1975. Polen e esporos do Quaternário de Santos (Brasil). Hoehnea 5: 1–26.

Ab'Saber, A.N., 2000. Fundamentos da geomorfologia costeira no Brasil atlântico inter e subtropical. Rev. Bras. Geomorfol. 1, 27–43. https://doi.org/10.20502/rbg.v1i1.67

Allen, G.P., Posamentier, H.W., 1993. Sequence stratigraphy and facies model of an incised valley fill; the Gironde Estuary, France. Journal of Sedimentary Research 63, 378–391. https://doi.org/10.1306/D4267B09-2B26-11D7-8648000102C1865D

Alongi, D.M., 2008. Mangrove forests: Resilience, protection from tsunamis, and responses to global climate change. Estuarine, Coastal and Shelf Science 76, 1–13. https://doi.org/10.1016/J.ECSS.2007.08.024

ANA (National Waters Agency), 2020. Accessed: January 2020. Available: http://www.snirh.gov.br/hidrotelemetria/Mapa.aspx

Aziz, I., Khan, M.A.M., 2001. Effect of Seawater on the Growth, Ion Content and Water Potential of Rhizophora mucronata Lam. Journal of Plant Research 114, 369–373. https://doi.org/10.1007/PL00013998

Beerbower, J.R., 1964. Cyclothems and cyclic depositional mechanisms in alluvial plain sedimentation. In: D.F. Merriam (Ed.), Symposium on Cyclic Sedimentation. Kansas Geological Survey Bulletin 169:31–42.

Behling, H., Cohen, M.C.L., Lara, R.J., 2001. Studies on Holocene mangrove ecosystem dynamics of the Bragança Peninsula in north-eastern Pará, Brazil. Palaeogeography, Palaeoclimatology, Palaeoecology 167, 225–242. https://doi.org/10.1016/S0031-0182(00)00239-X

Behling, H., da Costa, M.L., 2000. Holocene environmental changes from the Rio Curua record in the Caxiuana region, Eastern Amazon Basin. Quaternary Research 53, 369–377. https://doi.org/10.1006/qres.1999.2117

Bigham, J.M., Fitzpatrick, R.W., Schulze, D.G., 2018. Iron Oxides. Soil Mineralogy with Environmental Applications 7, 323–366. https://doi.org/10.2136/SSSABOOKSER7.C10

Blasco, F., Saenger, P., Janodet, E., 1996. Mangroves as indicators of coastal change. CATENA 27, 167–178. https://doi.org/10.1016/0341-8162(96)00013-6

Blum, M., Martin, J., Milliken, K., Garvin, M., 2013. Paleovalley systems: Insights from Quaternary analogs and experiments. Earth-Science Reviews 116, 128–169. https://doi.org/10.1016/J.EARSCIREV.2012.09.003

Cameron, C.C., Palmer, C.A., 1995. The mangrove peat of the Tobacco Range islands, Belize Barrier Reef, Central America.

Catuneanu, O., 2019. Model-independent sequence stratigraphy. Earth-Science Reviews 188, 312–388. https://doi.org/10.1016/J.EARSCIREV.2018.09.017

Cecil, C.B., 2013. An overview and interpretation of autocyclic and allocyclic processes and the accumulation of strata during the Pennsylvanian-Permian transition in the central Appalachian Basin, USA. International Journal of Coal Geology 119, 21–31. https://doi.org/10.1016/j.coal.2013.07.012

Church JA, Clark PU, Cazenave A, Gregory JM, Jevrejeva S, Levermann A, Merrifield MA, Milne GA, Nerem RS, Nunn PD, Payne AJ, Pfeffer WT, Stammer D, Unnikrishnam AS. 2013. Sea level change. In Climate Change 2013: The Physical Basis, Contribution of Working Group I to the Fifth Assessment Report of the Intergovernmental Panel on Climate Change, Stocker TF, Qin D, Plattner G-K, Tignor M, Allen SK, Boschung J, Nauels A, Xia Y, Bex V, Midgley PM (eds). IPCC: Cambridge, pp. 1029–1136.

Church, K.D., Coe, A.L., 2003. Processes controlling relative sea- level change and sediment supply. In: Coe, A.L. (Ed.), The Sedimentary Record of Sea-level Change. Cambridge Universi- ty Press, pp. 99–117.

Cloern, J.E., Canuel, E.A., Harris, D., 2002. Stable carbon and nitrogen isotope composition of aquatic and terrestrial plants of the San Francisco Bay estuarine system. Limnology and Oceanography 47, 713–729. https://doi.org/10.4319/LO.2002.47.3.0713

Cohen, M.C.L., França, M.C., de Fátima Rossetti, D., Pessenda, L.C.R., Giannini, P.C.F., Lorente, F.L., Junior, A.Á.B., Castro, D., Macario, K., 2014. Landscape evolution during the late Quaternary at the Doce River mouth, Espírito Santo State, Southeastern Brazil. Palaeogeography, Palaeoclimatology, Palaeoecology 415, 48–58. https://doi.org/10.1016/j.palaeo.2013.12.001

Cohen, M.C.L., Pessenda, L.C.R., Behling, H., de Fátima Rossetti, D., França, M.C., Guimarães, J.T.F., Friaes, Y., Smith, C.B., 2012. Holocene palaeoenvironmental history of the Amazonian mangrove belt. Quaternary Science Reviews 55, 50–58. https://doi.org/10.1016/j.quascirev.2012.08.019

Cohen, M.C.L., Behling, H., Lara, R.J., 2005. Amazonian mangrove dynamics during the last millennium: The relative sea-level and the Little Ice Age. Review of Palaeobotany and Palynology 136, 93–108. https://doi.org/10.1016/j.revpalbo.2005.05.002

Colinvaux, P., De Oliveira, P.E., Patiño, J.E.M., 1999. Amazon Pollen Manual and Atlas. Harwood Academic Publishers, Dordrecht.

Color, M., 2009. Munsell Soil Color Charts, New Revised Edition. Macbeth Division of Kollmorgen Instruments, New Windsor, NY.

Cordero-Oviedo, C., Correa-Metrio, A., Urrego, L.E., Vázquez, G., Blaauw, M., Escobar, J., Curtis, J.H., 2019. Holocene establishment of mangrove forests in the western coast of the Gulf of Mexico. CATENA 180, 212–223. https://doi.org/10.1016/J.CATENA.2019.04.025

Daidu, F., Yuan, W., Min, L., 2013. Classifications, sedimentary features and facies associations of tidal flats. Journal of Palaeogeography 2, 66–80. https://doi.org/10.3724/SP.J.1261.2013.00018

Dalrymple, R.W., Choi, K., 2007. Morphologic and facies trends through the fluvial-marine transition in tide-dominated depositional systems: A schematic framework for environmental and sequence-stratigraphic interpretation. Earth-Science Reviews 81, 135–174. https://doi.org/10.1016/j.earscirev.2006.10.002

Decker, V., Falkenroth, M., Lindauer, S., Landgraf, J., Al-Lawati, Z., Al-Rahbi, H., Franz, S.O., Hoffmann, G., 2021. Collapse of Holocene mangrove ecosystems along the coastline of Oman. Quaternary Research 100, 52–76. https://doi.org/10.1017/QUA.2020.96

Deines, P., 1980. The isotopic composition of reduced organic carbon. In: Fritz P and Fontes JC (eds) Handbook of Environmental Isotope Geochemistry. The Terrestrial Environment, Vol.1. Amsterdam: Elsevier, 329–406.

Ellison, J.C., 2008. Long-term retrospection on mangrove development using sediment cores and pollen analysis: A review. Aquatic Botany 89, 93–104. https://doi.org/10.1016/J.AQUABOT.2008.02.007

Emery, K.O., Aubrey, D.G., 1991. Sea Levels, Land Levels, and Tide Gauges. Sea Levels, Land Levels, and Tide Gauges. https://doi.org/10.1007/978-1-4613-9101-2

Erdtman, G., 1960. The acetolysis method: in a revised description. Svensk Botanisk Tidskrift Lund 54: 561–564.

FAPESPA. Amazon Foundation for Studies and Research Support. Pará Municipal Statistics: Igarapé-Miri. Belém, 2016. Accessed: June 2019. Available: https://www.fapespa.pa.gov.br/node/201

Ferreira, C.S., 1977. Fácies da Formação Pirabas (Mioceno Inferior): Novos conceitos e ampliações. (Projeto específicos ABe. FINEP) - Anais Academia Brasileira de Ciências, 49: 353.

Fontes, N.A., Moraes, C.A., Cohen, M.C.L., Alves, I.C.C., França, M.C., Pessenda, L.C.R., Francisquini, M.I., Bendassolli, J.A., Macario, K., Mayle, F., 2017. The impacts of the middle holocene high Sea-Level stand and climatic changes on mangroves of the jucuruÇu river, southern Bahia-Northeastern Brazil. Radiocarbon 59, 215–230. https://doi.org/10.1017/RDC.2017.6

França, M.C., Alves, I.C.C., Castro, D.F., Cohen, M.C.L., Rossetti, D.F., Pessenda, L.C.R., Lorente, F.L., Fontes, N.A., Junior, A.Á.B., Giannini, P.C.F., Francisquini, M.I., 2015. A multi-proxy evidence for the transition from estuarine mangroves to deltaic freshwater marshes, Southeastern Brazil, due to climatic and sea-level changes during the late Holocene. CATENA 128, 155–166. https://doi.org/10.1016/J.CATENA.2015.02.005

Freitas, M.A.B., Magalhães, J.L.L., Carmona, C.P., Arroyo-Rodríguez, V., Vieira, I.C.G., Tabarelli, M., 2021. Intensification of açaí palm management largely impoverishes tree assemblages in the Amazon estuarine forest. Biological Conservation 261, 109251. https://doi.org/10.1016/J.BIOCON.2021.109251

Góes, A.M., Rossetti, D. de F., Nogueira, A.C.R., Toledo, P.M. de, 1990. Modelo Deposicional preliminar da Formação Pirabas no Nordeste do Estado do Pará. Boletim do Museu Paraense Emílio Goeldi, Ciências da Terra 2, 3–15.

Grimm, E.C., 1987. CONISS: a FORTRAN 77 program for stratigraphically constrained cluster analysis by the method of incremental sum of squares. Computers & Geosciences 13, 13–35. https://doi.org/10.1016/0098-3004(87)90022-7

Guimarães, J.T.F., Cohen, M.C.L., Pessenda, L.C.R., França, M.C., Smith, C.B., Nogueira, A.C.R., 2012. Mid- and late-Holocene sedimentary process and palaeovegetation changes near the mouth of the Amazon River. Holocene 22, 359–370. https://doi.org/10.1177/0959683611423693

Guimarães, J.T.F., Sahoo, P.K., de Figueiredo, M.M.J.C., da Silva Lopes, K., Gastauer, M., Ramos, S.J., Caldeira, C.F., Souza-Filho, P.W.M., Reis, L.S., da Silva, M.S., Pontes, P.R., da Silva, R.O., Rodrigues, T.M., 2021. Lake sedimentary processes and vegetation changes over the last 45k cal a bp in the uplands of south-eastern Amazonia. Journal of Quaternary Science 36, 255–272. https://doi.org/10.1002/jqs.3268

Guimarães, J.T.F., Cohen, M.C.L., Pessenda, L.C.R., França, M.C., Smith, C.B., Nogueira, A.C.R., 2012. Mid- and late-Holocene sedimentary process and palaeovegetation changes near the mouth of the Amazon River. Holocene 22, 359–370. https://doi.org/10.1177/0959683611423693

Haines, E.B., 1976. Stable carbon isotope ratios in the biota soils and tidal water of a georgia USA salt marsh. Estuarine and Coastal Marine Science 4, 609–616.

Holbrook, J., Scott, R.W., Oboh-Ikuenobe, F.E., 2006. Base-Level Buffers and Buttresses: A Model for Upstream Versus Downstream Control on Fluvial Geometry and Architecture Within Sequences. Journal of Sedimentary Research 76, 162–174. https://doi.org/10.2110/JSR.2005.10

Irion, G., Müller, J., Morais, J.O., Keim, G., de Mello, J.N., Junk, W.J., 2009. The impact of Quaternary sea level changes on the evolution of the Amazonian lowland. Hydrological Processes 23, 3168–3172. https://doi.org/10.1002/HYP.7386

Iriondo, M., 1999. Climatic changes in the South American plains: Records of a continent-scale oscillation. Quaternary International 57–58, 93–112. https://doi.org/10.1016/S1040-6182(98)00053-6

Jayatissa, L.P., Wickramasinghe, W.A.A.D.L., Dahdouh-Guebas, F., Huxham, M., 2008. Interspecific Variations in Responses of Mangrove Seedlings to Two Contrasting Salinities. International Review of Hydrobiology 93, 700–710. https://doi.org/10.1002/iroh.200711017

Kim, W., Petter, A., Straub, K., Mohrig, D., 2014. Investigating the autogenic process response to allogenic forcing: Experimental geomorphology and stratigraphy. From Depositional Systems to Sedimentary Successions on the Norwegian Continental Margin 9781118920, 127–138. https://doi.org/10.1002/9781118920435.ch5

Kodikara, K.A.S., Jayatissa, L.P., Huxham, M., Dahdouh-Guebas, F., Koedam, N., 2018. The effects of salinity on growth and survival of mangrove seedlings changes with age. Acta Botanica Brasilica 32, 37–46. https://doi.org/10.1590/0102-33062017ABB0100

Kumaran, K.P.N., Shindikar, M., Limaye, R.B., 2004. Mangrove associated lignite beds of Malvan, Konkan: evidence for higher sea-level during the Late Tertiary (Neogene) along the west coast of India. Current Science 86, 335–340.

Lacerda, L.D., Ittekkot, V., Patchineelam, S.R., 1995. Biogeochemistry of Mangrove Soil Organic Matter: a Comparison BetweenRhizophoraandAvicenniaSoils in South-eastern Brazil. Estuarine, Coastal and Shelf Science 40, 713–720. https://doi.org/10.1006/ECSS.1995.0048

Lamb, A.L., Wilson, G.P., Leng, M.J., 2006. A review of coastal palaeoclimate and relative sea-level reconstructions using δ13C and C/N ratios in organic material. Earth-Science Reviews 75, 29–57. https://doi.org/10.1016/J.earscirev.2005.10.003

Lugo, A.E., Snedaker, S.C., 1974. The Ecology of Mangroves. Annual Review of Ecology and Systematics 5, 39–64. https://doi.org/10.1146/ANNUREV.ES.05.110174.000351

Malagnino, E.D., Strelin, j., 1996. Oscilaciones del enplazamiento en el brazo Norte del Lago Argentino y península Herminita desde el Holoceno Tardío hasta la actualidad. XIII Congr. Geol. Arg., Actas IV, pp. 290–308

Meyers, P.A., 1997. Organic geochemical proxies of paleoceanographic. Organic Geochemistry 27, 213–250.

Meyers, P.A., 1994. Preservation of elemental and isotopic source identification of sedimentary organic matter. Chemical Geology 114, 289–302. https://doi.org/10.1016/0009-2541(94)90059-0

Miall, 1978. Facies types and vertical profilemodels in braided river deposits: a summary. In: Miall, A.D. (Ed.), Fluvial Sedimentology. Canadian Society of Petroleum Geologists, Calgary, pp. 597–604

Novello, V.F., Cruz, F.W., Vuille, M., Stríkis, N.M., Edwards, R.L., Cheng, H., Emerick, S., de Paula, M.S., Li, X., Barreto, E.D.S., Karmann, I., Santos, R. v., 2017. A high-resolution history of the South American Monsoon from Last Glacial Maximum to the Holocene. Scientific Reports 2017 7:1 7, 1–8. https://doi.org/10.1038/srep44267

Pepper, I.L., Gentry, T.J., 2015. Earth Environments. Environmental Microbiology: Third Edition 59–88. https://doi.org/10.1016/B978-0-12-394626-3.00004-1

Posamentier, H.W., Vail, P.R., 1988. Eustatic control on clastic deposition II—sequence and system tract models. In: Wilgus, C.K., Hastings, B.S., Kendall, C.G.C., Posamentier, H.W., Ross, C.A., Van Wagoner, J.C. (Eds.), Sea-Level Changes: An Integrated Approach: SEPM Special Publication, 42, pp. 125–154.

Potter, I.C., Chuwen, B.M., Hoeksema, S.D., Elliott, M., 2010. The concept of an estuary: A definition that incorporates systems which can become closed to the ocean and hypersaline. Estuarine, Coastal and Shelf Science 87, 497–500. https://doi.org/10.1016/J.ECSS.2010.01.021

Prabakaran, N., 2020. Mangrove community response to subsidence inflicted sea level change in Car Nicobar Island, India. Botanica Marina 63, 419–427. https://doi.org/10.1515/BOT-2019-0088/MACHINEREADABLECITATION/RIS

Prestes, Y.O., Borba, T.A. da C., Silva, A.C. da, Rollnic, M., 2020. A discharge stationary model for the Pará-Amazon estuarine system. Journal of Hydrology: Regional Studies 28. https://doi.org/10.1016/j.ejrh.2020.100668

Ratajczak, Z., Carpenter, S.R., Ives, A.R., Kucharik, C.J., Ramia- dantsoa, T., Stegner, M.A., Williams, J.W., Zhang, J., Turner, M.G., 2018. Abrupt change in ecological systems: inference and diagnosis. Trends in Ecology & Evolution 33, 513–526.

Reading, H.G., 1996. Sedimentary Environments: Processes, Facies and Stratigraphy. 3rd Edition, Blackwell, Oxford, 689 p.

Reis, L.S., Guimarães, J.T.F., Souza-Filho, P.W.M., Sahoo, P.K., de Figueiredo, M.M.J.C., de Souza, E.B., Giannini, T.C., 2017. Environmental and vegetation changes in southeastern Amazonia during the late Pleistocene and Holocene. Quaternary International 449, 83–105. https://doi.org/10.1016/J.quaint.2017.04.031

Ribeiro, S.R., Batista, E.J.L., Cohen, M.C.L., França, M.C., Pessenda, L.C.R., Fontes, N.A., Alves, I.C.C., Bendassolli, J.A., 2018. Allogenic and autogenic effects on mangrove dynamics from the Ceará Mirim River, north-eastern Brazil, during the middle and late Holocene. Earth Surface Processes and Landforms 43, 1622–1635. https://doi.org/10.1002/esp.4342

Ribeiro, S.R., Valadão, R.C., 2021. Efeitos marinho e fluvial na dinâmica dos ambientes inundáveis do Estuário Superior do Rio Pará, Norte do Brasil. Revista Brasileira de Geomorfologia 22, 876–898. https://doi.org/10.20502/RBG.V22I4.2017

Ribeiro, S.R., Valadão, R.C., 2020. Processos fluviomarinhos associados à formação da Ilha Rasa, Sul da Baía de Marapatá, Nordeste do Pará, Brasil. Arquivos de Ciências do Mar 53, 110–119. https://doi.org/10.32360/acmar.v53,supl.,42659

Ribeiro, S.R., Valadão, R.C., Gomes, M.O.S., Bittencourt, J.S., Alves, R.A. (Submitted). Paleoecological indicators of the highstand sea level on the Amazonian supralittoral until the last two millennia. Journal of South American Earth Sciences.

Ribeiro, S.R., Valadão, R.C. (Submitted) Spatial and temporal patterns of coastal drainage rearrangement by large tropical rivers in a passive margin setting. Geomorphology.

Rich, V.I., Maier, R.M., 2015. Aquatic Environments. Environmental Microbiology: Third Edition 111–138. https://doi.org/10.1016/B978-0-12-394626-3.00006-5

Ridd, P. v., Stieglitz, T., 2002. Dry Season Salinity Changes in Arid Estuaries Fringed by Mangroves and Saltflats. Estuarine, Coastal and Shelf Science 54, 1039–1049. https://doi.org/10.1006/ECSS.2001.0876

Rossetti, D.F., Truckenbrodt, W., Góes, A.M., 1989. Estudo paleoambiental e estratigráfico dos Sedimentos Barreiras e Pós-Barreiras na região Bragantina, nordeste do Pará. Boletim do Museu Paraense Emílio Goeldi, Série Ciências da Terra 1, 25–74.

Roubik, D.W., Moreno, J.E., 1991. Pollen and Spores of Barro Colorado Island. Missouri Botanical Garden: St Louis.

Shennan, I., 2019. Peat. In: Charles W.F., Christopher, M. (Eds.), Encyclopedia of Coastal Science. Springer Nature Switzerland AG, pp. 1364–1367.

Shennan, I., Long, A.J., Rutherford, M.M., Green, F.M., Innes, J.B., Lloyd, J.M., Zong, Y., Walker, K.J., 1996. Tidal marsh stratigraphy, sea-level change and large earthquakes, I: A 5000 year record in Washington, U.S.A. Quaternary Science Reviews 15, 1023–1059. https://doi.org/10.1016/S0277-3791(96)00007-8

Sifeddine, A., Martin, L., Turcq, B., Volkmer-Ribeiro, C., Soubiès, F., Cordeiro, R.C., Suguio, K., 2001. Variations of the Amazonian rainforest environment: a sedimentological record covering 30,000 years. Palaeogeography, Palaeoclimatology, Palaeoecology 168, 221–235. https://doi.org/10.1016/S0031-0182(00)00256-X

Smith, C.B., Cohen, M.C.L., Pessenda, L.C.R., França, M.C., Guimarães, J.T.F., Rossetti, D. de F., Lara, R.J., 2011. Holocene coastal vegetation changes at the mouth of the Amazon River. Review of Palaeobotany and Palynology 168, 21–30. https://doi.org/10.1016/j.revpalbo.2011.09.008

Souza-Filho, P.W.M., Lessa, G.C., Cohen, M.C.L., Costa, F.R., Lara, R.J., 2009. The Subsiding Macrotidal Barrier Estuarine System of the Eastern Amazon Coast, Northern Brazil. Lecture Notes in Earth Sciences 107, 347–375. https://doi.org/10.1007/978-3-540-44771-9_11

Szymański, W., Skiba, M., 2013. Distribution, Morphology, and Chemical Composition of Fe-Mn Nodules in Albeluvisols of the Carpathian Foothills, Poland. Pedosphere 23, 445–454. https://doi.org/10.1016/S1002-0160(13)60037-5

Tatumi, S.H., Silva, L.P. da, Pires, E.L., Rossetti, D.F., Góes, A.M., Munita, C.S., 2008. Datação de Sedimentos Pós-Barreiras no Norte do Brasil: implicações paleogeográficas. Revista Brasileira de Geociências 38, 514–524. https://doi.org/10.25249/0375-7536.2008383514524

Thornton, S.F., McManus, J., 1994. Application of Organic Carbon and Nitrogen Stable Isotope and C/N Ratios as Source Indicators of Organic Matter Provenance in Estuarine Systems: Evidence from the Tay Estuary, Scotland. Estuarine, Coastal and Shelf Science 38, 219–233. https://doi.org/10.1006/ecss.1994.1015

Vedel, V., Behling, H., Cohen, M., Lara, R., 2006. Holocene mangrove dynamics and sea-level changes in northern Brazil, inferences from the Taperebal core in northeastern Pará State. Vegetation History and Archaeobotany 15, 115–123. https://doi.org/10.1007/s00334-005-0023-9

Yao, Q., Liu, K.B., 2017. Dynamics of marsh-mangrove ecotone since the mid-Holocene: A palynological study of mangrove encroachment and sea level rise in the Shark River Estuary, Florida. PLOS ONE 12, e0173670. https://doi.org/10.1371/JOURNAL.PONE.0173670

Walker R.G., 1992. Facies, facies models and modern stratigrahic concepts. In Facies Models – Response to Sea Level Change, Walker RG, James NP (eds). Geological Association of Canada: Ontario; 1–14.

Wells, J.T., 1995. Tide-dominated estuaries and tidal rivers. In: Perillo, G. M. E. (org.). Geomorphology and Sedimentology of estuaries. Amsterdam: Elsevier. pp. 179–205. https://doi.org/10.1016/S0070-4571(05)80026-3

Weng, C., Bush, M.B., Athens, J.S., 2002. Holocene climate change and hydrarch succession in lowland Amazonian Ecuador. *Review of Palaeobotany and Palynology* 120(1–2). Elsevier: 73–90. DOI: 10.1016/S0034-6667(01)00148-8

Supplementary Data

The biomass removal demonstrates irregularity features along the Terra Firme (TFi) morphological unit surface. These negative features up to a depth of 30 cm are described as the most striking morphological component of this environment domain, likely incised during relative sea-level fall.

CAPÍTULO 5:

DA COMPARTIMENTAÇÃO DO OBJETO À CONSTRUÇÃO DE UMA TESE

1. Integrando escalas e cenários

O trânsito multiescalar é intrínseco à investigação em Geografia Física e em Geomorfologia (CAILLEUX & TRICART, 1956; THOMBURY, 1969; AB'SÁBER, 1977; CHRISTOFOLETTI, 1977; WHITE, 1982; ABREU, 1983; SCHUMM, 1985; GAO & XIA, 1996; GOODIE, 2000; UNWIN, 2002). A multiescalaridade que transcende fronteiras artificialmente construídas e que acaba por delinear compartimentos espaciais e temporais ditados pelo objeto constitui necessidade lógico-científica que vai ao encontro de nossas tentativas por compreender a complexidade evolutiva da superfície da Terra, de maneira simplificada e elucidativa (BOER, 1992; SHERMAN & BAUER, 1993; BAUER, 1996). Essa compartimentação, tal como feito nesta investigação da foz do Rio Tocantins, reflete também restrições disciplinares, visto que as escalas espaciais de um problema são ditadas pelos métodos usados para atacá-los (BAUER, 1996). O termo compartimentação faz referência a *compartmentalization*, empregado por Bauer (1996), e denota o ajuste entre problema investigado e perspectiva de análise, mediante a subdivisão em escalas espaço-temporais.

A compartimentação do objeto, seguida pelo desacoplamento de processos e segmentação da profundidade de tempo, útil para descrever a história passada ou inversamente para explicar as mudanças observadas no presente, se, por um lado, resolve satisfatoriamente questões maiores da investigação geomorfológica, por outro, permite, talvez, que lacunas sejam abertas e uma fração dos registros e informações geomórficas sejam perdidas. Se essa afirmativa for verdadeira, difícil é caracterizar e dimensionar o que foi perdido. Certo é que, ao fim da investigação, a consequente conclusão é de que uma fração da evolução da paisagem corresponde, invariavelmente, a *gaps*. Nesse sentido, reconhecer a limitação intrínseca a esse procedimento metodológico desperta o senso da autoavaliação crítica sobre a produção do conhecimento e, ao mesmo tempo, desenvolve no pesquisador maior rigor sobre a hierarquia da compartimentação e controle sobre a escala adotada.

Reunir os resultados e integrar as múltiplas escalas na tentativa de superar limitações e incompletudes que foram se aderindo à investigação, consiste, também, na somatória de lacunas. Portanto, a pesquisa geográfica consta de desafios de ordem metodológica claramente não superados, capazes de apresentar resultados não inteiramente conclusivos, pois questões abertas talvez pudessem ter adequada resposta nos *gaps*.

Posto de lado tais dimensionamentos, a presente contribuição pode ser designada como contribuitiva ao campo da Geomorfologia Histórica (cf. BECKINSALE & CHORLEY, 1991; BAKER & TWIDALE 1992; KENNEDY 1992), o que significa que a investigação se baseou

em referências temporais bem definidas, de sorte que os processos, forçantes, mecanismos ou fenômenos naturais receberam maior atenção dentro de limites espaço-temporais circunscritos, embora sua repercussão não atenda necessariamente aos ditames dessas escalas. De acordo com Bauer (1996), a pesquisa geomorfológica histórica preocupa-se com a compreensão da evolução da paisagem como uma sequência de eventos, mesmo que por vezes graduais (BRUNSDEN, 1996), e, portanto, lida com a identificação explícita de elementos distintos no curso do tempo.

Às premissas estabelecidas na Introdução deste volume deve-se o norte desta pesquisa. Os procedimentos metodológicos endereçados a diversos níveis hierárquicos de investigação e os consequentes resultados revelados, com explicação adequada, demonstram apropriada verdade concernente às premissas: o ajuste do Rio Tocantins representa o estágio central da paleogeografia costeira ocidental do Estado do Pará. A paisagem insular comunica uma gradação de processos articulados às influências marinha e fluvial, com contrapartes principais na neotectônica, mudança no nível do mar e na hidrodinâmica estuarina. Sabe-se que variações climáticas controlaram as mudanças no nível do mar, contudo, sua assinatura [fase úmida *versus* seca] na componente ecológica não tem sido detectada com clareza. A esse respeito, no entanto, investigações são recomendadas.

As forçantes com atuação em longo prazo e/ou expressas no tempo presente na foz do Tocantins foram caracterizadas com base nos padrões de assinaturas geomórficas, ecológicas e estruturais, bem como através do registro no sistema deposicional e na assinatura geoquímica da paleoprodutividade orgânica que os preenche. Nesse sentido, é plausível sustentar que o Complexo Insular, tem de fato, raízes morfogenéticas ancoradas no contexto espaço-temporal profundo.

O Complexo Insular tem origem no continente, de onde foi destacado sob efeito de um regime tectônico transcorrente que tomou lugar durante o Holoceno. O desenvolvimento estratigráfico desse trecho continental, Série Holoceno, foi controlado majoritariamente pelo mecanismo marinho, apesar de localizado a 180 km do litoral, na foz de largos sistemas fluviais tropicais. A fonte orgânica do material sedimentar está associada a grupamento de árvores, demonstrando que florestas bem desenvolvidas ocupavam o contexto espacial desde o Holoceno Inicial. Mediante adequada caracterização do papel das forçantes e da colocação em perspectiva dos resultados alcançados, o cenário evolutivo sub-regional através de referências temporais pôde ser reconstituído.

Antes de tudo, defende-se que o Rio Tocantins foi o principal modelador da paisagem costeira na região nordeste do Estado do Pará; do rebaixamento dos platôs, às menores formas

esculpidas nos limites de sua bacia de drenagem podem ser atribuídos ao trabalho fluvial desse rio. O estágio inicial desse protagonismo corresponde ao ajuste costeiro que sofreu. O Tocantins fluía em direção à foz do Amazonas, provavelmente até o Pleistoceno Superior. Eventos de ordem tectônica direcional dextral E-W, que surgiram no quadro neotectônico regional durante o Quaternário, desacoplou o Tocantins da Bacia Amazônica. Simultaneamente, o regime estrutural dextral NE-SW, levou à abertura de uma fenda a montante de Baião, que, propagando-se até o litoral, formou uma zona de fraqueza erosiva. Essa zona deu vazão à nova via fluvial do Tocantins para leste, esvaziando-se no Atlântico. Consequentemente, o antigo curso oeste foi inativado.

Na transição Pleistoceno-Holoceno, com nível do mar abaixo do atual e a linha de costa posicionada mais adentro da bacia oceânica, a declividade da plataforma exposta favoreceu a energia do fluxo exorreico, ativando a erosão remontante de vales fluviais. A eficiência da erosão e a posição dessas feições fluviais foi favorecida por descontinuidades estruturais resultantes do quadro tectônico emergente. Nesse contexto, abre-se o vale do Maratauíra, gatilho para a separação do trato continental reconhecido por Complexo Insular. A partir deste evento, a evolução paleogeográfica pôde ser rastreada e as mudanças engendradas ao longo do Holoceno tornaram-se mais bem conhecidas pelos métodos aqui empregados.

O evento seguinte de forte implicação na paisagem ocorreu no Holoceno Inicial com a elevação do nível do mar, que afogou antigos vales previamente escavados. Maratauíra foi inteiramente afogado, evoluindo para ria, precisamente em 8410 anos cal AP (6459 anos cal AC). Múltiplas evidências da influência marinha, mais intensa que a dos dias atuais, são fornecidas por pólen, microforaminífera, razão isotópica da matéria orgânica e fácies sedimentares.

A vegetação, como síntese da condição do meio físico, sugere o desenvolvimento de um ambiente salobro, no qual o manguezal se estabeleceu e prosperou nas planícies de maré do Holoceno Inicial até o Tardio. Por volta de 1490 anos cal AP (466 anos cal DC) o manguezal foi severamente impactado. A condição salobra cessou no supralitoral, enquanto a vegetação de água doce surgiu, emergindo a várzea, ecossistema tipicamente adaptado à inundação. Essa marcante mudança, que impactou a paisagem ecológica, a natureza do aporte sedimentar e a incisão de rede de drenagem demarca mudança no nível relativo do mar, interpretado como em estágio de queda, para posição pouco abaixo a do nível atual.

A morte do mangue se rendeu à formação de turfeiras, cuja camada de detrito orgânico contínuo supera 2 m, depositados entre ~1500 a 700 anos cal AP. Atribui-se à configuração de inundação estuarina a formação do ambiente redutor e o suprimento sedimentar de textura

lamosa, favorável ao rápido soterramento da matéria orgânica, antes de sua decomposição. As sucessões lamosas e heterolíticas que sustentam, e igualmente se sobrepõem às turfeiras, refletem um ambiente de baixa energia, no qual planícies estuarinas se desenvolveram. De outra forma, mediante o padrão de empilhamento sedimentar, atividades relacionadas à migração de canais estuarinos foram reconhecidas.

O capítulo final da evolução da paisagem é pontuado como iniciado após 700 anos cal AP. A vegetação, constituída por espécies de água doce, com presença de uma franja de manguezal, pode ser atribuída diretamente à subida do nível relativo do mar, alcançando a posição atual ao longo desses 7 séculos, favorecido também por eventos de subsidência. Adicionalmente, a extensa rede de canais de maré previamente aberta é afogada, conferindo ao CIOA o intrínseco caráter multi-insular. Esse ambiente contemporâneo tem sua dinâmica regida por mesomarés, cuja variação de até 3.78 m durante a sizígia sujeita, aproximadamente, 40% do CIOA a eventos de inundação. O gradiente é limnético, em função do elevado aporte fluvial ao longo do ano, o que promove a diluição do gradiente salobro a jusante dessa região.

Embora as marés, englobadas na forçante hidrodinâmica, tenham sua assinatura impressa na evolução da paisagem desde ~8,4 ka AP, a competência da neotectônica e de variações no nível do mar assumiram maior protagonismo na estruturação da paisagem até aproximadamente os últimos dois milênios. É mediante o enfraquecimento de ambas que a hidrodinâmica assume controle sobre o ambiente insular, influenciando os aspectos morfológico, ecológico e sedimentar da várzea conhecida atualmente.

Endereçada a uma região com escassas investigações no âmbito da Geografia Física, buscou-se adequadamente colocar esta pesquisa no contexto da literatura existente, partindo de avanços trazidos por outros campos do saber, confrontando resultados e buscando abrir espaço para novos debates sobre as interpretações fornecidas aos achados nela reunidos.

Ao lado da reconstituição da paisagem, entre os principais achados, consta a detecção de atividades de forte controle tectônico nesta margem passiva, estruturando os elementos mais proeminentes da paisagem, como a foz do Tocantins, o desenho do Maratauíra, a posição do CIOA e de ilhas adjacentes e o arranjo dos estratos holocênicos. Esse último apresenta deslocamento de pacotes sedimentares formados até no último milênio, o que sugere firmemente pulsos tectônicos que atravessaram o Holoceno. O domínio geotectônico passivo não restringiu o papel dos ajustes neotectônicos.

Enfatiza-se que os estudos voltados à Amazônia devem ter um olhar cuidadoso sobre a neotectônica. Para tanto, distintos padrões espaço-temporais de abordagem são úteis, pois permitem obter dados estruturais de alta resolução, geralmente com aderência sensível à menor

escala, tal como os revelados aqui. Esses achados permitem levantar indagações, tais como: houve de fato um período de quiescência tectônica na Amazônia? O emprego dessa terminologia traduz a ausência de fenômenos estruturais ou a escassez de estudos? Quiescência tectônica resiste às investigações em menor/pequena escala? Ao que tudo indica, a dimensão da região amazônica, marcada pela coexistência de ambientes diversos, parece contrastar com a Geomorfologia calcada na generalização.

Compartimentar o objeto e reduzir a escala de espaço e tempo no levantamento investigativo pode revelar fenômenos geomórficos facultativos ao rastreio em maior escala. Por isso, a adoção de distinto padrão espaço-temporal mostra-se um caminho adequado no expediente das investigações nos campo da Geomorfologia, em particular, a Estrutural.

Outro destaque deve ser dado ao nível do mar, visto que a evidência *multi-proxy* permite interpretar que a sua posição já esteve acima do nível atual até, aproximadamente, ~1500 anos cal AP. De acordo com as idades obtidas por radiocarbono, o mar atravessou o litoral amazônico ainda no *Greenlandian*. Não há dúvidas que a competente migração do ambiente salobro para o interior do continente tenha sido favorecida pela fase climática mais seca à montante da área de estudo, que reduziu o volume da drenagem fluvial. Em contraste, o clima parece ter sido menos importante na transição ambiental cronocorrelata aos últimos 2 milênios.

A mudança espacial na vegetação testemunhada pela paisagem durante o Holoceno tardio, com emergente florescimento da vegetação de água doce, concomitante à disrupção do manguezal, é coerente com uma rápida queda no nível relativo do mar. É importante notar que condições tropicais úmidas já estavam presentes na região há pelo menos 2 mil anos (i.e., 4–3,5 ka AP), antes do declínio dessa comunidade halófila; tal assincronia temporal torna a hipótese climática inconsistente na explicação da dinâmica paleoecológica. A retração no nível relativo marinho mostra-se um fato coerente. Portanto, esses sinais possibilitam propor um nível do mar alto no supralitoral paraense até o Holoceno tardio, seguido de uma queda relativamente brusca antes de sua estabilização no nível atual, o que significa novas perspectivas naquelas discussões travadas acerca de paleoníveis no litoral da Amazônia, em particular no campo supralitorâneo, sob a tríplice influência dos rios Pará, Tocantins e Maratauíra.

As novas concepções relativas ao comportamento do nível relativo do mar fundamentam-se, ainda, na seleção dos locais de amostragem que foram designados de campo distante. Este é o primeiro estudo voltado à detecção de sinais de influência marinha do Holoceno realizado em região estabelecida 100 km além da linha de costa ao longo do litoral brasileiro. O campo distante é inexplorado e potencialmente sensível aos estudos de rastreamento de influências

marinhas. Contudo, devido à possibilidade da entrada e deposição alóctone de pólen da vegetação halófila, recomenda-se, em tais abordagens, o emprego de indicadores adicionais, tais como os provenientes da geomorfologia, fácies sedimentares e geoquímica isotópica para a geração de um índice robusto. Essa integração de procedimentos possibilita traçar confiavelmente o efeito marinho fora da linha costeira, onde ele é tipicamente bem investigado, devido apresentar maior potencial de preservação do avanço oceânico.

Nesses termos, considera-se que esta Tese – termo aqui grafado em maiúsculo para se referir à coletânea dos resultados desta pesquisa – traz significativos avanços no âmbito das Geociências, em especial da Geografia Física e Geomorfologia, mediante a ênfase no diálogo com a Geologia, a Paleoecologia e a Paleoclimatologia, a Oceanografia e áreas afins. A pesquisa foi construída também com métodos e procedimentos inerentes a esses campos do saber. O raciocínio geomorfológico, de modo algum, exclui a interdisciplinaridade. A formação do geógrafo físico e do geomorfólogo requer um expediente de interdisciplinaridade mais forte que o discurso. De igual modo, requer experiência de campo e laboratório, tanto quanto demanda-se em gabinete.

Por fim, avalia-se que as interevidências reunidas podem melhorar os dados para reconstrução do quadro paleogeográfico da interface terra-mar da porção do nordeste costeiro do Estado do Pará, incluindo contribuições para a ciência geomorfológica, face à demonstração de ilha como produto do rearranjo fluvial. Em conjunto, esses avanços ajudam a compreender melhor a evolução da Amazônia através do Quaternário em termos de lacunas paleogeográficas que persistem.

Referências

ABREU, A. A. A teoria geomorfológica e sua edificação. Rev. Instituto Geológico, v. 4, p. 5–23,1983.

AB'SABER, A. N. Os domínios morfo-climáticos da América do Sul. São Paulo. Geomorfologia. IGEOG-USP, v. 52, p. 1–21, 1977.

BECKINSALE, R. P.; CHORLEY, R. J. The History of the Study of Landforms or the Development of Geomorphology, Vol. 3; Historical and Regional Geomorphology, 1890–1950, Routledge, London. 1991.

BAKER, V. R.; TWIDALE, C. R. The reenchantment of geomorphology. Geomorphology, v. 4, p. 73–100, 1991.

BAUER, B. O. Geomorphology, geography, and science. In: B.L. Rhoads and C.E. Thorn, (Eds), The Scientific Nature of Geomorphology: Proceedings of the 27th Binghamton Symposium in Geomorphology, 27–29 September 1996. John Wiley and Sons Ltd, p. 381–413, 1996.

BRUNSDEN, D. Geomorphological events and landform change. Z. Geomorphol., v. 40, p. 273–288, 1996.

CHRISTOFOLETTI, A. As tendências atuais da geomorfologia no Brasil. Notícia Geomorfológica Campinas, v. 17, p. 35– 91, 1977.

CAILLEUX, A.; TRICART, J. Le problème de la classification des faits géomorphologiques. Ann. de Géogr., v. 65, p. 162 –186, 1956.

BOER, D. H. de. Hierarchies and spatial scale in process geomorphology: a review. Geomorphology, v. p. 4, 303–318, 1992.

GAO, J.; XIA, Z. Fractal in physical geography. Progress in Physical Geography, v. 20, p. 178–191, 1996.

GOODIE, A. S. The integration of physical geography. Geographica Helvetica, v. 3, p.163–168, 2000.

KENNEDY, B. A. Hutton and Horton: views of sequences, progressions and equilibrium in geomorphology, in Geomorphic Systems, edited by J.D. Phillips and W.H. Renwick, Geomorphology, v. 5, p. 231–250, 1992.

SCHUMM, S. A. Explanation and extrapolation in Geomorphology: seven reasons for deologyc uncertainty. Transactions. Japanese Geomorphological Union, v. 6, p. 1–18, 1985.

SHERMAN, D. J.; BAUER, O. B. Dynamics of beach-dune systems. Progress in Physical Geography, v. 17, p. 413–447, 1993.

THORNBURY, W.D. Principles of Geomorphology, 2nd edn. Wiley, New York. 1969.

UNWIN, T. The Place of Geography. Longman Scientific & Technical, New York, p. 273, 1992.